THE UNIVERSITY OF CHICAGO

# ANTIBODY TARGETING OF ANTIGEN TO ENDOGENOUS IMMUNE SURVEILLANCE PATHWAYS FOR THE INDUCTION OF TOLERANCE

A DISSERTATION SUBMITTED TO
THE FACULTY OF THE PRITZKER SCHOOL OF MOLECULAR ENGINEERING
IN CANDIDACY FOR THE DEGREE OF
DOCTOR OF PHILOSOPHY

BY
ELYSE ANDREA WATKINS

CHICAGO, ILLINOIS
MARCH 2021

To my parents, John and Silvia Watkins, for always standing by my side, fostering in me a sense of curiosity about the world, and encouraging me to shoot for the stars.

"Nothing in life is to be feared, it is only to be understood. Now is the time to understand more, so that we may fear less" - Marie Curie

# TABLE OF CONTENTS

# LIST OF FIGURES

# LIST OF TABLES

# ACKNOWLEDGMENTS

I am so thankful to have been blessed with a village of people that helped me survive and thrive during my graduate studies.

I would above all like to thank my graduate advisor, Jeffrey Hubbell. Since day one, his curiosity about science and discovery has been infectious. He has allowed me the opportunity to pursue even the wildest ideas, and although many did not pan out, I will always cherish the fun in that exploration. He has always spoken to me as a peer, instead of as a boss, which has allowed me to freely bounce around ideas and concerns without the fear of judgment. He also cares deeply about the people in his laboratory. He has fostered a collaborative environment, where everyone enjoys working together and exchanging ideas, which makes the science and experience that much better. Finally, and importantly, he has taught me how to make a great Negroni.

I would like to thank my committee members, Marisa Alegre, Jun Huang, and Patrick Wilson. I would first like to thank them for their patience, as my project has changed so many times and they stuck with me through it all. I thank them for all of the one-on-one meetings where they came up with new ideas and they made me think more deeply about my science. I look forward to continuing to work with them for years to come.

I would like to thank the many mentors I have had throughout the years. I would like to thank Chris Lee, my first mentor in research at Georgia Tech, who would always make sure I knew why I was doing something instead of just performing the task. His style of mentorship has completely influenced how I mentor new students that work with me. I would like to thank my former research advisors Tom Barker and Sai Reddy, both of whom also worked with Jeff, who really sparked my passion for science, and who have continued to mentor me throughout the past 10 years. I would particularly like to thank Sai for hosting me twice in his lab in Switzerland, and for all of the wonderful people and lasting friendships I made while I was there. I would like to thank four mentors I have had in the lab since I started. Marcin Kwissa enabled me to start working in the lab when everything was unfamiliar and there was

no one else around. I will always remember fondly the times I spent asking him countless questions about science, distracting him from getting any work done. Michelle Miller really taught me all things about mouse work, and was such an amazing immunologist and patient mentor. Scott Wilson has an endless stream of all knowledge, and was the hardest worker I have met to date. I thank him for all of the life and scientific advice he gave me in the many late nights we spent in lab. I also thank Jun Ishihara, who taught by example that science is best done in teams. I am so thankful to have learned that from him, and I know it will guide how I do research in the years to come.

There are so many people in the lab I would like to thank. First, Robert DeLoera, Anya Dunaif, and Jaeda Roberts, the three undergraduates in the lab that I mentored who together worked with me for 6 years. They dedicated so many hours to helping with the project, and stuck with me through many, many frustrating days of experiments not working. I would like to thank the other students I have had the complete privilege of mentoring – Jenni Antane, Rachel Wallace, Joe Reda, Erica Budina, and now Brendan Berg. They have all helped me so much with my projects, and helped me grow as a researcher and mentor. It has been such a pleasure seeing them grow into amazing scientists, and teach me things all of the time. They also taught me never to underestimate someone that is new to a technique – people are capable of learning much more quickly than we think they are.

I would like to thank Andrew Tremain, who has been such a leader in the lab and has invested so much time and effort into making it better since day one. He has also provided moral and scientific support, as we struggled through our PhD careers at the same time. Thank you to Stephan Kontos, who though not in the lab, pioneered my project and has provided so much guidance along the way. I would like to thank many others in the Hubbell and Swartz labs – and in particular Tiffany Marchell, Lea Maillat, Rachel Weathered, Suzana Gomes, Mindy Nguyen, John Michael Williford, Peyman Hosseinchi, Nick Mitroussis, and Sarah MacEwan, for your friendship, guidance, and support. Everyone in these labs has made it such a wonderful environment to conduct science. When experiments wouldn't

work, at least we could laugh.

I would like to thank many in the Kossiakoff lab, and in particular Tomasz Slezak, who went out of his way to help me with all things dealing with antibodies and protein production. Thank you to Mat Schnorenberg, who in addition to helping me with everything dealing with Fab conjugation to polymerosomes, has also been by my side since the beginning of PME and has become a lifelong friend. Thank you to Ani Solanki, who has done thousands of mouse injections for me, never complaining about my chronic lateness. Thank you to Mike Olson, Bert Ladd, and David Lerec at the flow cytometry core facility, for the long hours and patience spent on flow sorting. Thank you to Bill in the DNA Sequencing Core for sequencing the millions of Fabs I have sent to him, and providing me with fresh produce from his garden.

I would like to thank my many classmates and friends at UChicago who have made my experience so great – Alyson Yee, Zack Jarin, Yu Kambe, Kevin Miao, Christine McIntosh, Viktor Rosza, Moshe Dolejsi, Alex Crook, and countless others. I would also like to thank many faculty and staff at the PME who have been influential throughout the whole process – Juan de Pablo, Matt Tirrell, Diana Morgan, Laura Rico-Beck, Rovana Popoff, Novia Pagone, and Kimberly McGee.

Finally, and most importantly, I would like to thank my family. My parents, John and Silvia Watkins, have sacrificed everything in their lives to make sure I had the most perfect childhood and best education. They never forced me in any direction, and let pursue whatever I wanted to. By their example they taught me to work hard, but never put pressure on me when I would fail. They endured the last 6 years of me complaining about my experiments, and told me that it would always work out in the end, and that hard work eventually pays off. Above all they taught me to be kind to others, and that is the best lesson I could learn. I would like to thank my grandmother, Alice Watkins, who is the best example of a strong woman, and who in her time achieved more than any man thought she could. She has supported me every step of the way. Finally, I would like to thank my sister,

Erica. She has been the rock by my side (literally - we were neighbors), always listening, never judging, and going out of her way to offer me support in any way she could. She is my absolute role model as a businesswoman, wife, and now mother, and I could not have survived these years in grad school without her.

# ABSTRACT

The overall goal of my thesis is to develop molecules to induce antigen-specific tolerance by co-opting endogenous tolerance mechanisms. To do this I developed antibody fragments that target the apoptotic pathway or the liver, and characterized the ensuing immune responses.

In Chapter 1, I introduce the field of immune tolerance. I discuss the mechanisms that the immune system employs to maintain tolerance to self, and avoid autoimmunity. I discuss the current standards of care in immunosuppression used to treat autoimmunity, allergy, transplantation, and prevention of anti-drug antibodies. Finally, I introduce emerging strategies that are in development to achieve antigen-specific tolerance.

In Chapter 2, I expand upon a previously developed technique in the laboratory to target apoptotic erythrocytes for immune tolerance. I conduct phage display on mouse erythrocytes using a human antibody fragment phage library, and characterize the resulting erythrocyte-binding antibody fragments. I target antigen to erythrocytes and determine that delivery to this pathways yields profound and lasting T cell dysfunction, both in transgenic and endogenous T cells. I further characterize the mechanism of tolerance induction as occurring in the spleen, and for CD8 T cells by Batf3+ dendritic cells.

In Chapter 3, I develop a method of targeting liver sinusoidal endothelial cells for their inherent tolerogenic properties. I conduct phage display on liver sinusoidal endothelial cell C-type lectin (LSECtin), for its specificity to LSECs in the liver. I characterize the Fabs from phage display, and determine that they are rapidly and specifically internalized by LSECs. I target antigen to LSECtin, and determine that this pathway reduces presentation to T cells. I use protein engineering strategies to enhance antigen presentation by developing cathepsin-cleavable linkers and endosomal escape peptides. Finally, I encapsulate antigen in polymerosomes decorated with anti-LSECtin Fab, and enhance presentation by LSECs.

In Chapter 4, I discuss the conclusions and future directions of this work. Furthermore, I discuss the limitations to the field of antigen-specific tolerance, and offer potential strategies to overcome these limitations.

# CHAPTER 1

# INTRODUCTION

Autoimmune disease, allergy, transplant rejection, and development of anti-drug antibodies (ADA) represent major causes of morbidity and mortality, and are caused by an unwanted immune response. In autoimmune disease, self-reactive lymphocytes that have escaped negative selection become activated in the periphery, and initiate immune-mediated organ destruction. In allergy, development of ADAs, and transplant rejection, the immune system recognizes innocuous foreign antigen as harmful, and mounts a subsequent attack on the antigen. Current treatments for these conditions are largely global immunosuppression, which not only leave individuals susceptible to infection, but unwanted side effects are also implicated in cancer, diabetes, and cardiovascular issues. There is therefore great interest in suppressing the immune response solely to the antigen(s) that is the subject of the immune attack, while leaving the rest of the immune system capable of mounting a productive immune response. Here we review endogenous mechanisms of T cell tolerance, the current state of immunosuppression, and emerging technologies for induction of antigen-specific tolerance.

## 1.1 Endogenous Mechanisms of Immune Tolerance

In order to develop therapeutics for tolerance induction, it is important to understand the different forms tolerance can take and the longevity of this tolerance.

### *1.1.1 Central Tolerance*

The immune system is designed to be tolerant to self, while maintaining responsiveness to all other foreign antigens that it might encounter in order to protect the host. T and B cells have a first checkpoint in primary lymphoid organs during their development, where they are subject to central tolerance in the thymus and bone marrow, respectively. While in these organs, immature T and B cells encounter self-antigen, and T cells are additionally

exposed to peripheral tissue antigens through an Aire-dependent mechanism [1]. If their T cell receptors (TCR) or B cell receptors (BCR) signal strongly, they will undergo clonal deletion, thereby largely ridding the repertoire of potentially autoreactive lymphocytes that may cause autoimmunity. However, lymphocytes with a low avidity to self-antigen will escape into the periphery, which may then have the potential to elicit disease if under the right circumstances. Although potentially dangerous for the host, purging all lowly autoreactive cells in the primary lymphoid organs would leave gaps in the repertoire of pathogen-specific response that would be even more costly to the host.

A safeguard to these low avidity autoreactive T cells are regulatory cells. Most prominently studied are FoxP3+ CD25+ CD4+ regulatory T cells (Tregs). Thymic-derived Tregs (tTregs) are developed in the thymus, and about 80% of total Tregs are thought to be tTregs [2]. tTregs depend on the transcription factor FoxP3, and mice and humans that lack or have mutations in FoxP3 develop severe autoimmunity [3, 4] .

Tregs are thought to suppress immune responses by a number of mechanisms. Tregs secrete immunosuppressive molecules such as TGF-$\beta$ and IL-10, which can act directly to curb activated T cell responses [5, 6]. Tregs express the high affinity IL-2R$\alpha$, CD25, and although there are conflicting reports, may sequester IL-2 such that it is not available for conventional T cells to promote activation [7]. They may also directly kill conventional T cells, through perforin and granzymes [8]. Tregs may act in a contact-dependent manner by taking molecules needed for naïve T cell activation from the membrane of the APC, a phenomenon known as trogocytosis. CTLA-4, which is highly expressed on Tregs, may trogocytose CD80 and CD86 on activated APCs such that it is not available to bind CD28 on conventional T cells [9]. A recent report has demonstrated that Tregs may act in antigen-specific mechanisms by trogocytosing peptide-MHCII complexes from an activated APC, such that the molecules are not available to activate naïve T cells [10].

tTregs have classically been thought to have a high degree of stability, which is essential to prevent autoimmunity. Most reports maintain that only a very small fraction of Tregs

lose expression of FoxP3 and may convert to pathogenic phenotype, whereas the large majority maintain suppressive capacity once created [11, 12]. This is not only dependent on FoxP3 expression, but also on a pattern of CpG hypomethylation that is required for suppressive capacity of Tregs and their long-term stability [13]. Although conflicting studies have demonstrated that Tregs may exhibit plasticity in their ability to lose suppressive and acquire effector functions, it is thought that a small proportion of contaminating conventional T cells, as well as T cells that only transiently expressed FoxP3, likely explain these contradictory findings [14–16]. It is now believed that the FoxP3+ CD25+ cells are a stable and committed lineage, whereas FoxP3+ CD25- cells are uncommitted and thereby may exhibit plasticity and conversion to effector cells [17].

### *1.1.2 Peripheral Tolerance*

Because not all self-reactive T cells are deleted in the thymus, and there are innocuous antigens such as food antigens present in the periphery that would not be present in the thymus, peripheral tolerance mechanisms exist that are important to prevent unwanted immune responses [18]. These include deletion, anergy, exhaustion, and induction of peripheral Tregs (pTregs) and other regulatory cells.

When T cells see their cognate antigen in the periphery, they rely on cues from the environment to determine whether they will undergo activation or tolerance. If naïve cells encounter antigen presented by APCs with the costimulatory molecules CD80 and CD86, the outcome of these response will likely be differentiation into effector T cells. There are further stimuli, such as the cytokine milieu, that will further determine the fate of the cells; for example IL-6 and TGF-$\beta$ along with the proper costimulatory molecules will produce Th17 cells.

### *1.1.3 Deletion*

In the absence of costimulatory molecules, naïve T cells that encounter antigen are likely to undergo deletion or anergy [19]. Initial exposure to antigen without costimulation will drive T cells to undergo Fas- and Bim-mediated deletion [20]. This plays a substantial role in peripheral tolerance, as mice and humans that lack or have mutations in apoptotic pathways develop autoimmune lymphoproliferative syndromes [21, 22]. This strategy has been employed extensively for potential treatments in autoimmune disease.

### *1.1.4 Anergy*

Cells that are spared from deletion may become anergic, a state of hyporesonsiveness characterized by the inability to produce IL-2 [23, 24]. TCR stimulation in the absence of costimulation leads to NFAT1 expression without formation of the AP-1 complex [25]. After repeated stimulation, this leads to NFAT1-driven expression of the E3 ubiquitin ligases such as Cbl-b, GRAIL, and Itch that impair TCR signaling [26]. Furthermore, NFAT1 without AP-1 induces the expression of transcription factors Egr2, Egr3, Ikaros, and CREM, which repress the *Il2* gene.

There is debate about the fate of anergic cells. *In vitro*, addition of IL-2 to anergic cells allows them to regain effector function, whereas this is insufficient *in vivo* [27]. Early studies suggested that removal of antigen could reverse the anergic state in T cells [28]. However, newer studies suggest that the initial program of the tolerant, anergic state is permanent, and transfer of anergic cells into a new lymphopenic host may temporarily lead to acquisition of effector functions, but the cells are eventually restored to tolerance even in the absence of antigen [29]. Similarly, co-stimulation blockade during allogeneic transplantation provides TCR stimulation without co-stimulation, yielding dysfunctional T cells that do not reject the organ. Upon exposure to an inflammatory context, such as infection with Listeria monocytogenes, T cells are rendered temporarily capable of acquiring effector functions and rejecting the organ, but the dysfunctional state is eventually recovered [30]. Because of this

longevity of a dysfunctional program, anergy induction by tolerogenic APCs *in vitro* and *in vivo* has been explored as a therapeutic approach to treat a variety of autoimmune disease such as type 1 diabetes (T1D), rheumatoid arthritis (RA), and multiple sclerosis (MS) [31].

### *1.1.5 Peripheral Tregs and Other Peripherally Induced Regulatory Cells*

In an alternative to deletion or anergy, T cells that encounter antigen in the periphery may also become Tregs (pTreg). pTregs perform a nonredundant role to tTregs in suppression of autoimmunity and inflammation, particularly at mucosal tissue sites [32, 33]. This conversion to a Treg as opposed to the other fates is largely dependent on the environment. For example, a large proportion of pTregs are found in the gut, where TGF-$\beta$, retinoid acid, and short chain fatty acids, all molecules that may contribute to Treg induction, are found in abundance [34, 35]. These pTregs recognize dietary antigens and likely recognize commensal microbes, and are thought to control pathogenic inflammation to these foreign antigens [36, 37]. pTregs are also found abundantly in the placenta, where decidual macrophages play a role in their induction, and contribute to maternal-fetal tolerance [38, 39]. Interestingly, tumors also harbor immunosuppressive microenvironments, including the production of TGF-$\beta$, which may contribute to the induction of pTregs specific for tumor antigens capable of suppressing tumor immunity [33, 40].

Other peripherally-induced regulatory cells include T regulatory type 1 cells (Tr1), CD8 Tregs, and regulatory B cells (Breg). Although they do not constitutively express FoxP3, Tr1 cells produce high levels of IL-10 and TGF-$\beta$, have suppressive capacity, and upregulate a number of inhibitory molecules including LAG-3, PD-1, and CTLA-4 [41]. Tr1 induction is antigen-specific, and likely a result of priming by DCs that highly express IL-10 [42]. Tr1 cells may, like Tregs, exert their suppressive functions via antigen-specific and antigen-nonspecific mechanisms, and are associated with improved outcomes in autoimmunity and transplantation, and worse outcomes in cancer [43, 44]. Tr1 are not as well-defined as Tregs, but recent studies suggest that Tr1 cells maintain a stable suppressive identity over time,

and cells do not become effector cells when faced with a viral challenge [45, 46].

A role for B cells in restraining autoimmunity was first suggested when mice deficient in B cells had impaired recovery in experimental autoimmune encephalomyelitis (EAE), a mouse model of multiple sclerosis [47]. This was confirmed with studies demonstrating that mice with IL-10-deficient B cells develop non-remitting EAE [48]. Bregs in mice and humans are thought to contribute to downregulation of Th1 and Th17 responses in autoimmunity and other inflammatory contexts. [49–52]. Although potentially powerful suppressors, a number of factors preclude their immediate therapeutic development. The predominant issue is that there lacks a standardized method of identifying Bregs aside from IL-10 production [53]. Furthermore, there is little known about Breg induction, specificity, and stability, which are essential to understand in order to develop a viable therapy.

Similarly, CD8 Tregs, otherwise known as suppressor CD8 T cells, represent a similarly heterogenous population that may be important in suppressing aberrant immune responses. CD8+CD25+FoxP3+ Tregs are found in the steady state in the mouse and human, and have an *in vitro* suppressive capacity equal to or greater than CD4 Tregs [54]. Another class of CD8 Tregs are Qa1-restricted, an HLA class 1b MHC molecule, and are FoxP3-. These CD8 Tregs primarily act on CD4 T cells, suppressing Tfh cells from promoting lupus-like disease, and suppressing CD4 T cells in EAE from promoting pathogenesis [55–57]. Although promising, more studies need to be conducted on these cells before they are used in the clinic.

### *1.1.6 Exhaustion*

Exhaustion was first described as a T cell fate resulting from chronic infection [58, 59]. Following chronic activation, T cells had a reduced capacity to produce effector cytokines and control the viral infection. Since these seminal studies were performed over 20 years ago, the program of T cell exhaustion has also been well characterized in many viral infections and cancer, and there is an emerging role for exhausted cells and in autoimmunity and transplantation [60–63]. Exhausted cells are characterized by reduced ability to proliferate

produce cytokines such as interleukin 2 (IL-2), tumor necrosis factor alpha (TNF$\alpha$), and interferon gamma (IFN$\gamma$), and degranulate [60]. Exhausted T cells are also characterized by the upregulation of co-inhibitory molecules, such as PD-1, CTLA-4, LAG-3, TIM-3, and TIGIT, as well as transcription factors such as TOX [64].

Blocking these inhibitory molecules, known as checkpoint blockade, can reinvigorate exhausted T cells to become effector cells. Checkpoint blockade therapies, in particular those targeting PD-1/PD-L1 and CD28/CTLA-4 interactions, have been revolutionary in treating many forms of cancer [65, 66]. However, not all patients are responsive to checkpoint blockade, despite having exhausted tumor-specific T cells [66, 67]. One such reason is that only a subset of exhausted T cells, likely those expressing TCF-1, may be responsive to checkpoint blockade and mediate tumor killing [68–70]. Furthermore, this responsiveness may only be temporary, as epigenetic programming may establish a permanent exhausted program and cells may revert to dysfunction after blockade [71]. Although detrimental for cancer and chronic infection, this stability of T cell exhaustion may prove a potential therapeutic avenue for treatment of autoimmunity and prevention of transplant rejection.

## 1.2 Current Standard of Care in Autoimmune Disease, Allergic Disease, Transplantation, and Anti-Drug Antibodies

### *1.2.1 Autoimmune Disease*

There are over 80 autoimmune diseases recognized by the NIH, that are characterized by a breakdown of immune tolerance to one's own tissues [72]. In autoimmunity, the weakly autoreactive cells that escape central tolerance become activated and attack self-tissue. The trigger for this breakdown of immune tolerance and subsequent development of autoimmunity is largely unknown, but is thought to involve a complex interaction between genetics and the environment. Studies in monozygotic twins often demonstrate a significant link between genetics and development of disease; however, in many autoimmune diseases there is only

up to a 30% penetrance between monozygotic twins, indicating a substantial contribution of the environment [73]. Echoing this, the prevalence of autoimmune disease has increased substantially over the past 30 years, with 11.5% between 1988-1991 and 15.9% between 2011-2012 of the US population testing positive for antinuclear antibodies, the most common biomarker of autoimmunity [74]. Because genetics are unlikely to change substantially over the course of 30 years, it is likely a number of environmental factors have contributed to this uptake in disease. Prior infection, changes in microbiota, and toxin exposure such as tobacco and heavy metals are thought to contribute to development of disease.

There are currently no drugs available to treat the underlying cause of autoimmunity and reverse the course of disease. Instead, treatments to suppress an ongoing immune response must often be taken over a lifetime. A typical first line of therapy is corticosteroids for their rapid efficacy, which, among other things, act on glucocorticoid receptors to interfere with transcriptional activation of NF-$\kappa$B and AP-1, transcription factors involved in initiating an inflammatory response [75]. Methotrexate, originally used to treat cancer by inhibiting folate's role in purine synthesis, has also been very effective in treating rheumatic diseases, albeit likely by a distinct mechanism [76]. Hydroxychloroquine, an anti-malarial drug, is another anti-rheumatic drug commonly used to treat systemic lupus erythematosus (SLE) and RA, in part by increasing the lysosomal pH and reducing antigen presentation in antigen presenting cells (APC) [77].

Although these common small molecule drugs are inexpensive and easy to use, they often act on ubiquitous cellular pathways, and long-term use is associated with a number of systemic adverse side effects. Such side effects include hypertension, bone fracture, de novo diabetes, gastrointestinal issues, hepatotoxicity, myopathy, and retinopathy [75, 77, 78]. Relatively newer biotherapeutics, or biologics, aim to suppress the immune system more specifically, thereby limiting some of these side effects. The most common of these neutralize the effect of inflammatory cytokines such as TNF$\alpha$, a cytokine that is important in the immune response to pathogens, but is also dysregulated in many autoimmune diseases

and central to pathogenesis [79]. Some biologics reduce inflammation by reducing T cell trafficking to sites of disease, such as the gut and spinal cord, by blocking the interaction of T cell integrins $\alpha 4\beta 7$ and $\alpha 4\beta 1$ integrins with vascular adhesion molecules [80, 81]. In more severe cases that are refractory to other treatments, lymphodepleting biologics are utilized. For example, anti-CD20 antibody that depletes B cells is used to treat moderate to severe RA and SLE [82, 83]. Paradoxically, one of the most common biologics to treat MS is interferon beta (IFN$\beta$), a molecule involved in both dampening and eliciting an immune response to pathogens [84].

Even though they are more specific than small molecule drugs, these biologics still have substantial effects on the immune system, which may leave patients severely immunocompromised. A desirable alternative would be to shut down the aberrant immune response to a specific autoantigen, while sparing the rest of the immune system, an outcome known as antigen-specific tolerance. A significant challenge in this approach is identifying the relevant autoantigens in these diseases. There are known autoantigens for only 45 autoimmune diseases [72]. Of these, some have singular autoantigens, such as acetylcholine receptor in myasthenia gravis, desmogleins 1 and 3 in pemphigus vulgaris, and aquaporin 4 in neuromyelitis optica [85–87]. In other autoimmune diseases, such as T1D, MS, and SLE, a variety of autoantigens are associated with pathogenesis [88–90]. The relative contribution of each of the antigens, and how many autoantigens are needed to induce tolerance to in order to reverse disease, is not known. Furthermore, in diseases such as type 1 diabetes, once patients present with poor glycemic control much of the autoimmune-mediated destruction has already been complete, necessitating early biomarkers of disease. Finally, in autoimmune diseases the autoreactive lymphocytes are already effector cells, and therefore a successful therapy would be required to induce deletion in these cells or render them dysfunctional and incapable of effector functions.

### *1.2.2 Allergic Disease*

Allergic diseases, including food allergy, atopic dermatitis, allergic rhinitis, sinusitis, asthma, urticaria (hives), and venom hypersensitivity, are the 6th leading cause of chronic illness in the United States, affecting 10-30% of the population [91]. The allergic response is characterized by crosslinking of the Fc$\varepsilon$RI on mast cells and basophils by IgE-antigen complexes. This leads to subsequent mast cell and basophil degranulation, including release of histamines and lipids, and later release of cytokines and inflammatory mediators which recruit other inflammatory cells and propagate the response [92, 93]. In severe cases, this may lead to anaphylaxis, and at least 5% of adults in the US have suffered an anaphylactic reaction [94].

The cause of allergy is largely unknown. The past 100 years have seen a substantial rise in cases of allergy, associated with westernization [95]. There have been various theories to explain this rise in allergy, such as an altered microbiota because of antibiotics and a westernized diet, exposure to environmental toxins, sedentary lifestyle, and lack of exposure to vitamin D during immune development. Despite this rise in allergy, treatment remains limited.

Antihistamines are common and inexpensive treatments that have been used for over 50 years to control the allergic response, particularly in allergic rhinitis and urticaria [96]. Corticosteroids are another class of common drugs used for a variety of allergic diseases, most commonly including asthma and atopic dermatitis [97]. Severe anaphylactic reactions to allergens are treated with epinephrine. Other common treatments, depending on the allergic disease being treated, include $\beta$2-adrenoceptor agonists and phosphodiesterase inhibitors [98].

More recently, biologics have been developed for chronic allergies that are refractory to other treatments. Omalizumab, which binds soluble IgE and inhibits its interaction with Fc$\varepsilon$RI as well as clears it from circulation, is clinically approved for the treatment of asthma and urticaria [99]. Other antibody drugs that are either approved or in late stage clinical trials block the action of mediators of the T helper 2 (Th2) allergic response, including

interleukin-4 (IL-4) and interleukin-5 (IL-5) [100]. Although effective, their very high cost in comparison to other approved drugs has limited their use to primarily severe cases.

Although the aforementioned treatments are effective in reducing the symptoms associated with allergic disease, they do not affect the underlying cause of the disease, an aberrant T and B cell response to an innocuous antigen. Allergy immunotherapy (AIT), a form of antigen-specific tolerance similar to that previously described for delivery of unmodified antigen in autoimmunity, is the only disease-modifying treatment proven effective to treat some allergic diseases [100]. Treatment typically involves either subcutaneous (SCIT) or sublingual (SLIT), administration of an escalating dose of allergen followed by a maintenance dose, as frequently as weekly for SCIT and daily for SLIT over the course of 3-5 years [101]. AIT is thought to function by desensitizing T cells over time to their cognate antigen and reducing the number of Th2 cells, while inducing conventional Tregs, Tr1, and IgG4 antigen-specific antibodies, an isotype of IgG associated with favorable outcomes [102]. This strategy is relatively inexpensive and has proven safe for the treatment of asthma, allergic rhinitis, and venom allergy; however, particularly in the attempt to expand treatment to oral immunotherapy for treatment of food allergy, systemic adverse reactions and anaphylaxis are often reported [103–105]. Another limitation of AIT is compliance. In SCIT the 3-year compliance rate has been shown to be 57%, whereas for the safer but more frequent strategy, SLIT, the compliance is closer to 10% [106]. Although already quite effective, a strategy is needed for allergy treatment that achieves the same safety and efficacy as the current AIT, but with fewer doses to achieve greater compliance.

### *1.2.3 Transplantation*

Transplantation has become a major treatment for end-organ failure, with over 30,000 solid organ transplants done annually [107]. The major hurdle in transplantation is recognition of the donor graft as foreign by the recipient's immune system, and subsequent rejection of the graft. The donor graft contains human leukocyte antigens (HLA), responsible for presenting

foreign antigen to T cells. HLA is the most polymorphic human locus, with over 25,000 alleles [108, 109]. Each individual has 6 class I HLA molecules and 6 class II HLA molecules. In the 1970s, it was found that matching the transplant HLA to the recipient HLA increased graft survival [110]. However, unless the organ is donated from a close relative, the probability of an exact match of HLA is very low. When the HLA are not a perfect match, the recipient's T and B cells can recognize the HLA molecules as foreign, either by direct recognition on the organ or by indirect recognition of donor HLA peptides presented on recipient HLA, and attack the organ. B cells may mount a subsequent donor specific antibody (DSA) response, the presence of which is highly correlated with graft rejection [111]. Thus, in most cases, lifelong immunosuppression is necessary to prevent the recipient from rejecting the organ.

Over the past 40 years, immunosuppressive regimens have largely been able to prevent acute rejection, and over 90% of many solid organ transplants have at least a 1-year survival [112]. These new regimens typically involve induction and maintenance phases. The induction phase occurs during the perioperative period, and has historically involved high doses of the same drugs used in the maintenance phase. In the last 10 years, however, it has become common practice to use antibody therapy in the induction phase to prevent acute rejection, such as targeting CD52 or CD3 to deplete lymphocytes or T cells, respectively, or IL-2R on activated T cells to prevent IL-2 ligation and subsequent proliferation [113–115]. This induction phase is followed by a maintenance phase that includes a triple therapy of a calcineurin inhibitors, anti-proliferative agents, and corticosteroids [112]. Calcineurin inhibitors, such as tacrolimus, and corticosteroids are the most widely used drugs for immunosuppression in transplantation, and transplants recipients will generally take these drugs throughout their lifetime [116]. However, these are associated with a number of adverse side effects, including nephrotoxicity, increase in cardiovascular episodes, hypertension, diabetes, hyperlipidemia, and obesity [117]. To overcome these significant side effects, new therapies are emerging in clinical trials [117]. CTLA-4-Ig has been used during induction therapy, and allows for decrease in use of calcineurin inhibitors without compromising graft survival, but does not

show equivalent prevention of acute graft rejection as a monotherapy compared to current regimens. Making use of a similar pathway of blocking T cell co-stimulation, a non-depleting, blocking antibody to CD40 has shown safety and early signs of efficacy in kidney transplant [118, 119]. Other attempts at prolonging graft survival have included therapies that aim to minimize DSAs, such as intravenous immunoglobulin therapy or B cell and plasma cell depletion using an anti-CD20 antibody or proteasome inhibitor, respectively [120]. Treg therapy has also been shown to be effective in preventing or alleviating graft versus host disease, and has shown some promise in solid organ transplantation [121, 122].

Although new therapies utilizing biologics have shown promise and have better safety profiles than long term use of currently used immunosuppressants, their long-term efficacy remains to be seen. As with autoimmunity and allergy, the holy grail of transplant tolerance would be to have antigen-specific tolerance to the organ as opposed to global immunosuppression. However, there is an added layer of complexity in transplantation compared to autoimmunity because instead of tolerizing to a limited number of antigens, lymphocytes would need to be tolerized to all combinations of donor HLA with the peptides they are presenting.

### *1.2.4 Anti-Drug Antibodies*

Biotherapeutics, also known as biologics, are a class of drugs made of proteins that have revolutionized patient treatment across many sectors of medicine. Originating with the production of recombinant insulin in 1982, the global biopharmaceutical market for antibody therapies is valued at $125 billion [123]. A large part of their success compared to small molecule drugs is their specificity and therefore lack of off-target effects. However, this comes at the cost of these molecules containing T and B cell epitopes that may be perceived as foreign by the host's immune system, triggering the formation of anti-drug antibodies (ADA) [124]. In fact, many biologics trigger ADAs in 1-5% of patients, some can lead to ADAs in up to 40% of patients [125]. Immunogenicity of these molecules is of significant interest

to the biopharmaceutical industry, as ADAs may neutralize the activity of the biologics, reducing or eliminating their biological activity [126]. In more severe cases, ADAs may cause hypersensitivity reactions, or responses to endogenous proteins because of cross-reactivity [126].

Most strategies to reduce the immunogenicity of the biologics have focused on altering the molecule itself. The first strategy is to "humanize" the antibody, by mutating the foreign epitopes derived from the original host, typically mouse, to reflect a native human sequence [127]. New strategies involve *in silico* modeling to determine which sequences on the biologic could fit into the most common human HLA, and introduce point mutations that would abrogate binding to HLA while maintaining proper structure and function [124]. In the newest efforts to increase tolerance to biologics, groups have sought to introduce predicted Treg epitopes (Tregitopes) in the hopes of getting bystander Treg suppression to other foreign epitopes on the molecule [128]. Biologics are an ideal candidate for induction of antigen-specific tolerance, because unlike in autoimmunity and allergy, before patients receive the drug they have no prior immunity to it, offering a blank slate for the induction of tolerance before receiving the drug.

## 1.3 Emerging Technologies for the Induction of Antigen-Specific Tolerance

### *1.3.1 Therapeutic Immunization with Autoantigens*

Glatiramer acetate, which has been used for nearly 30 years to reduce the number of relapses in MS, is the first approved drug that achieves a form of antigen-specific tolerance [129]. It is a combination of peptides of varying lengths whose sequences resemble that of myelin basic protein (MBP), an autoantigen in MS, and is thought to act both as a decoy and an altered peptide ligand that can fit into the major histocompatibility complex (MHC) groove and divert MBP-reactive T cells to an anti-inflammatory phenotype.

Similar strategies to deliver auto-antigens in the absence of inflammatory signals to induce tolerance have been employed across many autoimmune diseases, but have largely not met therapeutic outcomes in clinical trials [130]. In MS, clinical trials have attempted subcutaneous delivery of MBP-derived peptides, skin patches with peptides from three different MS autoantigens, and intradermal delivery of four MBP peptides, demonstrating fewer lesions but no therapeutic benefit. In T1D, there have been attempts to deliver oral, intranasal, or subcutaneous insulin, which failed clinical trials, and glutamic acid decarboxylase (GAD) with the adjuvant alum, which demonstrated preservation of insulin secretion [131]. For Celiac disease, an intradermally administered cocktail of disease-relevant gliadin peptides that bind the MHC molecule most prevalent amongst Celiac patients failed to show efficacy in clinical trials [132]. For RA, oral administration of a peptide from the dnaJP1 heat shock protein showed promising results in phase II clinical trials, but was not pursued further [133]. The most encouraging results have been in SLE, where phase III clinical trials with subcutaneous administration of a peptide derived from small nuclear ribonuclear protein showed amelioration of disease, although not statistically different from current standard of care [134].

DNA vaccines utilize a similar premise to therapeutic peptide immunization, whereby peripheral cells can present antigen to circulating T cells in the absence of co-stimulation. With therapeutic DNA vaccines in development, plasmid encoding an autoantigen is delivered intramuscularly, and the cells that phagocytose the DNA plasmid can immediately express the protein to be processed and presented on MHC in the absence of inflammatory signals. A DNA vaccine encoding myelin basic protein was tested in Phase I/II clinical trials, and demonstrated not only safety, but also a reduction in gadolinium-enhancing lesions, IFN$\gamma$-producing antigen-specific CD4 T cells, and anti-myelin antibody titers [135, 136]. In another trial, a DNA vaccine encoding a non-secreted version of proinsulin was used to treat patients with recent onset of T1D. This plasmid was engineered such that the potentially TLR9-stimulatory CpG motifs were mutated and replaced with non-stimulatory and com-

peting GpG motifs [137]. This trial demonstrated higher levels of C-peptide compared to placebo, as well as a reduction in islet-specific CD8 T cells [138]. This DNA vaccine is still undergoing clinical trials in a diverse set of patient groups.

### *1.3.2 In Vitro-Generated Tolerogenic Dendritic Cells*

Efforts to deliver unmodified antigen continue despite the modest efficacy, but newer strategies have utilized actively immunosuppressive pathways to enhance tolerance. One such strategy has been to use immature or tolerogenic dendritic cells (tolDCs), for their antigen-presenting capacity, lack of costimulatory molecules, and potential to secrete an anti-inflammatory milieu [139]. In one approach, autologous monocytes were derived from patient peripheral blood and differentiated into monocyte-derived tolDCs using granulocyte-macrophage colony-stimulating factor (GM-CSF), IL-4, and dexamethasone [140]. They were then pulsed with a cocktail of cytokines and either myelin peptides or the myelin peptides in addition to an aquaporin 4 peptide, and injected i.v. to treat MS and neuromyelitis optica, respectively. This approach was well tolerated and led to antigen-specific IL-10 production by peripheral blood mononuclear cells (PBMC) as well as induction of Tr1 cells. In a separate phase I trial, tolDCs were similarly manufactured from autologous monocytes, with the addition of calcitriol, the bioactive form of vitamin D3. TolDCs were then pulsed with a TLR4 ligand and autologous synovial fluid and administered arthroscopically to inflamed knee to treat RA [141]. This approach was well-tolerated, but there was a small reduction in disease activity only in the highest dose of tolDCs, and there were no detectable systemic immunomodulatory outcomes. A more successful attempt to treat RA developed tolDCs by inhibiting NF-$\kappa$B in monocyte-derived DCs, and pulsed them with a variety of citrullinated disease relevant peptides [142]. This led to a reduction in disease activity score, higher Treg: effector T cell ratio, reduction in inflammatory cytokines in the serum, and reduced antigen-specific effector responses.

### *1.3.3 Targeting Tolerogenic Antigen Presenting Cells In Vivo*

An indirect cell-based approach seeks to target tolerogenic APCs *in vivo*. A strategy to achieve this is to target the apoptotic pathway, which has tolerogenic properties. In one approach, six myelin peptides were coupled to autologous PBMCs and injected into patients with MS [143]. This strategy demonstrated a good safety profile and cellular profile with reduced responsiveness to the myelin antigens, but has not yet been followed up in subsequent trials.

In transplantation a similar approach is employed in donor specific transfusions, whereby the recipient receives donor bone marrow at the same time or shortly before as the solid organ [144]. Because of the potential for development of graft versus host disease whereby the donor's lymphocytes attack the host's tissues, this is typically done in cancer patients requiring bone marrow transplant. However, clinical trials have been conducted on patients without malignancies and have demonstrated acceptance of renal transplants after weaning off of immunosuppression [145].

In an alternative approach of targeting tolerogenic APCs *in vivo* by targeting the apoptotic pathway, our lab and others have utilized erythrocytes as an endogenous source of apoptotic cells. These strategies have included targeting autoantigen to the erythrocytes *in vivo* with an erythrocyte-binding molecule, *ex vivo* loading erythrocytes with antigen, or genetically engineering erythrocyte precursors to express autoantigens. These strategies have been tested in preclinical trials for avoidance of anti-drug antibodies in enzyme replacement therapy, and in T1D, EAE, and Celiac disease [146–148].

An early approach in nonspecifically targeting APCs was the development of nanoparticles with antigen conjugated to the surface that would be taken up by the spleen and in the absence of inflammation, induce tolerance [149]. These nanoparticles have progressed to phase II clinical trials in the treatment of Celiac disease, and have demonstrated a reduction in antigen-specific IFN$\gamma$ production upon gluten challenge and small intestine pathology [150]. Newer versions of nanoparticles contain other bioactive molecules to further enhance

tolerogenic antigen presentation. Liposomes have been developed that contain calcitriol, that produce tolDCs in the draining lymph nodes. These have been encapsulated with collagen II peptides in phase I clinical trials to treat RA, and have demonstrated a PD-L1-dependent expansion of pTregs [151]. PLA-PEG nanoparticles have been developed to encapsulate rapamycin, which also induce tolDCs. These nanoparticles co-administered with a tolerogen are being explored to induce tolerance for avoidance of an antibody response to adeno-associated viruses, and are currently in phase II clinical trials with coadministration of a PEGylated uricase to avoid anti-uricase antibodies in gout treatment [152].

Other groups have developed nanoparticles that are not formulated with autoantigen, but act to broadly expand Tregs with the aim of a portion of these being antigen specific or act by bystander suppression. One strategy involves nanoparticles carrying alpha-galactosylceramide, which is taken up by APCs and presented on CD1d to invariant Natural Killer T cells (iNKT) to activate them. This iNKT activation promotes expansion of tTregs and responders (patients that saw increase in Tregs) saw reduction in graft versus host disease (GvHD) [153]. Another strategy, that is still in preclinical development, utilizes nanoparticles encapsulating a molecule that activates aryl hydrocarbon receptor in APCs to promote Treg-mediated suppression [154, 155].

Aside from targeting classical APCs such as DCs and macrophages, there have been efforts to target nonclassical APCs in the liver, to exploit its natural tolerogenic environment. One strategy to target the liver employed polymers of glycans conjugated to autoantigens. This capitalized on the natural scavenger function of the liver, with many cells containing lectins that recognize glycans and are able to present antigen in the anti-inflammatory liver milieu. These conjugates are in phase I clinical trials for Celiac disease [156]. In a separate liver-targeting approach, nanoparticles coated with autoantigen were targeted nonspecifically to liver sinusoidal endothelial cells by virtue of their size, are in clinical trials to treat pemphigus vulgaris [157].

### *1.3.4 Ex Vivo-Modified T Cell Therapy*

Although seemingly contradictory, a strategy for treatment of MS was to deliver patient-expanded antigen-specific T cells [158]. Before reintroduced into the patient, these T cells were irradiated, such that they could not exacerbate autoimmunity. This approach was tested in phase IIb clinical trials but did not meet endpoints potentially because of trial design, and has subsequently not been followed.

Another cell-based strategy is Treg therapy, which has ongoing clinical trials in T1D, SLE, pemphigus vulgaris, Crohn's disease, autoimmune hepatitis, and transplantation [159, 160]. Most trials involve sorting CD4+CD25+CD127low cells, which are primarily Tregs, and expanding them using high dose IL-2, CD3/CD28 ligation, and often rapamycin. Notably, these are a polyclonal repertoire likely containing a very small number of antigen-specific cells, suggesting the mechanism is likely a mix of antigen-specific and non-specific suppression. These trials are in their early stages but have demonstrated safety, efficacy, and stability and long-term persistence of the Tregs.

Induced Tregs (iTreg), or Tregs generated *in vitro*, hold promise in preventing unwanted immune responses. However, the method of induction determines their stability. Although Tregs induced by TGF-$\beta$ demonstrate high levels of FoxP3, they have incomplete demethylation, and can acquire effector functions upon TCR stimulation without TGF-$\beta$ [161]. However, addition of IL-2 and blockade of CD28 ligation produces the appropriate hypomethylation, which is stable *in vivo* [161]. These have not yet been attempted as a strategy in the clinic, but offer a promising avenue due to the ability to generate large number of cells, compared to the relatively small frequency of tTregs *in vivo*.

Given the limitation of the polyclonality of isolating total Tregs, a new strategy has emerged to develop Tregs with chimeric antigen receptors (CAR-Treg) recognizing transplant or autoantigens. In these strategies, polyclonal Tregs are sorted and expanded using IL-2, anti-CD3/CD28, and rapamycin, and transduced with CARs. Upon CAR recognition of antigen, they secrete anti-inflammatory molecules. For treatment of transplantation, human

polyclonal Tregs were transduced with a CAR specific for a human MHC-I molecule, which showed promise in human skin xenograft mouse model [162]. This approach has also been attempted in preclinical models of GvHD, colitis, and EAE [163]. Long term stability of the Treg phenotype and suppressive capacity needs to be demonstrated before progressing into human trials.

### *1.3.5 In Vivo T Cell Targeting*

Strategies have also been developed to target antigen-specific T cells *in vivo* to trigger their deletion, induction of anergy, or conversion to pTregs. The first strategy to do so was to use covalently linked peptide-MHC complexes. A peptide from human cartilage glycoprotein 39 was covalently linked to a human MHC-II molecule and delivered i.v. to patients with RA. Patients demonstrated a modest reduction in clinical score with the therapy, particularly in the short term. A limitation to this technology is the low affinity of pMHC-TCR interaction, and subsequent short-lived efficacy of a single treatment. To overcome this limitation, nanoparticles have been developed that contain many peptide-MHC on the surface, and are able to have stable interactions with T cells [164, 165]. In preclinical trials, they have demonstrated remarkable efficacy in preclinical models of T1D and EAE, and in PBMC responses of humanized mice. Mechanistically, this is due to induction and proliferation of autoregulatory CD8 T cells, Tr1 cells, and Bregs, and lower production of inflammatory cytokines in antigen-specific T cells.

# CHAPTER 2

# PERSISTENT ANTIGEN EXPOSURE VIA THE ERYPTOPTIC PATHWAY LEADS TO TERMINAL T CELL DYSFUNCTION

## 2.1 Abstract

Although most current treatments of autoimmunity involve broad immunosuppression, recent efforts have attempted to regulate T cells in an antigen-specific manner. One such effort is through targeting antigen to the apoptotic pathway. Erythrocytes are an attractive candidate to target because of their high rate of eryptosis. Here we develop an approach that binds antigens to erythrocytes and achieves profound T cell dysfunction. Transcriptomic and phenotypic analyses revealed signatures of self-tolerance and dysfunction, including upregulation of PD-1, CTLA4, LAG-3, 4-1BB and TOX, and downregulation of effector molecules. T cells were incapable of responding to an adjuvanted antigenic challenge even months after antigen clearance. This strategy was able to induce tolerance in a polyclonal endogenous repertoire and was antigen-specific, as mice were fully capable of responding to an irrelevant antigen. Furthermore, with this strategy we reversed pathology in an adoptive transfer model of murine experimental autoimmune encephalomyelitis. CD8 and CD4 T cell education occurred in the spleen, and for CD8 T cells was dependent on cross-presenting Batf3+ dendritic cells. Macrophages were also important for CD8 T cell dysfunction, but dispensable for CD4 T cell dysfunction. Despite upregulation of perforin by CD8 T cells, CD8-derived perforin was not necessary for tolerance. Thus, we demonstrate that antigens associated with eryptotic erythrocytes induce lasting T cell dysfunction that could be protective in downregulating pathogenic T cells.

## 2.2 Introduction

Clearance of apoptotic cells plays an essential role in the resolution of inflammation, by limiting necrosis and consequent release of danger-associated molecular patterns, as well as by acting directly on phagocytes to promote the release of anti-inflammatory mediators [166]. The importance of apoptotic cell clearance is clearly demonstrated in an inflammatory response. During a typical inflammatory response, there is a high degree of granulocytic infiltration, in particular by neutrophils. During the resolution phase, these neutrophils and other infiltrating peripheral blood mononuclear cells (PBMC) are no longer required, and undergo apoptosis. Macrophage clearance of these apoptotic neutrophils is necessary for the resolution of inflammation [167, 168]. In the lungs, the absence of macrophage clearance of apoptotic neutrophils leads to a chronic inflammatory response, which has been associated with chronic obstructive pulmonary disorder and pulmonary fibrosis [169, 170].

The role of apoptotic cell clearance is also evident in the steady state. It is estimated that billions of cells undergo apoptosis daily in the human, yet there are few detectable non-engulfed apoptotic cells, suggesting rapid clearance from the body [171]. Mice deficient in receptors that recognize apoptotic cells, such as MERTK, SCARF-1, AXL, and TYRO3, develop systemic autoimmunity characterized by widespread inflammation and development of antinuclear antibodies [171–173]. This is also evident in humans, where it has been shown that in systemic lupus erythematosus (SLE), an autoimmune disorder characterized by the development of anti-nuclear antibodies, there is a high level of circulating apoptotic peripheral blood mononuclear cells, suggesting a defect in clearance of apoptotic debris [174]. GWAS studies have demonstrated a link between polymorphisms in MERTK and multiple sclerosis, and mice deficient in AXL experience worse pathology in experimental autoimmune encephalomyelitis (EAE) than wild type controls [175, 176].

Mechanistically, apoptotic cells seem to act on phagocytes via phosphatidylserine and other conserved motifs to induce a pro-tolerogenic phenotype in these APCs. The earliest mechanistic experiments demonstrated that macrophages treated with apoptotic neutrophils

decrease secretion of proinflammatory cytokines such as IL-1$\beta$, TNF$\alpha$, and GM-CSF [177]. Not only does apoptotic cell engagement suppress APC activation, but it also triggers the release of TGF-$\beta$1 from macrophages, which is dependent on phosphatidylserine ligation [178]. A potential mediator of this phenomenon was proposed when it was discovered that stimulation of dendritic cells with Gas6, a molecule that serves as a bridge between phosphatidylserine and the receptor MERTK on many APCs, can reverse TLR9-induced activation [179].

The anti-inflammatory properties of targeting the apoptotic pathway can be recapitulated by intravenous injection of apoptotic cells. Antigen coupled to these apoptotic cells have led to antigen-specific tolerance in a number of mouse models, including contact hypersensitivity, EAE, and islet transplantation [180–182]. Cells accumulated in the splenic marginal zone, and triggered IL-10 production and regulatory T cell induction [183]. Additionally, apoptotic cells also triggered secretion of indoleamine 2,3-dioxygenase (IDO) in the spleen, and chronic exposure of IDO-deficient mice to apoptotic cells leads to lupus-like pathology [184]. This strategy of antigen-coupled cells moved forward to phase I clinical trials for multiple sclerosis, demonstrating safety and a reduction in antigen-specific T cells [143].

The previous source of apoptotic cells was exogenous, which requires *ex vivo* manipulation of cells. In an attempt to avoid the need for *ex vivo* manipulation, our lab developed a method of targeting a large population of apoptotic cells *in vivo* [147]. Erythrocytes undergo apoptosis, or erytptosis, at a rate of nearly 1% per day in humans and are immediately cleared from circulation. Kontos et al. developed a method of targeting erythrocytes in vivo by a peptide that binds glycophorin A. Antigen conjugated to this peptide and injected intravenously led to rapid proliferation and antigen-specific CD8 T deletion. Furthermore, recombinant expression of a single chain antibody fragment that recognized erythrocytes with a peptide specific to pancreas islets led to prevention of disease in a TCR transgenic model of diabetes. Further studies demonstrated that this strategy could lead to prevention of a humoral response to *E. coli* asparaginase, a typically immunogenic therapeutic protein

used to treat cancer, and that mechanistically this pathway was synergistically dependent on PD-1 and CTLA-4 ligation during priming [146, 185]. The purpose of this study was to conduct an in-depth analysis of the molecular characteristics of both CD4 and CD8 T cells upon encounter of self-associated antigen bound to erythrocytes, induce tolerance in an endogenous repertoire of T cells, and to understand the mechanisms involved in uptake and presentation of erythrocyte-associated antigen.

Using phage display of a human antibody fragment (Fab) library, we discovered a novel Fab, A8B1, that binds to mouse erythrocytes with high affinity and specificity, and we fused recombinant antigen to this Fab to develop a tolerogen. We conducted RNA-seq on antigen-specific CD8 and CD4 T cells that had recently experienced erythrocyte-associated antigen, and we found that a single exposure to antigen led to transcriptional signatures of anergy and early exhaustion, but not of effector functions. We conducted an in-depth phenotypic and functional analysis of the antigen-specific T cells, which in both the CD8 and CD4 compartments revealed signatures of terminal exhaustion, even after challenge with adjuvanted antigen. T cells remained in circulation and dysfunctional for months after initial antigen priming, despite only short-term initial exposure to erythrocyte-associated antigen. We demonstrated that this was true not only for TCR-transgenic T cells, but also for an endogenous repertoire, and that this dysfunction was antigen-specific. Furthermore, endogenous myelin oligodendrocyte glycoprotein (MOG)-activated T cells were rendered incapable of driving pathology in experimental autoimmune encephalomyelitis (EAE) after treatment with A8B1-MOG. Finally, we found that antigen presentation occurred in the spleen, and, in the MHC-I:CD8 T cell context, Batf3-dependent cross-presenting dendritic cells were necessary to render cells dysfunctional. This study has implications not only for the field of developing therapeutics for antigen-specific tolerance, but also reveals insights into the fate of T cells experiencing antigen derived from apoptotic cells in the periphery.

## 2.3 Results

### *2.3.1 Development of an Anti-Erythrocyte Antibody Fragment*

Previous studies in our laboratory identified a peptide that binds erythrocytes, or utilized a single chain variable fragment (scFv) Ter119 that binds erythrocytes. However, a single copy of the peptide has low affinity, requiring chemical conjugation of multiple copies to an antigen, thereby limiting its versatility compared to recombinant expression. Ter119 has poor biophysical characteristics and was prone to aggregation. To overcome these limitations, and to improve the translational potential, we sought to find a new binder to mouse erythrocytes. We utilized a M13 phage display antibody fragment library based on the 4D5 trastuzumab human antibody [186]. This library has no diversity in the complementarity determining regions (CDR) light chain (L) 1 and L2, minimal diversity in L3, heavy chain (H)1, and H2, and a high degree of diversity in H3. The observed diversity of the library is 3 X $10^{10}$.

We conducted phage display whole mouse erythrocytes, while negatively selecting on mouse peripheral blood mononuclear cells (PBMCs) to ensure binding specificity to erythrocytes (Figure 2.1a). After each round of display, the phage library was tested by flow cytometry for binding to erythrocytes, demonstrating enrichment of the library for binding (Figure 2.1b). After four rounds of selection, single colonies were grown up, and 96 individual phage clones were tested for binding to erythrocytes via flow cytometry, demonstrating strongly, weakly, and non-binding clones (Figure 2.1c).

The clones that bound most strongly to erythrocytes were sequenced, and three of the most frequent sequences were cloned into protein expression vectors, expressed in HEK293T cells, and purified with a Protein A column by fast protein liquid chromatography (Figure 2.2a). To choose between the three, we conducted half-life, humoral immunogenicity, and pull-down assays. To assess half-life, 10 $\mu$g of Fabs were injected once intravenously (i.v.), and mice were bled at various time points. Erythrocytes were stained with a fluorescently conjugated anti-Fab secondary antibody and fluorescence was measured by flow cytometry,

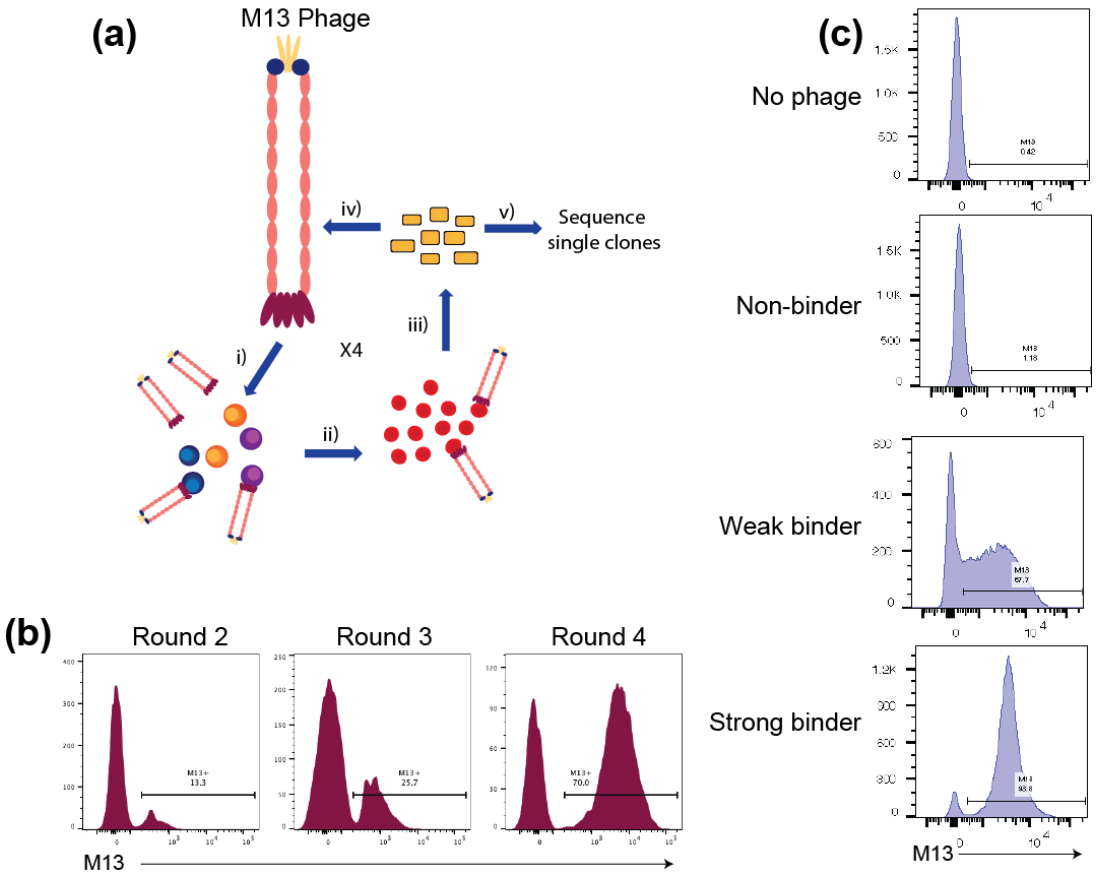


Figure 2.1: Phage display on mouse erythrocytes with human Fab phage library. a) Strategy for phage display. i) M13 phage library was incubated with mouse PBMCs, and bound phage was discarded. ii) Unbound phage was incubated with mouse erythrocytes. Phage that did not bind erythrocytes was washed off, and iii) bound phage was eluted off of erythrocytes and propagated overnight in *E. coli* with helper phage. After overnight incubation, phage was precipitated from *E. coli* supernatant. This panning was repeated 4 times, and single colonies were sent for sequencing after the fourth round of display. b) Binding by flow cytometry of bulk library to mouse erythrocytes after each day of display. c) After the fourth round of display, 96 single clones were tested for binding to erythrocytes via flow cytometry. Representative non-binding, weakly binding, or strongly binding phage clones to mouse erythrocytes.

indicating that A8B1 had the longest half-life of 72 hours (Figure 2.2b). To assess immunogenicity, 10 $\mu$g of Fabs were injected i.v. every week and mice were bled three days after injection to measure anti-Fab IgG antibody titers (Figure 2.2c). As the Fab is a human protein, repeated injection should lead to development of antibodies against the foreign protein. E2A3 demonstrated development of high titers of antibodies in 4/5 mice tested, whereas only

one mouse that received A8B1 or F3F1 developed a titer. In A8B1, there was no detectable titer in the last two weeks tested. To determine what the Fabs bound to, Fabs were incubated with mouse erythrocyte ghost, solubilized with detergent, and complexes were pulled down with magnetic protein A beads (Figure 2.2d). Although there was no single band pulled down, likely because of strong interactions between the proteins, the bands pulled down corresponded to those on the Band3 complex of proteins, which includes Band3, glycophorins A and B, Protein 4.2, CD47, ankyrin, and spectrin. Given these data, the clone A8B1 was chosen for future studies.

To determine the affinity of A8B1 for mouse erythrocytes, a binding assay was conducted on PBMC-depleted mouse blood (Figure 2.3a). Erythrocytes were incubated with fluorescently labeled A8B1 at various concentrations, Fab was washed off, and mean fluorescence intensity (MFI) determined by flow cytometry. The calculated affinity of the interaction was 320 pM. To determine the specificity of the Fabs, fluorescent A8B1 was incubated with mouse erythrocytes (CD45-) or PBMCs (CD45+) in the blood, and binding was assessed by flow cytometry. A8B1 demonstrated strong binding to CD45- cells, and lacked binding to CD45+ cells (Figure 2.3b). To determine if binding would affect hematological parameters, 1 $\mu$g was injected three times, and various hematological parameters were assessed. There was no measurable effect on red blood cell count, hemoglobin, hematocrit, mean cell volume, mean cell hemoglobin, or platelet count (Figure 2.3c).

### *2.3.2 Erythrocyte-Targeted Antigen Reveals Transcriptional Signatures of Anergy in Antigen-Specific T cells*

The immunogenicity data in Figure 2.2c suggested that conjugating antigen to A8B1 would lead to tolerance. To test its effect on T cells, A8B1 was recombinantly expressed as a fusion with the model antigen ovalbumin (OVA) on the C-terminus of the heavy chain to yield A8B1-OVA. TCR transgenic OT-I and OT-II cells, which recognize the immunodominant CD8 and CD4 epitopes of OVA in C57BL/6 mice, respectively, were labeled with carboxyflu-

(a)

| Name | CDRL1 | CDRH1 | CDRH2 | CDRH3 |
|---|---|---|---|---|
| A8B1 | MGQGLI | VYSSSI | SISSYSSYTS | YSIYWWWYGEGL |
| E2A3 | YSYSASLV | LSSYSI | SYSSSGYTS | GSFGWFYGYYIMGL |
| F3F1 | SSSSLI | ISSYSI | SIYSYSGSTS | YGLYWWWYQAGL |

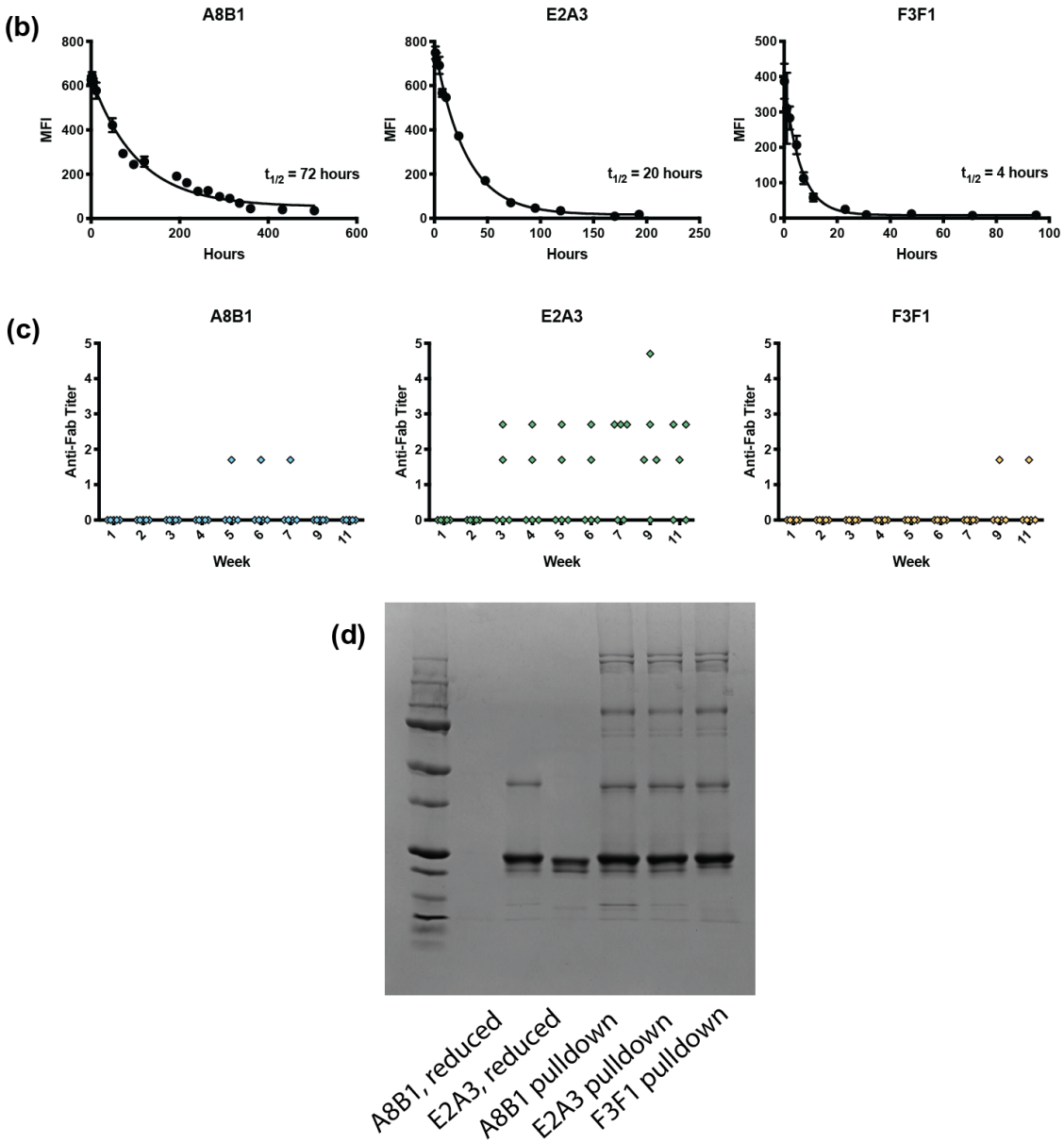


Figure 2.2: Characterization of Fab hits from phage display. a) Complementarity determining regions of three clones selected from phage sequences based on convergence. b) *In vivo* half-life of selected Fabs, as measured by mean fluorescence intensity binding to erythrocytes at different time points. c) 10 $\mu$g Fabs were injected weekly, and mice were bled weekly for development of anti-Fab IgG antibody titer. d) SDS-PAGE gel of a pulldown of Fabs on erythrocyte membranes.

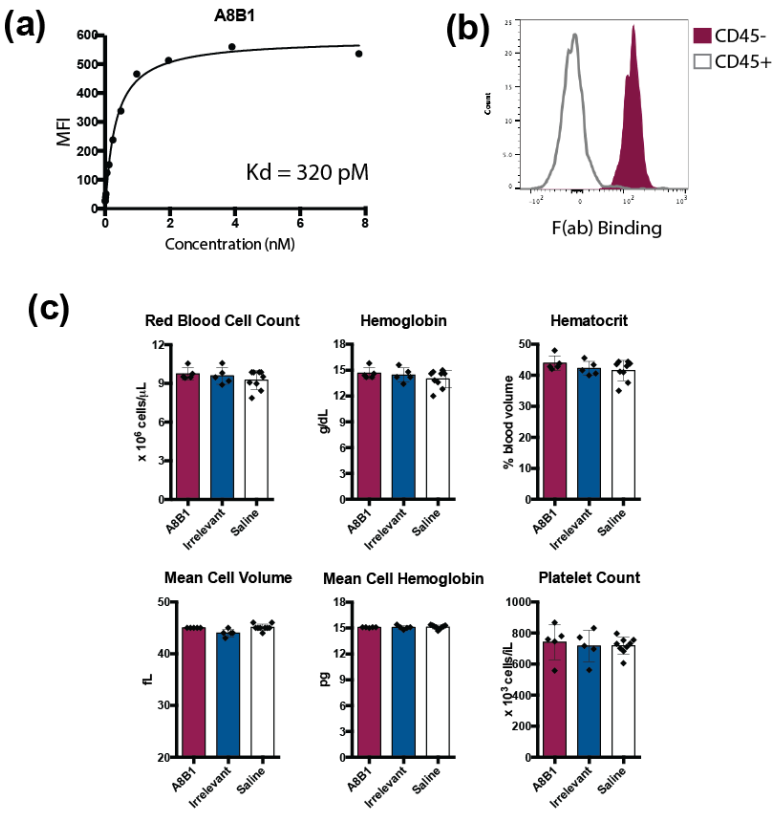


Figure 2.3: Properties of selected Fab A8B1. a) A8B1 was fluorescently labeled and added in increasing concentrations to mouse erythrocytes *in vitro*. Mean fluorescence intensity of Fab was measured by flow cytometry, and affinity was determined using a one-site specific binding nonlinear curve fit. b) Binding of A8B1 to CD45+ or CD45- (erythrocytes) cells in mouse blood. c) 1 $\mu$g A8B1, irrelevant Fab, or saline were injected i.v. every third day for a total of three injections. 24 hr after the final injection, mice were bled and red blood cell count, hemoglobin, hematocrit, mean cell volume, mean cell hemoglobin, and platelet count of whole blood was measured.

orescein succinimidyl ester (CFSE) to track rounds of proliferation, and were adoptively transferred into wild type C57BL/6 mice. 1 $\mu$g A8B1-OVA, an equimolar dose of OVA ($OVA^{low}$), or tenfold higher dose of OVA ($OVA^{high}$) was injected intravenously, and mice were sacrificed 4 d later. A8B1-OVA demonstrated almost complete CFSE dilution in OT-I cells (Figure 2.4a). Almost no proliferation could be seen in the equimolar $OVA^{low}$ dose, and the ten-fold higher $OVA^{high}$ dose had almost equivalent levels of proliferation to that of A8B1-OVA, suggesting that the erythrocyte-associated pathway of antigen presentation on both class I (MHC-I) and class II (MHC-II) major histocompatibility complex was more

efficient than soluble antigen alone.

To determine the transcriptional signature of targeting this self-associated pathway, OT-I and OT-II cells were adoptively transferred into naïve mice, and 24 hr later mice received either A8B1-OVA, $OVA^{low}$, $OVA^{high}$, or saline (Figure 2.4b). Four days later mice were sacrificed, and OT-I and OT-II cells were sorted and processed for RNA-seq; we utilized this time point to capture the initial T cell program, and analyze cells while still in the expansion phase prior to their undergoing contraction by deletion. Unsupervised clustering demonstrated that $OVA^{low}$ clustered with naïve samples, and upon comparison of naïve to $OVA^{low}$ in both the OT-I and OT-II cell compartments, there were no significantly upregulated genes (Figure 2.4c-d). This, coupled with the lack of proliferation noted in Figure 2.4a, indicated a lack of antigen experience. Thus, for all statistical evaluations, groups were compared to $OVA^{high}$ to account for similar levels of antigen experience.

OT-I and OT-II upregulated genes associated with anergy and exhaustion, while downregulating genes involved in effector functions (Figure 2.5a). Gene signatures revealed a variety of similarly regulated pathways in OT-I and OT-II, with 159 of the same differentially expressed genes in A8B1-OVA compared to the $OVA^{high}$ dose (Figure 2.5b). Both OT-I and OT-II showed upregulation of *Egr2* and *Egr3*, transcription factors that are necessary for induction of anergy, inhibit T-bet-mediated cytokine production in effector T cells, and are expressed in dysfunctional tumor-infiltrating T cells, compared to free OVA [187–191]. OT-I and OT-II cells also upregulated *Rgs16*, which is highly upregulated in T cells that have been pre-determined upon initial antigen encounter to re-establish tolerance, even after antigenic challenge in a lymphopenic host [29]. Both OT-I and OT-II cells upregulated many molecules and receptors frequently involved in T cell exhaustion. OT-I cells significantly upregulated *Pdcd1* (PD-1), *Lag3*, *Cd200*, and *Tox*, while OT-II cells upregulated *Pdcd1*, *Cd160*, *Ikzf2*(Helios), and *Cd200* (Figure 2.5c) [192–194]. OT-I and OT-II cells upregulated *Tnfrsf9* (4-1BB), a target of *Egr2*, which although classically thought of as a costimulatory molecule, has been shown to be upregulated in dysfunctional cells [195]. OT-I

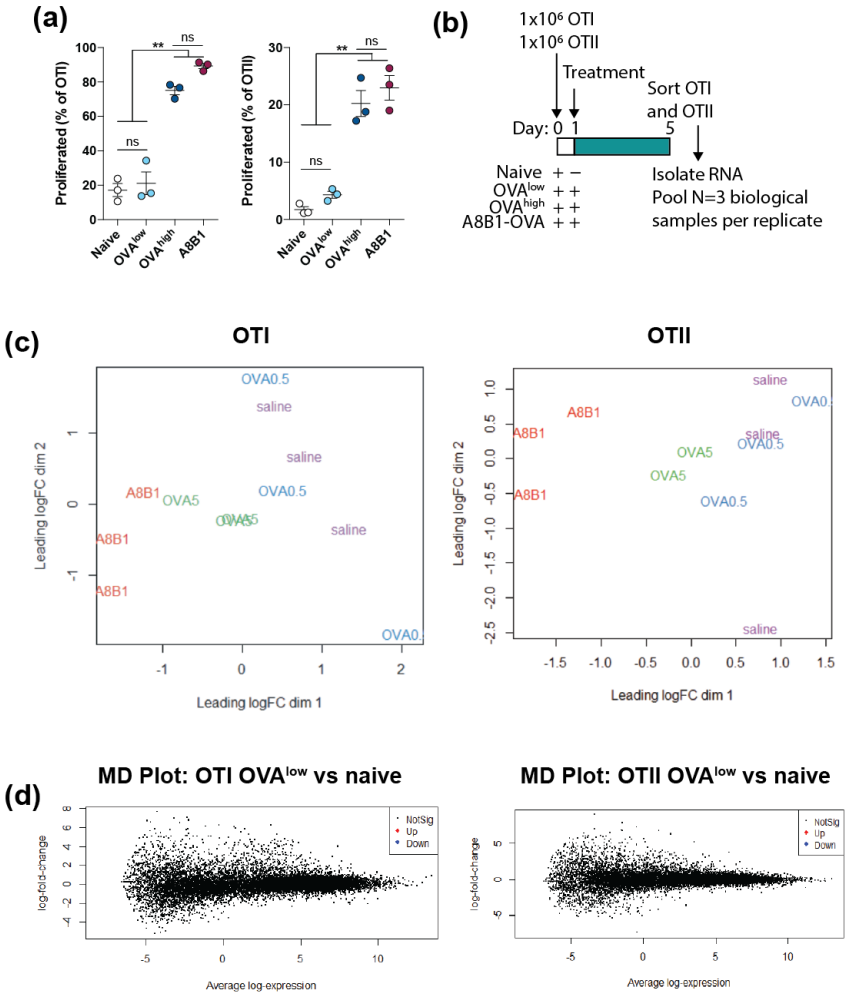


Figure 2.4: Targeting antigen to erythrocytes leads to robust antigen-specific T cell proliferation. a) Naïve mice were adoptively transferred with 500,000 OT-I and OT-II. 24 hr later, 1 g A8B1-OVA, an equimolar dose of OVA ($OVA^{low}$), 10-fold greater dose of OVA ($OVA^{high}$), or saline were administered i.v. Four days later, mice were sacrificed and OT-I and OT-II and assessed for proliferation. b) Strategy for RNA-seq. Mice were adoptively transferred with OT-I and OT-II and treated as in a). Four days later, mice were sacrificed and OT-I and OT-II sorted and cells processed for RNA-seq. For all groups n= 3, except for OT-II $OVA^{high}$, n=2. Each replicate is pooled from 3 mice. c) Multidimensional scaling plot of naïve and $OVA^{low}$. d) Mean difference plots of $OVA^{low}$ vs naïve in OT-I and OT-II.

cells downregulated effector molecules such as *Gzmb* and *Gzmm*, as well as *Klrg1*, *Prdm1* (Blimp-1), integrins *Itgax* and *Itga4*, and chemokine receptors *Ccr2* and *Ccr5*, indicating that cell-associated antigen led to reduced effector functions than free antigen alone (Figure 2.5c). Interestingly, both OT-I and OT-II cells upregulated *Xcl1*, suggesting a means for

recruiting XCR1+ cross-presenting DCs to enhance priming [196]. Together this suggests induction of a program of self-tolerance and movement away from effector functions with a single dose of erythrocyte-targeted antigen.

To probe similarity to T cell signatures in similar contexts of antigen experience, upregulated and downregulated genes were compared to genes in published gene sets using gene set enrichment analysis (GSEA) (Figure 2.6). For these analyses, there was no consistent control similar to free antigen; thus, DEGs of A8B1 vs. Naïve and OVA vs. Naïve were utilized. A self-tolerant set was derived from a study conducted in a TCR transgenic mouse whose CD8 T cells were specific for an autoantigen, escaped negative selection, and were tolerized in the periphery [29]. To establish a comparison of T cells activated in a similar time frame, genes were compared CD8 or CD4 T cells from day 6 of LCMV infection [197, 198]. To compare to chronic exhaustion in a self context, we compared to tumor-infiltrating CD8 T cells [199]. To determine if there are similar signatures seen in pathogens that target erythrocytes, transgenic CD4 T cells from a blood-stage malaria infection were compared [200]. Finally, we compared this signature to that of CD8 T cells undergoing deletional tolerance [201]. Of the data sets tested, both OT-I and OT-II cells were most similar to self-tolerant T cells. The OT-I compartment also matched closely to tumor-infiltrating CD8 T cells in a human melanoma, suggesting a similar state of T cell exhaustion as commonly attributed to melanoma [202]. Interestingly, OT-II cells also matched closely to a gene set derived from effector CD4 TCR transgenic T cells recognizing a parasitic antigen in a mouse model of blood-stage malaria infection [200].

### *2.3.3 Brief Exposure to Antigen Begins to Drive Dysfunctional T Cell Phenotype*

Because the transcriptional signature suggested an inhibitory state of the antigen-specific T cells, we sought to confirm this phenotype and probe other molecules involved in these pathways. Mice were adoptively transferred with OT-I and OT-II cells and received one dose

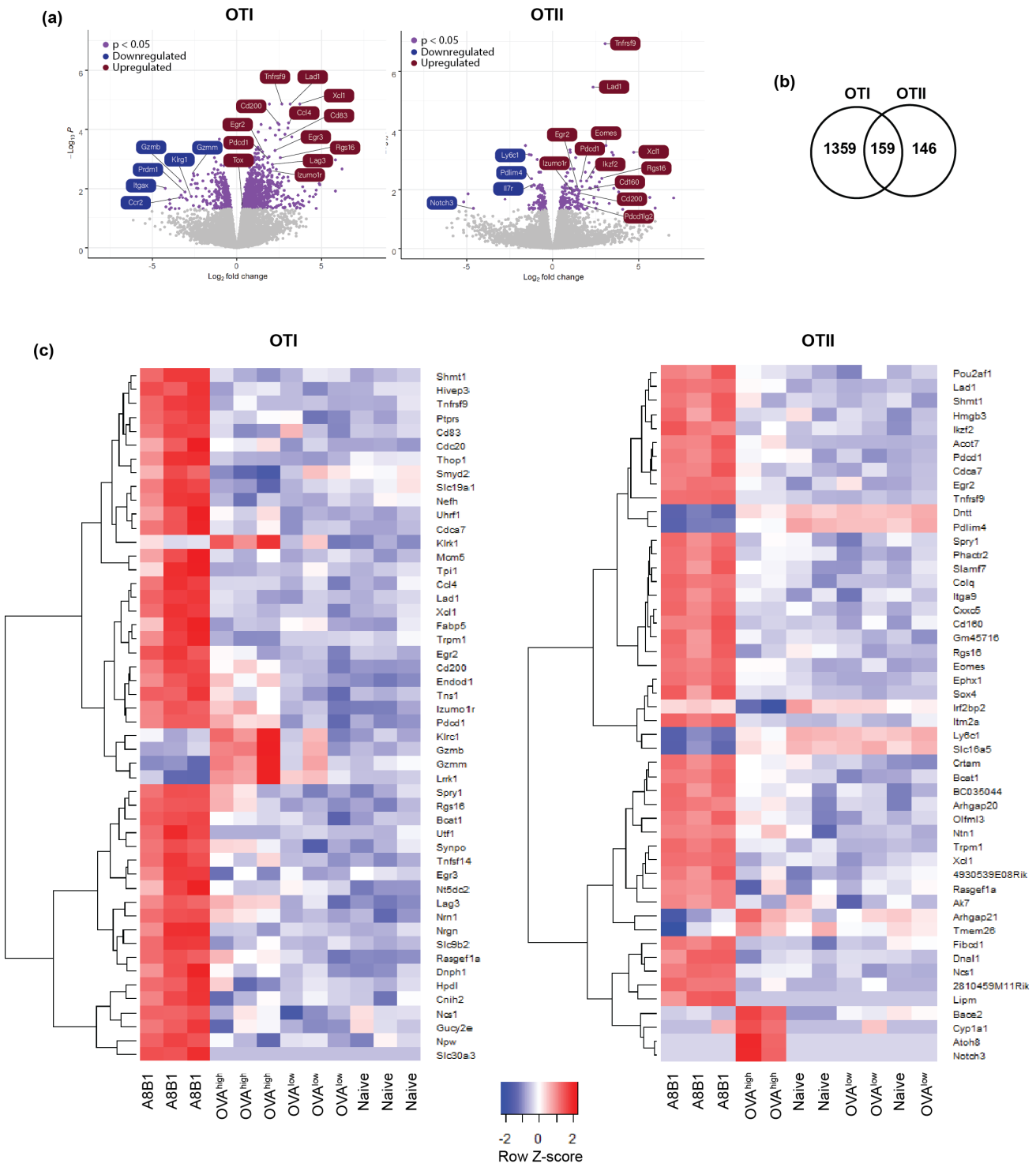


Figure 2.5: Initial T cell exposure to erythrocyte-associated antigen drives molecular signatures of anergy and early exhaustion. a) Volcano plots of A8B1-OVA vs OVA$^{high}$ in OT-I and OT-II. In purple, genes $p < 0.05$. b) The number of differentially expressed genes of A8B1-OVA compared to OVA$^{high}$ in OT-I and OT-II. c) Heat map of unbiased clustering of top 50 differentially expressed genes (DEG).

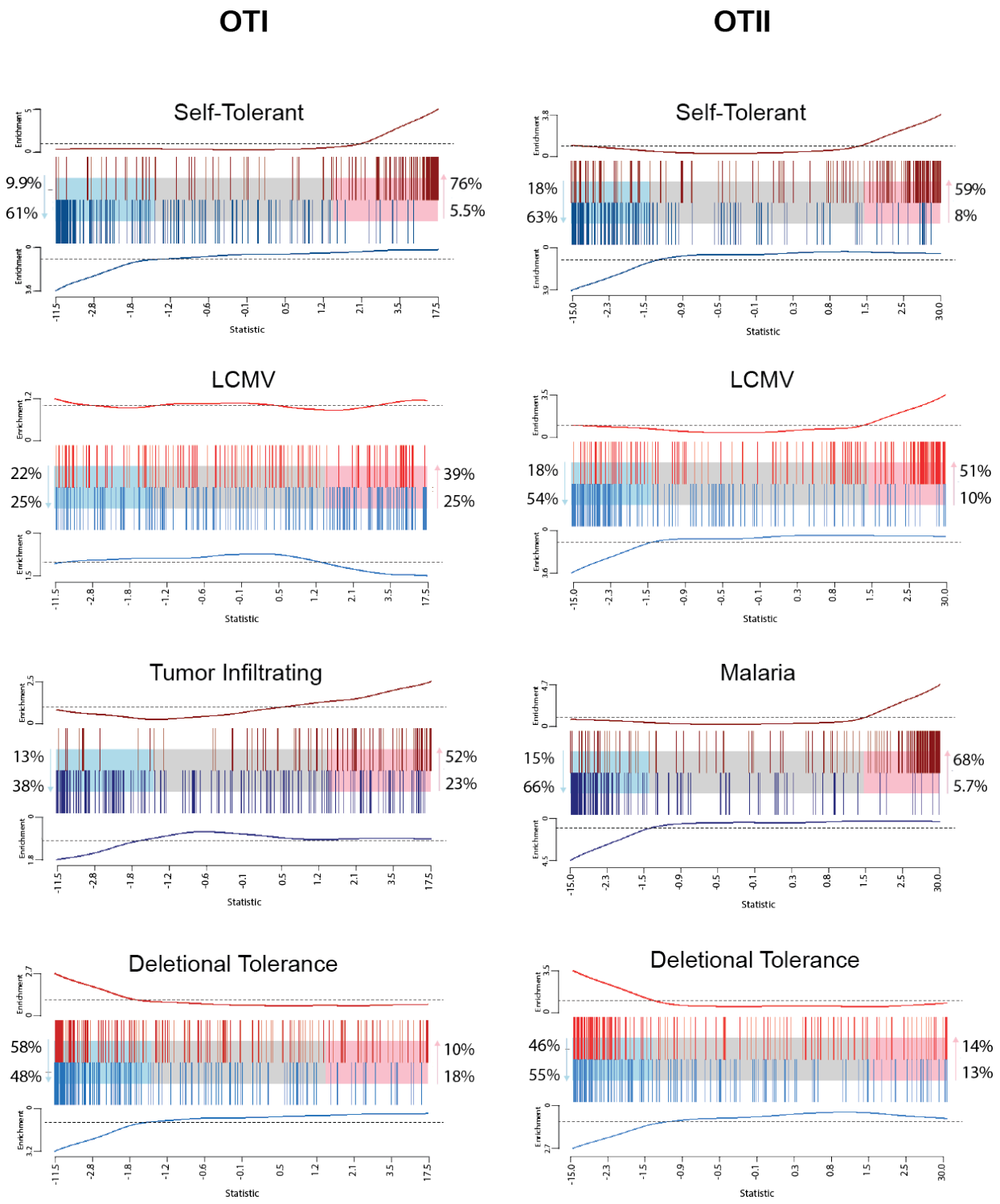


Figure 2.6: Gene set enrichment analysis demonstrates similarities to self-tolerant T cells. Bar code plots of top differentially expressed genes in A8B1 vs Naïve compared to top differentially expressed genes from published gene sets.

of A8B1-OVA, OVA, or saline. Four days later, splenocytes were analyzed by flow cytometry (Figure 2.7a). Confirming the RNA-seq data, both OT-I and OT-II highly upregulated Egr2 compared to free OVA, suggesting early induction to a program of anergy (Figure 2.7b). Also consistent with the transcriptomic data, OT-I and OT-II upregulated inhibitory receptors, such as PD-1, CTLA-4, and LAG-3, to a higher level than free antigen (Figure 2.7c). Likewise, there was a strong induction of TOX on OT-I, a transcription factor thought to drive T cell exhaustion in the context of chronic antigen stimulation, which was to a high degree co-expressed with PD-1 (Figure 2.7d) [64]. Additionally, there was a higher proportion of TCF-1+ PD-1+ Eomes$^{lo}$ cells, considered a population that is fated to become terminally exhausted (Figure 2.7e) [70]. Although these data suggest that the cells may be going down a pathway fated for exhaustion, 4 d after initial dose could also reflect robust activation. Thus, studies were conducted at later time points.

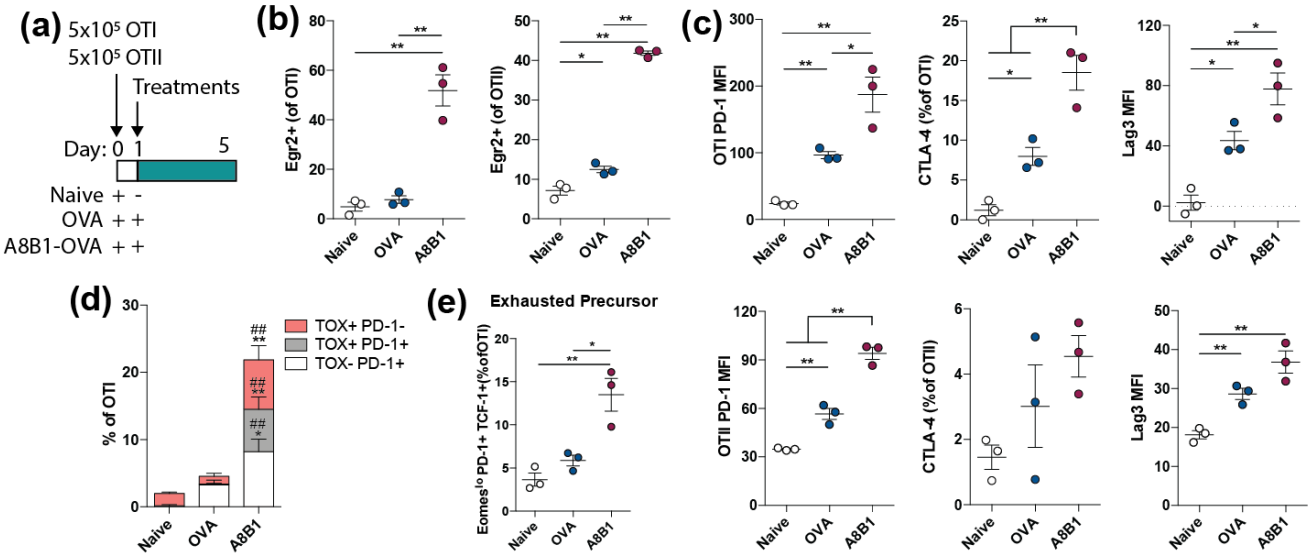


Figure 2.7: Exposure to erythrocyte-associated antigen leads to early phenotypic indication of anergy and exhaustion. a) 500,000 OT-I and OT-II were adoptively transferred into C57BL/6 mice. Mice received an intravenous injection of 1 $\mu$g of A8B1-OVA or 10-fold higher molar equivalent OVA, and sacrificed 4 d later. b) Percentages of Egr2+ OT-I and OT-II in the spleen. c) Expression of PD-1, CTLA-4, and LAG-3 on OT-I and OT-II. d) Percentage of TOX+ PD-1+ cells of OT-I. * vs Naïve, vs OVA. e) Percentage of exhausted precursor (Eomes$^{lo}$PD-1+TCF-1+) cells of OT-I. Statistical analyses were performed using one-way ANOVA with Tukey's test. *P $<$ 0.05 and **P $<$ 0.01.

In order to control for molecular size of A8B1-OVA compared to free OVA alone, an irrelevant Fab control was synthesized to contain an identical backbone to A8B1, but with complementarity determining regions that bind to the xenoantigen outer surface protein A from *Borrelia burgdorferi*, thus lack binding to erythrocytes (Figure 2.8a) [203]. It was recombinantly expressed with OVA on the C-terminus of the heavy chain, yielding Irrelevant-OVA. Because erythrocyte-bound OVA is more efficient at antigen presentation than free OVA, we chose to inject three times to ensure that all T cells receiving Irrelevant-OVA would have experienced antigen, as measured by CD44 induction (Figure 2.8b).

The inhibitory molecules upregulated could be a result of recent antigen experience as opposed to a lasting dysfunctional program. To test this, OT-I and OT-II cells were adoptively transferred, and mice received 3, 1 $\mu$g doses of A8B1-OVA or Irrelevant-OVA (Figure 2.8c). Mice were sacrificed 15 d after the first exposure to Fab-OVA, as opposed to 4 d, and lymph nodes (LN) and spleen were analyzed for cell function. In the LN, there appeared to be fewer OT-I and OT-II in mice receiving A8B1-OVA than control, whereas in the spleen there appeared equal numbers of cells (Figure 2.8d). In the OT-I compartment, both cells in the LN and spleen drastically downregulated T cell receptor compared to control, suggesting overstimulation and a mechanism of self-inhibition (Figure 2.8e) [204]. Consistent with this inhibition, CD8 T cells in the LN and spleen, and CD4 T cells in the spleen, highly upregulated the inhibitory molecule PD-1 as well as TOX (Figure 2.8f-g). Interestingly, CD8 T cells downregulated CXCR3, which could restrict homing to sites of infection or inflammation (Figure 2.8h) [205]. To assess functional capacity, splenocytes were restimulated *ex vivo* with $OVA_{257\text{-}264}$ (SIINFEKL) or $OVA_{323\text{-}339}$ (ISQAVHAAHAEINEAGR, abbreviated as ISQ) for OT-I and OT-II cells, respectively. OT-I and OT-II cells both greatly reduced their capacity to produce TNF$\alpha$, but OT-I maintained some ability to produce IFN$\gamma$, which has been described for both T cell exhaustion and anergy (Figure 2.8i-j) [64, 206].

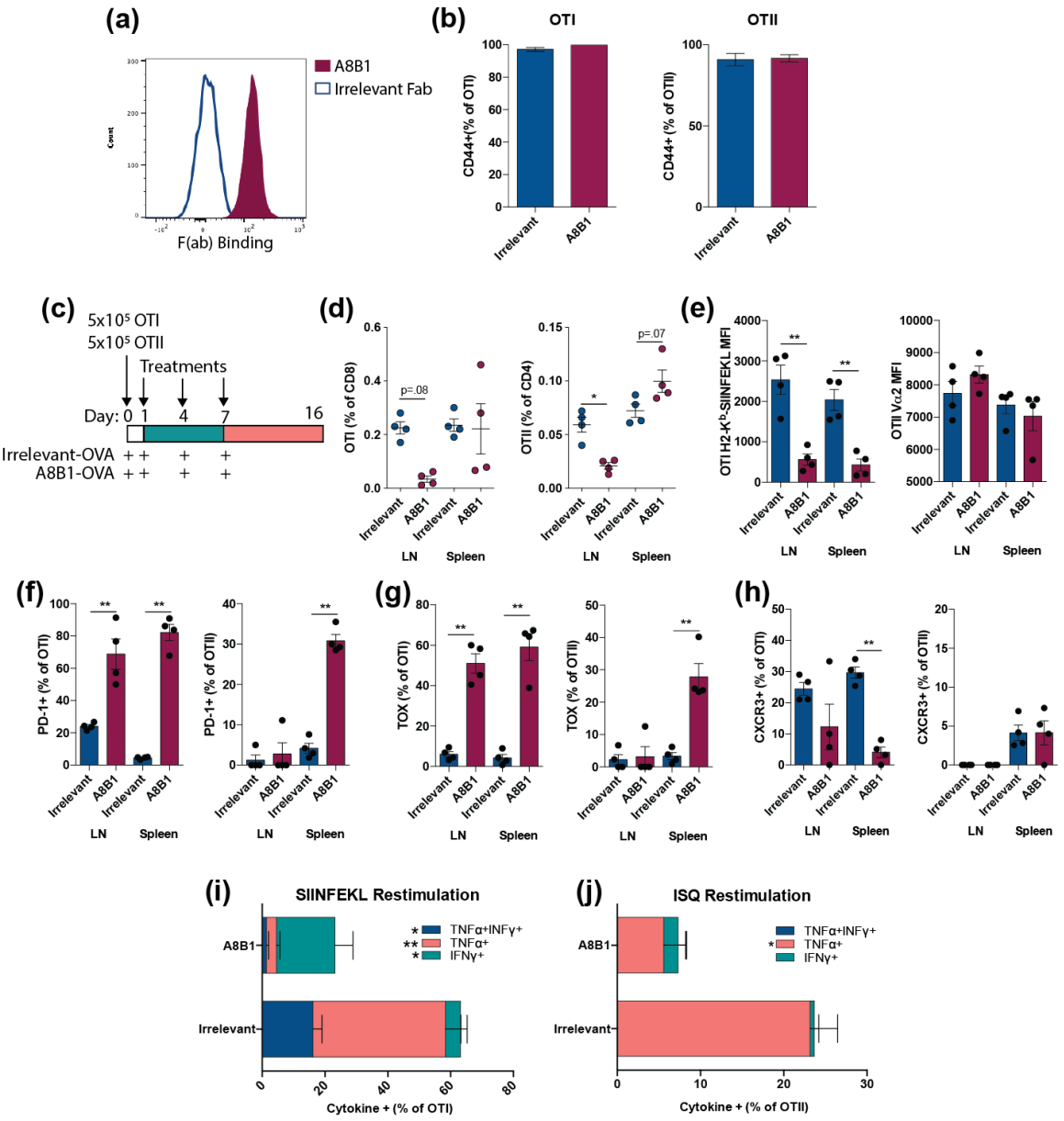


Figure 2.8: Prolonged exposure to erythrocyte-associated antigen leads to further T cell dysfunction. (Continued on next page)

### *2.3.4 Exhausted T Cell Phenotype and Dysfunction is Maintained After Antigenic Challenge.*

Because the *ex vivo* restimulation indicated reduced functionality of antigen-specific T cells *in vitro* (Figure 2.8), we next tested if OT-I and OT-II cells in mice receiving A8B1-OVA would be less capable of responding to an adjuvanted antigenic challenge in vivo. Mice were

Figure 2.8, continued: Prolonged exposure to erythrocyte-associated antigen leads to further T cell dysfunction.a) Irrelevant-Fab-OVA was synthesized to control for size and expression vector of antigen. Irrelevant Fab or A8B1 were incubated with erythrocytes and assessed for binding by flow cytometry to erythrocytes. b) Mice were adoptively transferred with OT-I and OT-II and received 3, 1 $\mu$g doses of Fab-OVA, and CD44 expression was analyzed 9 d after the final dose. c) Mice were adoptively transferred with OT-I and OT-II and dosed every 3 d with 1 $\mu$g A8B1-OVA or Irrelevant Fab-OVA, and sacrificed 9 d after final dose. d) Percentage of OT-I and OT-II in LN (axillary, brachial, inguinal, popliteal) and spleen. e) Mean fluorescence intensity (MFI) of H2-$K^b$-SIINFEKL pentamer on OT-I (left) or V$\alpha$2 on OT-II (right). f) Percentage of PD-1+ OT-I and OT-II cells. g) Percentage TOX+ cells of OT-I and OT-II. h) Percentage CXCR3+ cells of OT-I and OT-II. Lymphocytes from the draining lymph nodes were restimulated for 6 hr with i) SIINFEKL peptide or j) ISQ peptide and stained for intracellular cytokine production. Data are shown as mean  SEM. This experiment was performed twice. Statistical analyses were performed using one-way ANOVA with Tukey's test. *P $<$ 0.05 and **P $<$ 0.01.

treated as in Figure 2.8, and 9 d after the final dose, when A8B1-OVA had largely been cleared from circulation, mice were challenged s.c. with OVA and lipopolysaccharide (LPS) (Figure 2.9a). Both the OT-I and OT-II cells that had experienced erythrocyte-associated antigen had severely reduced ability to proliferate in response to challenge compared to Irrelevant-OVA, and both OT-I and OT-II reached similar levels to naïve control (Figure 2.9b). OT-I maintained high levels of PD-1+ TOX+ cells, whereas controls upregulated TOX but had low levels of double positive cells (Figure 2.9c). Despite a challenge, OT-I and OT-II cells maintained a downregulated T cell receptors (TCR), (Figure 2.9d). Inhibitory receptors CTLA-4, 4-1BB, and LAG-3 remained high compared to Irrelevant-OVA (Figure 2.9e). OT-I had low levels of TCF-1 and T-bet compared to controls, suggesting the cells are no longer in an activated state due to recent exposure of antigen, but rather a terminal program of dysfunction (Figure 2.9e-f). In support of this, OT-I cells had a higher proportion of $Eomes^{hi}$ PD-1+ TCF-1-T-bet- cells, a population thought to be in a terminally exhausted state (Figure 2.9h). (43) On OT-II cells, there was a weak induction of regulatory T cells, suggesting they may play a minor role in the inability to respond to challenge (Figure 2.9i).

To confirm that these were not memory and effector cells, and that they maintained dysfunction in response to antigen, cells from dLN were restimulated *ex vivo* with cognate

peptides. As before challenge with LPS, OT-I and OT-II cells had a greatly reduced capacity to produce TNF$\alpha$ but maintained capacity to produce IFN$\gamma$ (Figure 2.9j). Unlike what has been demonstrated for anergic cells, addition of IL-2 to the restimulation media did not restore the capacity to produce cytokines in OT-I or OT-II from mice receiving A8B1-OVA (Figure 2.9k). Interestingly, addition of IL-2 did enhance capacity of OT-II cells to produce cytokines in mice receiving Irrelevant-OVA.

### *2.3.5 CD8 T Cell Dysfunction is Lasting*

The observed T cell dysfunction in response to erythrocyte-associated antigen was not due to recent overexposure to antigen, nor was it temporary. OT-I cells from mice that received A8B1-OVA and were challenged 3 months after dosing accumulated in far fewer numbers than in control mice both in the LN and spleen (Figure 2.10a-b). This could be reflective of a smaller pool of cells in the mice receiving A8B1-OVA as opposed to a lack of proliferation. However, the cells still phenotypically and functionally appeared dysfunctional. Remarkably, TCR remained significantly downregulated in the OT-I cells (Figure 2.10c). OT-I retained high expression of PD-1, and in the spleen had higher levels of TOX expression (Figure 2.10d-e). Functionally, the remaining OT-I were crippled in their capacity to produce cytokines (Figure 2.10f). This suggests that although OT-I cells remained in circulation, they maintained their dysfunctional program. Interestingly, OT-II cells did not demonstrate the same reduction in effector functions as did OT-I cells, and largely recovered to the effector functions of controls (Figure 2.10g).

### *2.3.6 Dysfunction is Antigen-Specific and Can Be Induced in an Endogenous Repertoire*

The previous studies were conducted using model systems in which the antigen-specific TCRs are identical and of high affinity, which is unlike a physiological response where there is a

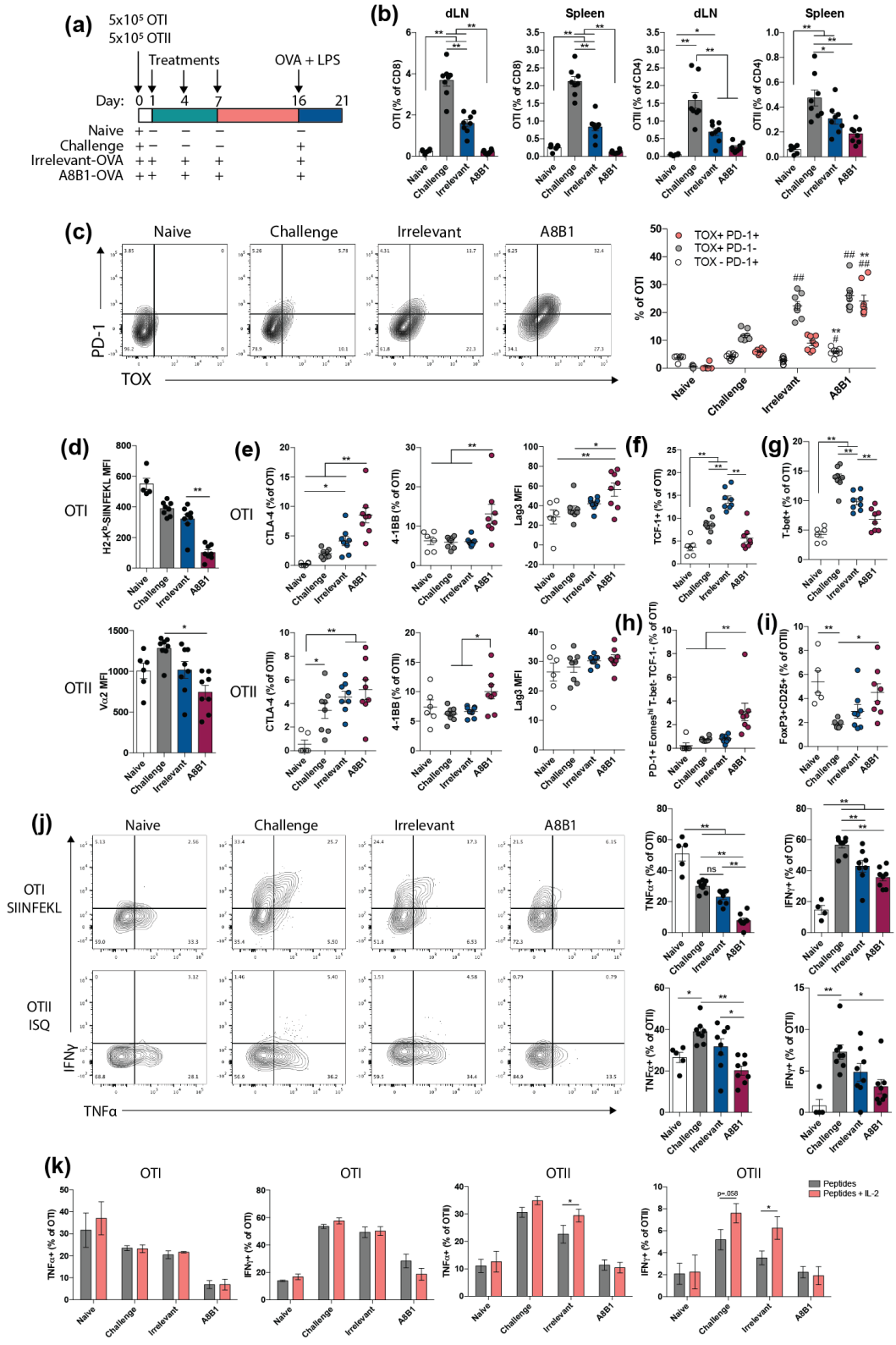


Figure 2.9: Exhausted T cell phenotype and dysfunction is maintained after antigenic challenge. (Continued on the following page.)

Figure 2.9, continued: Exhausted T cell phenotype and dysfunction is maintained after antigenic challenge. a) 500,000 OT-I and OT-II were adoptively transferred into C57BL/6 mice. Mice received an intravenous injection every 3 d of 1 $\mu$g of A8B1-OVA or Irrelevant-OVA, challenged with 20 $\mu$g OVA and 50 ng LPS 9 d subcutaneously after the final injection, and sacrificed for cellular analysis of draining LN (axillary, popliteal, inguinal, and brachial) and spleen 5 d after challenge. For challenge, Irrelevant-Fab, and A8B1 n=8; for naïve n=6. b) Percentages of OT-I and OT-II in the draining lymph nodes (dLN) and spleen. c) Percentage of TOX+ PD-1+ OT-I in the dLN. vs Challenge, * vs Irrelevant-OVA. d) MFI of T cell receptor on OT-I and OT-II in the dLN. e) Expression of CTLA-4, 4-1BB, and LAG-3 on OT-I and OT-II in the spleen. f) Percentage of TCF-1+ OT-I in the dLN. g) Percentage of T-bet+ OT-I in the dLN. h) Percentage of terminally exhausted cells of OT-I in the dLN. i) Percentage of regulatory T cells of OT-II in the dLN. j) TNF$\alpha$ and IFN$\gamma$ production in OT-I and OT-II after 6 hour *ex-vivo* restimulation of lymphocytes from dLN with SIINFEKL peptide or ISQ peptide. k) Cytokine expression in OT-I and OT-II after ex-vivo restimulation of splenocytes with SIINFEKL and ISQ peptides as in d) with or without exogenous mouse IL-2. Data are shown as mean  SEM. Data is representative of 3 repeat experiments. Statistical analyses were performed using one-way ANOVA with Tukey's test. *P $<$ 0.05 and **P $<$ 0.01.

diverse endogenous repertoire of TCRs of varying affinities. To test this in an endogenous repertoire, 1 $\mu$g A8B1-OVA or Irrelevant-OVA were administered every three days for 5 doses in WT C57BL/6 mice. Mice were challenged with OVA and CpG, and 7 d after the final dose, organs were analyzed for T cell responses. Analysis of dLN and spleen revealed deletion of OVA-specific CD8 T cells, as measured by H2-K$^{b}$-SIINFEKL pentamer staining (Figure 2.11a). There is no reliable tetramer to identify OVA-specific CD4 T cells. Analysis of antigen-specific CD8 cells revealed upregulation of molecules similar to those seen in the OT-I cells, including CTLA-4, LAG-3, and 4-1BB (Figure 2.11b). Interestingly, there was not a high induction of PD-1, as demonstrated in OT-I. Naive mice were excluded from this phenotypic analysis because of a lack of antigen-specific cells.

It is important to demonstrate that this strategy is antigen-specific, and does not affect the ability of the immune system to mount responses to other antigens, such as would be necessary in the course of an infection. Thus, mice were challenged with a separate antigen, NP, at the time of challenge to OVA. To avoid any potential for bystander suppression of OVA-specific cells onto NP-specific cells in the dLN of the challenge, mice were challenged

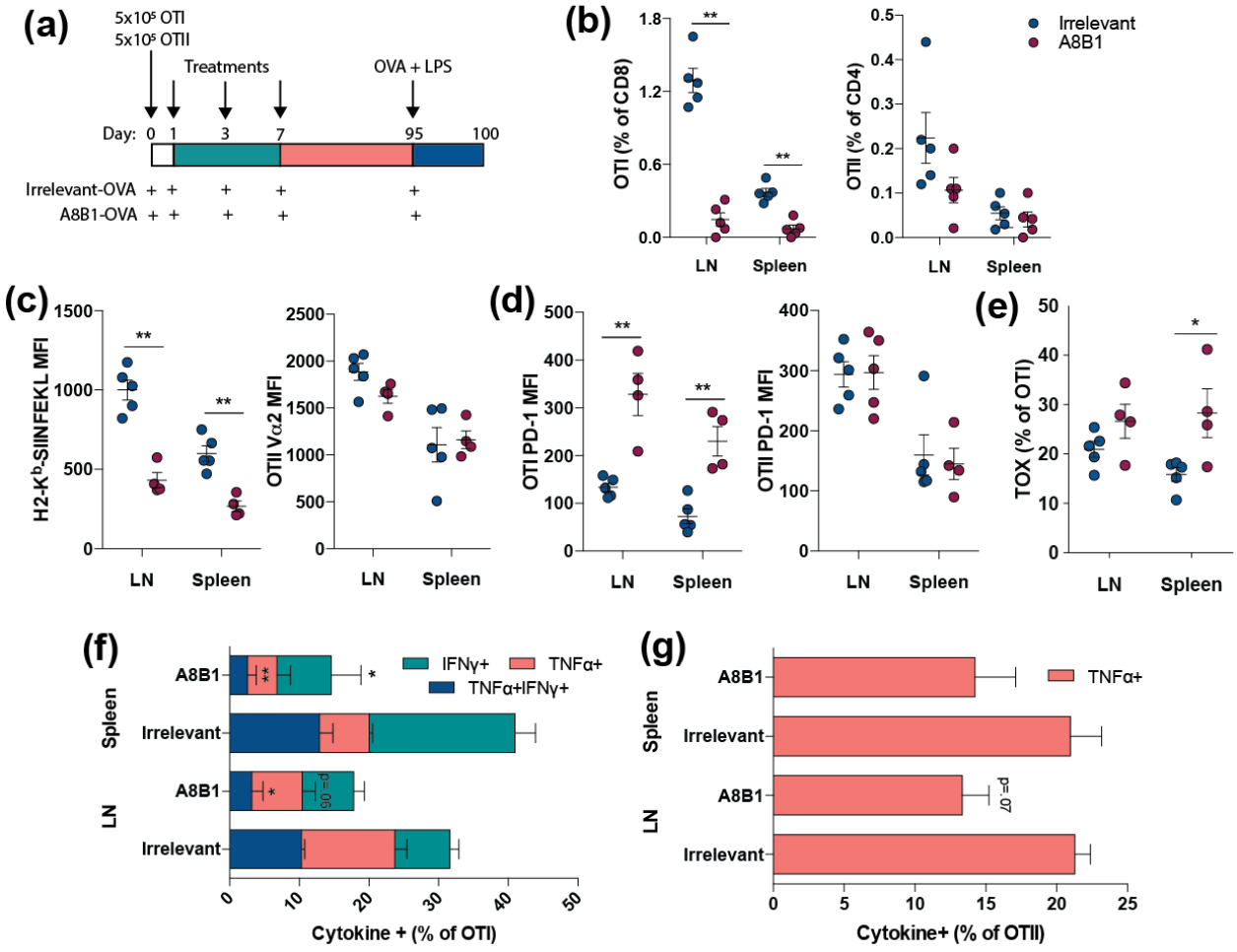


Figure 2.10: Erythrocyte-antigen induces durable CD8 T cell dysfunction. a) Experiment was conducted as in Figure 9, with mice being challenged three months after injection with Fab-OVA. b) Percentages of OT-I and OT-II in the dLN and spleen. c) MFI of H2-K$^b$-SIINFEKL pentamer on OT-I and V$\alpha$2 on OT-II. d) MFI of PD-1 on OT-I and OT-II. e) Percentage of TOX+ OT-I. Lymphocytes from dLN were restimulated for 6 hours *ex vivo* with f) SIINFEKL or g) ISQ peptide. Data are shown as mean  SEM. This experiment was performed once. Statistical analyses were performed using one-way ANOVA with Tukey's test. *P $<$ 0.05 and **P $<$ 0.01.

with the two antigens on separate sides. NP-specific CD4 and CD8 T cells were identified with I-A$^b$-NP$_{311\text{-}325}$ and H2-D$^b$-NP$_{366\text{-}374}$ tetramers, respectively. There was no defect in the ability of NP-specific T cells to respond to NP challenge in mice that had received A8B1-OVA (Figure 2.11c). Furthermore, splenocytes were restimulated with SIINFEKL and ISQ or NP$_{311\text{-}325}$ and NP$_{366\text{-}374}$. Mice that received A8B1-OVA had a reduced ability to

secrete inflammatory cytokines upon restimulation with OVA peptides, but were capable of responding to restimulation with NP peptides (Figure 2.11d-e). Together these data indicate that erythrocyte-targeting is able to induce dysfunctional T cells in an endogenous repertoire of T cells, and that this dysfunction is specific to the antigen that was directed to erythrocytes.

### *2.3.7 Erythrocyte-Associated MOG Protects Mice from EAE*

The adoptive transfer model of EAE was utilized to assess anergy and inhibition mechanisms in a setting of autoimmune pathology in an endogenous repertoire. B6.SJL mice were vaccinated with a peptide from myelin oligodendrocyte glycoprotein ($MOG_{35\text{-}55}$), and splenocytes were restimulated with $MOG_{35\text{-}55}$ to generate highly encephalitogenic T cells that were then injected into naïve mice. Mice received various treatment schedules of A8B1 recombinantly expressed with the $MOG_{35\text{-}55}$ peptide (A8B1-MOG). As a positive control for remission of EAE, the clinically relevant anti-VLA-4 antibody, which blocks lymphocyte infiltration into the spinal cord, was used [207]. Mice that received PBS succumbed to severe EAE after 10 d, and mice treated with anti-VLA-4 had a delayed progression of disease but eventually all developed EAE (Figure 2.12a-b). Conversely, animals treated with either a low dose or a high dose of A8B1-MOG at days 0, 7, and 17 initially began to develop disease, but it did not continue to progress after day 10, likely due to the second dose of A8B1-MOG at day 7 (Figure 2.12a). Remarkably, at the lower dose, dosing at days 0, 3, and 6 prevented the development of pathology, and even after the cessation of dosing mice did not develop disease, suggesting a lasting program (Figure 2.12b). Together these data demonstrated that targeting cell-associated antigen not only induced a dysfunctional state that left T cells less capable of responding to an antigenic challenge, but it was also able to prevent activated T cells from causing disease.

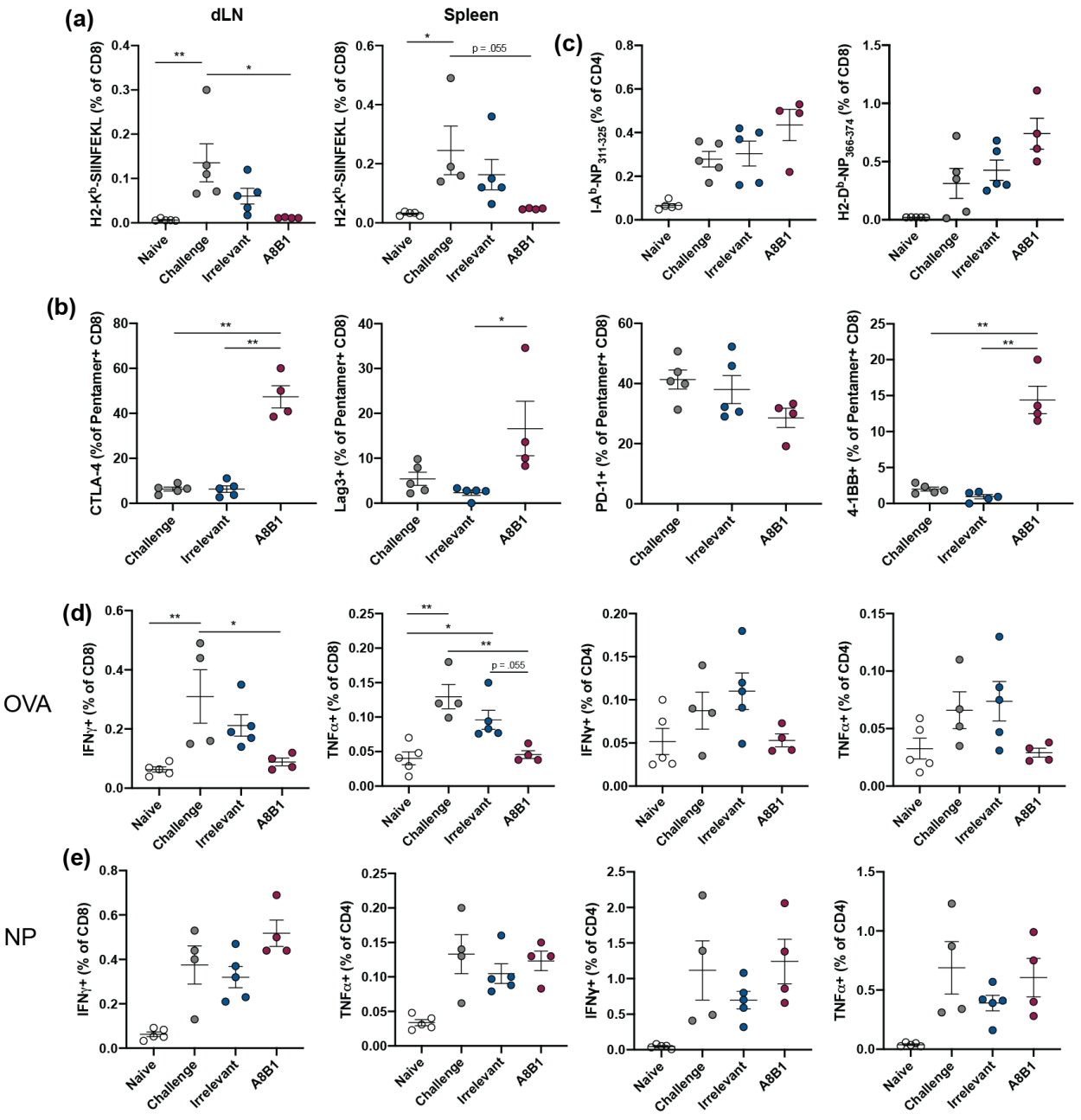


Figure 2.11: Erythrocyte-associated antigen induces endogenous and antigen-specific dysfunction. a-e) 1 $\mu$g A8B1-OVA or Irrelevant-OVA were administered to naïve mice every three days for a total of 5 doses, and mice were challenged with 10 $\mu$g influenza nucleoprotein (NP) and 10 $\mu$g OVA with 20 $\mu$g CpG 8 d after the final dose. Mice were sacrificed 7 days later. a) Percentage of H2-K$^b$-SIINFEKL endogenous cells of total CD8. b) Phenotype of H2-K$^b$-SIINFEKL CD8 T cells. c) Percentage of NP-specific CD4 (above) or CD8 (below) in the dLN. d-e) Splenocytes were restimulated with d) OVA peptides or e) NP peptides and intracellular cytokine secretion was quantified. Data are shown as mean  SEM. The experiment was performed once. Statistical analyses were performed using one-way ANOVA with Tukey's test. *P $<$ 0.05 and **P $<$ 0.01

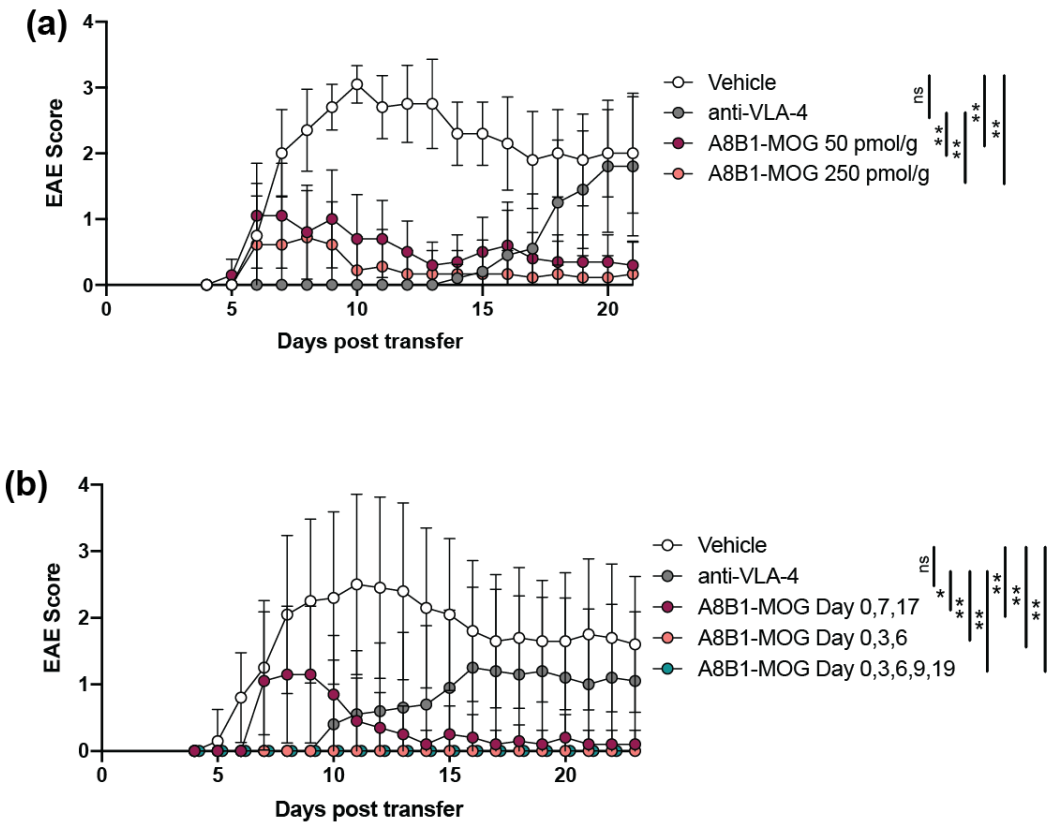


Figure 2.12: Erythrocyte-associated MOG protects mice from EAE. B6.SJL mice were vaccinated with $MOG_{35\text{-}55}$, and eleven days later spleens were harvested and encephalitogenic T cells were restimulated with $MOG_{35\text{-}55}$ peptide in the presence of IL-12 and anti-IFN$\gamma$. Cells were then injected intraperitoneally into naïve C57BL/6 mice. a) Mice were treated with 50 pmol/g or 250 pmol/g of A8B1-MOG at days 0, 7, or 17 after transfer of encephalitogenic T cells, or anti-VLA-4 antibody every other day (n=10). b) Mice were treated with 50 pmol/g A8B1-MOG at various dosing schedules (n=10). Data are shown as mean  SD. Each experiment was performed once. Statistical analyses were performed at the final time point using one-way ANOVA with Tukey's test. *P $<$ **P $<$ 0.01.

### *2.3.8 The Spleen is Necessary for Induction of CD8 and CD4 T Cell Dysfunction*

After demonstrating that exposure to erythrocyte-associated antigen left T cells not only incapable of responding to a future challenge but also induced dysfunction in already activated cells, there was interest in determining the route of antigen presentation of erythrocyte-associated antigen and if the robust T cell stimulation observed was due solely to its pro-

longed circulation time.

Dying and damaged erythrocytes are cleared by phagocytes in both the liver and spleen [208]. Because antigen presentation of apoptotic debris is often associated with the spleen, we hypothesized that presentation of erythrocyte-associated antigen primarily occurs in the spleen [209]. To test this, we first adoptively transferred CFSE-labeled OT-I and OT-II cells into splenectomized mice or mice that received a sham surgery, treated once with A8B1-OVA, and assessed proliferation in the LN 4 d later. Proliferation index revealed that the spleen was necessary for robust OT-I proliferation (Figure 2.13a). It is possible that it is necessary for OT-II proliferation, however, the small sample size precludes that conclusion.

To determine if the spleen was necessary for tolerance, mice were adoptively transferred with OT-I and OT-II, received A8B1-OVA or Irrelevant-OVA, and were challenged with OVA and LPS 9 d after the final dose. Results indicated that the spleen was necessary for T cell dysfunction in both the OT-I and OT-II compartments in mice receiving A8B1-OVA, whereas it was completely dispensable in mice receiving Irrelevant-OVA (Figure 2.13b). In splenectomized mice receiving A8B1-OVA, there was no longer deletion of OT-II cells, and a similar trend could be seen for OT-I (Figure 2.13b). High levels of PD-1 were reversed in OT-I and OT-II upon splenectomy, back to control levels (Figure 2.13c). Likewise, TCR downregulation and TOX upregulation were largely reversed (Figure 2.13d-e). Interestingly, in OT-I cells, TCR downregulation and TOX upregulation did not quite return to control levels. This could be indicative of non-splenic cells presenting some erythrocyte-associated antigen that would lead to persistent TCR signaling but would not involve the same tolerogenic milieu as the eryptotic pathway in the spleen. Splenectomy inhibited induction of Tregs of OT-II (Figure 2.13f). Finally, OT-I and OT-II from splenectomized mice had restored ability to produce inflammatory cytokines upon antigen restimulation (Figure 2.13g-i).

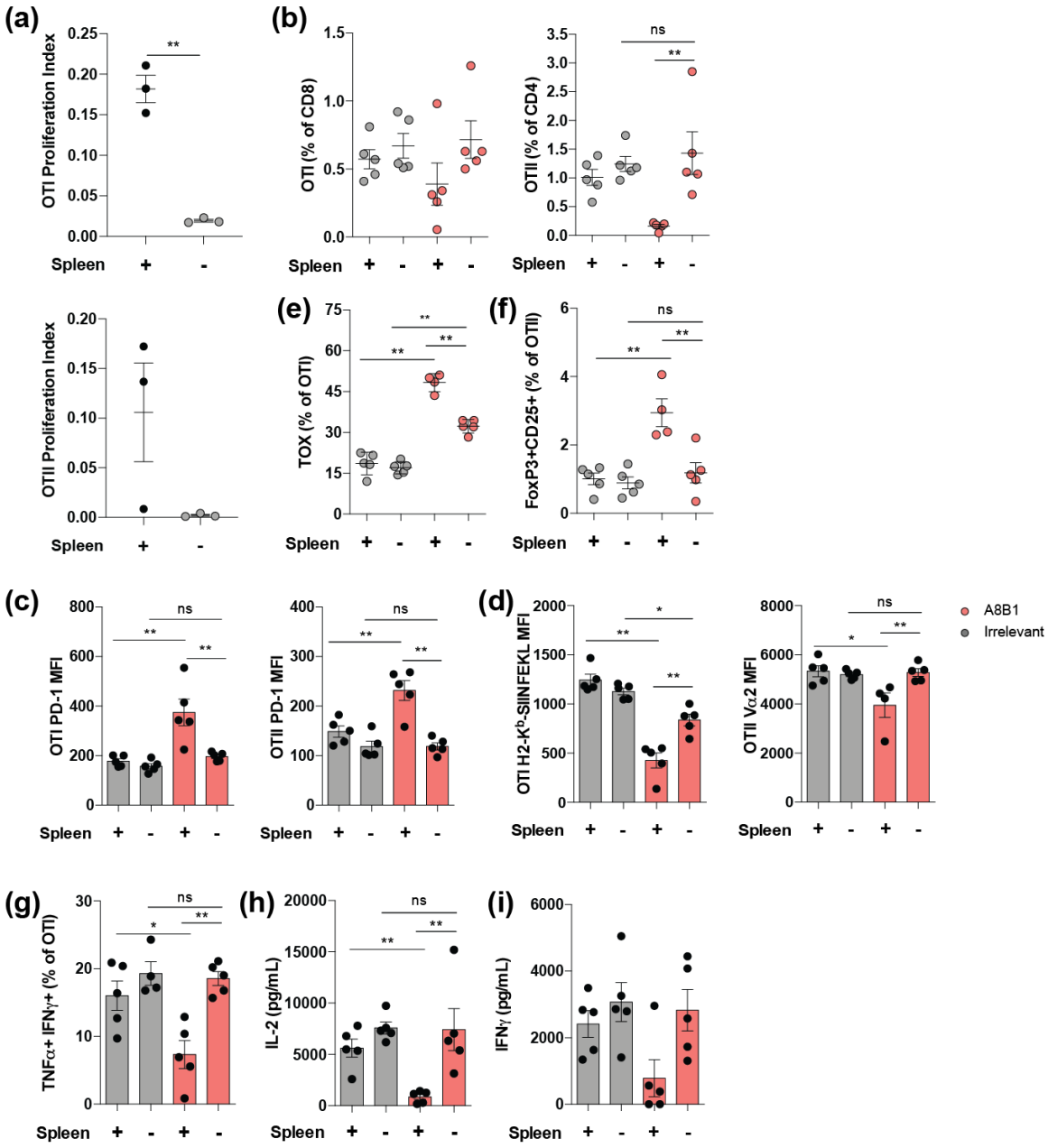


Figure 2.13: The spleen is necessary for induction of CD8 and CD4 T cell dysfunction. a-e) Mice followed dosing regimen as in Figure 2.9a), either in splenectomized or sham splenectomized mice (n=5). a) Percentages of OT-I and OT-II in the dLN. b) MFI of PD-1 on OT-I and OT-II cells. c) MFI of H2-K$^{b}$-SIINFEKL pentamer on OT-I and V$\alpha$2 on OT-II. d) Percentage of TOX+ OT-I cells. e) Percentage of FoxP3+ CD25+ regulatory T cells OT-II cells. f) Cytokine production in OT-I cells after 6 hr *ex vivo* restimulation of lymphocytes from dLN with SIINFEKL peptide. Cytokine levels in supernatant after 3 d restimulation of lymphocytes from dLN with g) ISQ peptide or h-i) full OVA protein. Data are shown as mean  SEM. The experiment was performed once. Statistical analyses were performed using one-way ANOVA with Tukey's test. *P $<$ 0.05 and **P $<$ 0.01

### *2.3.9 Fab Persists on Erythrocytes and is Capable of Stimulating T Cells for Days After Initial Dose*

The spleen contains interendothelial slits that are highly sensitive to changes in erythrocyte deformability, and are responsible for clearing altered erythrocytes from circulation [210]. It is possible that an initial bolus injection of antigen led to erythrocytes with altered deformability, that were rapidly cleared from circulation. If this were the case, the antigen presentation observed would be an artifact of this mechanism of clearance as opposed to uptake and presentation of self-apoptotic antigen. Thus, we wanted to test if removal of the spleen drastically changed altered antigen clearance, favoring prolonged circulation as opposed to a bulk clearance of antigen. We conducted a half-life study in splenectomized or sham splenectomized mice. Fluorescently labeled A8B1 or Irrelevant Fab was injected, mice were bled at various times, and erythrocytes were assessed by flow cytometry for erythrocyte-associated fluorescent Fab (Figure 2.14a). The initial clearance of A8B1 was indistinguishable between splenectomized and sham splenectomized mice. However, beginning 72 hr after injection, a small but statistically lower amount of A8B1 was exhibited in circulation of mice with a spleen compared to mice without a spleen. This demonstrates that there are alternative pathways of erythrocyte clearance, and that the spleen slowly clears a small number of erythrocytes and their bound antigenic payload. Presumably, the cleared erythrocytes are those undergoing apoptosis as part of their normal life cycle, and this slow turnover is what leads to T cell dysfunction.

To determine how long antigen circulating on erythrocytes could be presented to T cells, mice received 1 $\mu$g A8B1-OVA 1 d, 4 d, 9 d, or 45 d before adoptive transfer of CFSE-labeled OT-I and OT-II. 4 d later, mice were sacrificed and spleens analyzed for T cell proliferation. The 45 d time point was chosen because that is the lifespan of an erythrocyte in mice [211]. At 9 d, sufficient antigen remained on erythrocytes to trigger a small amount of proliferation in OT-I (Figure 2.14b-c). Interestingly, the same was not true for OT-II. With antigen delivered 4 d before adoptive transfer, there was almost undetectable levels of

OT-II proliferation. It is possible that antigen is being cross-presented more efficiently on MHC-I than presented on MHC-II. Because T cells require a high threshold for activation in the absence of co-stimulation, about 8000 TCRs, it is likely that the OT-II cells are not encountering sufficient pMHC to trigger proliferation [212]

To further confirm the hypothesis that tolerance was not due to bulk clearance of antigen, we injected A8B1-OVA 24 hr before adoptive transfer of OT-I and OT-II cells, during which time any bulk clearance of antigen would have been completed. In the OT-I compartment, injection 24 hr before adoptive transfer drove the same level of deletion and exhaustion as injection 24 hr after adoptive transfer (Figure 2.15a-d). This confirms that a bolus immediate clearance of antigen does not drive overstimulation and exhaustion.

### *2.3.10 CD8 Dysfunction is Lost in the Absence of Batf3+ Cross-Presenting Dendritic Cells*

With the knowledge that the spleen was necessary for antigen presentation, we further investigated the APC populations that could contribute to presentation. We investigated the necessity of cross-presenting DCs (cDC1), as they have been shown to take up blood-borne apoptotic cells in the marginal zone, and cross-present the antigen to CD8 T cells in the T cell zone [213]. The Batf3-deficient mouse, which lacks cDC1s, was utilized [214]. We confirmed the lack of XCR1+ CD8+ cross-presenting dendritic cells in the spleen of a Batf3$^{-/-}$ mouse (Figure 2.16a). CFSE-labeled OT-I and OT-II were adoptively transferred into WT or Batf3$^{-/-}$ mice and dosed with A8B1-OVA. Proliferation of OT-I was abrogated in the Batf3$^{-/-}$ mouse, whereas proliferation of OT-II was not affected (Figure 2.16b). When challenged with OVA, OT-I deletion was also abrogated in the Batf3$^{-/-}$ mouse, and there was little to no effect on OT-II deletion (Figure 2.16c). As might be expected, the OT-I response to OVA and LPS challenge was blunted in the absence of cDC1s, offering a narrow dynamic range to observe OT-I deletion in A8B1-OVA treated mice compared to control. However, the contribution of cDC1s to T cell dysfunction could still readily be observed, as OT-I cells

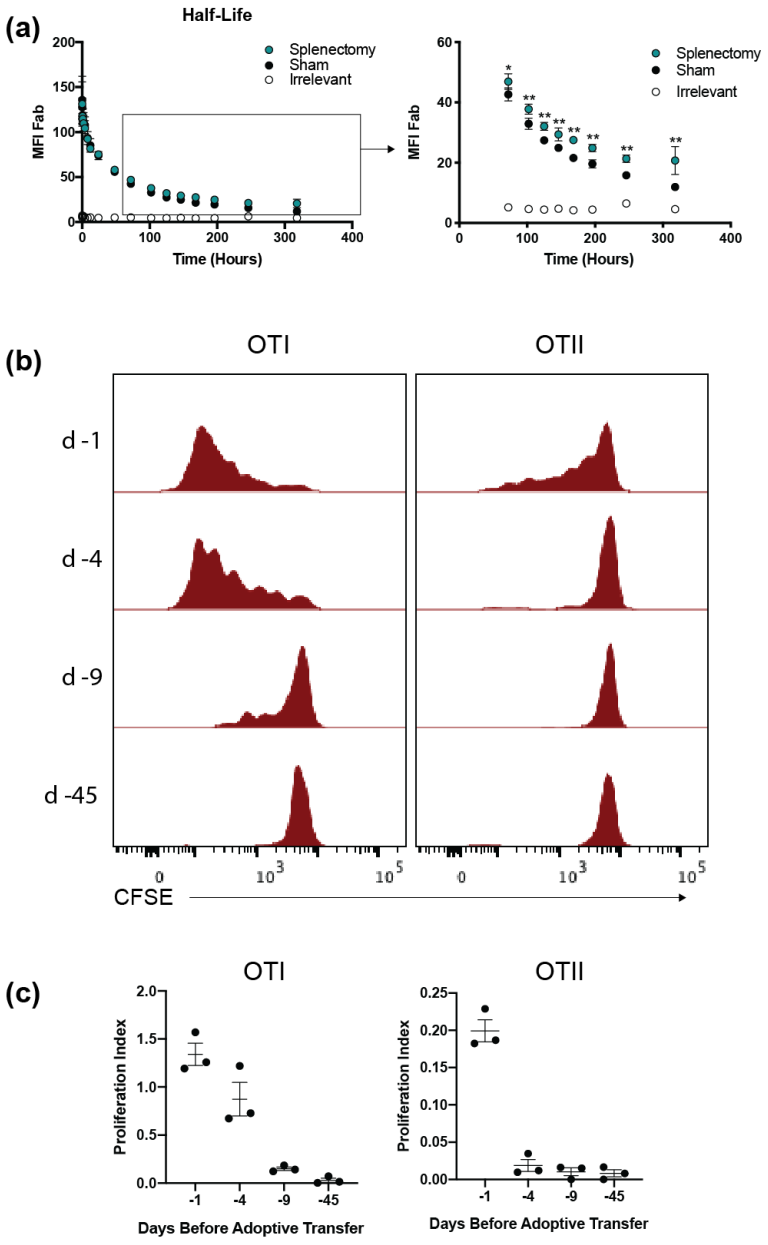


Figure 2.14: Fab persists on erythrocytes and is capable of stimulating T cells for days after initial dose. Fluorescently labeled A8B1 was injected into splenectomized or sham splenectomized mice, and mice were bled at various time points (n=4) to measure Fab bound to erythrocytes. Fluorescent Irrelevant Fab was injected in sham splenectomized mice as control. Data is represented as mean fluorescence of Fab measured by flow cytometry and data is analyzed at each time point via t-test. b-c) 1 $\mu$g A8B1-OVA 1 d, 4 d, 9 d, or 45 d before adoptive transfer of CFSE-labeled OT-I and OT-II. 4 d later, mice were sacrificed and spleens analyzed for T cell proliferation. Representative histograms of CFSE dilution in T cells at different time points. c) Proliferation index quantifying extent of proliferation (n=3).

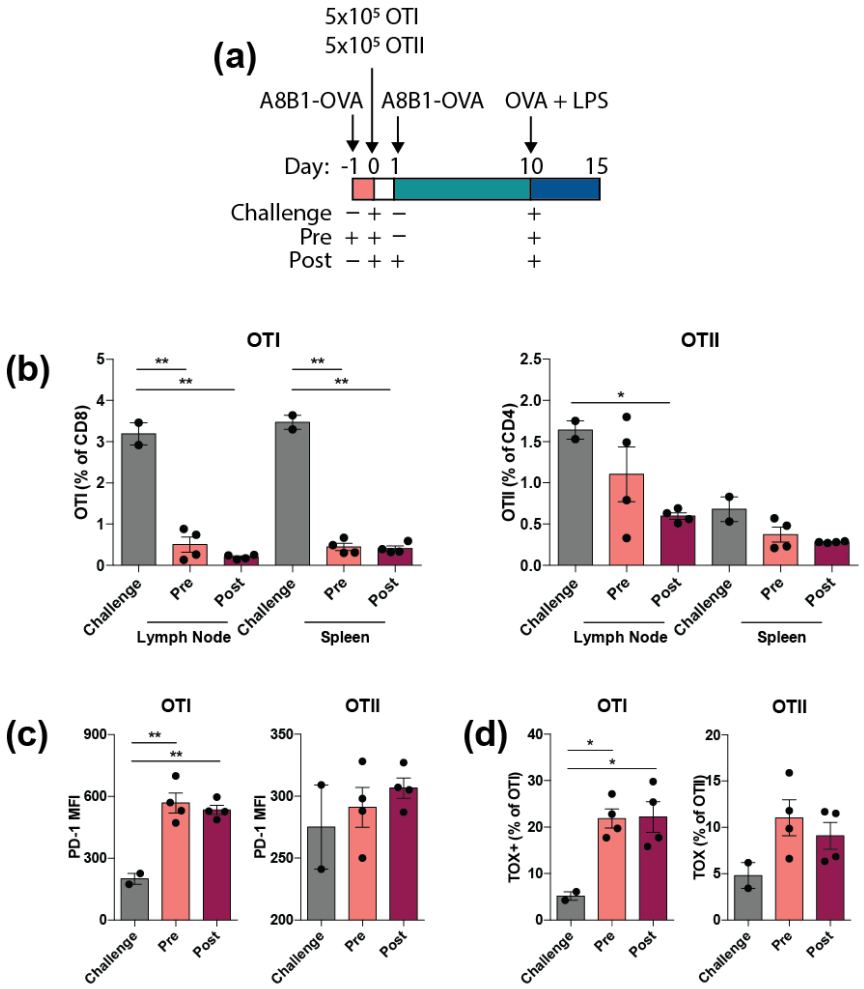


Figure 2.15: T cell dysfunction is not due to bolus of antigen presentation immediately after injection. a) Mice received a single dose of A8B1-OVA either 24 hr before (Pre) or 24 hr after (Post) adoptive transfer of OT-I and OT-II, challenged with OVA and LPS, and sacrificed 5 d later. For Pre and Post groups, n=4, for challenge control n=2. b) Percentages of OT-I and OT-II in the LN and spleen at sacrifice. c) MFI of PD-1 on OT-I and OT-II. d) TOX expression in OT-I and OT-II. Data are shown as mean  SEM and analyzed by one-way ANOVA. *P $<$ 0.05 and **P $<$ 0.01.

in Batf3$^{-/-}$ mouse did not upregulate PD-1, and were rescued in their ability to produce TNF$\alpha$ (Figure 2.16d-e). Conversely, cDC1s had no effect on PD-1 upregulation on OT-II or their blunted capacity to produce cytokines (Figure 2.16f-g).

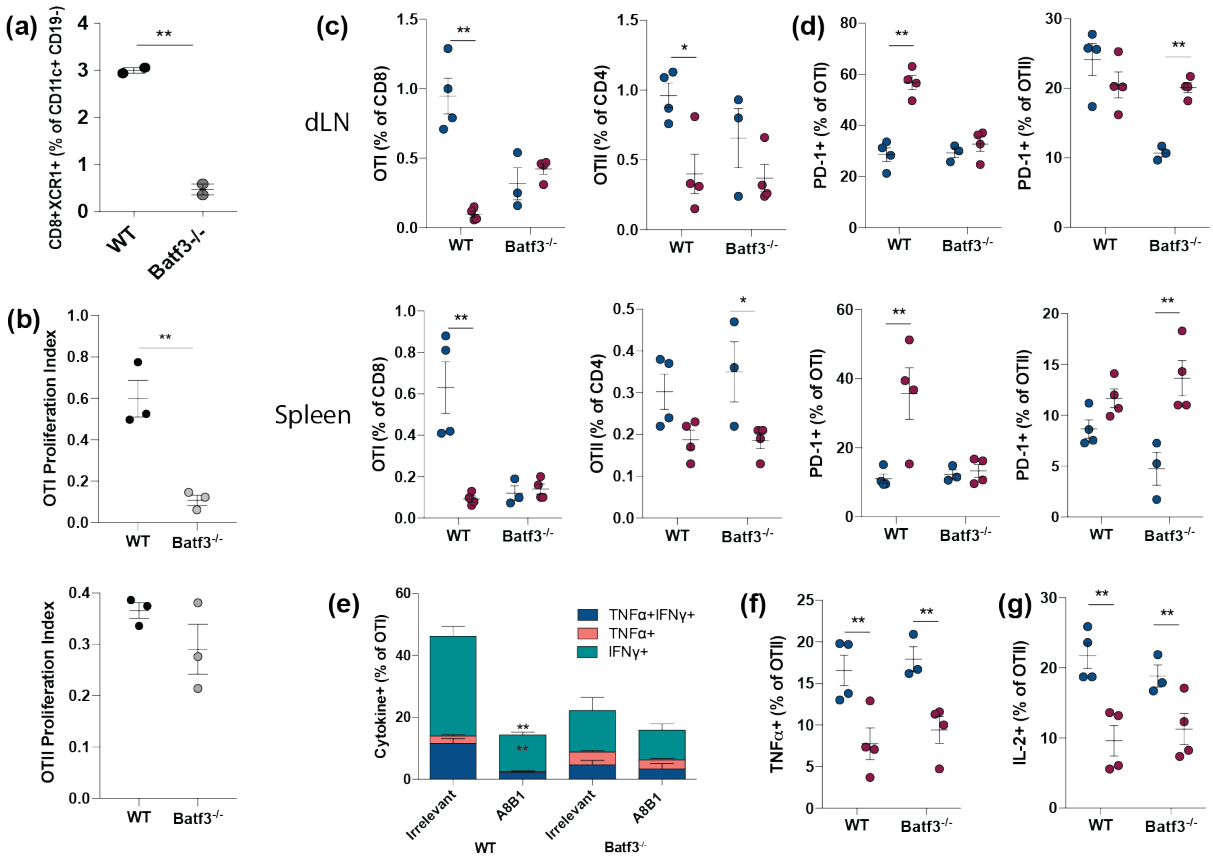


Figure 2.16: CD8 T cell dysfunction is lost in mice lacking Batf3+ cross-presenting DCs. a) Percentage of cross-presenting dendritic cells in the spleen of a Batf3$^{-/-}$ or WT mouse. b) Proliferation index of CFSE-labeled OT-I and OT-II in the spleen of mice that received 1 $\mu$g A8B1-OVA and were analyzed 4 d later. c-g) Mice followed dosing regimen as in Figure 9a, either in WT or Batf3$^{-/-}$ mice (n=4 for all groups except Irrelevant Fab Batf3$^{-/-}$, n=3). c) Percentage of OT-I and OT-II in the dLN and spleen. d) Percentage of PD-1+ cells in the dLN (above) or spleen (below). Lymphocytes from the dLN were restimulated with e) SIINFEKL or f-g) ISQ peptide and intracellular cytokines measured by flow cytometry. These experiments were performed once. Experiments a-b were analyzed via t-test, and all others were analyzed using a one-way ANOVA with Tukey's test. *P $<$ 0.05 and **P $<$ 0.01.

### *2.3.11 Macrophage Depletion Reverses CD8 Dysfunction*

Splenic macrophages are also a likely candidate, as they have been extensively described to engulf apoptotic cells. Red pulp macrophages (RPM) are typically associated with uptake of senescent erythrocytes, but the contribution of RPM to presentation of apoptotic debris is unknown [215–217]. CD169+ marginal metallophillic and MARCO+ marginal zone

macrophages have been described to take up apoptotic debris for presentation to T cells, the consequence of which, when in the absence of danger signals, is associated with tolerance [218, 219].

To investigate the role of macrophages in presentation of erythrocyte-associated antigen, we first attempted to deplete macrophages with an anti-CSF1R antibody, however it was insufficient to deplete RPM (Figure 2.17a). In an alternative approach, we utilized clodronate liposomes, which have been described extensively to deplete splenic macrophages [220]. Indeed, one intravenous injection was sufficient to deplete all splenic macrophages, while sparing splenic DCs (Figure 2.17b). Dosing with clodronate liposomes every 3 to 4 d throughout dosing with Fab-OVA, it was determined that macrophages were necessary for OT-I deletion, but dispensable for OT-II deletion (Figure 2.17c). Dosing with clodronate also reversed PD-1 upregulation, TCR downregulation, and TOX induction (Figure 2.17d-f). Dosing with clodronate liposomes reversed PD-1 in OT-II (Figure 2.17d). However, there was little effect on TCR downregulation or Treg induction in OT-II (Figure 2.17e,g). Thus, it appears that macrophages are important for induction of CD8 T cell dysfunction, but it is unclear if they are important for CD4 T cell dysfunction.

Although this indicated that cDC1s and macrophages are necessary for OT-I dysfunction, these results do not enable us to distinguish between cDC1s directly phagocytosing erythrocytes and presenting A8B1-OVA, or if macrophages, such as RPM or marginal zone macrophages, engulf the cells and transfer antigen to cDC1s for presentation [221–224]. Additionally, although one dose of clodronate liposomes spared cDC1s, it is possible that such frequent dosing may kill cDC1s, and further experiments need to confirm that they are spared after repeated dosing.

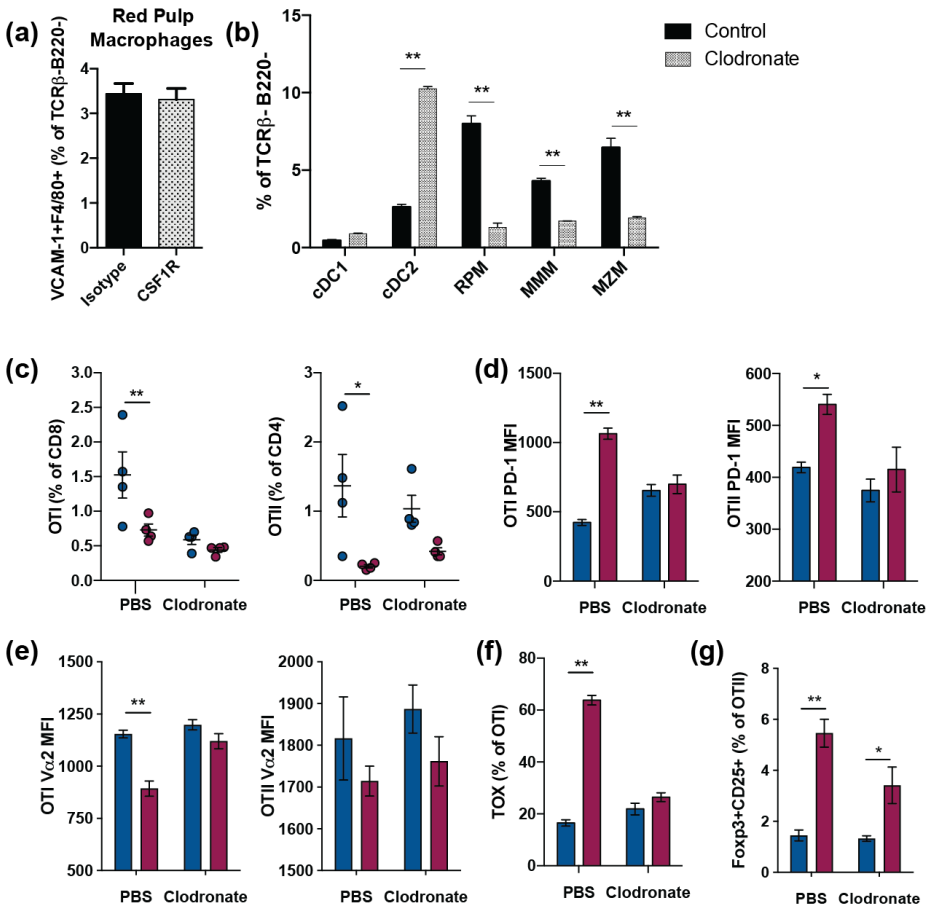


Figure 2.17: Macrophages are important for induction of CD8 T cell dysfunction. a) Percentage of red pulp macrophages of lineage- cells in the spleen after administration of two i.p. 400 $\mu$g doses of anti-CSF1R antibody. b) Percentage of APC subsets in the spleen 24 hr after one i.v. dose of clodronate or PBS-loaded liposomes. c) Percentage of OT-I and OT-II in the dLN. d) Mean fluorescence intensity of PD-1 on OT-I and OT-II. e) Mean fluorescence intensity of TCR on OT-I and OT-II. f) Percentage TOX+ cells of OT-I. G) Percentage of FoxP3+ CD25+ cells of OT-II.

### *2.3.12 Tolerance to CD8 Epitopes May Lead to Cross-Tolerance of CD4 Epitopes*

Previously in the laboratory it was demonstrated that mice adoptively transferred with OT-I only, dosed with a peptide that binds erythrocytes conjugated to OVA, and received a subsequent adoptive transfer of OT-I and OT-II had a blunted OT-II response to OVA challenge [185]. This demonstrated that there may have been a dominant tolerant effect

of the OT-I on the OT-II in suppression of expansion. However, one cannot exclude the possibility that ISQ-specific endogenous T cells suppressed the subsequent transfer of OT-II.

To overcome this potential confounding factor of endogenous antigen-specific CD4 T cells, we recombinantly expressed A8B1 or Irrelevant Fab with SIINFEKL or ISQ on the heavy chain. We adoptively transferred OT-I or OT-II and followed the same 21 d dosing strategy as previously. However, the dose of Fab-SIINFEKL or Fab-ISQ was dosed to be the same molar equivalent of Fab-OVA, about 0.5 $\mu$g. Mice received Fab-SIIN, Fab-ISQ, or both Fab-SIIN and Fab-ISQ. Mice that received A8B1-ISQ only before challenge demonstrated no ability to suppress proliferation of OT-I, suggesting a lack of CD4 OT-II dominant tolerance (Figure 2.18a). Unexpectedly, in mice receiving A8B1-SIIN only, there was not the typical suppression of OT-I responses typically observed with erythrocyte targeting. This is likely due to a lack of CD4 T cell help. This is suggested by the fact that dosing with A8B1-ISQ at the same time as A8B1-SIIN, which would provide CD4 T cell help, led to deletion closer to the typical deletion observed. However, the deletion was still not to the same level as expected, which could be because the SIIN and ISQ were not on the same antigen, would could lead to different cells presenting the antigen to OT-I and OT-II at different times. A lack of CD4 help was also reflected by the lack of typical PD-1 upregulation and TCR downregulation on OT-I cells (Figure 2.18b-c).

Unlike with the OT-I cells, 0.5 $\mu$g of A8B1-ISQ was very effective at inducing deletion of OT-II, with or without co-administration of A8B1-SIIN (Figure 2.18d). Dosing with A8B1-SIIN only had little to no effect on the ability of OT-II to respond to challenge. This discrepancy between the OT-I dominant tolerance observed by Grimm et al. and this study could be a result of the lack of CD4 help in this system, whereas with ERY1-OVA mice received a much greater dose of 10 $\mu$g. Interestingly, although there was no ability of the OT-II T cells to suppress OT-I, Tregs composed a large percentage of the remaining OT-II cells (Figure 2.18e).

Because 0.5 $\mu$g of A8B1-SIIN was insufficient to trigger the typical OT-I dysfunction

observed, it was not possible to conclude that there was no dominant tolerance of OT-I cells acting on OT-II cells. A 10-fold higher dose of A8B1-SIIN was instead used, which would provide sufficient antigen to trigger a CD8 response even in the absence of robust CD4 help. Consistent with this, dosing with this higher dose of A8B1-SIIN triggered the usual OT-I deletion observed with erythrocyte targeting (Figure 2.18f). Dysfunction was confirmed by the inability of OT-I to produce cytokines upon SIINFEKL restimulation *ex vivo* (Figure 2.18g). In order to have both CD4 and CD8 epitopes on the same antigen, Fab was recombinantly expressed with both ISQ and SIINFEKL epitopes and a natural cleavage site between the peptides, to yield Fab-SIIN-ISQ. Interestingly, when both CD4 and CD8 epitopes were on the same antigen, this seemed to lead to overstimulation of the OT-I, and a loss of tolerance, compared to having the epitopes on separate proteins, or having A8B1-SIIN alone (Figure 2.18a).

When 5 $\mu$g of A8B1-ISQ was injected, this seemed to have an opposite effect on OT-II compared to 0.5 $\mu$g A8B1-ISQ, appearing to cause expansion instead of deletion (Figure 2.18h). When A8B1-SIIN was co-administered with A8B1-ISQ, some deletion of OT-II was observed. When A8B1-SIIN-ISQ was administered, there was even greater deletion of OT-II, suggesting cross-talk with OT-I, and a potential for dominant tolerance. Dosing with A8B1-SIIN alone, there were trends towards deletion of OT-II compared to Irrelevant Fab control (Figure 2.18h). The OT-I tolerance seemed to occur through deletion only, because there was little difference in ability of OT-II to produce cytokines (Figure 2.18i). These data indicate that a lower dose of CD4 epitope is superior to a higher dose, and a higher dose of CD8 epitope superior to a low dose, with erythrocyte targeting. Additionally, this suggests that there may be dominant tolerance of OT-I, likely acting by deletion.

### *2.3.13 CD8-Derived Perforin is Dispensible for Tolerance*

Others have demonstrated that suppressor CD8 T cells act in a perforin-dependent mechanism to delete CD4 T cells. Interestingly, we observed upregulation of perforin in OT-I

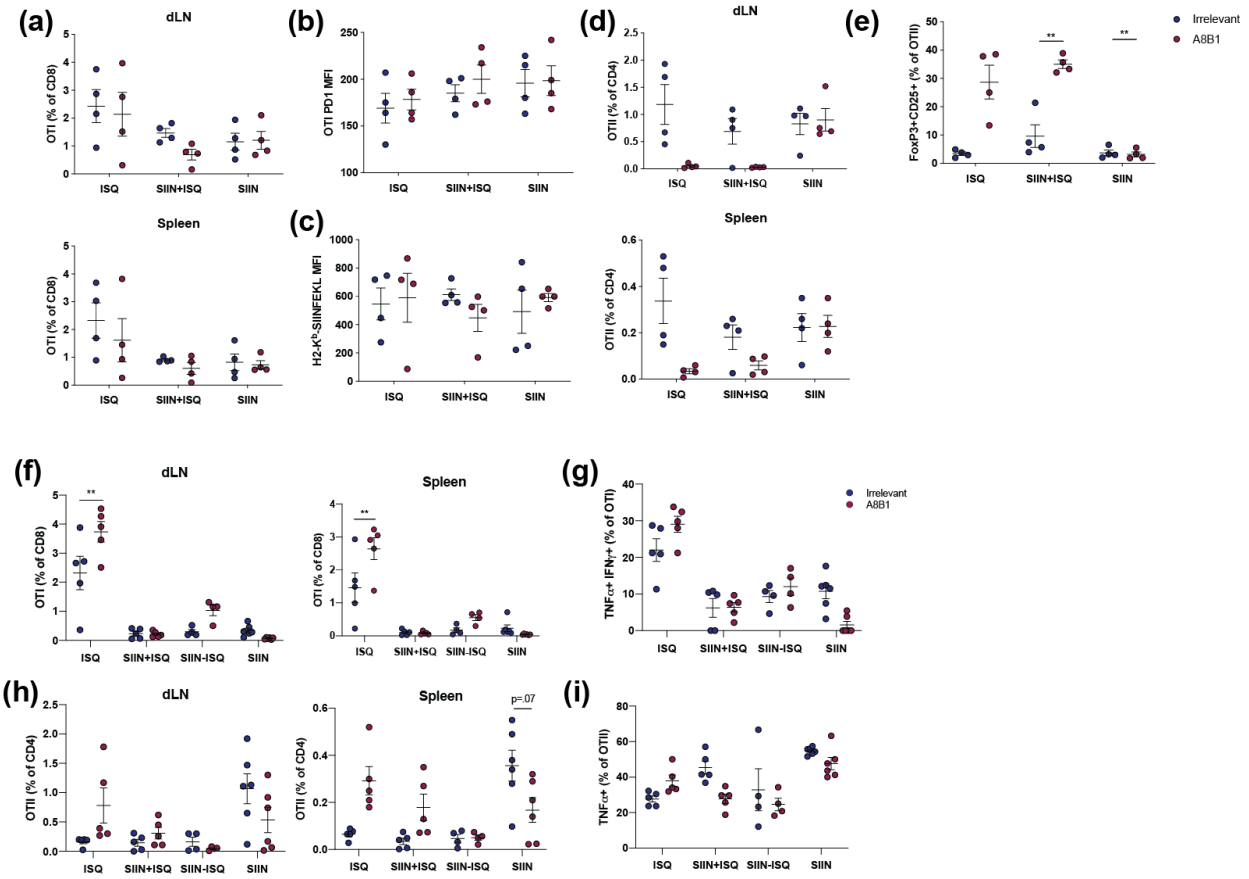


Figure 2.18: Tolerance to CD8 epitopes may lead to cross-tolerance of CD4 epitopes. a-d) Mice were dosed as in Figure 9a, but instead of Fab-OVA, mice received 0.5 $\mu$g of Fab-SIINFEKL, Fab-ISQ, or both. a) Percentage of OT-I in the dLN and spleen. b) MFI of PD-1 on OT-I. c) MFI of TCR on OT-I. d) Percentage of OT-II in the dLN and spleen. e) Percentage FoxP3+CD25+ Tregs on OT-II. f-j) Mice were dosed as in a) but instead with 5 $\mu$g Fab-SIIN, Fab-SIIN-ISQ, Fab-ISQ, or Fab-SIIN + Fab-ISQ. f) Percentage of OT-I in the dLN and spleen. g) Intracellular cytokine expression in OT-I after restimulation of cells from the dLN with SIINFEKL. h) Percentage of OT-II in the dLN and spleen. i) Intracellular cytokine expression in OT-II after restimulation of cells from the dLN with ISQ. Data are shown as mean  SEM. The experiment was performed once. Statistical analyses were performed using one-way ANOVA with Tukey's test. *P $<$ 0.05 and **P $<$ 0.01

T cells after treatment with A8B1-OVA (Figure 2.19a). Upon restimulation with cognate peptide, OT-I had reduced perforin, likely indicating release of perforin granules upon seeing antigen. Perforin upregulation was reversed in the absence of a spleen, and in Batf3$^{-/-}$ mice (Figure 2.19b-c). The perforin+ OT-I cells were not secreting other cytokines. Upon *ex vivo* restimulation with SIINFEKL after dosing with A8B1-OVA, OT-I were positive for either

perforin or TNF$\alpha$ (Figure 2.19c). Similarly, there were almost no OT-I cells that secreted both perforin and IL-2 (Figure 2.19d). This suggests that the OT-I cells containing perforin granules were not inflammatory.

To test the necessity of perforin for induction of T cell dysfunction, OT-I were crossed to perforin Prf1$^{-/-}$ deficient mice, yielding OT-I Prf1$^{-/-}$. OT-I Prf1$^{-/-}$ or littermate controls were CFSE labeled along with WT OT-II and adoptively transferred into mice. Mice received a single dose of A8B1-OVA and were sacrificed 4 d later. There were no differences in the number of OT-I or OT-II in the lymph nodes or spleen of mice receiving WT or Prf1$^{-/-}$ OT-I (Figure 2.19e). There were likewise no differences in the extent of proliferation, or upregulation of TOX and PD-1 (2.19f-g).

It is possible that the effect of perforin in OT-I would not be apparent until cells were faced with an adjuvanted challenge. Thus, the 21 d challenge experiment was conducted as previously with either WT or Prf1$^{-/-}$ OT-I and WT OT-II. Unexpectedly, Prf1$^{-/-}$ were less capable of responding to OVA and LPS challenge, both in mice that received Irrelevant-OVA and A8B1-OVA (Figure 2.19h). Despite impaired ability of OT-I Prf1$^{-/-}$ to respond to challenge, there was still greater deletion in mice that received A8B1-OVA compared to Irrelevant-OVA. Even more strikingly, in mice that received Prf1$^{-/-}$ OT-I, OT-II cells were incapable of responding to challenge, both in mice that received A8B1-OVA and Irrelevant-OVA (Figure 2.19i). Also interesting is the observation that PD-1 upregulation was greater in perforin deficient than WT mice (Figure 2.19j). These data indicate that perforin in CD8 T cells may actually enhance an immunogenic response in both CD8 and CD4 T cells, and is likely dispensable for erythrocyte-mediated tolerance induction.

## 2.4 Discussion

Induction of tolerance for therapeutic purposes will require a detailed mechanistic approach to be successful in the clinic. This study demonstrated that targeting antigen to erythrocytes in vivo leads to efficient presentation of antigen to T cells, the result of which drives antigen-

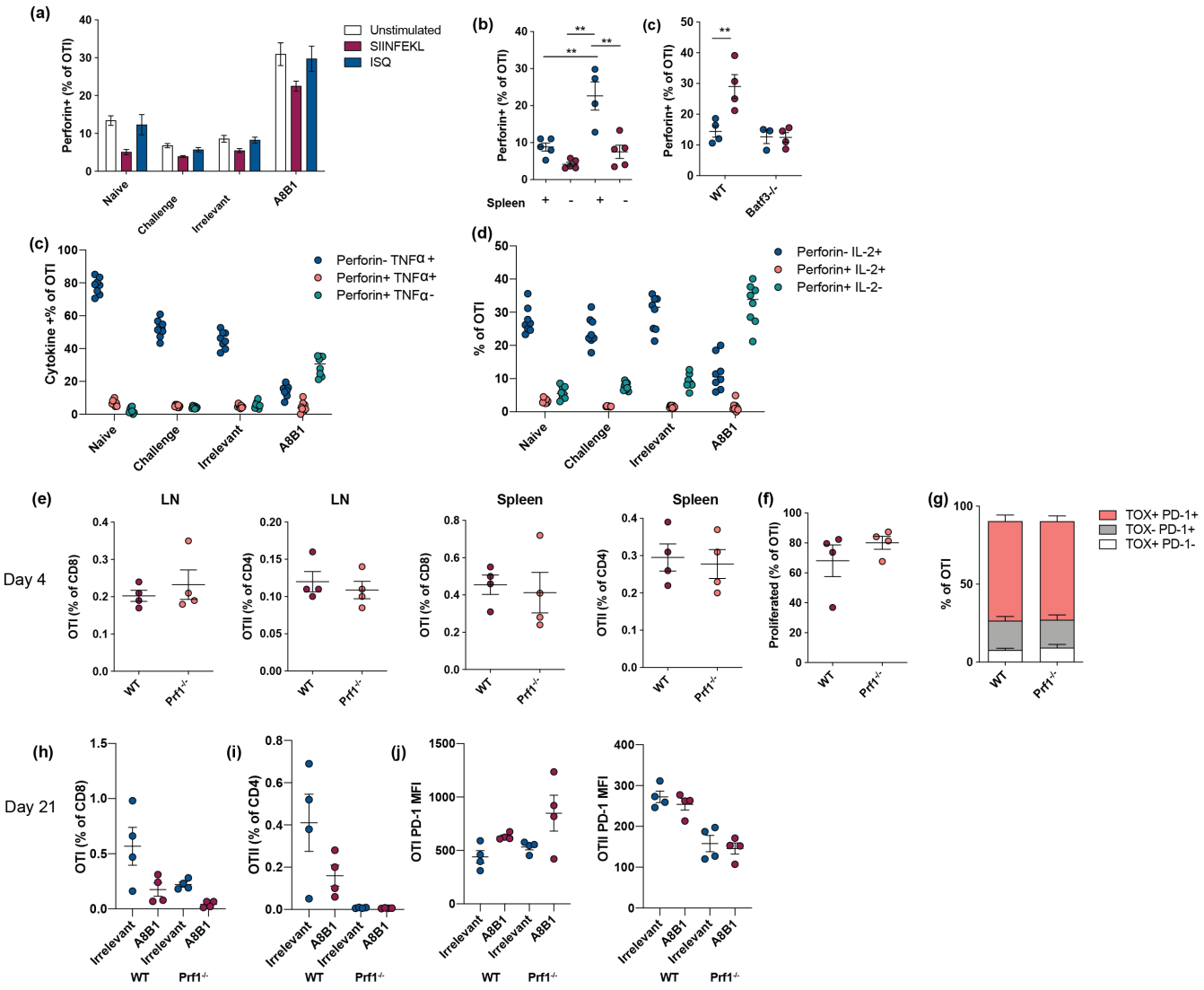


Figure 2.19: CD8 Perforin is dispensable for tolerance. Mice were dosed as in Figure 9a for a-j). a) 5 days after challenge, mice were sacrificed and restimulated with SIINFEKL or ISQ peptide, or left unstimulated. Perforin+ of OT-I. b) Perforin+ cells of OT-I in b) splenectomized or c) Batf3$^{-/-}$ mice. Cells from the LN were restimulated with SIINFEKL peptide and stained for intracellular cytokines. Percentage of OT-I that are positive for perforin and c) TNF$\alpha$ or d) IL-2. CFSE labeled WT or Perforin$^{-/-}$ OT-I were injected with OT-II into WT mice, and mice received 1 dose of 1 $\mu$g A8B1-OVA and spleens and LN were analyzed 4 days later. e) Percentage of OT-I and OT-II in the spleen and LN. f) Percentage of OT-I that have diluted CFSE. g) Percentage TOX+ PD-1+ cells of OT-I. h) Prf1$^{-/-}$ or WT OT-I were injected with OT-II into WT mice and dosed as previously. h) Percentage of OT-I dLN. i) Percentage of OT-II in the dLN. j) MFI of PD-1 on OT-I and OT-II in the dLN.

specific T cells to dysfunction. We developed an antibody fragment, A8B1, that binds with high affinity to mouse erythrocytes. A single, low dose of antigen was sufficient to drive rapid proliferation of cognate T cells, and the gene signature was one of self-tolerance, anergy, and exhaustion. Consistent with this, when compared to gene sets of other forms of T cell antigen encounter, the transcriptional profile was most similar to that of T cells that had escaped negative selection and seen self-antigen in the periphery [29]. Interestingly, the OT-I profile was also similar to that of human tumor-infiltrating T cells [29]. This could be because in cancer, tumors are continually shedding apoptotic cells and apoptotic bodies [225]. This, along with the immunosuppressive microenvironment of the tumor, provides continual antigen exposure to T cells with potent immunosuppression, a similar context to that of uptake of erythrocyte-associated antigen. The OT-II profile also correlated strongly with that of CD4 T cells in infection with *Plasmodium chabaudi*, a mouse model of malaria used to study blood-stage immunity [200, 226]. This suggests that parasites may be co-opting this eryptotic pathway to drive T cell dysfunction, as an association with inhibitory molecules on T cells has been associated with poor prognosis in patients with malaria [227, 228]. It is unlikely that this pathway would be co-opted by many viruses, however, because toll-like receptor stimulation of cDC1s would trigger activation of these cells and an inflammatory environment, which would overcome the tolerogenic environment of this pathway.

Aside from anergic signatures, upregulation of other co-inhibitory molecules commonly attributed to T cell exhaustion were upregulated, indicating that a single low dose of erythrocyte-associated antigen could be driving cells to exhaustion. However, at this early time point, these molecules could be upregulated due to overactivation. Still, the low expression compared to free antigen of effector molecules, such as granzymes and chemokines, suggests that the cells are not simply activated.

Consistent with this, flow cytometric analysis of T cells over a week after dosing with erythrocyte-associated antigen, and even after an adjuvanted antigenic challenge, led to upregulation of many molecules involved in exhaustion, including the master regulator of

exhaustion, TOX. This phenotype of exhaustion was associated with an inability to express TNF$\alpha$, even after addition of IL-2, but the retention in ability to produce some IFN$\gamma$. Although not to equivalent levels of erythrocyte-targeted antigen, soluble antigen alone was able to drive proliferation and deletion of OT-I cells. This is likely due to its presentation, perhaps through mannose receptor via the natural mannosylation of OVA, in the absence of costimulation [229]. However, the remaining T cells retained effector capacity, evidenced by both the RNA-seq data and their ability to produce inflammatory cytokines. Consistent with this, OT-I from mice experiencing free antigen had higher expression of TCF-1 and T-bet than with erythrocyte-associated antigen. This would suggest that with free antigen, cells would likely still be capable of responding to challenge with effector functions [68, 230]

T cells also strongly downregulated the TCR complex. This has been demonstrated in a number of contexts, including tumor infiltrating lymphocytes, peripheral tolerance, and in a high affinity parasite-specific TCR [204, 231, 232]. This likely serves as a means of increasing the threshold for stimulation, to both limit a pathogenic amount of T cell activation and to avoid a monoclonal response to a pathogen. In the presence of co-stimulatory molecules this could likely be overcome; Viola et al. demonstrated that triggering 8000 TCRs was necessary for a productive response and, with co-stimulation, that could be reduced to 1500. However, due to the high levels of co-inhibitory molecules, the threshold is likely high [212].

The effect of erythrocyte targeting was long-lasting in the OT-I compartment, as CD8 T cells had a reduced capacity to respond to antigen months following administration, long after the antigen was cleared from circulation. PD-1 remained upregulated, and remarkably, TCR remained downregulated. Future studies would need to be conducted to determine if PD1/PDL1, CTLA-4, and LAG-3 blockade months after initial dosing could restore functionality in these cells.

In the OT-II compartment there was little indication of lasting dysfunction. It is possible that 1 g was insufficient to drive sufficient CD4 dysfunction, and CD8 and CD4 T cells would require different amounts of antigen to lead to the same level of dysfunction. Alternatively,

the initial dysfunction seen in the OT-II cells could have been dependent on persistent exposure to antigen, and the cells reverted to functionality after antigen was removed. Lorentz et al. demonstrated that with erythrocyte-targeting, lasting humoral tolerance was achieved to a foreign antigen [146]. This suggests that CD4 tolerance is achievable, perhaps with an optimized dosing routine.

Consistent with this, in the EAE model utilized, which is driven primarily by pathogenic CD4 T cells, A8B1-MOG was able to drive the prevention of T cell activation and development of pathology in EAE, which was maintained even after we ceased dosing with antigen. This is consistent with studies that have demonstrated that dose and duration of the antigen exposure are important for driving T cell dysfunction [233, 234].

The benefit of early, more frequent dosing in this model could be explained by the fact that not all of the antigen-specific cells encountered erythrocyte-associated antigen with the amount dosed on day 0, and the cells that escape contribute to pathology. However, the fact that the high dose group with less frequent dosing still began to develop pathology suggests that most cells likely did encounter antigen. The more likely explanation is the duration of TCR stimulation in the erythrocyte-associated context. Figure 2.14b-c suggests that there is insufficient antigen presented to CD4 T cells 4 d after antigen dosing. Thus, dosing every 3 d likely maintained high levels of presentation to MOG-reactive CD4 T cells, and this persistent signaling led to dysfunction, which prevented the T cells from acquiring effector functions and causing pathology. Conversely, dosing every 7 d would limit the persistent exposure to MOG-reactive T cells. Future studies would need to be conducted to determine the appropriate dosing to achieve lasting CD4 and CD8 responses.

We were able to demonstrate tolerance not only to transgenic T cells, but also to OVA in a polyclonal naïve repertoire. It was also crucial to determine antigen-specificity of this approach. In the clinic, patients need to be suppressed only to the autoantigen, but be capable of responding to infections. We were able to demonstrate that mice were responsive to an irrelevant antigen, but hyporesponsive to OVA after administration of A8B1-OVA.

We demonstrated that the spleen is necessary for presentation of erythrocyte-associated antigen. This is consistent with a study that demonstrated that clearance of exogenously administered apoptotic cells is dependent on the spleen, and in particular on IL-10 production by splenic macrophages [183]. This suggests that a combination of persistent antigen exposure, as well as the immunosuppressive environment created by uptake of apoptotic cells, leads to the profound T cell dysfunction observed. Interestingly, in the half-life study, there was an initial bulk clearance of antigen that progressed over 24 hr that was independent of the spleen. Although this is much longer than the half-life of a typical protein this size, it was in contrast to a subsequent, longer half-life that took days. Over time, mice with a spleen began to clear erythrocyte-associated antigen faster than mice without a spleen, suggesting the spleen is responsible for clearance of a small amount of likely eryptotic erythrocytes per day.

Kontos et al. demonstrated accumulation of erythrocyte-associated antigen in the liver [147]. It is possible that this initial bulk clearance of antigen largely occurs in the liver, as do most proteins. Interestingly, that study also demonstrated presentation of antigen on class I MHC in the liver. This could explain some of the TOX upregulation in the absence of the spleen; the persistent antigen turnover could drive some T cell proliferation but is insufficient to drive the same level of dysfunction as when the spleen is present.

Batf3-dependent cross-presenting DCs were necessary for CD8 dysfunction. It is possible that macrophages took up antigen and transferred it to cDC1s, or that cDC1s took up erythrocytes directly and presented antigen [213]. Interestingly, both OT-I and OT-II cells showed upregulation of *Xcl1* in the RNA-seq data, suggesting that T cells could be producing XCL1 to attract these XCR1+ cDC1s to the T cell zone in the spleen [213]. For CD4 T cells, it is then likely that another cell type, such as conventional cDC2s, presented the erythrocyte-associated antigen. Administration of clodronate also prevented tolerance in the OT-I cells, suggesting that macrophages may engulf antigen for transfer to cDC1s. It is unclear how the CD4 T cells would then encounter antigen.

Although it is unclear how antigen is presented to CD4 T cells, it is clear that both CD4 and CD8 epitopes likely need to be present on the same antigen presenting cell, or in close proximity, to achieve maximal T cell stimulation and consequent dysfunction (Figure 2.18). It is evident that in the absence of CD4 help when dosing with A8B1-SIIN alone, there was poor presentation of antigen to CD8 T cells, as is immunological dogma. However, it is interesting that there also seems to be cross-talk from the CD8 T cells to the CD4 T cells. At a higher dose of A8B1-ISQ, CD4 T cells were robustly activated, instead of being tolerized. When A8B1-SIIN was dosed at the same time as A8B1-ISQ, there were fewer CD4 T cells at sacrifice. When both epitopes were on the same antigen, yielding A8B1-SIIN-ISQ, there were almost no CD4 T cells at sacrifice. This effect seemed to only be apparent with erythrocyte-targeted antigen, as Irrelevant-OVA did not lead to this phenomenon.

This leads us to pose the hypothesis that perhaps antigen is presented by an unknown cell type to CD4 T cells, to activate them. This CD4 T cell may then interact with a cDC1 presenting antigen to CD8 T cells, and thereby activate the CD8 T cells by providing the necessary IL-2, as is consistent with the canonical three-cell hypothesis. In a low dose setting, endogenous CD8 Fab-specific T cells may be sufficient to lead to OT-II deletion (Figure 2.18d), whereas in a high dose setting, a higher number of CD8 T cells, provided by the OT-I cells, is needed to promote OT-II T cell deletion (Figure 2.18h). The mechanism by which OT-I contribute to OT-II deletion is likely not through perforin, as perforin-deficient OT-I had little effect on OT-II tolerance (Figure 2.19). However, the OT-II cells were not able to expand in mice receiving perforin-deficient OT-I and Irrelevant-OVA either, limiting its interpretation.

Although this technology is effective in inducing tolerance via T cell dysfunction, a limitation is in the setting of an active B cell response. If an autoantigen was delivered to erythrocytes, it would allow for a long circulating time of the autoantigen, and thus accumulation of anti-autoantigen antibody and immune complex accumulation on the erythrocyte. This would trigger robust immune activation. To overcome this, B cells and plasma cells

would need to be depleted with an anti-CD20 antibody and bortezomib, respectively, before dosing. Alternatively, prophylactic tolerance could be induced in this setting.

This study provides insight into the use of erythrocyte-associated antigen for therapeutic tolerance. We demonstrated the ability to not only prevent the induction of a potent T cell response to both TCR transgenic and endogenous T cells, but also to induce dysfunction in already activated T cells. In the prophylactic setting, this has implications for induction of tolerance to therapeutic biological drugs to avoid an anti-drug antibody response. In the therapeutic context, it has implications for a variety of autoimmune diseases, for which there are known autoantigens, to reverse the course of disease after depleting B cells. Furthermore, this technology may be used as a simple tool to study T cell exhaustion and dysfunction, particularly to apoptotic antigen.

## 2.5 Materials and Methods

### *2.5.1 Mice*

Mice were maintained in a specific pathogen-free facility at the University of Chicago. The experiments and procedures in this study were performed in accordance with the Institutional Animal Care and Use Committee. Female C57BL/6 mice were used as wild type mice in all studies purchased from The Jackson Laboratory. OT-I (stock no: 003831) and OT-II (stock no: 004194) were crossed to CD45.1 mice (stock no: 002014) to yield congenically labeled OT-I and OT-II. Batf3$^{-/-}$ were bred in house. Splenectomized and sham splenectomized C57BL/6 mice were purchased from The Jackson Laboratory. OT-I were crossed in house with Prf1$^{-/-}$ (stock no: 002407) from the Jackson Laboratory to yield OT-I Prf1$^{-/-}$.

### *2.5.2 Phage Display*

M13 phage library containing a synthetic human Fabs based on the 4D5 scaffold was generously provided by Anthony Kossiakoff. Peripheral blood mononuclear cells (PBMCs) were

isolated from C57BL/6 mice. The library was incubated with PBMCs for 1 hr on ice. Cells were spun down, and supernatant was added to 10 million mouse erythrocytes for 1 hr on ice. Cells were washed 4 times, and phage was eluted with sodium citrate pH 2.6. Phage was propagated overnight in XL1-blue E. coli. Phage was precipitated by addition of 1/5 volume 20% PEG 8K, 2.5 M NaCl and resuspended in PBS. Panning was repeated for a total of 4 rounds. After the second, third, and fourth rounds of panning, a sample of phage library was added to erythrocytes and subjected to flow cytometry using an anti-M13 secondary antibody (Biolegend) to assess enrichment. After the fourth round of panning, XL1-blue cells were infected with phage, and plated on LB-agar plates overnight. Single colonies were picked and grown in 2 mL cultures supplemented with Ampicillin and M13K07 helper phage (New England Biolabs). Supernatant was collected after 16-20 hr, and phage was precipitated. 96 individual phage clones were added to mouse erythrocytes, and flow cytometry was conducted using the anti-M13 antibody to assess binding. The best binders were sequenced using sanger sequencing, and top clones were cloned into mammalian protein expression vectors.

### *2.5.3 Fab Cloning*

Fab sequences were cloned out of the M13 vectors and into a human endothelial kidney (HEK) expression vector, Abvec2.0 (Table 2.1). For Fab payload sequences, such as ovalbumin, DNA was purchased from Genscript and cloned into the HEK vectors at the C terminus of the heavy chain. Amino acid sequence of antigens can be found on Table 2.2.

Table 2.1: Primers to amplify Fabs out of M13 vector

| **Primer** | **Sequence** |
|---|---|
| Forward VL | 5'-tgtgcctggccggccgcgccctggccgatatccagatgacccagtccccga-3' |
| Reverse VL | 5'-acgctaggggcagccaccgtacgtttgatctccaccttggtaccctgtccga-3' |
| Forward VH | 5'-gcctggctgggcgcgccctggccgaggttcagctggtggagtctgg-3' |
| Reverse VH | 5'-cccttggtgctagccgaggagacggtgaccagggtt-3' |

### *2.5.4 Fab Expression and Purification*

Fabs were expressed in HEK293T suspension cells in FreeStyle 293 Expression Medium (Thermo Fisher Scientific). At 1 million cells/mL in log-phase growth, cells were transfected with 1 $\mu$g of plasmid and 2 $\mu$g of polyethylenamine in 40 $\mu$L OptiPRO SFM (Gibco) per million cells. Transfected cells were cultured for 6 d in shake flasks. The cells were then pelleted by centrifugation, and the supernatant was filtered through a 0.22 $\mu$mfilter and pH-adjusted to 7.0 using 1 M Tris buffer, pH 9.0. The Fabs were then purified by affinity chromatography using a 5 mL HiTrap Mabselect Protein A column (GE Life Sciences) via fast protein liquid chromatography. The column was first equilibrated with 5 column volumes (CVs) of PBS at 5 mL/min. The crude Fab solution was then flowed over the column at 5 mL/min and the column washed with 10 CVs of PBS at 2 mL/min. Fab was then eluted with 0.1 M glycine-HCl, pH 2.6, and neutralized with1 M Tris buffer, pH 9.0. Elution peaks were pooled and dialyzed into PBS. Where necessary, Fabs were concentrated (Amicon). Because the Fabs are prone to aggregation, dynamic light scattering was conducted on samples and filtered through 0.22 $\mu$m PES filters until the sample was >95% pure by intensity. For all studies, produced proteins were verified to contain <.01 endotoxin units by HEK-TLR4 assay. Proteins were aliquoted and frozen at -80.

### *2.5.5 Fab Characterization*

To characterize binding to erythrocytes and PBMCs, mouse blood was isolated using Histopaque per manufacturer's protocol. Erythrocytes and PBMCs were collected from respective fractions in the gradient were diluted in PBS+2% BSA. Fab was fluorescently labeled with an NHS-ester conjugated dye that reacts with free amines on the Fab (Dyomics). Erythrocytes were stained on ice with increasing concentrations of Fab in 5 mL polystyrene tubes in PBS + 2% BSA for 20 min and protected from light. Erythrocytes were washed in PBS+2% BSA and flowed immediately. Fixation using standard buffers was avoided because it lysed the erythrocytes. For assessment of Fab binding to PBMCs by flow cytometry, Fab was added

Table 2.2: Amino acid sequences of A8B1 Fab payload

| Payload | Sequence |
|---|---|
| OVA | GSGGGGSGGGGSGGGGSGGGGSMGSIGAASMEFCFD<br>VFKELKVHHANENIFYCPIAIMSALAMVYLGAKDSTR<br>TQINKVVRFDKLPGFGDSIEAQCGTSVNVHSSLRDILN<br>QITKPNDVYSFSLASRLYAEERYPILPEYLQCVKELYRG<br>GLEPINFQTAADQARELINSWVESQTNGIIRNVLQPSSV<br>DSQTAMVLVNAIVFKGLWEKAFKDEDTQAMPFRVTE<br>QESKPVQMMYQIGLFRVASMASEKMKILELPFASGTM<br>SMLVLLPDEVSGLEQLESIINFEKLTEWTSSNVMEERK<br>IKVYLPRMKMEEKYNLTSVLMAMGITDVFSSSANLSG<br>ISSAESLKISQAVHAAHAEINEAGREVVGSAEAGVDA<br>ASVSEEFRADHPFLFCIKHIATNAVLFFGRCVSP |
| MOG | MEVGWYRSPFSRVVHLYRNGK |
| SIIN | GSGGGSGLEQLESIINFEKL |
| ISQ | GSGGGSAESLKISQAVHAAHAEINEAGR |
| SIIN-ISQ | GSGGGSGLEQLESIINFEKLTEWTSSGGGSAESLKISQA<br>VHAAHAEINEAGR |

at 200 nM and incubated for 20 minutes on ice.

### *2.5.6 Determination of In Vivo Fab Half-Life*

10 $\mu$g of each Fab was injected into WT mice. Mice were bled by making a small incision over the injection site, and subsequently 2-5 $\mu$L blood were taken from this site. Blood was washed and anti-human Fab (Jackson Immunoresearch) was added at a 1:400 dilution in PBS+2% BSA for 15 minutes at room temperature. Samples were flowed immediately after washing.

### *2.5.7 Determination of Antibody Titer*

ELISA plates (Nunc Maxisorp, ThermoFisher) were coated overnight with 10 $\mu$g/mL Fab. Mice were dosed weekly with 10 $\mu$g A8B1, E2A3, or F3F1 Fab, and bled three days later. Blood was collected in a heparinized capillary tube per IACUC protocol. Blood was spun down at 300xg for 5 minutes to pellet erythrocytes, and plasma was collected. Plasma was

diluted in 2% BSA 1:100 for the first dilution, and 10-fold dilutions subsequently. After washing and blocking plates coated with Fab, diluted plasma was added for 2 hours at room temperature, and washed. Antibodies were detected using an HRP-conjugated anti-mouse IgG antibody for one hour at room temperature diluted in 2% BSA (Southern Biotech). TMB solution was added, and 10% sulfuric acid to stop the reaction. Titers were calculated by averaging 4 blank wells, adding 4 times the standard deviation of these wells, and subtracting this value from the optical density (OD) readings of all samples. The reciprocal of the last dilution with detectable signal is the titer plotted.

### *2.5.8 Fab Pulldown on Erythrocyte Membranes*

1 mL of mouse blood was centrifuged with a Histopaque-1077 (Sigma) gradient to remove PBMCs and plasma. ACK lysis buffer (Gibco) was added at a ratio of 10:1 initial volume of blood in 1.5 mL microcentrifuge tubes. Lysis was conducted on ice to prevent proteolysis for 5 minutes. Microcentrifuge tubes were spun down at 21,000 x g for 5 minutes to pellet ghosts. This was repeated 10 times, until ghosts were white. Subsequently, 10 $\mu$g Fab were incubated with 10 $\mu$g erythrocyte ghost for 30 minutes in PBS. 20 $\mu$L Protein A magnetic beads (Dynabeads, Invitrogen) were washed in PBS and incubated with the ghost and Fab for 30 minutes in a volume of 200 $\mu$L. Fab-ghost complexes were washed 5 times, and eluted with Laemmli buffer + 50 $\mu$M beta mercaptoethanol. Elutions were boiled at 95°C for 10 minutes and loaded onto an SDS-PAGE gel.

### *2.5.9 Determination of Hematological Parameters*

Mice were bled 24 hr after dosing with 3 doses of Fab-OVA every third day. 50 $\mu$L of blood were analyzed for complete blood count (CBC) on a Beckman Coulter AcT.

### *2.5.10 Adoptive Transfer*

Spleens and lymph nodes were isolated from TCR transgenic mice. OT-I and OT-II T cells were isolated by negative magnetic bead selection using a CD8 (Stemcell) and CD4 (Stemcell) negative selection kit, respectively. In experiments assessing T cell proliferation, cells were labeled with 5 M carboxyfluorescein succinimidyl ester (CFSE). For RNA sequencing, 1 million OT-I and OT-II in DMEM were injected through the tail vein. For tolerance experiments, 500,000 OT-I and 500,000 OT-II in DMEM were injected intravenously through the tail vein.

### *2.5.11 RNA Sequencing Library Preparation*

Mice were adoptively transferred with 1 million OT-I and 1 million OT-II at day 0. At day 1, mice received saline, 1 $\mu$g A8B1-OVA, molar equivalent of ovalbumin, or 10-fold greater molar equivalent of ovalbumin (Endograde). Four days later, mice were sacrificed and spleens and lymph nodes were pooled. OT-I and OT-II were sorted into Trizol using fluorescence activated cell sorting (FACS) and frozen at -80°C. RNA was extracted (Qiagen), and three mice were pooled per replicate. RNA integrity was measured by the Agilent 2100 Bioanalyzer, and all samples had a RNA integrity number greater than 8.3. RNA was converted to cDNA using SmartSeq-v4 (Takara, cat no. R400752). Library was prepared using Nextera XT DNA library preparation kit (Illumina, cat no. FC-131-1096). All samples were pooled and sequenced using Illumina HiSeq 4000 (2x100 paired-end).

### *2.5.12 RNA Sequencing Analysis*

Unless otherwise specified, all data analyses were performed under the R programming and software environment for statistical computing and graphics version 3.6 (R Core Team, 2019). FastQ file for each sample was assessed for quality using the FastQC tool (version 0.11.5). For mRNAseq, raw reads were aligned to the GRCh38 primary genome assembly

using Spliced Transcripts Alignment to a Reference (STAR) aligner (version 2.7.2a) 1-pass algorithm [235]. After sorting the bam files in lexicographical order with the sambamba program [236] (v0.5.4), we assigned the reads to exon features annotated in Ensembl Mus musculus GRCm38 annotation (release 97) using the FeatureCounts tool from the subread package (version 1.5.2) and summarized the read counts by genes [237]. The post alignment quality control was carried out with Picard tools (version 2.18.7). Specifically, we examined the QC data regarding the alignment summary, gene body coverage, read distribution, and ribosomal RNA depletion rate. We used alignment-free transcriptome quantification method kallisto (v0.46.1) to estimate the transcript abundance of each sample [238]. We then summarize the transcript-level estimates for gene-level analysis using R package tximport and GRCm38 annotation. After removing the genes with zero read counts across all samples, we calculated the normalization factors to scale the raw library sizes using the calcNormFactors function in the edgeR R package with trimmed mean of M-values (TMM) option enabled [239]. The normalized count per million (CPM) value was log2-transformed for each gene. We removed heteroscedascity from the count data using the voomWithQualityWeights function from the limma package. We then fit a linear model for each gene using the limma algorithm and ranked the genes for differential expression using the empirical Bayes method. The differentially expressed genes were identified using the Benjamini–Hochberg procedure for multiple testing correction. The adjusted P-value threshold was set at 0.05.

Self-contained gene set tests were performed with the mroast function with publicly available microarray gene sets on GSEA (https://www.gsea-msigdb.org/gsea/msigdb/search.jsp), which provide the top 200 differentially expressed genes between two groups of interest [240]. Where not available on GSEA, microarray data was accessed on the Gene Expression Omnibus (https://www.ncbi.nlm.nih.gov/geo/) and analyzed with the GEO2R. Top 200 differentially expressed genes by fold change were used for analyses.

### *2.5.13 Challenge*

For experiments where mice received only ovalbumin challenge, mice were challenged with 20 °Cg EndoGrade OVA (Hyglos) and 50 ng LPS (Sigma) total in the 4 hocks while mice were anesthetized with isofluorane. In endogenous tolerance experiments, mice were challenged with 10 $\mu$g influenza nucleoprotein (Anaspec) and 10 $\mu$g Endograde OVA (Hyglos) with CpG ODN 1826 (InvivoGen).

### *2.5.14 Preparation of Single-Cell Suspensions*

Draining lymph nodes (axillary, brachial, inguinal, and popliteal) and spleen were isolated from mice. Lymph nodes were digested for 45 min at 37°C in DMEM with 1 mg/mL collagenase IV (Worthington). LN and spleen were homogenized using syringe plungers onto 70 $\mu$M strainers. Spleens were lysed using 3 mL ACK lysis buffer (Gibco) for 5 min and quenched with 30 mL DMEM. Cells were counted using a fluorescent cell counter.

### *2.5.15 Flow Cytometry*

For phenotypic analysis, 2-4x$10^6$ cells were stained in PBS with 1:200 CD16/CD32 Fc Block (Biolegend) and 1:500 Live/Dead fixable dye (ThermoFisher) at 4°C for 15 minutes. Cells were washed in PBS + 2% FBS. Cells were stained with 1:200 surface antibodies at 4°C for 20 minutes. Cells were washed in PBS + 2% FBS and fixed in 2% paraformaldehyde. For intracellular staining, cells were fixed and permeabilized using Cytofix/Cytoperm (BD Biosciences) at 4°C for 20 minutes, and cells stained intracellularly in Perm Wash Buffer (Biolegend) with 1:200 antibodies at 4°C for 30 minutes. For transcription factor stain, FoxP3 Transcription Factor Kit (eBioscience) was used per manufactures protocol, and nuclear stains were applied for 1 hour at 4°C. Tetramer staining was conducted after Live/Dead staining. First, cells were incubated at 37°C for 30 minutes in 50 nM dasatinib. Tetramers were added directly to the cells in dasatinib, and stained for 1 hr at room temperature.

H2-$K^b$-SIINFEKL pentamer was purchased from ProImmune, and used at a final dilution of 1:10. NP tetramers were provided by the NIH, and used at a final concentration of 50 nM. After tetramer stain, cells were washed and surface stain performed as described above.

### *2.5.16 Ex Vivo Restimulation*

For restimulations involving flow cytometry analysis of intracellular cytokines, 2 million splenocytes or LN cells were plated in 200 $\mu$L of DMEM + 1% penicillin/streptomycin + 10% fetal bovine serum in a round bottom 96-well plate. SIINFEKL (Genscript)and ISQ (Genscript) peptides were added at a final concentration of 1 $\mu$g/mL. CD8 NP peptide (Anaspec) was added at 10 $\mu$g/mL, and CD4 NP peptide (Anaspec) at 2.5 $\mu$/mL. After 2 hr of restimulation with peptide, brefeldin A (GolgiPlug, BD Biosciences) was added to block secretion of cytokines. Four hours after addition of brefeldin A, cells were washed and stained for flow cytometry. For 3 day *ex-vivo* restimulation, 1 million splenocytes or LN cells were plated in a 96-well round bottom plate. SIINFEKL or ISQ were added at a final concentration at 1 $\mu$g/mL, and Grade V ovalbumin (Sigma) at a final concentration of 100 $\mu$g/mL. For experiments involving IL-2, IL-2 was added to restimulation at 100U/mL. After 3 d, supernatant was taken for cytokine analysis via ELISA.

### *2.5.17 EAE Model*

B6.SJL mice were vaccinated with $MOG_{35-55}$ (Hooke Labs) emulsified in complete Freud's adjuvant. Eleven days later, spleens were harvested, and single cell suspensions created. To enhance the encephalitogenic T cells, cells were restimulated with $MOG_{35-55}$ peptide (20 $\mu$g/mL) and cultured in the presence of IL-12 (20 ng/mL) (RD Systems) and anti-IFN$\gamma$ (7 $\mu$g/mL) (BioXCell, Clone PS/2) for 3 d. Cells were spun down and washed, counted, and 10 million cells were injected intraperitoneally into naïve C57BL/6 mice, which received various treatment schedules of A8B1 recombinantly expressed with the $MOG_{35-55}$ peptide. As a positive control for reversal of EAE, 10 mg/kg anti-VLA-4 antibody (BioXCell, clone

XMG1.2) was injected i.p. every 2 d. Mice were scored daily starting from day 4 until the study's termination. Scoring was performed blind, by a person unaware of treatment or previous scores.

### *2.5.18 Macrophage Depletion*

To deplete macrophages, two doses of 400 $\mu$g of anti-CSF1R antibody (Clone AFS98, BioX-Cell) were injected i.p. every 4 days and spleens were analyzed 24 hours after the last injection. In an alternative strategy, 200 $\mu$L clodronate liposomes or PBS-loaded liposomes (Liposoma B.V.) were administered i.v. every 3 or 4 days beginning the day before adoptive transfer of OT-I and OT-II cells and throughout the duration of the experiment, until sacrifice.

### *2.5.19 Statistical Analysis*

Statistically significant differences between experimental groups were determined using Prism software (v6, GraphPad). All statistical analyses are stated specifically in the figure legends for all experiments. For most experiments, unless otherwise specified in figure legend, one-way ANOVA was performed with a Tukey's post-hoc test to correct for multiple comparisons. Comparisons were significant if $p < 0.05$. For the RNA-seq experiment, a detailed description of the statistical analysis can be found in Methods.

## 2.6 Author Contributions

Jennifer Antane performed analysis of RNA sequencing data. Andrew Tremain assisted in animal experiments for RNA-seq experiments and aided in RNA extraction and library preparation. Jaeda Roberts and Anya Dunaif assisted in protein production and purification. Roberto De Loera aided in characterization of biophysical parameters and binding of erythrocyte Fabs. Jaeda Roberts, Anya Dunaif, Mindy Nguyen, Rachel Wallace, and Rachel

Weathered aided in performing mouse experiments. Lucas Bailey led the phage panning on erythrocytes. Kristen Lorentz and Sarah Zuerndorfer synthesized A8B1-MOG and led EAE experiments. Stephan Kontos and Jeffrey Hubbell guided and advised the experiments presented.

## 2.7 Funding

This work was supported by funding from the National Science Foundation Graduate Research Fellowship Program, University of Chicago, and Anokion S.A.

## 2.8 Acknowledgements

I am grateful to members of the Hubbell laboratory for helpful comments and suggestions. I thank J.M. Williford and S. Gomes for technical assistance. I would like to thank Ani Solanki in the Animal Resources Center, who was essential in performing a number of mouse procedures, including injections and bleeding. I would like to thank the DNA Sequencing Core Facility at the University of Chicago. Flow cytometry data was acquired using the Cytometry and Antibody Technology Core Facility, with special help from Michael Olson and David Leclerc. The phage library was kindly provided by Anthony Kossiakoff. I would like to thank Tomasz Slezak and Elena Davydova for their guidance in phage display and Fab characterization. I thank the Center for Research Informatics, which is funded by the Biological Sciences Division at the University of Chicago with additional funding provided by the Institute for Translational Medicine, CTSA grant number UL1 TR000430 from the National Institutes of Health, and The University of Chicago Comprehensive Cancer Center Support Grant (NIH P30CA014599).

## 2.9 Data Availability

Gene expression data obtained by RNA-seq have been deposited in the NCBI Gene Expression Omnibus with the accession number GSE155679.

## 2.10 Conflicts of Interest

This work was funded in part by Anokion SA. J.A.H, K.M.L and S.K. are inventors on patents associated with this work which are licensed to Anokion. J.A.H. consults for and holds equity in Anokion. S.Z and S.K. are employees of Anokion, and K.M.L. was at the time of study an employee of Anokion; these authors hold equity in Anokion.

# CHAPTER 3

# DEVELOPMENT OF AN ANTIBODY FRAGMENT TO TARGET LIVER SINUSOIDAL ENDOTHELIAL CELLS FOR TOLERANCE

## 3.1 Abstract

The liver is known to harbor immunomodulatory properties. In the steady state, it is primed to induce immune tolerance, since it is constantly exposed to toxins and microbial byproducts and must avoid a pathogenic state of inflammation. Liver sinusoidal endothelial cells have been shown to contribute to this tolerogenic environment, with their ability to induce T cell deletion and regulatory T cells. The purpose of this study was to target antigen to liver sinusoidal endothelial cells (LSEC) specifically, by targeting liver and lymph node sinusoidal C-type lectin (LSECtin). An antibody fragment was developed to target LSECtin with high affinity and specificity. Antigen targeted to LSECtin was presented less efficiently than free antigen alone, and this could not be overcome by cathepsin cleavage of the targeting molecule from the antigen, or by the addition of endosomal escape peptides. Encapsulation of antigen in polymerosomes decorated in the targeting molecule were able to target LSECs and induce proliferation of cognate T cells, but at the doses tested appeared not to induce tolerance.

## 3.2 Introduction

The liver's main functions in the body are in detoxification, metabolism, and production of important substances such as albumin and bile. However, an underappreciated role of the liver is in immunity. The liver is subject to blood-borne pathogens to which it must mount a productive immune response, such as during infection with hepatitis viruses. It is home to the largest population of tissue resident macrophages, Kupffer cells, as well as the largest concentration of Natural Killer cells and Natural Killer T cells [241]. Furthermore,

the anatomy of the liver is suited for immune interactions. Blood slows significantly as it passes through the liver sinusoids, and the endothelium is fenestrated and lacking a basement membrane, exposing sub-endothelial cells residing in the space of Disse to circulating cells [242]. The low shear enables intimate interactions between circulating lymphocytes with liver sinusoidal endothelial cells (LSECs) as well as the sub-endothelial cells, without the need for lymphocyte rolling, adhesion, and extravasation necessary in other tissues [243].

However, the liver receives 70-80% of its blood from the portal vein, which contains byproducts derived from the intestines [244]. These byproducts are primarily dietary nutrients, but also include microbial byproducts such as lipopolysaccharide (LPS) [245]. These intestinal byproducts and other potential immunogenic molecules in systemic circulation have the potential to trigger robust immune activation in the liver, but because of the hundreds of essential functions of the liver it is crucial to limit inflammation and downregulate immune activation. In fact, much of the pathology observed during liver infection by hepatitis viruses is a result of inflammation of the liver as opposed to viral destruction itself [244]. Liver inflammation, if unchecked, leads to liver fibrosis, cirrhosis, and end stage organ failure [246].

Consistent with this need to downregulate immune responses to avoid unnecessary inflammation, there have long been reports of the tolerogenic nature of the liver. Among the first reports of a tolerogenic role of the liver was in transplants. It was found that transplanted porcine livers were accepted across Major Histocompatibility Complex (MHC) barriers in the absence of immunosuppression, whereas other organs were readily rejected [247]. Additionally, in humans, transplant of a liver simultaneously with a kidney was more effective at prolonging graft survival than sequential kidney transplants, suggesting systemic immunosuppression mediated by the liver to alloantigens [248]. Futhermore, injection of allogeneic cells into the portal vein results in tolerance to alloantigens, and intestinal drainage of oral antigen into the liver is required for oral tolerance [249, 250].

A cell type critically involved in the dichotomy between immunity and tolerance in the

liver is the LSEC. As the first point of contact in the liver, LSECs are continuously surveilling the blood for toxins, waste, and pathogens, and they are thought to be the most efficient cell type in the body for endocytosis [251, 252]. To accomplish this essential role of clearance and surveillance, they have many scavenger receptors, such as SR-A1, SR-B1, CD36, stabilin 1, stabilin 2, LOX-1, LYVE-1, and LRP-1 [253]. With these receptors, LSECs perform a vital role in clearing physiological byproducts, such as LDL, HDL, advanced-glycation end products, aldehyde-modified proteins, hyaluronan, and C-reactive protein, but also microbial byproducts such as LPS and lipoteichoic acid. LSECs also contain various lectins, such as mannose receptor, L-SIGN, and liver and lymph node sinusoidal endothelial cell C-type lectin (LSECtin) [254]. These are important pattern recognition receptors that recognize conserved carbohydrates on viruses including Hepatitis C virus and SARS-CoV. LSECs also express high levels of the immunoglobulin Fc receptors Fc$\gamma$RIIb and FcRn, consistent with a role in regulation of an immune response [255, 256].

LSECs express components necessary for T cell activation, including MHC class II and co-stimulatory molecules [252]. LSECs can process and present antigen to CD4+ T cells, but they may also cross present antigen to CD8 T cells, a capability that has otherwise only been described in dendritic cells and subset of macrophages [257]. LSECs express seven TLRs that enable them to recognize pathogen associated molecular patterns (PAMP) and mount subsequent productive immune responses [258]. Upon TLR stimulation, LSECs have been shown to produce immunogenic cytokines such as IFN$\beta$, IL-6, and IL-12, and may activate CD8+ T cells as well as control hepatitis B virus replication in hepatocytes [258–260]. In a recent immunoengineering approach, nanoparticles coated with melittin, a natural defense peptide, were preferentially targeted to LSECs compared to unmodified nanoparticles. This triggered robust activation of LSECs, evidenced by upregulation of costimulatory molecules and secretion of proinflammatory cytokines, which overcame their pro-tolerogenic niche in the liver and led to a prevention of liver metastases in a number of cancer metastases models [261].

Although capable of mounting a productive response, in the physiological, non-inflamed state, LSECs are important for suppression of inflammation. LSECs have been shown to present antigen to CD4 T cells, the result of which is diversion away from a Th1 fate, Treg induction, and even suppression of inflammatory CD4 T cells [242, 262–264]. In the absence of inflammatory signals, LSECs can cross-present antigen to trigger CD8 T cell deletion and hyporesponsiveness, and may contribute to CD8 tolerance of tumor antigens [257, 263, 265]. It has further been shown that LSECs can in fact deter dendritic cells from inducing immunity *in vivo* [266]. This may be partially explained by the fact that LSECs exposed to LPS, which is abundant in the portal blood, have reduced nuclear localization of NF-$\kappa$B, downregulate lymphocyte adhesion and costimulatory molecules, and therefore have a reduced capacity to present antigen to T cells in an inflammatory manner [267].

Thus, there is an interest in specifically targeting LSECs for immunological purposes. It has been demonstrated that antigen delivered to LSECs via the mannose receptor *in vivo* leads to efficient cross-presentation of antigen to CD8 T cells, and a functional hyporesponsiveness of these T cells [257]. Although a promising target, mannose receptor is also highly expressed by Kupffer cells and hepatic dendritic cells in the liver, as well as widely on APCs throughout the body, which could potentially lead to activation as opposed to tolerance [268, 269]. The candidate explored here is liver and lymph node C-type lectin (LSECtin), as it is expressed very highly on LSECs, and LSECs are the only cells that express this receptor in the liver [270]. It is a scavenger receptor that is capable of binding mannose and N-acetyl-glucosamine. Although also found on lymphatic endothelial cells and subsets of plasmacytoid dendritic cells, because antigen is quickly delivered to the liver when administered systemically, it is reasonable to imagine that antigen targeted to LSECtin would be engulfed exclusively by the many LSECs lining the liver sinusoids. Given the role of mannose in cross presentation, it is also reasonable to hypothesize that targeting a similar C-type lectin, LSECtin, would also lead to cross-presentation, and that this antigen would be presented efficiently to circulating T cells. No method of targeting LSECtin was available;

thus, the purpose of this study was to develop a binder to LSECtin, deliver antigen to this route, and determine if we could induce tolerance to the antigen.

## 3.3 Results

### *3.3.1 Liver Sinusoidal Endothelial Cell Isolation and Characterization*

Given the heterogeneity in isolation and identification of LSECs in the literature, we first aimed to conduct a phenotypic analysis to choose the best method of identifying the cells [271]. A common method for isolation is density centrifugation, which is beneficial in that is leaves cells largely undisturbed; however, it yields low purity, confounding potential results [272]. Another method is immunomagnetic sorting based on expression of CD146 [273]. Although improved over density centrifugation, this method still only yields 80-90% purity, because CD146 is reported to be expressed by other cells in the liver, such as hepatic stellate cells [274]. Thus, we opted to use fluorescence activated cells sorting (FACS) to isolate LSECs.

Stabilin-2 is a scavenger receptor highly expressed by LSECs and most other sinusoidal endothelial cells in the body [275]. CD31 is a common marker of endothelial cells, and although there are mixed reports of surface expression, we sought to determine if it will be a reasonable marker to identify LSECs [276]. We perfused mice as described previously and conducted a centrifugation gradient to remove most hepatocytes and lymphocytes [277]. Flow cytometry revealed populations with differential expression of CD31 and Stabilin-2 (Figure 3.1a). To determine which populations were LSECs, we analyzed each population for expression of other canonical LSEC markers, such as CD54 (ICAM-1), CD32b (Fc$\gamma$RIIb), CD36, and Lyve-1 (Figure 3.1b). Analysis revealed that the CD31 high Stabilin-2 high population most reliably identified LSECs. This co-expression was confirmed by immunofluorescence microscopy on mouse liver sections, which demonstrated co-localization of CD31 and Stabilin-2 to the sinusoids (Figure 3.1c). Thus, these were used for all future analyses and

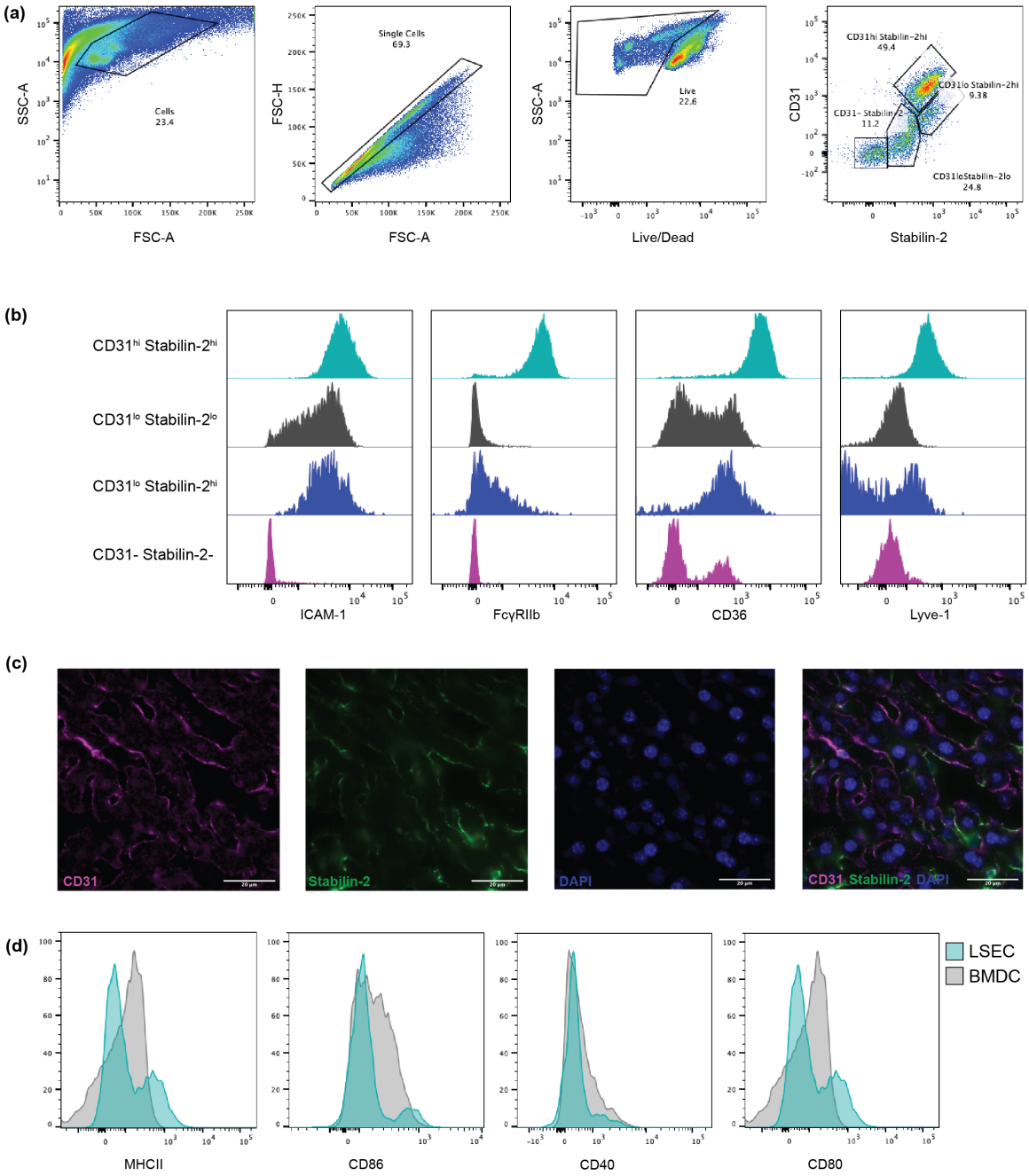


Figure 3.1: Phenotypic characterization of liver sinusoidal endothelial cells. a) Gating strategy on liver cells to identify LSECs. b) Expression of LSEC markers ICAM-1, Fc$\gamma$RIIb, CD36, and Lyve-1 on population of differentially expressing CD31 Stabilin-2 positive cells as identified in a). c) Immunofluorescence microscopy of mouse liver sections to identify CD31 and Stabilin-2 expressing cells. d) Expression of co-stimulatory molecules on CD31+Stabilin-2+ cells.

sorting. Additionally, to remove contaminating Kupffer cells during sorting, we sorted out F4/80+ cells.

To determine LSEC capacity to present antigen, we analyzed surface markers associated with antigen presentation, MHC-II, CD40, CD86, and CD80. Interestingly, CD31+ Stabilin-2+ LSECs had mostly low expression of these costimulatory molecules (Figure 3.1d). However, there was a small population of LSECs that were positive for these costimulatory molecules, to similar levels of bone marrow-derived dendritic cells. This is consistent with the finding in single cell RNA sequencing that different subsets of LSECs have differential expression of costimulatory molecules [278].

Once we had characterized LSECs, we sought to target an endocytic receptor that was specific to LSECs in the liver. Analysis of the literature revealed that the C-type lectin liver and lymph node sinusoidal endothelial cell C-type lectin (LSECtin) had high transcription in LSECs and nearly none in hepatic stellate cells, Kupffer cells, and hepatocytes [279]. Although it is expressed on lymphatic endothelial cells and colonic macrophages in the mouse, and in plasmacytoid dendritic cells (DC) in the human, LSECs would be targeted to a much greater degree due to the high volume of blood flow through the liver sinusoids [270, 280, 281]. LSECtin has also been described to trigger rapid internalization upon ligation, which would be beneficial for introducing an autoantigen and clearing it rapidly from circulation [280].

### *3.3.2 Phage Display on Recombinant Mouse LSECtin*

Because there were no available monoclonal antibodies targeting mouse LSECtin, we conducted phage display using a human phage antibody fragment (Fab) library on the 4D5 backbone, as used in Chapter 2 [186]. A variant of LSECtin was expressed that contained a minimal portion of the transmembrane domain, containing a potentially stabilizing glycosylation site, and the entire carbohydrate recognition domain (CRD), in order to maximize phage hits to the CRD, which in C-type lectins often triggers internalization (Figure 3.2a) [282]. The protein was expressed recombinantly with a SNAP-tag on the N-terminus. This

(a)


(b)

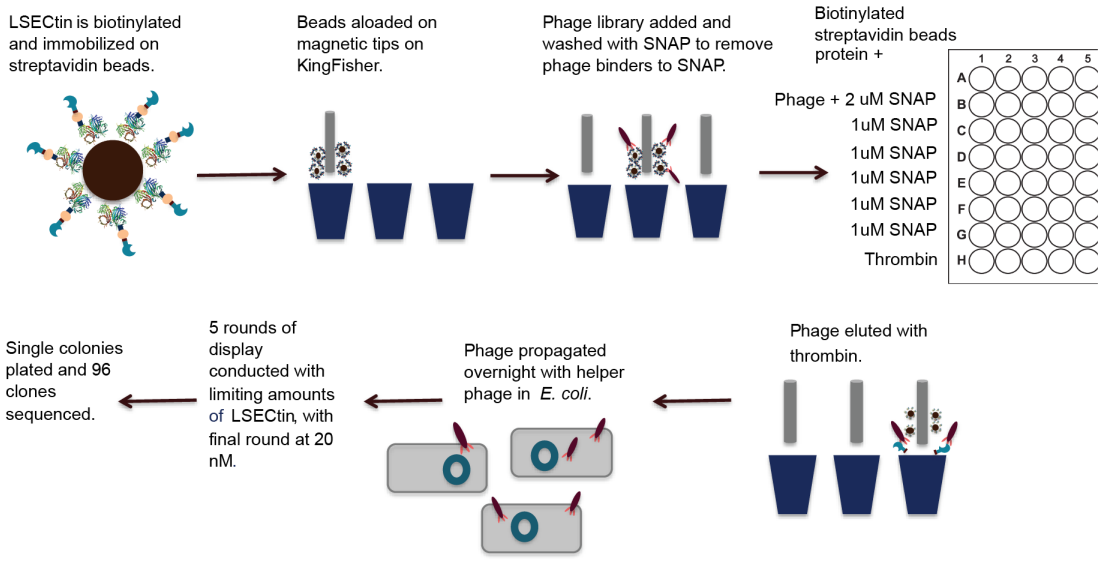


(c)

| Name | CDRL3 | CDRH1 | CDRH2 | CDRH3 |
|---|---|---|---|---|
| A1A1 | SYWYPV | LSSSSI | SISSYYGYTY | NDDWYIWDWYYTRWYGL |
| E1B2 | SPWWGPI | FSYYSI | SIYPYSGYTS | YSYEYWRLYLFQYFWLGL |
| A6B8 | SSSSLI | VYYSSI | SISPSSSYTS | WYWYDYFWWWHQEAL |
| D3C9 | YVRYYGPI | ISSSSI | SISPSYGSTY | YWHWWGFSYWAYGYYGF |

Figure 3.2: Phage display on mouse LSECtin yields anti-LSECtin Fabs. a) Design of LSECtin for phage display. b) Strategy for phage display against LSECtin. c) CDRL3, CDRH1, CDRH2, and CDRH3 sequences from top hits of phage display.

19 kD protein is a modified DNA repair enzyme that reacts with O6-benzylguanine (BG) to form a covalent bond [283]. There are a variety of molecules, such as biotin and fluorophores, that have been modified with BG and therefore allow for site-specific labeling of SNAP-tagged proteins. In this system, site-specific biotinylation would enable LSECtin to be immobilized on magnetic streptavidin beads in the same conformation, as opposed to the alternative of nonspecific biotinylation. The former allows for the same epitopes to be exposed to the phage library, whereas the latter is nonhomogeneous and leaves different

epitopes exposed, which would make library enrichment challenging. The protein was also designed with a thrombin cleavage site to allow for simple cleavage from streptavidin magnetic beads on which the LSECtin is immobilized, to co-elute protein and bound phages. Finally, there is a 6X-histidine tag to allow for purification via a nickel-NTA column by fast protein liquid chromatography.

Phage display was conducted as described in Figure 3.2b. LSECtin was site-specifically biotinylated using BG-biotin, and immobilized on streptavidin magnetic beads. Beads were loaded on a KingFisher device, which contains magnetic probes. Phage library was added to the magnetic probes, and washed numerous times with free SNAP protein to remove any phage binders to SNAP-tag. Finally, protein and attached phage were eluted with thrombin, and phage were propagated overnight in *E. coli* with M13 helper phage. After 5 rounds of display, single colonies were picked from infected *E. coli* and sequenced. Sequencing revealed convergence primarily on two clones – A1A1 and A6B8, with others appearing less frequently (Figure 3.2c).

### *3.3.3 Characterization of Fabs from Phage Display*

The most frequent sequences were cloned out of the phage vectors and cloned into mammalian expression vectors. Binding to purified LSECtin was determined via ELISA, revealing A1A1 had the highest affinity followed by A6B8, which mirrored the highest and second highest frequencies of sequences from display (Figure 3.3a). Next, Fabs were assessed for binding to CD31+ Stabilin-2+ LSECs, and lack of binding to other hepatic cells (Figure 3.3b). E1B2 demonstrated the highest binding, but showed some binding to the non-LSEC cells. Conversely, A1A1 and A6B8 had a high level of binding to LSECs, and low level to other cells. A Fab with CDRs specific for a xenoantigen was used as a negative control for experiments, as described in Section 2.3.3.

Antibodies derived from phage display although specific, are often polyreactive [284]. To assess polyreactivity, we tested binding to LSECtin versus binding to a panel of antigens,

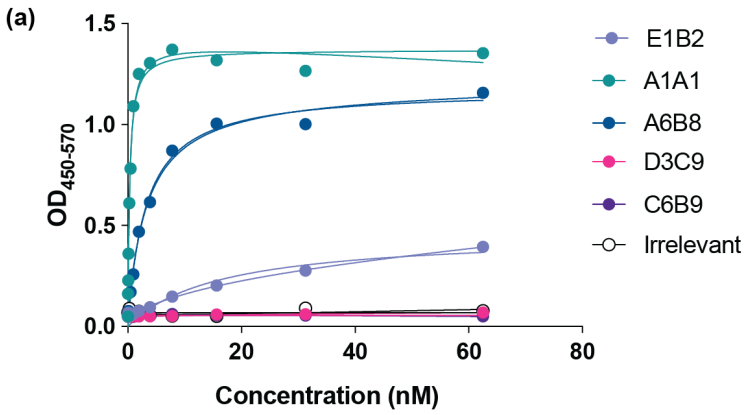


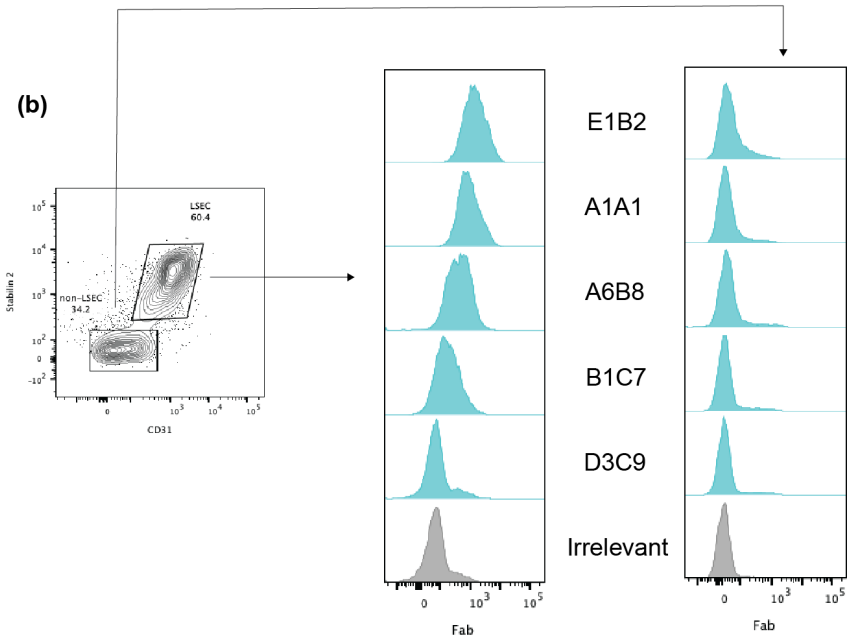


(c)

| | LPS | Insulin | dsDNA | OVA |
|---|---|---|---|---|
| **E1B2** | 1.11 | 1.63 | 1.6 | 2.36 |
| **A1A1** | 1.48 | 2.52 | 3.12 | 3.93 |
| **A6B8** | 0.34 | 0.65 | 0.64 | 1.05 |
| **B1C7** | 0.28 | 0.56 | 0.56 | 1.02 |
| **D3C9** | 0.37 | 0.54 | 0.54 | 1.05 |

Figure 3.3: Characterization of Fab hits from phage display. a) Binding curves of Fabs to recombinant mouse LSECtin via ELISA. b) Flow cytometry of selected recombinantly expressed Fabs to LSECs. c) Polyreactivity assay for Fab binding to double stranded DNA (dsDNA), LPS, insulin, and OVA, as measured by ELISA. Data is represented as fold-change of binding to LSECtin over binding to polyreactive antigens.

including LPS, double stranded DNA, and insulin, commonly used in the literature for polyreactivity assays [285]. Of all Fabs tested, A1A1 was the least polyreactive (Figure 3.3c). As the strongest binder with the lowest polyreactivity, A1A1 was selected for future studies.

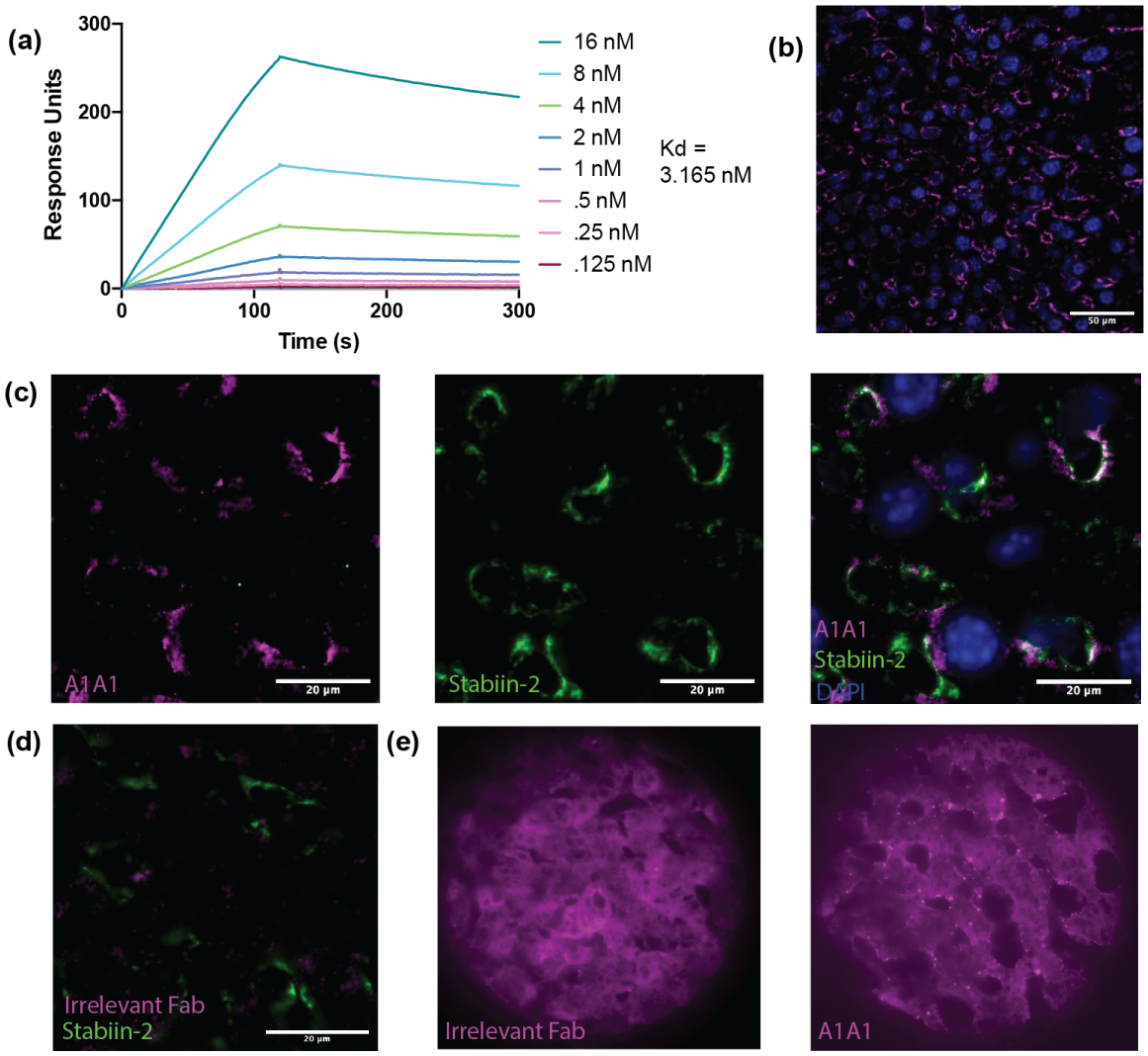


Figure 3.4: A1A1 binds with high affinity to mouse LSECtin and localizes to the sinusoids. a) Surface plasmon resonance of A1A1 onto immobilized mouse LSECtin. b) Immunofluorescence of A1A1 binding to mouse liver sections under 20x magnification. c) A1A1 colocalizes with the LSEC marker Stabilin-2 on mouse liver sections. d) Binding of irrelevant Fab and Stabilin-2 to mouse liver sections. e) Binding of Irrelevant Fab or A1A1 to mouse liver sections.

### *3.3.4 A1A1 Fab Binds LSECtin with High Affinity and Localizes to Mouse Sinusoids*

We next aimed to further characterize A1A1. We conducted surface plasmon resonance on immobilized LSECtin and determined an affinity of 3.165 nM (Figure 3.4a). To determine if A1A1 specifically stained LSECtin, mouse liver sections were stained with A1A1, using an anti-human Fab secondary antibody. A1A1 clearly stained the sinusoids (Figure 3.4b). Staining was co-localized with Stabilin-2, demonstrating that A1A1 specifically stained LSECs (Figure 3.4c). This staining was not due to human Fab non-specific staining, as the irrelevant Fab showed no staining over background (Figure 3.4d). A1A1 also co-localized to monkey liver sections, enhancing its translational potential (Figure 3.4e). This is unsurprising, because the region of mouse LSECtin expressed for display has 69% sequence identity with monkey LSECtin.

### *3.3.5 LSECtin-Binding Fab is Rapidly Internalized by LSECs In Vitro and In Vivo*

To determine if the anti-LSECtin A1A1 Fab preferentially reached the liver, A1A1 or irrelevant Fab were fluorescently labeled with a near-infrared dye and injected into mice. 30 minutes after injection, there was an initial accumulation of A1A1 compared to irrelevant Fab in the liver as evidenced by *in vivo* imaging (Figure 3.5a). At 60 minutes, irrelevant Fab also accumulated, consistent with the finding that most proteins are taken up by the liver. At 24 hours, however, irrelevant Fab was cleared, but A1A1 remained. This suggests that LSECtin may undergo recycling and release A1A1 payload back into the bloodstream, that it does not undergo internalization and Fab remains bound on the surface of the cell, or that it is shuttled into the cell without being degraded. To assess the first possibility, a blood half-life study was conducted on an irrelevant Fab vs A1A1. Although A1A1 appeared to have a longer half-life, it was undetectable in the blood after 5 hours (Figure 3.5b). This

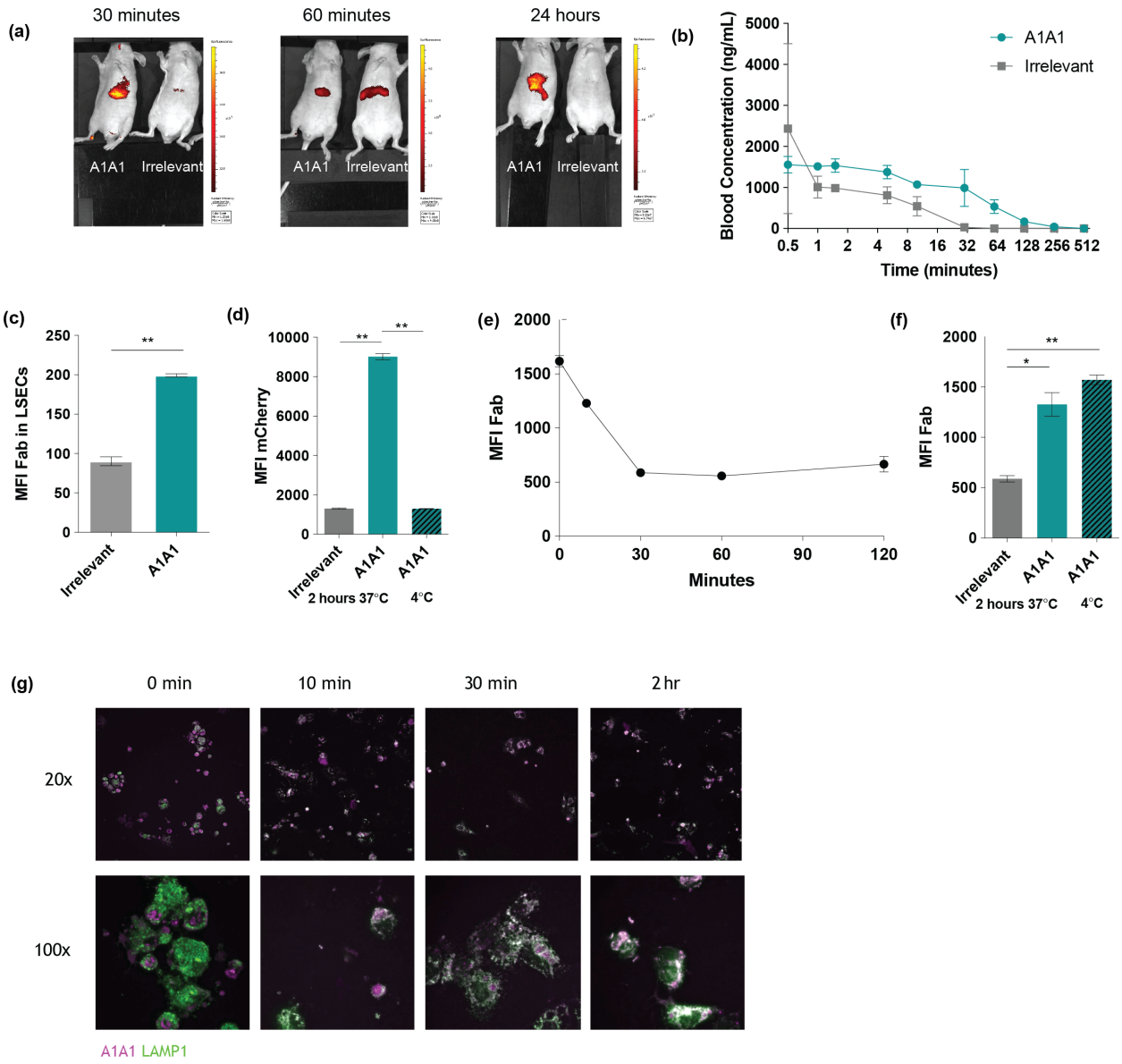


Figure 3.5: A1A1 is rapidly internalized by LSECs *in vitro* and *in vivo*. Continued on the following page.

suggests that if A1A1 is recycled back to the bloodstream and then is repeatedly endocytosed by LSECs, it is not the primary reason for persistence in the liver.

To confirm that uptake was specifically by LSECs, and not by other hepatic cells, fluorescent Fabs were injected i.v., and livers were perfused 30 minutes after injection. Fab uptake by various cell types was assessed by flow cytometry. Although both A1A1 and irrelevant Fab were found in LSECs, which is consistent with LSECs being the first cell type exposed

Figure 3.5, continued: A1A1 is rapidly internalized by LSECs *in vitro* and *in vivo*. a) 25 $\mu$g A1A1 or irrelevant Fab were labeled with a near-infrared dye, injected into nude mice i.v., and imaged for various time points over 24 hours with an *in vivo* imaging system (IVIS). b) 2.5 $\mu$g were fluorescently labeled and injected i.v. Mice were perfused through the inferior vena cava and single cell suspensions were created from livers. Data is represented as mean fluorescence intensity (MFI) of Fab in CD31+ Stabilin-2+ LSECs. c) Mice were injected i.v. with 2.5 $\mu$g Fab and bled at various time points. ELISAs were conducted on plasma to determine Fab blood concentration. d-g) LSECs were isolated from mice as described previously and flow sorted based on the expression of CD31 and Stabilin-2. Fab was recombinantly expressed with mCherry on the heavy chain. d) LSECs were incubated with A1A1-mCherry or Irrelevant-mCherry for 2 hours at 37°C, and washed after two hours. Data is represented as MFI of mCherry. e) LSECs were incubated with A1A1-mCherry on for 20 minutes at 4°C, washed, and incubated for 120 minutes at 37°C to allow for internalization. LSECs were washed and stained with an anti-Fab secondary antibody, and data is MFI of secondary antibody measured by flow cytometry. f) LSECs were incubated with A1A1-mCherry or Irrelevant-mCherry for 2 hours at 37°C, washed after two hours and stained with an anti-human Fab secondary antibody. g) LSECs were cultured on glass coverslips and pulsed with A1A1-AF647 for 20 minutes at 4°C. Cells were washed to remove excess Fab and incubated at 37°C for various time points and fixed with 2% paraformaldehyde. Cells were stained for the lysosomal marker Lamp1 and imaged on a confocal microscope. Statistical analyses were performed using one-way ANOVA with Tukey's test. *P $< 0.05$ and **P $< 0.01$.

to blood-borne particles, the mean fluorescence intensity (MFI) of A1A1 was greater than irrelevant Fab (Figure 3.5c).

To exclude the possibility that the fluorescent small molecule was being degraded by different kinetics than that of the protein, mCherry, a fluorescent protein, was expressed as a fusion protein on the C-terminus of A1A1 or irrelevant Fab, yielding a fully polypeptide fluorescent protein.

LSECs were isolated by flow cytometry as previously described, and *in vivo* uptake studies were conducted. LSECs were incubated continuously with A1A1-mCherry or Irrelevant-mCherry for 2 hours at 37°C, and cells were washed and measured for MFI of mCherry by flow cytometry. Results indicated high uptake of A1A1-mCherry, but not Irrelevant-mCherry (Figure 3.5d). This was not due solely to surface-bound A1A1-mCherry, as cells stained at 4°C, which would inhibit uptake, and measured for MFI of mCherry had much lower levels of mCherry fluorescence (Figure 3.5d, striped bars). To determine the kinetics of

uptake, LSECs were incubated at 4°C with A1A1-mCherry, which would enable binding but not internalization. LSECs were washed to remove excess Fab and incubated at 37°C. At various time points, LSECs were removed and assessed by flow cytometry for surface-bound Fab. After 30 minutes, all surface A1A1 was internalized, indicating rapid internalization (Figure 3.5e). To determine if LSECtin was being degraded after this internalization, or if it was being recycled back to the surface, we incubated LSECs continuously with A1A1-mCherry or Irrelevant-mCherry. After 2 hours, LSECs were washed and stained for surface Fab. Irrelevant-mCherry unsurprisingly had background levels of surface Fab, as it does not bind LSECs (Figure 3.5f). There were still high levels of A1A1-mCherry on the surface after 2 hours, indicating that although LSECtin is internalized, it is recycled back to the surface, where it could capture new A1A1.

To investigate the fate of A1A1-mCherry, LSECs were cultured on glass coverslips and incubated at 4°C for 20 minutes with A1A1-mCherry, washed, and incubated at 37°C. At various time points, cells were fixed and stained for LAMP-1, a lysosomal marker (Figure 3.5g). After 30 minutes, A1A1-mCherry appeared to co-localize with LAMP-1, indicating it was being shuttled to lysosomal compartments. Together these results indicate that LSECtin is rapidly internalized, and likely recycled back to the cell surface. Bound payload is delivered to lysosomal compartments, but given the short time point of 2 hours the fate of the Fabs remains unknown.

### *3.3.6 Targeting Antigen to LSECtin Leads to Reduced Antigen Presentation to T Cells Compared to Free Antigen*

With the knowledge that targeting LSECtin using A1A1 led to rapid uptake specifically by LSECs, we aimed to determine if this would lead to antigen presentation. A1A1 was recombinantly expressed with the model antigen ovalbumin (OVA) on the C-terminus, yielding A1A1-OVA. OT-I and OT-II cells, recognizing the CD8 or CD4 immunodominant epitopes of OVA, respectively, were adoptively transferred into C57BL/6 mice. Prior to adoptive trans-

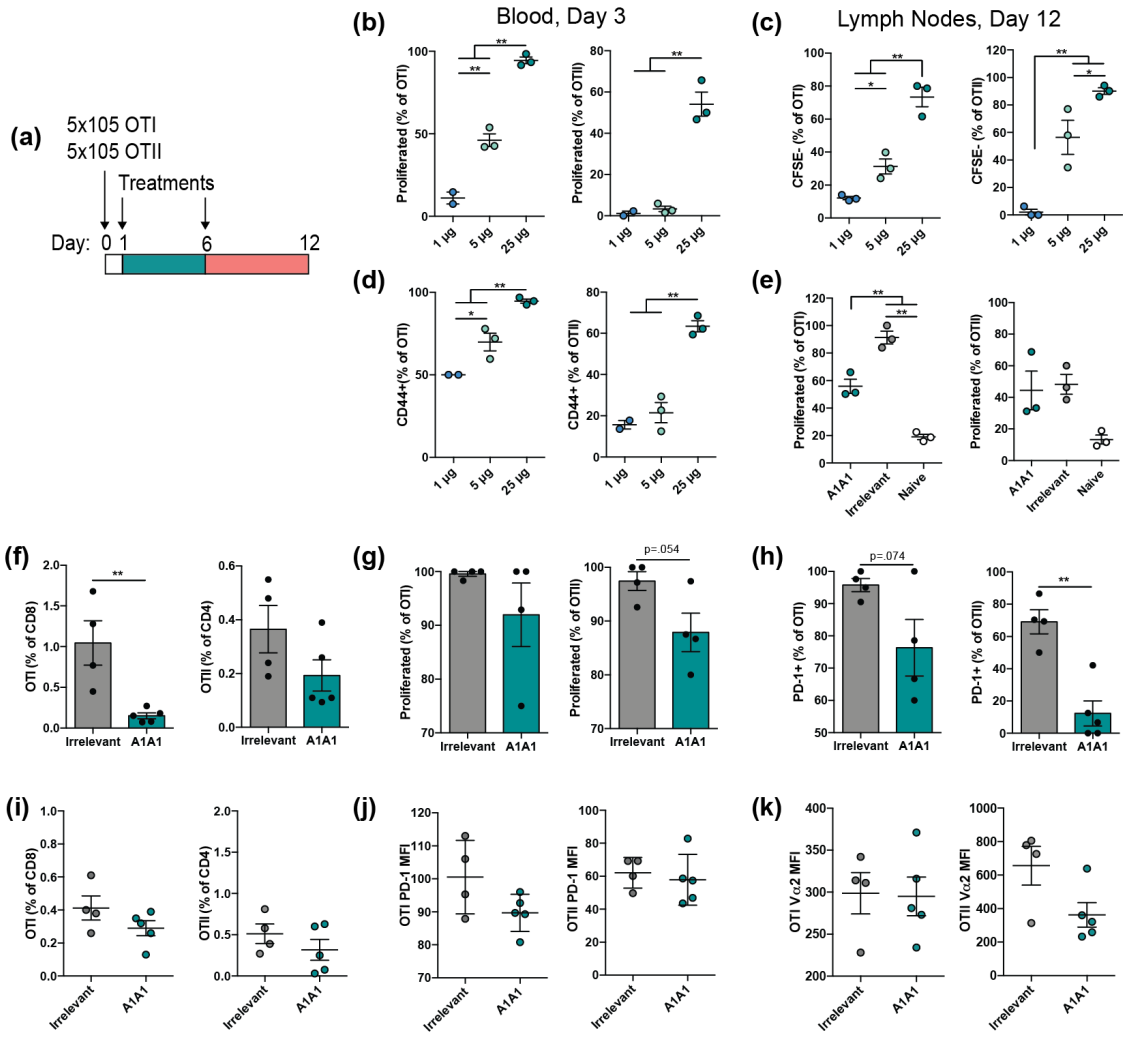


Figure 3.6: Targeting antigen to LSECtin leads to reduced antigen presentation compared to free antigen. a-d) Mice were adoptively transferred with 500,000 CFSE labeled OT-I or OT-II cells, dosed at days 1 and 6 with 1, 5, or 25 $\mu$g of A1A1-OVA, and sacrificed 6 days later. b) Mice were bled two days after initial dosing. Percent of OT-I and OT-II that have diluted CFSE. c-d) Lymph node analysis at sacrifice. c) Percent of OT-I and OT-II that have completely diluted CFSE. d) Percentage of CD44+ antigen-experienced OT-I and OT-II. e) Mice were dosed as in a) with 5 $\mu$g A1A1-OVA or Irrelevant-OVA. Percent of OT-I and OT-II that have diluted CFSE at d 12. f-k) Mice were dosed as in a) with 25 with $\mu$g A1A1-OVA or Irrelevant-OVA. f-h) Mice were bled at day 4. f) Percent of OT-I and OT-II in the blood. g) Percent of OT-I and OT-II that have diluted CFSE. h) Percent of PD-1+ cells of OT-I and OT-II. i-k) Analysis of lymph nodes at sacrifice. i) Percent of OT-I and OT-II. j) MFI of PD-1 on OT-I and OT-II. k) MFI of T cell receptor on OT-I and OT-II.

fer, cells were labeled with carboxyfluorescein succinimidyl ester (CFSE) to track rounds of proliferation. Various doses were tested to determine the dose at which antigen was

presented. After adoptive transfer, mice received two treatments with 1, 5, or 25 $\mu$g of A1A1-OVA (Figure 3.6a). 2 days after the first dose, mice were bled and proliferation assessed (Figure 3.6b). 1 $\mu$g of antigen was insufficient to trigger proliferation of OT-I, whereas 5 $\mu$g led to proliferation of nearly half of the OT-I, and 25 $\mu$g proliferation of all of the OT-I. Interestingly, neither 1 nor 5 $\mu$g was sufficient to lead to proliferation of OT-II, and 25 $\mu$g led to proliferation of half of the cells. 6 days after the last dose, mice were sacrificed, and lymph nodes analyzed. OT-I and OT-II in the lymph nodes had not completely diluted CFSE in the 1 or 5 $\mu$g groups, indicating low levels of presentation (Figure 3.6c). This was mirrored by the level of CD44 upregulation, a molecule that is upregulated upon antigen experience (Figure 3.6d).

Because 1 $\mu$g led to low levels of presentation and would not be relevant to induce tolerance, we decided to test a 5 $\mu$g dose compared to nontargeting Irrelevant-OVA. Mice were dosed as in Figure 3.6a, and lymph nodes analyzed at sacrifice. Again, OT-I proliferated to a lesser extent with LSECtin targeting than free antigen (Figure 3.6e). Interestingly, OT-II proliferation looked the same between LSECtin targeting and free antigen.

Because 5 $\mu$g still did not lead to complete proliferation, we tested a 25 $\mu$g dose. Three days after the first dose, there were fewer OT-I and OT-II in the blood, and this was likely due to greater proliferation with free antigen alone (Figure 3.6f-g). Consistent with this, OT-I and OT-II that received free antigen upregulated PD-1, which becomes upregulated with high exposure to antigen (Figure 3.6h). At sacrifice, 6 days after the second dose, OT-I and OT-II were indistinguishable in terms of numbers, upregulation of PD-1, and MFI of the T cell receptor (TCR) (Figure 3.6i-k).

Together these data suggested that at low doses, antigen targeted to LSECtin is presented poorly, whereas at higher doses it is presented to similar levels to free antigen. It is possible that LSECtin leads to a non-presenting pathway, and when A1A1 binds to LSECtin it gets shuttled to lysosomes without presentation because it is degraded rapidly. It may also remain in compartments without being degraded. A similar phenomenon has been observed

in lymphatic endothelial cells, known as antigen archiving, where the antigen remains in LECs for weeks entirely intact [286]. At higher doses, enough antigen may accumulate that some is sampled for presentation. A more likely hypothesis is that all LSECtin receptors get saturated at higher doses and are internalized, and other cells, likely the same that are presenting Irrelevant-OVA, present the non-internalized A1A1-OVA. Thus, it would be advisable to use a lower amount of antigen, and force presentation of the payload that has entered endosomal compartments.

### *3.3.7 Design of Cathepsin-Cleavable Linkers to Enhance Antigen Availability in the Endosome*

We hypothesized A1A1 was following LSECtin down a non-presenting pathway, and the OVA payload would have to be released in early endosomal compartments before it was shuttled to those pathways, so that it might get presented more efficiently by LSECs. One could achieve this by using a disulfide chemical linker that is sensitive to the reductive environment in endosomes, but a recombinant method is preferable due to ease of manufacturing and scalability. Thus, we aimed to develop a recombinant linker between the Fab and payload to promote cleavage in the endosome.

Cathepsins are proteases that are active in the endosomes at a pH of 6, but remain inactive at a blood pH of 7.4. Literature analysis revealed that LSECs preferentially express cathepsin L and cathepsin B [279]. Potential cleavage sequences were derived from a published set of sequences from proteins that had been degraded by cathepsins L and B to determine cleavage motifs (Figure 3.7a) [287]. Fabs were expressed with these linkers between the C-terminus of the Fab and mCherry for visualization or OVA for antigen presentation assays (Figure 3.7b). To determine if these linkers were cleaved, the Fab-Cts-mCherry sequences were incubated with cathepsin L (CtsL) or cathepsin B (CtsB) at a pH of 6 in reducing conditions at 37°C, to mimic endosomal compartments. Fab-CtsL-mCherry was efficiently cleaved by 5 minutes of incubation with cathepsin L at pH 6 but not at pH 7.4 (Figure 3.7c). When there was no Cts

linker present, the protein was not cleaved, indicating specificity (Figure 3.7d). Cathepsin B was able to cleave Fab-CtsB-mCherry, but it took longer than the CtsL linker (Figure 3.7e).

To test the effect that this would have *in vivo*, mice were adoptively transferred with OT-I and OT-II as previously, and received either A1A1-OVA or the constructs with a cleavage site, A1A1-CtsB-OVA and A1A1-CtsL-OVA, containing a cathepsin B or cathepsin L cleavage site, respectively (Figure 3.8a). Treatment with the modified A1A1-OVA constructs yielded no increase in T cell proliferation compared to the unmodified construct, and all remained far less efficient at presentation than Irrelevant-OVA (Figure 3.8b-c). This indicated that the cathepsins were not degrading the protein *in vivo*, or that separation from the Fab was insufficient to lead OVA to a presenting pathway.

### *3.3.8 Development of Endosomal Escape Fabs to Promote Antigen Presentation*

In an alternative effort to promote antigen presentation by LSECs, we took advantage of peptides that have been described to promote endosomal escape. Many endosomal escape peptides are derived from viruses, which enable viruses to burst open endosomes after being internalized and access the cytoplasm for replication [288]. One such peptide is derived from influenza hemagglutinin, which when protonated in the acidic environment of the endosome becomes hydrophobic, and is able to insert itself into the endosomal membrane [289]. This causes disruption of the membrane and release of the contents into the cytoplasm. Another peptide is derived from Syncytin-1, a protein found in an endogenous retrovirus, that aids in placental trophoblast fusion by a similar mechanism [290]. Engineered variants of these peptides, INF7 and Syn1 from hemagglutinin and Syncytin-1, respectively, have been described, and were used to aid in the endosomal escape of A1A1 [291, 292].

Cell-penetrating peptides may become trapped in the membrane, limiting release of the cargo into the cytoplasm. Groups have overcome this by using disulfide bonds between the peptide and cargo [293]. In an analogous method, we utilized the cathepsin-cleavable

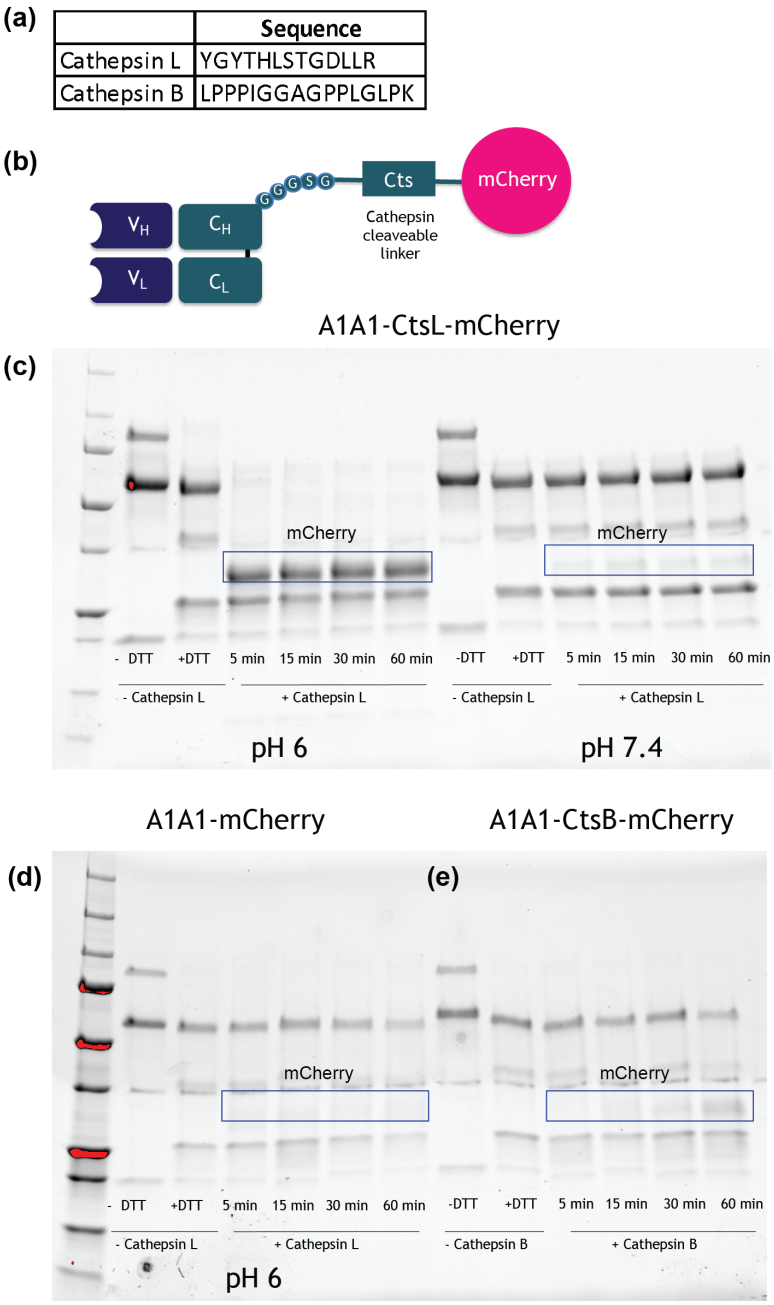


Figure 3.7: Design of cathepsin-cleavable linkers to enhance degradation in endosomes and subsequent antigen presentation. a) Design of constructs with Fab and payload separated by cathepsin-cleavable linkers. b) Sequences of cathepsin cleavable linkers tested. Fab-linker-mCherry were incubated in the presence of the reducing agent DTT at the endosomal pH of 6. Fab-CtsL-mCherry was incubated with recombinant cathepsin L at a pH of c) 6 or d) 7.4, and extent of cleavage was observed. d) Fab-mCherry, without a linker, was incubated with cathepsin L at a pH of 6. e) Fab-CtsB-mCherry was incubated with cathepsin B at a pH of 6.

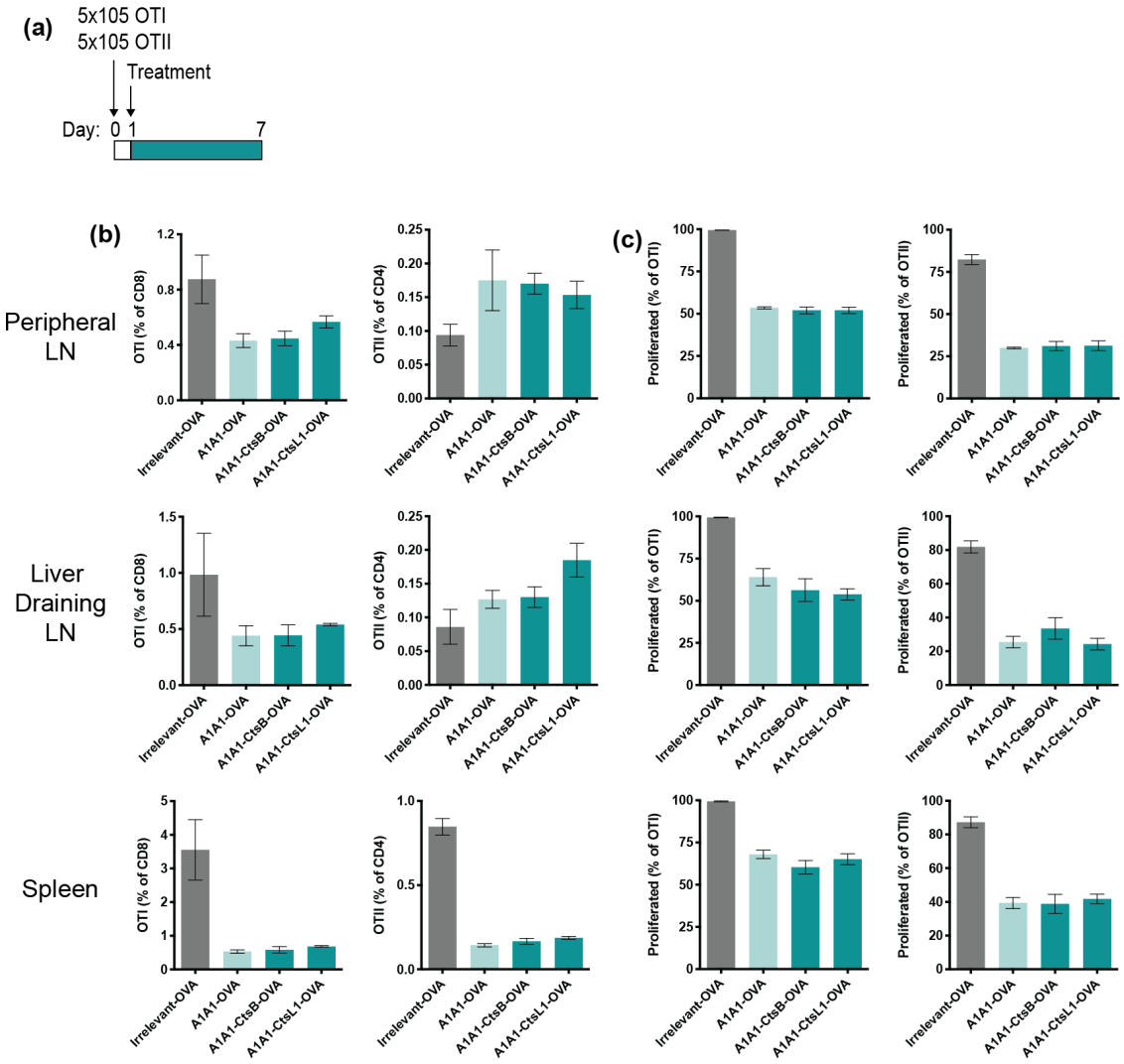


Figure 3.8: Cathepsin-cleavable linkers do not enhance antigen presentation. a) Mice were adoptively transferred with OTI and OTI, dosed once with Fab-Cts-OVA, and sacrificed 6 days later. b) Percentage of OT-I and OT-II in the peripheral lymph nodes, liver draining lymph nodes, and spleen at sacrifice. c) Percentage of OT-I and OT-II that have diluted CFSE.

linkers such that the proteins would be cleaved in an endosome after internalization, and the endosomal escape peptide would be free to insert itself into the membrane, and the cargo could be released into the cytoplasm (Figure 3.9a-c). To screen multiple peptides, we first tested their efficacy *in vivo* in BMDCs for their ability to promote antigen presentation to OT-I and OT-II. We could not use LSECs, as we were unable to maintain their phenotype and antigen-presenting capacity *in vivo*. However, BMDCs nonspecifically uptake antigen

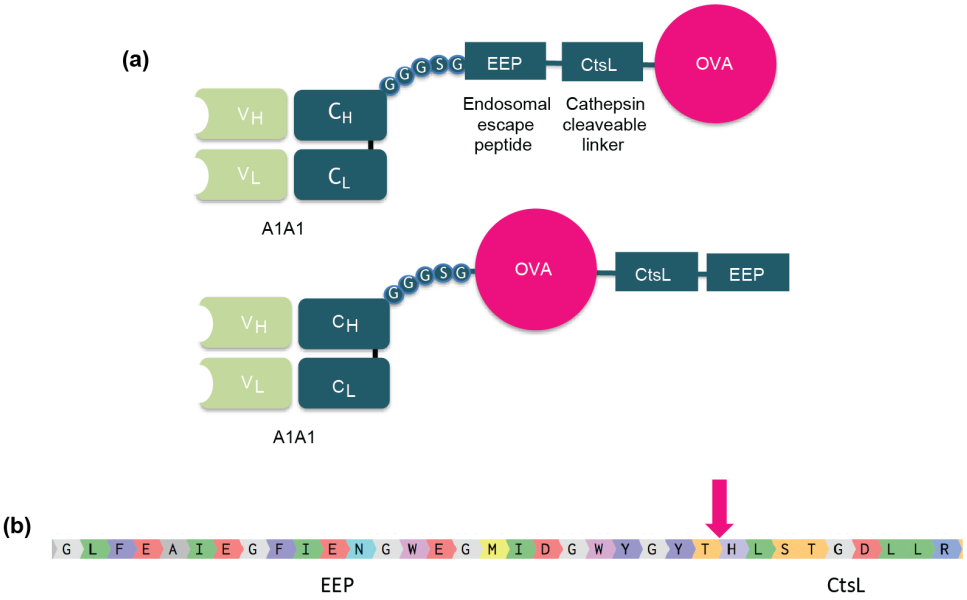


(c)

| | INF7 |
|---|---|
| EEP | GLFEAIEGFIENGWEGMIDGWYG |
| Fab-X-Cts-EEP | GGGGSGGGGSYGYTHLSTGDLLRGLFEAIEGFIENGWEGMIDGWYG |
| Fab-EEP-Cts-X | GGGGSGGGGSGAAAGLFEAIEGFIENGWEGMIDGWYGYTHLSTGDLLR |
| Fab-EEP-X | GGGGSGGGGSAAAGLFEAIEGFIENGWEGMIDGWYG |
| Fab-X-EEP | GGGSGGGSGLFEAIEGFIENGWEGMIDGWYG |

| | Syncytin 1 |
|---|---|
| EEP | PFVIGAGVLGALGTGIGGI |
| Fab-X-Cts-EEP | GGGGSGGGGSLFIGGLSFETPFVIGAGVLGALGTGIGGI |
| Fab-EEP-Cts-X | GGGGSGGGGSGAAAPFVIGAGVLGALGTGIGGLSFE |
| Fab-EEP-X | GGGGSGGGGSGAAAPFVIGAGVLGALGTGIGGI |
| Fab-X-EEP | GGGSGGGSPFVIGAGVLGALGTGIGGI |

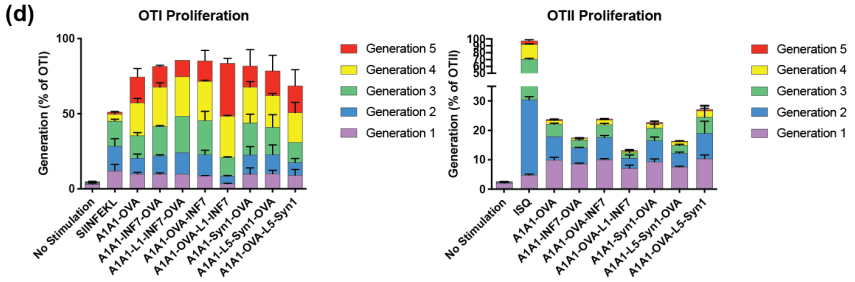


Figure 3.9: Design of Fabs with endosomal escape peptides. a) Graphical representation of endosomal escape Fabs. b) Example of the location of cleavage between endosomal escape peptide and payload. c) Sequences used for endosomal escape peptide-cathepsin linker fusions. d) Bone marrow derived dendritic cells were incubated with endosomal escape Fabs and pulsed with CFSE-labeled OT-I and OT-II. Data are presented as the percentage of OT-I or OT-II in a generation of proliferation, as measured by CFSE dilution.

for presentation, and would do so with the constructs.

BMDCs pulsed with antigen-escape Fabs demonstrated that A1A1-OVA-CtsL1-INF7 led to the highest proliferation in OT-I, consistent with escape and release into the cytoplasm (Figure 3.9d). It also led to the least presentation of antigen to OT-II, which is consistent with transfer from one presentation pathway to the other, and cross-presentation primarily occurring in the cytoplasm and presentation on MHCII occurring primarily in the endosomal compartments.

We next attempted to try these constructs *in vivo*, using the same dosing strategy as previously (Figure 3.10a). There were no differences in presentation in the blood after three days (Figure 3.10b-c). Similarly, there were no differences in numbers with or without the endosomal escape peptides at sacrifice (Figure 3.10d). Interestingly, OT-II had identical numbers across dose and with or without endosomal escape Fab. The lack of difference is likely because at low doses, a high enough concentration in the endosome could not be reached, and the escape peptide could not sufficiently destabilize the membrane, and at higher doses all LSECtin receptors were saturated.

### *3.3.9 Anti-LSECtin Polymerosomes Encapsulated with Antigen Enhance Antigen Presentation to CD8 and CD4 T cells*

In a final effort to promote presentation, we sought to deliver OVA encapsulated in a vehicle that promoted presentation. Previously in the lab, we used the amphiphile poly(ethylene glycol) (PEG)-poly(propylene sulfide) (PPS) that spontaneously form polymerosomes [294]. These polymerosomes had a hydrophilic core, enabling encapsulation of protein antigen. Delivery to dendritic cells led to escape of OVA into the cytoplasm and efficient cross-presentation to CD8 T cells. The polymerosomes themselves had little effect on the activation status of the dendritic cells unless they also contained TLR agonists. Thus, they served as a potential method of delivering OVA to the cytoplasm of LSECs for presentation without their activation.

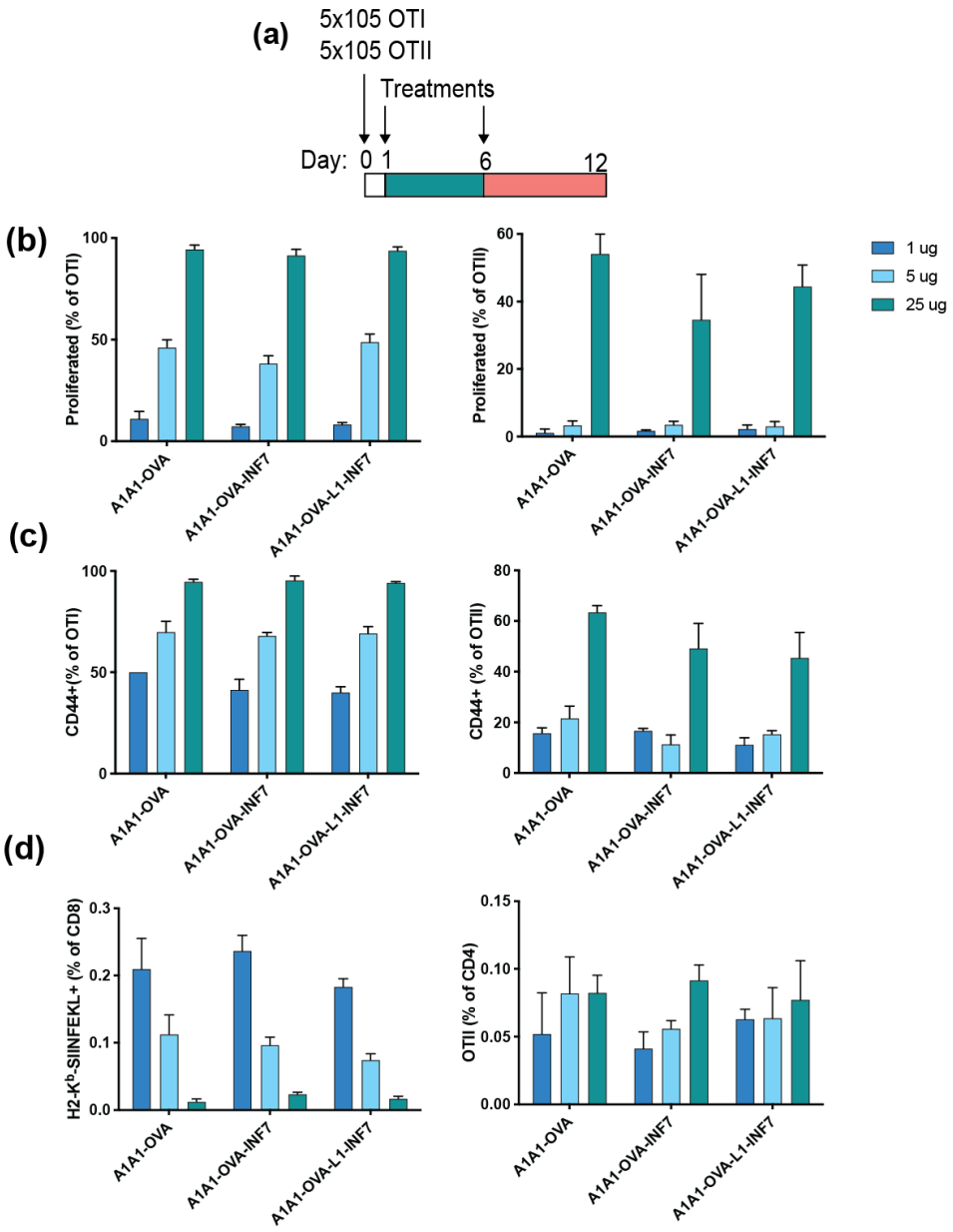


Figure 3.10: Endosomal escape peptides do not enhance antigen presentation of LSECtin-targeted antigen. a) Mice were adoptively transferred with CFSE-labeled OT-I and OT-II, and received 1, 5, or 25 $\mu$g endosomal escape Fabs at days 1 and 6. b) Percent of OT-I and OT-II that have diluted CFSE in the blood at day 4. c) Percentage of CD44+ OT-I and OT-II in the blood at day 4. d) Percentage of OT-I and OT-II in the lymph nodes at sacrifice.

To achieve this, Fabs were expressed with a free cysteine on the C-terminus and modified with a dibenzocyclooctyne linker. These were conjugated to OVA-loaded polymerosomes using azide-modified PEG-PPS, yielding polymerosomes decorated with Fab (A1A1-

PS or Irrelevant-PS) (Figure 3.11a). We verified that polymerosomes maintained binding to LSECtin by immobilizing biotinylated LSECtin on streptavidin beads, incubating with polymerosomes, detecting with an anti-Fab secondary antibody, and measuring binding by flow cytometry (Figure 3.11b). To determine if the A1A1-PS were delivered to LSECs in *in vivo*, we injected A1A1-PS or Irrelevant-PS and perfused mice 30 minutes later. Livers were sectioned and stained for Stabilin-2 and anti-Fab secondary antibody for immunofluorescence microscopy. A1A1-PS localized to the sinusoids, and co-localized with Stabilin-2 (Figure 3.11c-d). Irrelevant-PS also was delivered to the liver, as are most nanoparticles of this size. However, there was low to no co-localization with sinusoids, suggesting that likely Kupffer cells, the primary cell type involved in clearing nanoparticles of this size (100-150 nM), had captured the Irrelevant-PS [295].

To test the effect on antigen presentation, Fab-OVA constructs were compared to Fab-PS constructs. OT-I and OT-II were adoptively transferred into mice. At day 1 mice received 1 or 4 $\mu$g OVA equivalents of Fab-OVA or Fab-PS (Figure 3.12a). Four days after dose, mice were bled (Figure 3.12b). A1A1-PS enhanced presentation of OVA to both CD8 and CD4 T cells compared to A1A1-OVA (Figure 3.12b-c). Interestingly, delivery via PS enhanced presentation to OT-II cells compared to Irrelevant-PS. At day 12 in the spleen, 4 $\mu$g of PS encapsulation led to a greater accumulation of OT-I (Figure 3.12d). Similar to what was observed in the blood, in the spleen there was a large expansion of OT-II with the PS, reaching as high as 10% of all CD4 cells in the spleen with the LSECtin-targeted PS. There was little difference in the proliferation index between irrelevant PS and LSECtin-targeted PS (Figure 3.3.12e). It did not appear that LSECtin-targeted PS led to tolerance at these doses, as in addition to a lack of deletion, there was a lack of PD-1 upregulation and Treg induction (Figure 3.12f-h).

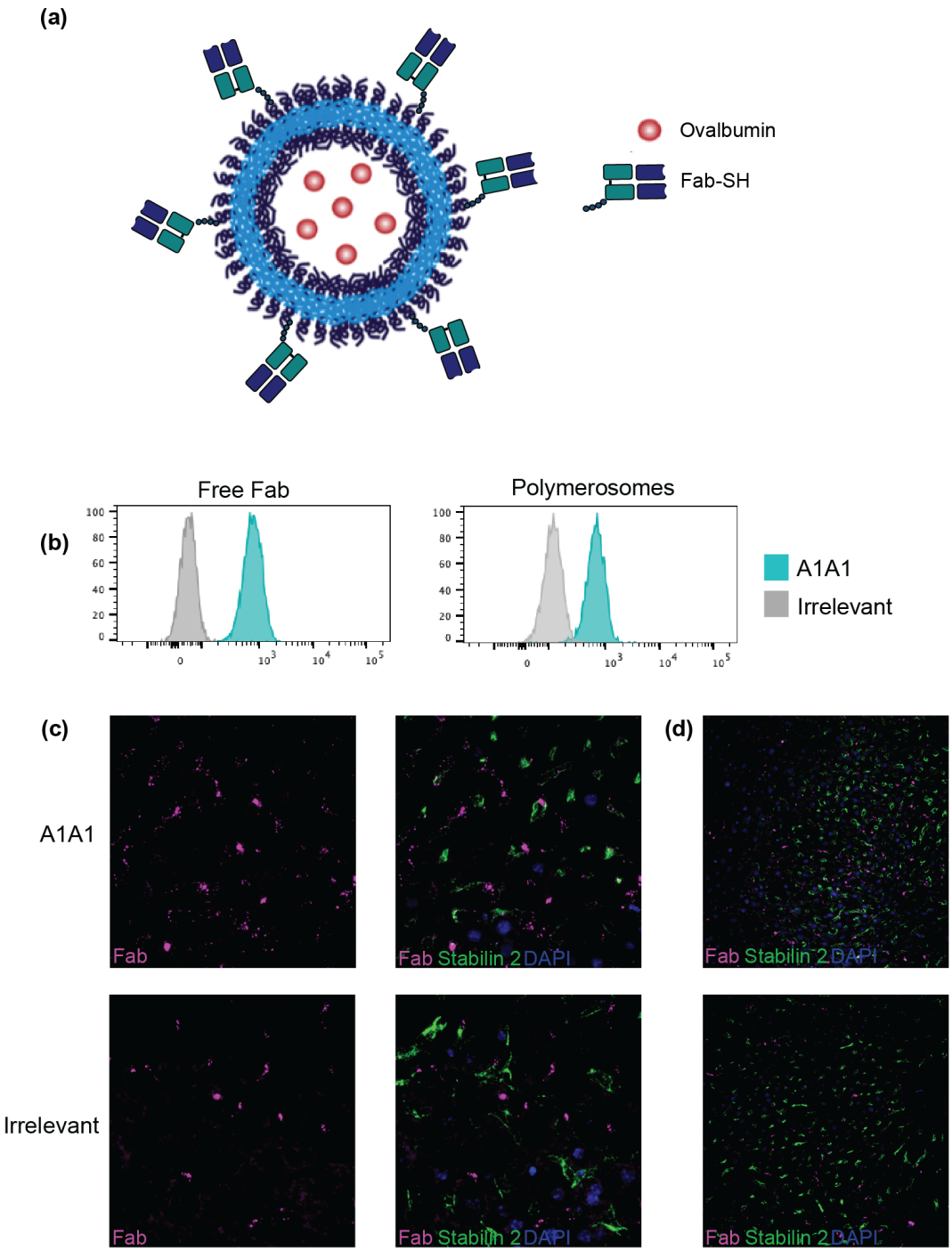


Figure 3.11: Design of Fab-coated polymerosomes to enhance antigen presentation. a) Graphical representation of PEG-PPS polymerosomes encapsulated with OVA and decorated in Fab on the surface. Graphic adapted from Michal Raczy. b) Binding of polymerosomes or free Fab to LSECtin-coated streptavidin beads measured by flow cytometry. c-d) Polymerosomes were injected i.v. and mice were perfused 30 minutes later and stained for immunofluorescence with a secondary anti-Fab antibody and Stabilin-2. c) 60x magnification and d) 20x magnification.

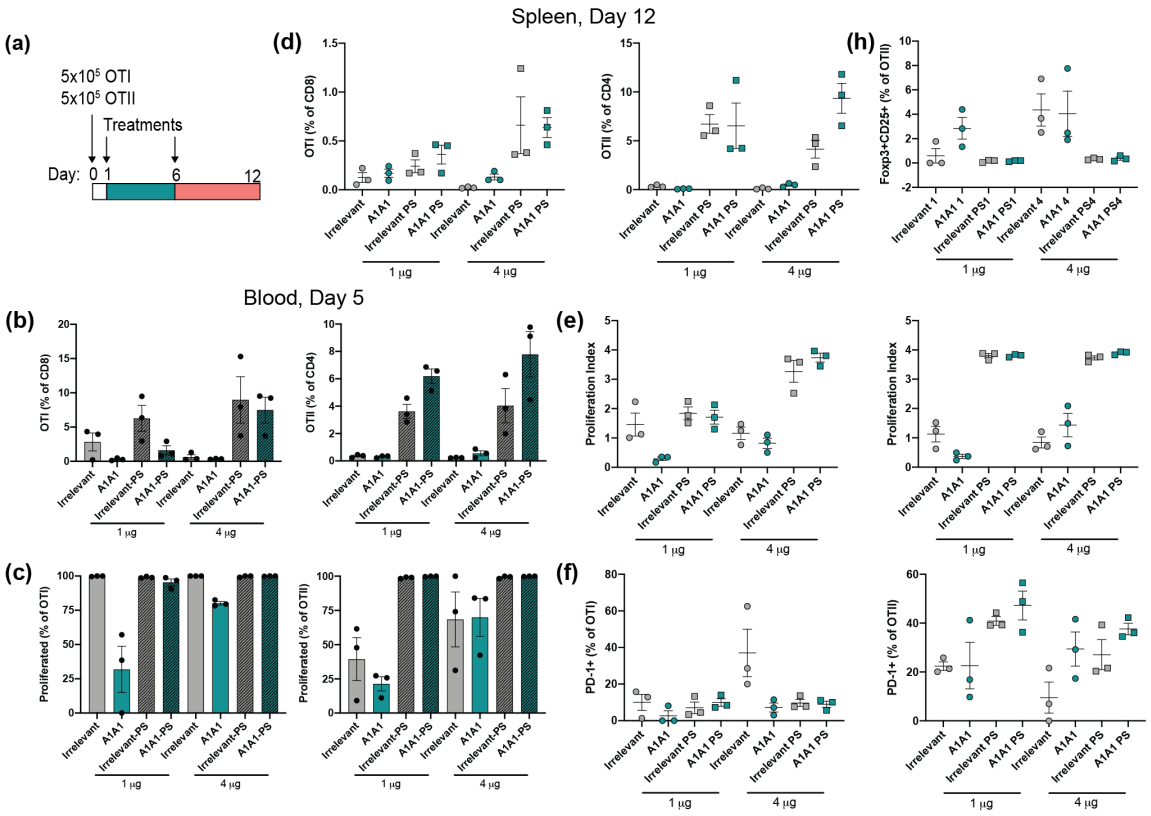


Figure 3.12: Delivery of OVA-loaded polymerosomes to LSECs enhance antigen presentation. a) Mice were adoptively transferred with CFSE-labeled OT-I or OT-II and either 1 or 4 $\mu$g Fab-OVA or Fab-PS. b-c) Blood was analyzed after 5 days for OT-I and OT-II b) numbers and c) proliferation. d) Percentage of OT-I and OT-II in the spleen at day 12. e) Proliferation index of OT-I and OT-II. f) Percentage of PD-1+ cells of OT-I and OT-II. h) Percentage of FoxP3+CD25+ Tregs of OT-II.

## 3.4 Discussion

In this study, we developed a method to target liver sinusoidal endothelial cells. We first sought to characterize LSECs, as the methods for their isolation and identification are non-standardized. We attempted to isolate purely by centrifuge gradients and selective attachment of Kupffer cells, but our purity was low. This is concerning, as many studies that have characterized the antigen presentation capacity of LSECs have been performed using this method, and as macrophages have the capacity to present antigen, this could confound the reported results.

Thus, we opted for specific isolation of cells. CD146+ magnetic bead purification led

to a reasonable purity, but with 5% contaminating cells. To enhance specificity, we sorted based on expression of CD31 and Stabilin-2. Some studies have reported that LSECs do not express CD31. These studies have been conducted using microscopy. We noted that Stabilin-2 negative large vessel endothelial cells had a much higher expression of CD31, which could potentially overwhelm a positive signal in LSECs and lead to a false negative result. We confirmed expression of CD31 by LSECs by immunofluorescence, flow cytometry, and polymerase chain reaction.

Once we had isolated LSECs, we attempted culture systems, but LSECs lost phenotype with all conditions tested after 24 hours, thus prohibiting any antigen presentation experiments *in vitro*. As such, any antigen presentation experiments had to be conducted *in vivo*. A primarily cell line was purchased, but these cells lacked expression of LSECtin.

We then sought to develop a new method of binding these cells, and opted to target LSECtin. This receptor was chosen primarily for its specificity; in the liver, it is unique to LSECs. It has been described to be in other cells in the body; however, we anticipated that protein is first delivered to the liver when injected i.v. and passes through the sinusoids. Because LSECtin has been reported to be rapidly internalized, we hypothesized that targeting LSECtin would rapidly sequester the payload in the LSEC before it could reach other cells.

We conducted phage display using a humanized antibody fragment library on a variant of mouse LSECtin that had just the carbohydrate recognition domain and a stalk region that contained a potentially stabilizing glycosylation motif. Phage display yielded multiple potential phage hits; however, many of them were quite polyreactive. This is not unusual in antibodies derived from synthetic libraries; thus, it is important to verify polyreactivity if one is to use display-derived antibodies *in vivo*. We decided on A1A1 for its high affinity, low polyreactivity, and potential cross-reactivity with monkey LSECtin.

We next sought to determine if A1A1 was endocytosed specifically by LSECs. *In vivo* imaging revealed rapid uptake by the liver, compared to an irrelevant Fab. Interestingly, A1A1 was still in the liver at 24 hours, suggesting that the Fab was not being degraded.

However, we cannot exclude the possibility that the protein component was fully degraded, and the dye was not. To overcome this, we recombinantly made the fluorescent protein mCherry, and confirmed that it was rapidly endocytosed by LSECs. After two hours, it was transported to lysosomal compartments, but we do not know the subsequent fate of the protein. It is possible that the antigen traveled to compartments in which it was archived, a process that has been demonstrated in lymphatic endothelial cells to occur for weeks following a viral infection to allow for sustained protection [286].

We determined that targeting low dose antigen to this pathway leads to very little cross-presentation of antigen, compared to an irrelevant Fab. Levels of presentation on MHC-II were reduced compared to irrelevant Fab, but not as low as presentation on MHC-I. We developed cathepsin cleavable linkers between the antigen and Fab, but these did not enhance presentation. This may be because there are low levels of active cathepsins in the compartments that LSECtin is shuttled into. LSECtin may also shuttle cargo to a non-presenting pathway, in which case cleavage of cargo would not be relevant, compared to other C-type lectins in the LSEC. Wilson et al. saw antigen presentation on class I MHC with delivery of N-acetyl glucosamine and N-acetyl galactosamine- conjugated antigens [156]. It is unknown which C-type lectins these bind to, but it suggests that different C-type lectins may lead to different antigen processing pathways. Additionally, A1A1 was delivered as a monomer, whereas these glycans are polymers, similar to what is found on viruses. LSECtin crosslinking by polymeric ligation might lead to a presentation pathway, whereas monomeric ligation does not. This is seen in a number of receptors, such as the neonatal Fc receptor which does not lead to presentation with monomeric IgG, but does lead to presentation with multimeric IgG complexes [296].

Endosomal escape peptides also did not enhance presentation, potentially because a high enough concentration was not reached in the endosome to disrupt the endosome and allow for escape. In BMDCs, there was such a high concentration in the supernatant, and macropinocytosis would lead to a high concentration of endosomal escape Fab in the

endosome, which would allow for endosomal escape.

Finally, we decided to attempt endosomal escape and subsequent antigen presentation with polymerosomes designed to burst the endosome. By decorating the polymerosomes with A1A1, we were indeed able to see greatly enhanced presentation of antigen compared to soluble A1A1-OVA alone. This did not lead to differences in deletion, proliferation index, PD-1 upregulation, or Treg induction. It is possible that all LSECtin receptors were saturated at the doses administered. Because 1 $\mu$g of encapsulated OVA was sufficient to trigger robust proliferation, we could reduce the dose many-fold in order to ensure that only LSECs are internalizing the A1A1-decorated PS. We could then determine if a lower dose would induce the desired tolerance.

Additionally, we will characterize in greater depth the specificity to LSECs. We will first confirm that the antigen presentation is indeed occurring by LSECs. This will be accomplished by injecting the polymerosomes encapsulating OVA, and sorting LSECs out after 24 hours to determine if they can present antigen to OT-I and OT-II *in vitro*. Because the cells would already be presenting antigen on MHC and could immediately prime T cells, we would not be concerned with LSECs losing phenotype *in vitro*. In an alternative method, we could also stain for MHCI-SIINFEKL using an antibody that binds this complex. Next, we will determine if presentation by LSECs leads to T cell tolerance, in their inability to respond to an adjuvanted challenge. The advantage of the polymerosome is that it enables encapsulation of a multitude of antigens, which would be relevant in the many diseases in which the specific autoantigen is unknown. For example, membrane from beta cell or islet lysate could be encapsulated by the polymerosomes, which could potentially induce tolerance to all of the autoantigens. This would additionally be beneficial because the polymerosome would shield the encapsulated product from circulating autoantibodies. These could be injected into a NOD mouse to determine if the mouse would be protected from diabetes. If successful, this would also have implications in transplant and a number of other autoimmune diseases.

Thus, we developed a new method to target LSECs. Our study tested targeting LSECs for tolerance, however, LSECtin has a number of interactions that would be interesting to investigate. Specifically, LSECtin has been shown to interact with the glycans of a number of viral proteins, including Ebola virus glycoprotein, SARS-Cov spike, hepatitis C virus E2 protein, and filovirus glycoproteins [297–299]. A1A1 could be used to study the necessity of interactions of these viruses with LSECtin, if it is determined that it binds to the carbohydrate recognition domain of LSECtin. LSECtin has also been shown to interact with CD44 and LAG-3 on T cells to promote tolerance [300, 301]. A1A1 could potentially be used to probe this interaction.

Additionally, although this study was aimed for tolerance, it was shown that particles encapsulated in melittin lead to activation of LSECs, which promotes tumor clearance. A1A1 could be used to deliver other TLR agonists specifically to LSECs, as they are reported to express multiple TLRs and can respond to these stimuli with activation [258–260, 302]. This could promote viral clearance or reduce the number of tumor metastases by promoting a more inflammatory microenvinronment.

## 3.5 Materials and Methods

### *3.5.1 Isolation of Mouse LSECs*

LSECs were isolated from mouse livers as previously described. Briefly, mice were sacrificed and catheter was inserted in the inferior vena cava. The liver was perfused with 25 mL of calcium-free Hank's Buffered Salt Solution (HBSS) supplemented with 12.5 mM EGTA, 125 units heparin, 62.5 $\mu$L 40% glucose, 625 $\mu$M HEPES, and 1% penicillin/streptomycin. To digest the liver, it was then perfused under a heating lamp with IMDM supplemented with GlutaMax, 25 $\mu$g Collagenase IV (Worthington) and 2 $\mu$g DNAse I (Sigma). Liver was excised and cells were immediately removed in a petri dish and passed through a 70 $\mu$M cell strainer. Cells were centrifuged at 68 x g to remove pelleted hepatocytes. Supernatant

was centrifuged at 600 x g to pellet all remaining cells. Cells were resuspended in 10 mL of DMEM. A two-step Percoll gradient was created by placing 20 mL of 50% Percoll as the bottom layer, 20 mL of 25% Percoll as top layer, and layering 10 mL of cell suspension on top. Cells were immediately spun at 1350 x g with no brake. The resulting layer of cells between the two gradients was taken and washed with PBS.

### *3.5.2 Preparation of Liver Sections for Immunofluorescence Analysis*

Mice were perfused through the inferior vena cava with HBSS followed by zinc fixative to fix the liver. Livers were fixed overnight in zinc fixative, transferred to a 10% sucrose solution for 24 hours at 4C, and then to a 30% sucrose solution for 24 hours at 4C. Livers were flash frozen and cryosectioned in 8 mM slices. Sections were stained with 10 $\mu$g/mL A1A1 anti-LSECtin Fab or irrelevant Fab control and rat anti-mouse Stabilin-2 (MBL International) at 4°C in 0.5% casein in TBST. Sections were washed and stained with anti-human F(ab)2 Alexa Fluor 594 (Jackson Immunoresearch) and anti-rat Alexa Fluor 488 secondary antibodies for 1 hour at room temperature in 0.5% casein in TBST. Sections were mounted with ProLong Gold Antifade Mountant with DAPI (Life Technologies) and imaged on an Olympus confocal microscope.

### *3.5.3 Synthesis of LSECtin for Phage Display*

The full-length sequence of murine LSECtin was ordered from Genscript. To generate LSECtin protein lacking the transmembrane and cytosolic domain, PCR amplification was conducted to create a variants of LSECtin corresponding to amino acids 100-294. At the N-terminus of the vector, the secretion signal from Laminin-II was added to allow for expression of secreted soluble protein. Following the laminin subunit gamma II secretion signal ('MPALWLGCCLCFSLLLPAARNLAGT'), the sequence for SNAP tag (NEB) was added to enable site-specific biotinylation. At the C-terminus of the vector, a thrombin-cleavable site followed by a 6xHistidine tag was included to enable protein purification on a Ni-NTA

column. The entire sequence was cloned into the pHEK293 Ultra expression vector (Takara). The plasmid was tranfected into HEK suspension cells seeded at 1 million cells per mL. After 6-8 days of culture, supernatant was harvested, passed through a 0.22 $\mu$M filter, and purified on an HisTrap column on the Akta pure 25 M system (GE Healthcare). Protein was washed with 30 mM imidazole in 25 mM Tris-Hcl, 300 mM NaCl, and eluted with 500 mM imidazole in 25 mM Tris-HCl 300 mM NaCl. SNAP-LSECtin was dialyzed overnight against 5 L of 25 mM Tris-HCl, 150 mM NaCl, 10 mM CaCl2. For long term storage of SNAP-LSECtin, 10% glycerol was added and protein was stored at -80°C.

### *3.5.4 Selection of Phage Library*

The phage library used was kindly provided by Anthony Kossiakoff at the University of Chicago. The library consists of humanized Fab based on the anti-HER2 antibody 4D5. Of the six complementarity determining regions (CDR), CDR-L1 and CDR-L2 from the light chain are constant, CDR-L3, CDR-H1, and CDR-H2 have limited diversity, and CDR-H3 is completely randomized. The actual diversity of the library is $3x10^{10}$, which can cover a broad range of targets.

### *3.5.5 Phage Panning Against LSECtin*

1 mM of SNAP-LSECtin was biotinylated as per the manufacturer's protocol (SNAP-biotin, NEB). For the first round, $5x10^{12}$ phages were used for panning against 1 mM of LSECtin bound to 200 mL magnetic streptavidin beads (Promega) in PBST-BSA (PBS, 0.05% Tween, 0.5% bovine serum albumin) for 1 hour at room temperature. Magnetic beads were washed 4 times in PBST-BSA. Phages were eluted from beads with thrombin. Eluted phages were incubated with 5 mL of XL1 Blue with M13-K07 helper phage overnight at 37°C to propagate the phage. Cells were pelleted and supernatant containing phage was kept. PEG-NaCl (20% PEG 8k, 2.5 M NaCl) was added to supernatant at equal volumes to precipitate phage. Phage was centrifuged and resuspended in PBST-BSA for the next round of panning. For

subsequent panning, KingFisher plates were used with the KingFisher device in a plate setup as demonstrated in Figure 3.2b. The first row included streptavidin beads (Dynabeads) with 300 nM, 150 nM, 75 nM, or 20 nM biotinylated LSECtin, corresponding to the second, third, fourth, and fifth rounds of display. The next well row contained phage and 2 $\mu$M biotinylated SNAP protein, to remove potential SNAP binders. The following row contained 1 $\mu$M biotin to saturate biotin sites on the streptavidin beads. The following 4 rows contained 1 $\mu$M SNAP to wash. The last row contained thrombin, to elute phage. All steps contained TBS + 10 mM CaCl2. Eluted phage was incubated with XL1, helper phage, and ampicillin overnight at 37°C.

### *3.5.6 Phage Sequencing*

After 5 rounds of panning on LSECtin, XL1 with phage was plated on LB-agar plates supplemented with ampicillin. Single clones were grown overnight at 37°C in 96 deep well plates in 400 $\mu$L 2XYT supplemented with 100 mg/mL ampicillin and M13-K07 helper phage. Three plates corresponding to panning on the three variants of LSECtin were sent to the DNA Sequencing Core Facility at the University of Chicago.

### *3.5.7 Fab Cloning*

Fab sequences were cloned out of the M13 vectors and into a human endothelial kidney (HEK) expression vector, Abvec2.0 (Table 1). For Fab payload sequences, such as ovalbumin, DNA was purchased from Genscript and cloned into the HEK vectors at the C terminus of the heavy chain. Amino acid sequence of antigens can be found on Table 2.

Table 3.1: Primers to amplify Fabs out of M13 vector

| **Primer** | **Sequence** |
|---|---|
| Forward VL | 5'-tgtgcctggccggccgcgccctggccgatatccagatgacccagtccccga-3' |
| Reverse VL | 5'-acgctaggggcagccaccgtacgtttgatctccaccttggtaccctgtccga-3' |
| Forward VH | 5'-gcctggctgggcgcgccctggccgaggttcagctggtggagtctgg-3' |
| Reverse VH | 5'-cccttggtgctagccgaggagacggtgaccagggtt-3' |

### *3.5.8 Fab Expression and Purification*

Fabs were expressed in HEK293T suspension cells in FreeStyle 293 Expression Medium (Thermo Fisher Scientific). At 1 million cells/mL in log-phase growth, cells were transfected with 1 $\mu$g of plasmid and 2 $\mu$ of polyethylenamine in 40 $\mu$L OptiPRO SFM (Gibco) per million cells. Transfected cells were cultured for 6 d in shake flasks. The cells were then pelleted by centrifugation, and the supernatant was filtered through a 0.22 $\mu$m filter and pH-adjusted to 7.0 using 1 M Tris buffer, pH 9.0. The Fabs were then purified by affinity chromatography using a 5 mL HiTrap Mabselect Protein A column (GE Life Sciences) via fast protein liquid chromatography. The column was first equilibrated with 5 column volumes (CVs) of PBS at 5 mL/min. The crude Fab solution was then flowed over the column at 5 mL/min and the column washed with 10 CVs of PBS at 2 mL/min. Fab was then eluted with 0.1 M glycine-HCl, pH 2.6, and neutralized with1 M Tris buffer, pH 9.0. Elution peaks were pooled and dialyzed into PBS. Where necessary, Fabs were concentrated (Amicon). Because the Fabs are prone to aggregation, DLS was conducted on samples and filtered through 0.22 $\mu$m PES filters until the sample was >95% pure by intensity. For all studies, produced proteins were verified to contain <.01 endotoxin units by HEK-TLR4 assay. Proteins were aliquoted and frozen at -80. The sequences used for A1A1-OVA, A1A1-mCherry, and A1A1-Cys are listed in Table 3.2.

### *3.5.9 ELISA*

Nunc MaxiSorp plates were coated overnight at 4°C with 10 $\mu$g/mL LSECtin in sodium bicarbonate buffer. Plates were washed 3X in PBST with an ELISA plate washer. Plates were blocked for 2 hours in PBS + 2% BSA at room temperature. Plates were washed 3X with an ELISA plate washer. Fabs were added at concentrations from 30 pM to 125 nM in PBS + 2% BSA for 2 hours at room temperature. Plates were washed 5X in PBST with an ELISA plate washer. Horseradish peroxidase-conjugated anti-F(ab)$_2$ IgG (Jackson Immunoresearch) was added at 1:5000 dilution in PBS + 2% BSA for 1 hour at room

Table 3.2: Amino acid sequences of A1A1 Fab payload

| Payload | Sequence |
|---|---|
| OVA | GSGGGGSGGGGSGGGGSGGGGSMGSIGAASMEFCFD<br>VFKELKVHHANENIFYCPIAIMSALAMVYLGAKDSTR<br>TQINKVVRFDKLPGFGDSIEAQCGTSVNVHSSLRDILN<br>QITKPNDVYSFSLASRLYAEERYPILPEYLQCVKELYRG<br>GLEPINFQTAADQARELINSWVESQTNGIIRNVLQPSSV<br>DSQTAMVLVNAIVFKGLWEKAFKDEDTQAMPFRVTE<br>QESKPVQMMYQIGLFRVASMASEKMKILELPFASGTM<br>SMLVLLPDEVSGLEQLESIINFEKLTEWTSSNVMEERK<br>IKVYLPRMKMEEKYNLTSVLMAMGITDVFSSSANLSG<br>ISSAESLKISQAVHAAHAEINEAGREVVGSAEAGVDA<br>ASVSEEFRADHPFLFCIKHIATNAVLFFGRCVSP |
| mCherry | GSGGGGSGGGGSGAAASGGTGMVSKGEEDNMAIIKE<br>FMRFKVHMEGSVNGHEFEIEGEGEGRPYEGTQTAKL<br>KVTKGGPLPFAWDILSPQFMYGSKAYVKHPADIPDYL<br>KLSFPEGFKWERVMNFEDGGVVTVTQDSSLQDGEFI<br>YKVKLRGTNFPSDGPVMQKKTMGWEASSERMYPED<br>GALKGEIKQRLKLKDGGHYDAEVKTTYKAKKPVQLP<br>GAYNVNIKLDITSHNEDYTIVEQYERAEGRHSTGGMD<br>ELYKMEVGWYRSPFSRVVHLYRNGK |
| Cys | GSGGSSGSGC |

temperature. Plates were washed 5X with an ELISA plate washer. TMB substrate was added and quenched with 10% sulfuric acid. Plates were read with a spectrophotometer at 450 nm wavelength and 570 nm reference wavelength. For polyreactivity ELISAs, plates were coated in 5 $\mu$g/mL insulin, 10 $\mu$g/mL dsDNA, 10 $\mu$g/mL LPS, and 10 $\mu$g/mL OVA. in sodium bicarbonate buffer overnight at room temperature. Plates were washed with water, and blocked with 1 mM EDTA pH 8 0.05% Tween 20 in PBS for 1 hour at 37°C. Plates were washed in water and samples were added in PBS for 1 hour at room temperature. Plates were washed in water and an HRP-conjugated anti-F(ab)$_2$ IgG was added at 1:5000 in 1 mM EDTA pH 8 0.05% Tween for 1 hr at room temperature. Plates were washed and antibody detected as above.

### *3.5.10 Flow Cytometry on LSECs*

To confirm binding of Fabs to LSECs *in vivo*, Cells were first stained with Live/Dead Viability Dye (Invitrogen) and 1:50 Fc block (BD). Cells were washed with PBS + 2% FBS. Cells were stained for CD31, Stabilin-2 and CD45 and with 5 $\mu$g/mL Fab for 30 minutes at 4°C. Cells were washed in PBS + 2% FBS and stained with 1:400 dilution of anti-Fab for 15 minutes at 4°C. Cells were washed and fixed in 2% paraformaldehyde for 15 minutes at 4°C. Cells were washed and analyzed by flow cytometry.

### *3.5.11 In Vivo Fab Uptake*

To measure the ability to localize to LSECs *in vivo*, anti-LSECtin Fabs were conjugated to an amine-reactive DY-800 (Dyomics), a near infrared fluorescent small molecule. 25 $\mu$g of Fab-800 were injected *in vivo*, and fluorescence was measured in nude mice for 24 hours (IVIS, Perkin Elmer). To measure uptake specifically by LSECs, Fabs were conjugated to the fluorescent amine-reactive dye DY-649P (Dyomics). 2.5 $\mu$g of Fab-649 were injected into mice, and mice were sacrificed 30 minutes after injection. LSECs were isolated and analyzed by flow cytometry for mean fluorescence intensity of Fab.

### *3.5.12 In Vitro Fab Uptake*

LSECs were isolated from mice as described above and sorted based on the expression of CD31 and Stabilin-2 and lack of CD45 and F4/80. Fab was recombinantly expressed with mCherry on the heavy chain. Fab-mCherry was added to LSECs at 4°C for 20 minutes and washed to remove excess Fab. LSECs were incubated at 37°C to allow for endocytosis and subsequently stained with an anti-Fab antibody. LSECs were incubated with A1A1-mCherry or irrelevant Fab-mCherry 2 hours at 37°C and the fluorescence intensity of mCherry was measured by flow cytometry.

### *3.5.13 Cathepsin-Cleavable Assays*

Cathepsin cleaveable linkers were designed between the Fab and payload to allow for separation in acidic compartments and enhanced degradation and antigen presentation. RNAseq data reveals that the most prevalent cathepsins in LSECs are cathepsin L and cathepsin B. Potential sequences were obtained from Sudo et al. who performed mass spectrometry on peptide isolates after incubation of cells with the respective cathepsins and identified predicted cathepsin specificities. Sequences were chosen based on abundance and adherence to predicted cathepsin specificities. Fabs were designed to have a Gly4Ser linker, cathepsin cleaveable sequence, and payload (OVA or mCherry). To determine if Fab constructs with payload separated by cathepsin cleaveable linkers were cleaved by cathepsins, proteins were incubated at 0.2 $\mu$g/mL with 1:100 mouse cathepsin L in pH 6 or pH 7.5 for varying time points at 37°C.

### *3.5.14 Adoptive Transfer*

Spleens and lymph nodes were isolated from TCR transgenic mice. OT-I and OT-II T cells were isolated by negative magnetic bead selection using a CD8 (Stemcell) and CD4 (Stemcell) negative selection kit, respectively. In experiments assessing T cell proliferation, cells were labeled with 5 $\mu$M carboxyfluorescein succinimidyl ester (CFSE). For RNA sequencing, 1 million OT-I and OT-II in DMEM were injected through the tail vein. For tolerance experiments, 500,000 OT-I and 500,000 OT-II in DMEM were injected intravenously through the tail vein.

### *3.5.15 Preparation of Single-Cell Suspensions*

Draining lymph nodes (axillary, brachial, inguinal, and popliteal) and spleen were isolated from mice. Lymph nodes were digested for 45 min at 37°C in DMEM with 1 mg/mL collagenase IV (Worthington). LN and spleen were homogenized using syringe plungers onto

70 $\mu$M strainers. Spleens were lysed using 3 mL ACK lysis buffer (Gibco) for 5 min and quenched with 30 mL DMEM. Cells were counted using a fluorescent cell counter.

### *3.5.16 Bone Marrow Derived Dendritic Cell Presentation of Endosomal Escape Fabs*

BMDCs were generated as previously described (307). Briefly, cells were obtained from mouse bone marrow and cultured in the presence of 200 U/mL rmGM-CSF, which was added at days 0, 3, and 6. BMDCs were ready to use at day 8. BMDCs were pulsed with 10 $\mu$L/mL antigen for 6 hours, washed, and CFSE-labeled OT-I or OT-II were added for 3 days.

### *3.5.17 Polymer Synthesis*

PEG24-PPS40 (MW of ca. 3900, PEG weight fraction of 0.28) was synthesized as previously described [294]. Briefly, benzyl mercaptan was used to initiate the living polymerization of propylene sulfide. The terminal thiolate was end-capped with mPEG24-mesylate. The azide modified polymer, N3-PEG24-PPS40 was synthesized by end-capping the PPS terminal thiolate with N3-PEG24-mesylate. At the end of reaction, block copolymers were precipitated multiple times in cold methanol and dried in vacuum. The polymers were characterized by GPC and 1H NMR to determine the purity, composition and the molecular weight.

### *3.5.18 Polymersome Formulation*

Polymersomes were formed via flash nanoprecipitation as previously described [303]. Briefly, PEG-PPS was dissolved in tetrahydrofuran (THF) at 40 mg/mL in 500$\mu$L. The THF solution was impinged against a solution of endotoxin-free ovalbumin in PBS at 8mg/mL in 500$\mu$L into a reservoir of 2mL endotoxin-free PBS. This solution was purified by benchtop size exclusion chromatography using Sepharose CL-4B resin in order to remove THF and un-

encapsulated protein.

### *3.5.19 Fab Conjugation to Polymersomes*

Fabs were expressed with a free thiol with the sequence in Table 3.2. To ensure the free thiol was reduced, 0.85 molar equivalents of tris(2-carboxyethyl)phosphine (TCEP) were added for 90 min at 37°C in the presence of 1 mM EDTA. Fabs were then conjugated to a DBCO-Sulfo-Maleimide (Click Chemistry Tools) linker such that it could then be conjugated to polymerosomes. Fabs were incubated with 100x molar excess of DBCO for 30 minutes at room temperature. Excess DBCO was removed using a 5 mL 7000 MWCO spin desalting column (Zeba, ThermoFisher). Polymersomes were assembled as described above, with 25% N3-PEG-PPS and 75% mPEG -PPS. DBCO-functionalized Fabs at a 0.01% molar ratio were then reacted with the N3-labeled polymersomes. The smaller volume, the DBCO-functionalized Fabs, was added to the tube first, and the larger volume, the N3-functionalized polymersomes, was then added and immediately mixed by pipetting to ensure uniform distribution within the reaction. The click reaction was allowed to proceed overnight at room temperature. The samples were then either purified or stored at 4°C until purification. The Fab-functionalized polymersomes were purified by size into PBS by benchtop SEC using Sepharose CL-4B resin.

### *3.5.20 Flow Cytometry for Validation Polymerosome Binding to LSECtin*

1 uM SNAP-LSECtin was incubated with 1 uM BG-biotin (NEB) and 1 mM DTT for 30 minutes at room temperature. 100 $\mu$g of biotinylated SNAP-LSECtin was incubated with 100 $\mu$L Avidin polystyrene beads (Spherotech) in 800 $\mu$L of PBS on a rotator for 1 hour at room temperature. 30 $\mu$L of beads + SNAP-LSECtin was added to 5 mL polystyrene tubes (Falcon), washed with 2 mL PBS + 2% BSA and spun down at 2000 RPM for 5 minutes. Supernatant was discarded, and 200 nM Fabs or 10 $\mu$L polymerosomes were added for 15 minutes at room temperature. Samples were washed with 2 mL PBS + 2% BSA and spun

down at 2000 RPM for 5 minutes. Anti-human F(ab)2- Alexa Fluor 594 secondary antibody (Jackson Immunoresearch) was added at a final concentration of 1 $\mu$g/mL for 15 minutes at room temperature and washed as previously. Samples were run on the Fortessa (BD) for flow cytometric analysis.

### *3.5.21 Statistical Analysis*

Statistically significant differences between experimental groups were determined using Prism software (v6, GraphPad). All statistical analyses are stated specifically in the figure legends for all experiments. For most experiments, One-way ANOVA was performed with a Tukey's post-hoc test to correct for multiple comparisons. Comparisons were significant if $p < 0.05$.

## 3.6 Author Contributions

Jennifer Antane assisted in LSEC isolation and experimental design. Tomasz Slezak led phage display against LSECtin. Anya Dunaif assisted in LSEC phenotypic characterization and culture methods, and well as protein production. Rachel Wallace and Michal Razcy assisted in polymerosome synthesis. Anya Dunaif, Jaeda Roberts, Mindy Nguyen, and Rachel Wallace aided in performing animal experiments. Stephan Kontos and Jeffrey Hubbell guided and advised the experiments presented.

## 3.7 Funding

This work was supported by funding from the National Science Foundation Graduate Research Fellowship Program, University of Chicago, and Anokion S.A.

## 3.8 Acknowledgments

I am grateful to members of the Hubbell laboratory for helpful comments and suggestions. I thank Suzana Gomes for technical assistance. I would like to thank Ani Solanki in the

Animal Resources Center. I would like to thank the DNA Sequencing Core Facility at the University of Chicago. Flow cytometry data and sorting experiments were acquired using the Cytometry and Antibody Technology Core Facility, with special help from Michael Olson and David Leclerc. The phage library was kindly provided by Anthony Kossiakoff. I would like to thank Elena Davydova for her guidance in phage display and Fab characterization.

## 3.9 Conflicts of Interest

This work was funded in part by Anokion SA. J.A.H, T.S., and E.A.W are inventors on patents associated with this work which are licensed to Anokion. J.A.H. consults for and holds equity in Anokion.

# CHAPTER 4

# DISCUSSION, FUTURE DIRECTIONS, AND CONCLUSION

## 4.1 Discussion and Future Directions in Erythrocyte Targeting

In conclusion, these studies co-opted existing mechanisms of endogenous tolerance for therapeutic purposes. In one study, I developed an antibody fragment that bound erythrocytes, and demonstrated that persistent exposure to antigen in this pathway led to profound CD8 exhaustion. T cell transcriptional signatures early upon antigen experience revealed markers of anergy, consistent with antigen exposure without co-stimulation. Prolonged T cell exposure via this pathway then led to profound T cell dysfunction in CD8 T cells, consistent with a phenotype of exhaustion commonly seen in chronic viral infection and cancer. In the absence of the spleen or Batf3+ dendritic cells, this dysfunction was abrogated, suggesting that cross-presenting DCs present apoptotic-erythrocyte antigen.

Given that the T cell dysfunction demonstrated with erythrocyte targeting was associated with high expression of co-inhibitory molecules, it would be interesting to determine the stimuli that could overcome dysfunction. This could have implications not only in autoimmunity and transplant, but also in cancer. In the former, probing the criteria for overcoming tolerance is important in designing therapies. For example, infection with *Listeria monocytogenes* is sufficient to overcome tolerance in a cardiac transplant model, despite there being dysfunctional antigen-specific T cells [30, 304]. In our studies, challenge with the TLR agonists LPS and CpG were insufficient to completely reverse dysfunction to control levels, although cells did reacquire ability to produce some IFN$\gamma$. Although it is likely that these cells would eventually revert back to a dysfunctional state, if the temporary activation would be sufficient to contribute to autoimmunity is important to determine. This would be relevant in cancer because one could use this system in a simple way to probe requirements for overcoming CD8 T cell dysfunction, for example by blockade of PD-1 and CTLA-4.

For translational potential, it would also be important to determine if tolerance could

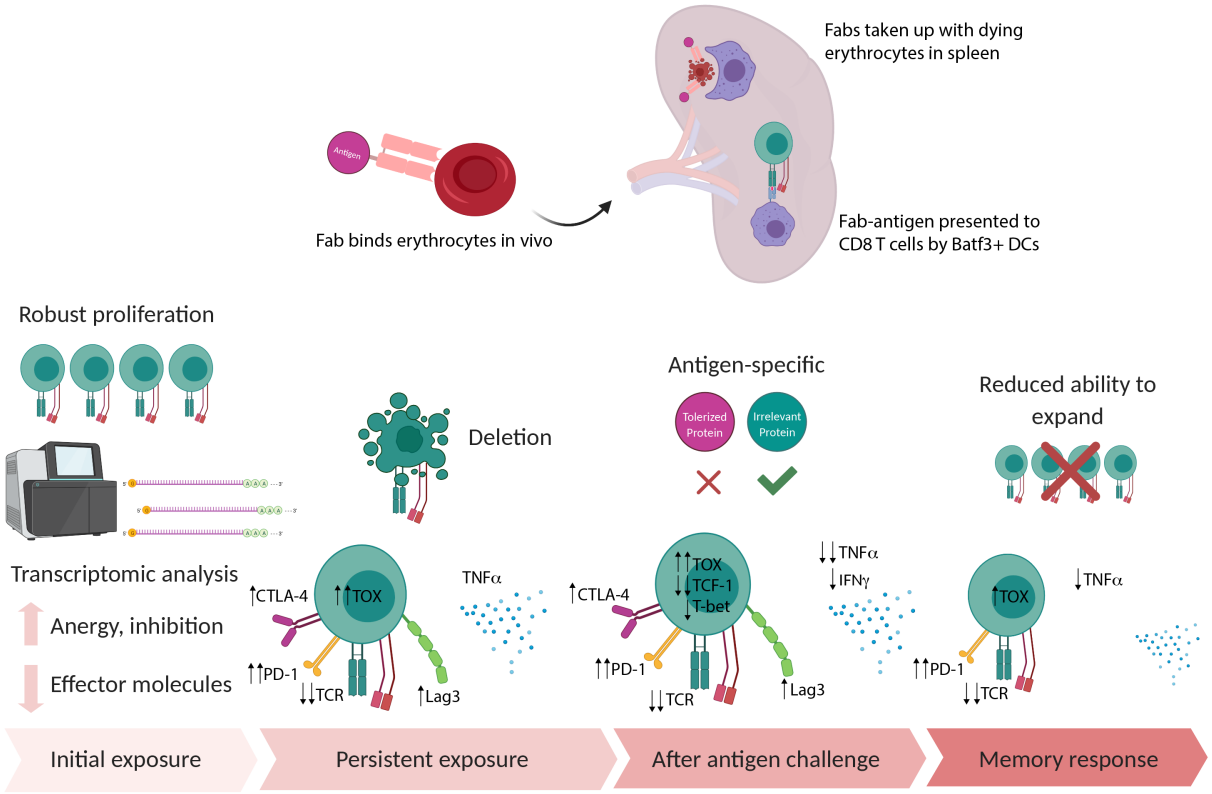


Figure 4.1: Fabs discovered by phage display bound with high affinity to erythrocytes. Dying erythrocytes were removed in the spleen, and associated antigen was presented by Batf3+ DCs to CD8 T cells, but it is unknown what cells presented to CD4 T cells. There was a high efficiency of presentation, as T cells proliferated extensively. Initial transcriptomics revealed signatures of anergy and inhibition, and not of effector functions, compared with free antigen. Prolonged exposure of antigen led to upregulation of inhibitory molecules such as PD-1, CTLA-4, and TOX, and downregulation of TCR. Cells had reduced capacity to respond to the tolerized antigen, maintaining high levels of the inhibitory molecules, downregulating TCF-1 and T-bet, and having reduced capacity to produce inflammatory cytokines. This strategy was antigen-specific, because cells could still respond to an irrelevant antigen. The cells remained in circulation for months after dosing, but still had reduced capacity to respond to antigen challenge.

be induced in the face of inflammation. In mouse models, there is typically little systemic inflammation. Humans, however, are constantly exposed to pathogens, and also often have many co-morbidities that increase systemic inflammation. It is possible that this approach relies on immature APCs to induce dysfunction, and therefore this strategy would need to be tested in models where there is ongoing systemic inflammation and potentially activated

APCs, such as in a mouse with a chronic inflammatory disease such as RA or that is infected with a pathogen.

It is interesting to note that the requirements for CD8 and CD4 T cell tolerance were different in this system. For CD8 T cells, even a 1 $\mu$g dose was sufficient to drive lasting dysfunction. For CD4 T cells, the parameters around dysfunction were unclear. Over time, CD8 T cells maintained dysfunction whereas CD4 T cells did not. A careful analysis of quantity and duration of dosing would need to be conducted to determine if terminal dysfunction could be achieved in the CD4 T cells. It is also interesting to note that for CD4 T cells, the gene signatures that matched most closely on IPA analysis were those related to mouse models of blood-stage malaria [200]. Consistent with this, there have been reports of T cell exhaustion in malaria patients [227]. It would be interesting to perform a more in-depth phenotypic and functional characterization to compare the two, as treatments to overcome the CD4 dysfunction could be tested in this simple model, without necessitating mouse infection with malaria. It would also be interesting to determine if there are similarities in viruses that might bind erythrocytes and co-opt this pathway to evade the immune system [305, 306].

## 4.2 Discussion and Future Directions in LSEC targeting

In the second study, I developed an antibody fragment that binds liver sinusoidal endothelial cells, in order to capitalize on their tolerogenic potential. These Fabs bound with high affinity to LSECtin and LSECs, and were rapidly internalized by LSECs. Ligation of LSECtin alone led to a reduction in antigen presentation to T cells, suggesting that LSECtin led to a non-presenting pathway. Protein engineering strategies were undertaken to enhance presentation, by means of endosomal escape peptides and cathepsin-cleavable linkers; however, these were unsuccessful. It is possible that LSECs sequester antigen until an inflammatory stimulus necessitates presentation. Alternatively, LSECs may just degrade LSECtin-bound antigen rapidly, preventing its presentation. Finally, we developed polymerosomes that rapidly burst

the endosome and decorated them in Fab, with antigen in the core of the polymerosome. This greatly enhanced presentation, particularly in the CD4 T cell compartment.

Because we finally saw enhanced presentation with polymerosomes, studies need to be conducted to determine if this presentation was tolerogenic, or if it was immunogenic. Additionally, a dosing study will be necessary, because the high amount of CD4 T cell presentation may not be beneficial. Similar studies would need to be conducted as with the erythrocyte-targeting project to investigate tolerance. As opposed to in a TCR transgenic model, it would be interesting to induce tolerance to other disease-relevant antigens in an endogenous repertoire, as this is more relevant to the clinic.

Polymerosomes also offer an interesting advantage over recombinant expression of protein for multiple reasons. The first is that by encapsulating antigen, it is shielded from antigen-specific antibodies in the periphery. This could enable tolerance induction in the face of an ongoing immune response. Consistent with this, many strategies for antigen-specific tolerance utilize nanoparticles encapsulated with autoantigens [307]. Another advantage of this system is the ability to encapsulate a breadth of antigens, as opposed to a single antigen as with recombinant expression. In many autoimmune diseases, there is either no defined autoantigen, or there are multiple autoantigens. One could imagine encapsulating whole lysate from islet beta cells for the treatment of T1D. Importantly, in this strategy the antigens do not need to be in the appropriate conformation, so proteins can be denatured and rendered dysfunctional so they do not have endogenous activity. One could also imagine transplant antigens such as from lysed donor PBMCs, which would contain MHC as well as peptides from the donor.

It may also be interesting to target LSECs for purposes other than immune tolerance using this technology. For example, nanoparticles coated in melittin triggered robust activation of LSECs, which led to a reduction in liver metastases [261]. One could imagine triggering activation in LSECs with polymerosome-encapsulated TLR ligands in the context of cancer or chronic liver infection with hepatitis B or C viruses. However, given the liver's essential

role to the body, there would have to be a careful titration of activation to avoid liver toxicity.

## 4.3 Limitations and Potential Solutions to Antigen-Specific Tolerance

### *4.3.1 Selection of Antigen*

A major limitation of antigen-specific tolerance lies in the choice of antigen. As described in Section 1.2.1, autoimmune diseases for which the autoantigens are known comprise roughly half of all known autoimmune diseases. Of the autoimmune diseases for which autoantigens are known, there are often many associated autoantigens, and the contributions of each to pathology are not well established. This is also particularly relevant in transplantation, where there is an almost infinite combination of peptide-MHC molecules to which tolerance must be induced. Furthermore, in some diseases such as SLE, the autoantigens are nucleic acids as opposed to protein antigens, and thus would not be targetable in the current strategies under investigation that rely on T cell tolerance. Finally, in some autoimmune diseases many autoreactive T cells recognize post-translationally modified peptides, such as hybrid peptides, citrullination, or transglutamination [308].

There are a few potential approaches to solving these issues. The first would be to induce tolerance to multiple known autoantigens, as opposed to just one. This strategy has been used extensively in MS and shows benefit over a single autoantigen (see Section 1.3.1). This, however, does not solve most of the aforementioned issues. Another alternative would be to use as the tolerogen a lysate of the affected tissues, obtained by a biopsy. Proteins could gently be denatured such that none of the antigens would be bioactive. This would enable tolerance to all of the patients' associated autoantigens. Limitations to this approach are availability of sufficient tissue, and vector of encapsulation. Although not patient-specific, cadavers, or eventually lab-generated organs, may offer a more feasible alternative to provide large quantities of antigen. A final approach could be delivery of a potent anti-inflammatory

molecules, such as rapamycin, IL-10, or calcitriol, specifically to the site of autoimmunity or antigen drainage. Our lab has developed serum albumin-IL-4 fusions that preferentially localize to the lymph nodes, and are effective in preventing EAE and reducing effector T cell functions in EAE [309]. It is possible that by interacting with pathogenic T cells as they encounter antigen, the IL-4 modulates its effects. Similarly, we can imagine other ways of delivering anti-inflammatory molecules to the site of autoimmunity by targeting specific receptors on the target organ, or by delivering the molecule to the specific draining lymph nodes. This could also potentially affect ongoing germinal center and B cell responses, which may be efficacious in inducing tolerance to non-T cell autoantigens.

### *4.3.2 Ongoing T Cell Responses*

Deletion of both naïve and pathogenic antigen-specific cells would be a clear way to prevent and reverse autoimmunity, respectively. With our strategy of erythrocyte targeting, we saw extensive deletion even with a large precursor frequency of naïve antigen-specific cells. This is complicated in an ongoing immune response, however, where there are already activated memory T cells. Providing antigen in this context could in theory activate T cells, which could exacerbate disease. Interestingly, this has not been observed in clinical trials that have sought to deliver free antigen for therapy (see Section 1.3.1). As these clinical trials have demonstrated, it is possible that high dose antigen alone would be sufficient to lead to some T cell deletion. In an alternative strategy to promote deletion of pathogenic T cells, one could imagine pulsing tolDCs engineered to overexpress FasL with autoantigen and delivering them to patients, such that memory cells expressing Fas that come into contact with their cognate antigen would be deleted, a strategy that is employed by HIV [310]. Using these strategies, however, it is unlikely that every antigen-specific cell would be deleted. Many of the antigen-specific cells during an ongoing immune response would likely be tissue resident, and therefore may never come into contact with the tolerogenically administered antigen. A lesser but nonzero concern is that over a lifetime, there would be new thymic emigrants

that are potentially autoreactive. Finally, it is unknown if only T cells with high TCR avidity would be deleted, sparing T cells with TCRs of low avidity. Thus, additional forms of tolerance are needed to supplement deletion.

A more feasible strategy than to delete pathogenic T cells is to induce their dysfunction. In transplant and cancer, this seems to be sufficient to prevent organ or tumor rejection, respectively, despite a multitude of neoantigens. With erythrocyte targeting and other strategies that employ persistent low dose antigen exposure in the absence of inflammation, it is possible to induce dysfunction. If autoreactive T cells are converted to being dysfunctional, this may be sufficient to prevent pathology. However, if there was an acute immune stimulus such as a strong infection, it may cause these cells to revert back to functionality and reinitiate autoimmune-mediated tissue destruction. If this would only be temporary, this may be acceptable in some cases of autoimmunity where flare ups would not be deadly. However, this would not be an acceptable strategy in transplant, where a reversal of tolerance could lead to irreversible organ destruction.

A component of tolerance that will likely be required for any antigen-specific treatment is the induction of Tregs. Even if T cells did escape deletion, or dysfunctional T cells regained effector capacity, Tregs could feasibly suppress these autoreactive T cells. Thus, one could imagine co-administering iTregs or CAR Tregs (see Section 1.3.4) with other strategies that induce deletion or dysfunction in the pathogenic T cells. This may require multiple Treg infusions over a lifetime, as the longevity of these transferred Tregs *in vivo* is still largely unknown. Other strategies that induce or amplify antigen-specific FoxP3+ Tregs or Tr1 cells *in vivo* (see Section 1.3.3) will be of even greater value because the T cells can directly suppress in an antigen-specific manner. However, there are even less data on the stability and longevity of these *in vivo* generated Tregs. Furthermore, although it has been recently demonstrated that conventional effector or memory T cells can convert to Tregs *in vivo* in the presence or newly discovered small molecules, there are little data on the ability of the antigen-specific therapies under investigation to do this [311, 312]. Thus, most of the

therapies that are allegedly Treg mediated are likely non-specific, or they amplify a small subset of specific T cells. Much more mechanistic investigation needs to be done on these strategies, as they will likely be crucial to inducing long-lasting tolerance.

### *4.3.3 Ongoing B Cell Responses*

Ongoing B cell responses are also of significant concern in autoimmunity, transplantation, and allergy. In many autoimmune diseases, such as SLE, RA, and T1D, there are many circulating autoantibodies [313]. If a strategy for antigen-specific tolerance involved naked antigen, it would likely be immediately opsonized and phagocytosed, precluding any potential for tolerance. To circumvent this, one could encapsulate antigen such that it is shielded from autoantibodies. If this approach produced sufficient Tregs, and in particular follicular regulatory T cells, it is possible that the B cell response might be mitigated. Alternatively, one could deplete B cells using anti-CD20 or other approved B cell-depleting strategies. This would have to be combined with depletion of plasma cells using bortezomib, as well as intravenous immunoglobulin therapy or FcRn inhibition to deplete circulating autoantibodies. If the antigen-specific treatment that followed was robust, this could prevent the reemergence of autoreactive B cells. Although less common than T cell tolerance approaches, there have been some approaches in clinical trials to deplete antigen-specific B cells, such as by liposomes carrying CD22 and antigen, that are able to trigger antigen-specific B cell apoptosis [314]. Combined with antibody and plasma cell depletion, this could also be an effective method of tolerance. Finally, one could imagine delivering antigen to sites of germinal center reactions along with cues that induce Bregs. However, this strategy is not immediately actionable, as the cues that lead to Breg differentiation are largely unknown (see Section 1.1.5.

### *4.3.4 Promise of Combination Therapies*

Antigen-specific tolerance offers a significant alternative to current broad immunosuppression utilized in the clinic, as outlined in the Introduction. Early approved therapies for antigen-specific tolerance may require many repeated doses, analogous to AIT in allergy. The eventual goal would be to achieve a state of lasting tolerance with few doses, that could not be overcome by infection or other chronic inflammation. In order to do this, it may be necessary to combine pathways of tolerance and have a combination therapy, analogous to treatments in other diseases. For example, cancer treatment often involves chemotherapy, radiotherapy, and immunotherapy to target tumor cell intrinsic and extrinsic pathways to rid the patient of cancer [315]. Similarly, to treat autoimmunity we may need to act on different components of the immune system to achieve tolerance, including B cell and T cell depletion, induction of T cell dysfunction, and induction of regulatory cells.

## 4.4 Conclusion

In conclusion, this work seeks to contribute to the burgeoning field of antigen-specific tolerance. We develop tools to target endogenous pathways of immune surveillance, and co-opt them for induction of immune tolerance. Developing therapies for the clinic will require a high degree of collaboration with immunologists, to not only develop reasonable strategies but also to properly characterize the developed technologies. There is so much potential for innovation in this field, and I hope that these types of technologies will lead to a better quality of life for the millions suffering from diseases of immune dysregulation.

# REFERENCES


[1] Mark S Anderson, Emily S Venanzi, Zhibin Chen, Stuart P Berzins, Christophe Benoist, and Diane Mathis. The Cellular Mechanism of Aire Control of T Cell Tolerance. *Immunity*, 23(2):227–239, 2005.

[2] Ludger Klein, Ellen A Robey, and Chyi-Song Hsieh. Central CD4+ T cell tolerance: deletion versus regulatory T cell differentiation. *Nature Reviews Immunology*, 19(1):7–18, 2018.

[3] Mary E Brunkow, Eric W Jeffery, Kathryn A Hjerrild, Bryan Paeper, Lisa B Clark, Sue-Ann Yasayko, J Erby Wilkinson, David Galas, Steven F Ziegler, and Fred Ramsdell. Disruption of a new forkhead/winged-helix protein, scurfin, results in the fatal lymphoproliferative disorder of the scurfy mouse. *Nature Genetics*, 27(1):68–73, 2001.

[4] Craig L Bennett, Jacinda Christie, Fred Ramsdell, Mary E Brunkow, Polly J Ferguson, Luke Whitesell, Thaddeus E Kelly, Frank T Saulsbury, Phillip F Chance, and Hans D Ochs. The immune dysregulation, polyendocrinopathy, enteropathy, X-linked syndrome (IPEX) is caused by mutations of FOXP3. *Nature Genetics*, 27(1):20–21, 2001.

[5] Soyoung A Oh and Ming O Li. TGF-$\beta$: Guardian of T Cell Function. *The Journal of Immunology*, 191(8):3973–3979, 2013.

[6] T H Sky Ng, Graham J Britton, Elaine V Hill, Johan Verhagen, Bronwen R Burton, and David C Wraith. Regulation of adaptive immunity; the role of interleukin-10. *Frontiers in immunology*, 4:129, 2013.

[7] Thomas Höfer, Oleg Krichevsky, and Grégoire Altan-Bonnet. Competition for IL-2 between Regulatory and Effector T Cells to Chisel Immune Responses. *Frontiers in immunology*, 3:268, 2012.

[8] Xuefang Cao, Sheng F Cai, Todd A Fehniger, Jiling Song, Lynne I Collins, David R Piwnica-Worms, and Timothy J Ley. Granzyme B and Perforin Are Important for Regulatory T Cell-Mediated Suppression of Tumor Clearance. *Immunity*, 27(4):635–646, 2007.

[9] Omar S Qureshi, Yong Zheng, Kyoko Nakamura, Kesley Attridge, Claire Manzotti, Emily M Schmidt, Jennifer Baker, Louisa E Jeffery, Satdip Kaur, Zoe Briggs, Tie Z Hou, Clare E Futter, Graham Anderson, Lucy S K Walker, and David M Sansom. Trans-endocytosis of CD80 and CD86: a molecular basis for the cell-extrinsic function of CTLA-4. *Science (New York, N.Y.)*, 332(6029):600–3, 2011.

[10] Billur Akkaya, Yoshihiro Oya, Munir Akkaya, Jafar Al Souz, Amanda H Holstein, Olena Kamenyeva, Juraj Kabat, Ryutaro Matsumura, David W Dorward, Deborah D Glass, and Ethan M Shevach. Regulatory T cells mediate specific suppression by depleting peptide-MHC class II from dendritic cells. *Nature immunology*, 20(2):218–231, 2019.

[11] Y P Rubtsov, R E Niec, S Josefowicz, L Li, J Darce, D Mathis, C Benoist, and A Y Rudensky. Stability of the Regulatory T Cell Lineage in Vivo. *Science*, 329(5999):1667–1671, 2010.

[12] Takahisa Miyao, Stefan Floess, Ruka Setoguchi, Hervé Luche, Hans Joerg Fehling, Herman Waldmann, Jochen Huehn, and Shohei Hori. Plasticity of Foxp3+ T Cells Reflects Promiscuous Foxp3 Expression in Conventional T Cells but Not Reprogramming of Regulatory T Cells. *Immunity*, 36(2):262–275, 2012.

[13] Naganari Ohkura, Masahide Hamaguchi, Hiromasa Morikawa, Kyoko Sugimura, Atsushi Tanaka, Yoshinaga Ito, Motonao Osaki, Yoshiaki Tanaka, Riu Yamashita, Naoko Nakano, Jochen Huehn, Hans Joerg Fehling, Tim Sparwasser, Kenta Nakai, and Shimon Sakaguchi. T Cell Receptor Stimulation-Induced Epigenetic Changes and Foxp3 Expression Are Independent and Complementary Events Required for Treg Cell Development. *Immunity*, 37(5):785–799, 2012.

[14] Xuyu Zhou, Samantha L Bailey-Bucktrout, Lukas T Jeker, Cristina Penaranda, Marc Martínez-Llordella, Meredith Ashby, Maki Nakayama, Wendy Rosenthal, and Jeffrey A Bluestone. Instability of the transcription factor Foxp3 leads to the generation of pathogenic memory T cells in vivo. *Nature Immunology*, 10(9):1000–1007, 2009.

[15] João H Duarte, Santiago Zelenay, Marie-Louise Bergman, Ana C Martins, and Jocelyne Demengeot. Natural Treg cells spontaneously differentiate into pathogenic helper cells in lymphopenic conditions. *European Journal of Immunology*, 39(4):948–955, 2009.

[16] G Lal, N Yin, J Xu, M Lin, S Schroppel, Y Ding, I Marie, D E Levy, and J S Bromberg. Distinct inflammatory signals have physiologically divergent effects on epigenetic regulation of Foxp3 expression and Treg function. *American journal of transplantation : official journal of the American Society of Transplantation and the American Society of Transplant Surgeons*, 11(2):203–14, 2011.

[17] Noriko Komatsu, Maria Encarnita Mariotti-Ferrandiz, Ying Wang, Bernard Malissen, Herman Waldmann, and Shohei Hori. Heterogeneity of natural Foxp3+ T cells: a committed regulatory T-cell lineage and an uncommitted minor population retaining plasticity. *Proceedings of the National Academy of Sciences of the United States of America*, 106(6):1903–8, 2009.

[18] Yan Xing and Kristin A Hogquist. T-cell tolerance: central and peripheral. *Cold Spring Harbor perspectives in biology*, 4(6):a006957–a006957, 2012.

[19] Daniel L Mueller. Mechanisms maintaining peripheral tolerance. *Nature immunology*, 11(1):21–7, 2009.

[20] Peter D Hughes, Gabrielle T Belz, Karen A Fortner, Ralph C Budd, Andreas Strasser, and Philippe Bouillet. Apoptosis regulators Fas and Bim cooperate in shutdown of chronic immune responses and prevention of autoimmunity. *Immunity*, 28(2):197–205, 2008.

[21] F Rieux-Laucat, F Le Deist, and A Fischer. Autoimmune lymphoproliferative syndromes: genetic defects of apoptosis pathways. *Cell Death & Differentiation*, 10(1):124–133, 2003.

[22] S Nagata. Human autoimmune lymphoproliferative syndrome, a defect in the apoptosis-inducing Fas receptor: A lesson from the mouse model. *Journal of Human Genetics*, 43(1):2–8, 1998.

[23] William L Redmond, Boris C Marincek, and Linda A Sherman. Distinct Requirements for Deletion versus Anergy during CD8 T Cell Peripheral Tolerance In Vivo. *The Journal of Immunology*, 174(4):2046–2053, 2005.

[24] Astrid Lanoue, Constantin Bona, Harald von Boehmer, and Adelaida Sarukhan. Conditions That Induce Tolerance in Mature CD4+ T Cells. *Journal of Experimental Medicine*, 185(3):405–414, 1997.

[25] Andrew D Wells. New insights into the molecular basis of T cell anergy: anergy factors, avoidance sensors, and epigenetic imprinting. *Journal of immunology (Baltimore, Md. : 1950)*, 182(12):7331–41, 2009.

[26] Pascal Chappert and Ronald H Schwartz. Induction of T cell anergy: integration of environmental cues and infectious tolerance. *Current opinion in immunology*, 22(5):552–9, 2010.

[27] C Garrison Fathman and Neil B Lineberry. Molecular mechanisms of CD4+ T-cell anergy. *Nature Reviews Immunology*, 7(8):599–609, 2007.

[28] B Rocha, C Tanchot, and H Von Boehmer. Clonal anergy blocks in vivo growth of mature T cells and can be reversed in the absence of antigen. *Journal of Experimental Medicine*, 177(5):1517–1521, 1993.

[29] Andrea Schietinger, Jeffrey J Delrow, Ryan S Basom, Joseph N Blattman, and Philip D Greenberg. Rescued tolerant CD8 T cells are preprogrammed to reestablish the tolerant state. *Science (New York, N.Y.)*, 335(6069):723–7, 2012.

[30] Michelle L Miller, Christine M McIntosh, Ying Wang, Luqiu Chen, Peter Wang, Yuk Man Lei, Melvin D Daniels, Elyse Watkins, Carolina Mora Solano, Anita S Chong, and Maria-Luisa Alegre. Resilience of T cell-intrinsic dysfunction in transplantation tolerance. *Proceedings of the National Academy of Sciences*, 116(47):23682–23690, 2019.

[31] Jaxaira Maggi, Carolina Schafer, Gabriela Ubilla-Olguín, Diego Catalán, Katina Schinnerling, and Juan C Aguillón. Therapeutic Potential of Hyporesponsive CD4(+) T Cells in Autoimmunity. *Frontiers in immunology*, 6:488, 2015.

[32] Dipica Haribhai, Jason B Williams, Shuang Jia, Derek Nickerson, Erica G Schmitt, Brandon Edwards, Jennifer Ziegelbauer, Maryam Yassai, Shun-Hwa Li, Lance M Relland, Petra M Wise, Andrew Chen, Yu-Qian Zheng, Pippa M Simpson, Jack Gorski,

Nita H Salzman, Martin J Hessner, Talal A Chatila, and Calvin B Williams. A requisite role for induced regulatory T cells in tolerance based on expanding antigen receptor diversity. *Immunity*, 35(1):109–22, 2011.

[33] Steven Z Josefowicz, Rachel E Niec, Hye Young Kim, Piper Treuting, Takatoshi Chinen, Ye Zheng, Dale T Umetsu, and Alexander Y Rudensky. Extrathymically generated regulatory T cells control mucosal TH2 inflammation. *Nature*, 482(7385):395–399, 2012.

[34] Nicholas Arpaia, Clarissa Campbell, Xiying Fan, Stanislav Dikiy, Joris van der Veeken, Paul deRoos, Hui Liu, Justin R Cross, Klaus Pfeffer, Paul J Coffer, and Alexander Y Rudensky. Metabolites produced by commensal bacteria promote peripheral regulatory T-cell generation. *Nature*, 504(7480):451–5, 2013.

[35] David Bauché and Julien C Marie. Transforming growth factor $\beta$: a master regulator of the gut microbiota and immune cell interactions. *Clinical & Translational Immunology*, 6(4):e136, 2017.

[36] E V Russler-Germain, S Rengarajan, and C-S Hsieh. Antigen-specific regulatory T-cell responses to intestinal microbiota. *Mucosal immunology*, 10(6):1375–1386, 2017.

[37] Kwang Soon Kim, Sung-Wook Hong, Daehee Han, Jaeu Yi, Jisun Jung, Bo-Gie Yang, Jun Young Lee, Minji Lee, and Charles D Surh. Dietary antigens limit mucosal immunity by inducing regulatory T cells in the small intestine. *Science (New York, N.Y.)*, 351(6275):858–63, 2016.

[38] Maria Salvany-Celades, Anita van der Zwan, Marilen Benner, Vita Setrajcic-Dragos, Hannah Ananda Bougleux Gomes, Vidya Iyer, Errol R Norwitz, Jack L Strominger, and Tamara Tilburgs. Three Types of Functional Regulatory T Cells Control T Cell Responses at the Human Maternal-Fetal Interface. *Cell reports*, 27(9):2537–2547.e5, 2019.

[39] Robert M Samstein, Steven Z Josefowicz, Aaron Arvey, Piper M Treuting, and Alexander Y Rudensky. Extrathymic Generation of Regulatory T Cells in Placental Mammals Mitigates Maternal-Fetal Conflict. *Cell*, 150(1):29–38, 2012.

[40] Mojgan Ahmadzadeh, Anna Pasetto, Li Jia, Drew C Deniger, Sanja Stevanović, Paul F Robbins, and Steven A Rosenberg. Tumor-infiltrating human CD4+ regulatory T cells display a distinct TCR repertoire and exhibit tumor and neoantigen reactivity. *Science immunology*, 4(31):eaao4310, 2019.

[41] Maria Grazia Roncarolo, Silvia Gregori, Rosa Bacchetta, Manuela Battaglia, and Nicola Gagliani. The Biology of T Regulatory Type 1 Cells and Their Therapeutic Application in Immune-Mediated Diseases. *Immunity*, 49(6):1004–1019, 2018.

[42] Abdelilah Wakkach, Nathalie Fournier, Valérie Brun, Jean-Philippe Breittmayer, Françoise Cottrez, and Hervé Groux. Characterization of Dendritic Cells that Induce Tolerance and T Regulatory 1 Cell Differentiation In Vivo. *Immunity*, 18(5):605–617, 2003.

[43] Caroline Pot, Lionel Apetoh, and Vijay K Kuchroo. Type 1 regulatory T cells (Tr1) in autoimmunity. *Seminars in Immunology*, 23(3):202–208, 2011.

[44] Belal Chaudhary and Eyad Elkord. Regulatory T Cells in the Tumor Microenvironment and Cancer Progression: Role and Therapeutic Targeting. *Vaccines*, 4(3):28, 2016.

[45] Tatiana Jofra, Roberta Di Fonte, Giuseppe Galvani, Mirela Kuka, Matteo Iannacone, Manuela Battaglia, and Georgia Fousteri. Tr1 cell immunotherapy promotes transplant tolerance via de novo Tr1 cell induction in mice and is safe and effective during acute viral infection: Tatiana Jofra et al. *European Journal of Immunology*, 48(8):1389–1399, 2018.

[46] N Gagliani, T Jofra, A Stabilini, A Valle, M Atkinson, M G Roncarolo, and M Battaglia. Antigen-Specific Dependence of Tr1-Cell Therapy in Preclinical Models of Islet Transplant. *Diabetes*, 59(2):433–439, 2009.

[47] Susan D Wolf, Bonnie N Dittel, Fridrika Hardardottir, and Charles A Janeway. Experimental Autoimmune Encephalomyelitis Induction in Genetically B Cell–deficient Mice. *Journal of Experimental Medicine*, 184(6):2271–2278, 1996.

[48] Simon Fillatreau, Claire H Sweenie, Mandy J McGeachy, David Gray, and Stephen M Anderton. B cells regulate autoimmunity by provision of IL-10. *Nature Immunology*, 3(10):944–950, 2002.

[49] Claudia Mauri and Anneleen Bosma. Immune Regulatory Function of B Cells. *Annual Review of Immunology*, 30(1):221–241, 2012.

[50] Fabian Flores-Borja, Anneleen Bosma, Dorothy Ng, Venkat Reddy, Michael R Ehrenstein, David A Isenberg, and Claudia Mauri. CD19+CD24hiCD38hi B cells maintain regulatory T cells while limiting TH1 and TH17 differentiation. *Science translational medicine*, 5(173):173ra23, 2013.

[51] Paul A Blair, Lina Yassin Noreña, Fabian Flores-Borja, David J Rawlings, David A Isenberg, Michael R Ehrenstein, and Claudia Mauri. CD19(+)CD24(hi)CD38(hi) B cells exhibit regulatory capacity in healthy individuals but are functionally impaired in systemic Lupus Erythematosus patients. *Immunity*, 32(1):129–40, 2010.

[52] Koichi Yanaba, Jean-David Bouaziz, Karen M Haas, Jonathan C Poe, Manabu Fujimoto, and Thomas F Tedder. A regulatory B cell subset with a unique CD1dhiCD5+ phenotype controls T cell-dependent inflammatory responses. *Immunity*, 28(5):639–50, 2008.

[53] C M Wortel and S Heidt. Regulatory B cells: Phenotype, function and role in transplantation. *Transplant immunology*, 41:1–9, 2017.

[54] Guillaume Churlaud, Fabien Pitoiset, Fadi Jebbawi, Roberta Lorenzon, Bertrand Bellier, Michelle Rosenzwajg, and David Klatzmann. Human and Mouse CD8(+)CD25(+)FOXP3(+) Regulatory T Cells at Steady State and during Interleukin-2 Therapy. *Frontiers in immunology*, 6:171, 2015.

[55] Hye-Jung Kim, Bert Verbinnen, Xiaolei Tang, Linrong Lu, and Harvey Cantor. Inhibition of follicular T-helper cells by CD8(+) regulatory T cells is essential for self tolerance. *Nature*, 467(7313):328–32, 2010.

[56] Naresha Saligrama, Fan Zhao, Michael J. Sikora, William S. Serratelli, Ricardo A. Fernandes, David M. Louis, Winnie Yao, Xuhuai Ji, Juliana Idoyaga, Vinit B. Mahajan, Lars M. Steinmetz, Yueh-Hsiu Chien, Stephen L. Hauser, Jorge R. Oksenberg, K. Christopher Garcia, and Mark M. Davis. Opposing T cell responses in experimental autoimmune encephalomyelitis. *Nature*, 572(7770):481–487, 2019.

[57] L Lu, H J Kim, M B F Werneck, and H Cantor. Regulation of CD8+ regulatory T cells: Interruption of the NKG2A-Qa-1 interaction allows robust suppressive activity and resolution of autoimmune disease. *Proceedings of the National Academy of Sciences*, 105(49):19420–19425, 2008.

[58] Allan J Zajac, Joseph N Blattman, Kaja Murali-Krishna, David J D Sourdive, M Suresh, John D Altman, and Rafi Ahmed. Viral Immune Evasion Due to Persistence of Activated T Cells Without Effector Function. *Journal of Experimental Medicine*, 188(12):2205–2213, 1998.

[59] Awen Gallimore, Ann Glithero, Andrew Godkin, Alain C Tissot, Andreas Plückthun, Tim Elliott, Hans Hengartner, and Rolf Zinkernagel. Induction and Exhaustion of Lymphocytic Choriomeningitis Virus–specific Cytotoxic T Lymphocytes Visualized Using Soluble Tetrameric Major Histocompatibility Complex Class I–Peptide Complexes. *Journal of Experimental Medicine*, 187(9):1383–1393, 1998.

[60] E John Wherry and Makoto Kurachi. Molecular and cellular insights into T cell exhaustion. *Nature reviews. Immunology*, 15(8):486–99, 2015.

[61] Peter P Lee, Cassian Yee, Peter A Savage, Lawrence Fong, Dirk Brockstedt, Jeffrey S Weber, Denise Johnson, Susan Swetter, John Thompson, Philip D Greenberg, Mario Roederer, and Mark M Davis. Characterization of circulating T cells specific for tumor-associated antigens in melanoma patients. *Nature Medicine*, 5(6):677–685, 1999.

[62] Eoin F McKinney, James C Lee, David R W Jayne, Paul A Lyons, and Kenneth G C Smith. T-cell exhaustion, co-stimulation and clinical outcome in autoimmunity and infection. *Nature*, 523(7562):612–6, 2015.

[63] Miguel Fribourg, Lisa Anderson, Clara Fischman, Chiara Cantarelli, Laura Perin, Gaetano La Manna, Adeeb Rahman, Bryna E Burrell, Peter S Heeger, and Paolo Cravedi. T-cell exhaustion correlates with improved outcomes in kidney transplant recipients. *Kidney international*, 96(2):436–449, 2019.

[64] Omar Khan, Josephine R Giles, Sierra McDonald, Sasikanth Manne, Shin F Ngiow, Kunal P Patel, Michael T Werner, Alexander C Huang, Katherine A Alexander, Jennifer E Wu, John Attanasio, Patrick Yan, Sangeeth M George, Bertram Bengsch, Ryan P Staupe, Greg Donahue, Wei Xu, Ravi K Amaravadi, Xiaowei Xu, Giorgos C Karakousis, Tara C Mitchell, Lynn M Schuchter, Jonathan Kaye, Shelley L Berger,

and E J Wherry. TOX transcriptionally and epigenetically programs CD8+ T cell exhaustion. *Nature*, 571(7764):211–218, 2019.

[65] Spencer C Wei, Colm R Duffy, and James P Allison. Fundamental Mechanisms of Immune Checkpoint Blockade Therapy. *Cancer discovery*, 8(9):1069–1086, 2018.

[66] James Larkin, Vanna Chiarion-Sileni, Rene Gonzalez, Jean Jacques Grob, C Lance Cowey, Christopher D Lao, Dirk Schadendorf, Reinhard Dummer, Michael Smylie, Piotr Rutkowski, Pier F Ferrucci, Andrew Hill, John Wagstaff, Matteo S Carlino, John B Haanen, Michele Maio, Ivan Marquez-Rodas, Grant A McArthur, Paolo A Ascierto, Georgina V Long, Margaret K Callahan, Michael A Postow, Kenneth Grossmann, Mario Sznol, Brigitte Dreno, Lars Bastholt, Arvin Yang, Linda M Rollin, Christine Horak, F Stephen Hodi, and Jedd D Wolchok. Combined Nivolumab and Ipilimumab or Monotherapy in Untreated Melanoma. *The New England journal of medicine*, 373(1):23–34, 2015.

[67] Whijae Roh, Pei-Ling Chen, Alexandre Reuben, Christine N Spencer, Peter A Prieto, John P Miller, Vancheswaran Gopalakrishnan, Feng Wang, Zachary A Cooper, Sangeetha M Reddy, Curtis Gumbs, Latasha Little, Qing Chang, Wei-Shen Chen, Khalida Wani, Mariana Petaccia De Macedo, Eveline Chen, Jacob L Austin-Breneman, Hong Jiang, Jason Roszik, Michael T Tetzlaff, Michael A Davies, Jeffrey E Gershenwald, Hussein Tawbi, Alexander J Lazar, Patrick Hwu, Wen-Jen Hwu, Adi Diab, Isabella C Glitza, Sapna P Patel, Scott E Woodman, Rodabe N Amaria, Victor G Prieto, Jianhua Hu, Padmanee Sharma, James P Allison, Lynda Chin, Jianhua Zhang, Jennifer A Wargo, and P Andrew Futreal. Integrated molecular analysis of tumor biopsies on sequential CTLA-4 and PD-1 blockade reveals markers of response and resistance. *Science Translational Medicine*, 9(379):eaah3560, 2017.

[68] Yifei Wang, Jianjun Hu, Yiding Li, Minglu Xiao, Haoqiang Wang, Qin Tian, Zhirong Li, Jianfang Tang, Li Hu, Yan Tan, Xinyuan Zhou, Ran He, Yuzhang Wu, Lilin Ye, Zhinan Yin, Qizhao Huang, and Lifan Xu. The Transcription Factor TCF1 Preserves the Effector Function of Exhausted CD8 T Cells During Chronic Viral Infection. *Frontiers in Immunology*, 10:169, 2019.

[69] Shawn D Blackburn, Haina Shin, Gordon J Freeman, and E John Wherry. Selective expansion of a subset of exhausted CD8 T cells by alphaPD-L1 blockade. *Proceedings of the National Academy of Sciences of the United States of America*, 105(39):15016–21, 2008.

[70] Zeyu Chen, Zhicheng Ji, Shin Foong Ngiow, Sasikanth Manne, Zhangying Cai, Alexander C Huang, John Johnson, Ryan P Staupe, Bertram Bengsch, Caiyue Xu, Sixiang Yu, Makoto Kurachi, Ramin S Herati, Laura A Vella, Amy E Baxter, Jennifer E Wu, Omar Khan, Jean-Christophe Beltra, Josephine R Giles, Erietta Stelekati, Laura M McLane, Chi Wai Lau, Xiaolu Yang, Shelley L Berger, Golnaz Vahedi, Hongkai Ji, and E John Wherry. TCF-1-Centered Transcriptional Network Drives an Effector versus Exhausted CD8 T Cell-Fate Decision. *Immunity*, 51(5):840–855.e5, 2019.

[71] K E Pauken, M A Sammons, P M Odorizzi, S Manne, J Godec, O Khan, A M Drake, Z Chen, D R Sen, M Kurachi, R A Barnitz, C Bartman, B Bengsch, A C Huang, J M Schenkel, G Vahedi, W N Haining, S L Berger, and E J Wherry. Epigenetic stability of exhausted T cells limits durability of reinvigoration by PD-1 blockade. *Science*, 354(6316):1160–1165, 2016.

[72] Scott M. Hayter and Matthew C. Cook. Updated assessment of the prevalence, spectrum and case definition of autoimmune disease. *Autoimmunity Reviews*, 11(10):754–765, 2012.

[73] Marco Salvetti, Giovanni Ristori, Roberto Bomprezzi, Paolo Pozzilli, and R.David G Leslie. Twins: mirrors of the immune system. *Immunology Today*, 21(7):342–347, 2000.

[74] Gregg E Dinse, Christine G Parks, Clarice R Weinberg, Caroll A Co, Jesse Wilkerson, Darryl C Zeldin, Edward K L Chan, and Frederick W Miller. Increasing Prevalence of Antinuclear Antibodies in the United States. *Arthritis & rheumatology (Hoboken, N.J.)*, 72(6):1026–1035, 2020.

[75] J Bradford Rice, Alan G White, Lauren M Scarpati, George Wan, and Winnie W Nelson. Long-term Systemic Corticosteroid Exposure: A Systematic Literature Review. *Clinical Therapeutics*, 39(11):2216–2229, 2017.

[76] Benjamin Friedman and Bruce Cronstein. Methotrexate mechanism in treatment of rheumatoid arthritis. *Joint Bone Spine*, 86(3):301–307, 2019.

[77] Eva Schrezenmeier and Thomas Dörner. Mechanisms of action of hydroxychloroquine and chloroquine: implications for rheumatology. *Nature reviews. Rheumatology*, 16(3):155–166, 2020.

[78] Wanying Wang, Hua Zhou, and Liang Liu. Side effects of methotrexate therapy for rheumatoid arthritis: A systematic review. *European Journal of Medicinal Chemistry*, 158:502–516, 2018.

[79] Amit K Mehta, Donald T Gracias, and Michael Croft. TNF activity and T cells. *Cytokine*, 101:14–18, 2016.

[80] Tim Wyant, Eric Fedyk, and Brihad Abhyankar. An Overview of the Mechanism of Action of the Monoclonal Antibody Vedolizumab. *Journal of Crohn's and Colitis*, 10(12):1437–1444, 2016.

[81] Michael Hutchinson. Natalizumab: A new treatment for relapsing remitting multiple sclerosis. *Therapeutics and Clinical Risk Management*, 3(2):259–268, 2007.

[82] Soheil Tavakolpour, Samira Alesaeidi, Mohammad Darvishi, Mojtaba GhasemiAdl, Sahar Darabi-Monadi, Meisam Akhlaghdoust, Somayeh Elikaei Behjati, and Arash Jafarieh. A comprehensive review of rituximab therapy in rheumatoid arthritis patients. *Clinical rheumatology*, 38(11):2977–2994, 2019.

[83] East Jeddah Hospital Jeddah Saudi Arabia, Department of Medicine, Fatma Alshaiki, Elaf Obaid, Umm Al-Qura University School of Medicine Makkah Saudi Arabia, Department of Medicine, Abdulqader Almuallim, Rabab Taha, Dr Sloiman Fakeeh Hospital Jeddah Saudi Arabia, Department of Medicine, Hadeel El-haddad, Hani Almoallim, and Umm Al-Qura University Makkah Saudi Arabia, Alzaidi Chair of Research in Rheumatic Diseases. Outcomes of rituximab therapy in refractory lupus: A meta-analysis. *European Journal of Rheumatology*, 5(2):118–126, 2018.

[84] Claus Madsen. The innovative development in interferon beta treatments of relapsing-remitting multiple sclerosis. *Brain and Behavior*, 7(6):e00696, 2017.

[85] Nils E. Gilhus. Myasthenia Gravis. *The New England Journal of Medicine*, 375(26):2570–2581, 2016.

[86] Enno Schmidt, Michael Kasperkiewicz, and Pascal Joly. Pemphigus. *The Lancet*, 394(10201):882–894, 2019.

[87] Sarah L. Patterson and Sarah E. Goglin. Neuromyelitis Optica. *Rheumatic Disease Clinics of North America*, 43(4):579–591, 2017.

[88] Craig E. Taplin and Jennifer M. Barker. Autoantibodies in type 1 diabetes. *Autoimmunity*, 41(1):11–18, 2009.

[89] Alyssa Nylander and David A. Hafler. Multiple sclerosis. *Journal of Clinical Investigation*, 122(4):1180–1188, 2012.

[90] G. Riemekasten and B. H. Hahn. Key autoantigens in SLE. *Rheumatology*, 44(8):975–982, 2005.

[91] Ruby Pawankar. Allergic diseases and asthma: a global public health concern and a call to action. *World Allergy Organization Journal*, 7(1):1–3, 2014.

[92] Hannah J Gould and Brian J Sutton. IgE in allergy and asthma today. *Nature reviews. Immunology*, 8(3):205–17, 2008.

[93] Kelly D Stone, Calman Prussin, and Dean D Metcalfe. IgE, mast cells, basophils, and eosinophils. *The Journal of allergy and clinical immunology*, 125(2 Suppl 2):S73–80, 2010.

[94] Robert A Wood, Carlos A Camargo, Philip Lieberman, Hugh A Sampson, Lawrence B Schwartz, Myron Zitt, Charlotte Collins, Michael Tringale, Marilyn Wilkinson, John Boyle, and F Estelle R Simons. Anaphylaxis in America: The prevalence and characteristics of anaphylaxis in the United States. *Journal of Allergy and Clinical Immunology*, 133(2):461–467, 2014.

[95] Thomas A E Platts-Mills. The allergy epidemics: 1870-2010. *The Journal of allergy and clinical immunology*, 136(1):3–13, 2015.

[96] F Estelle R Simons and Keith J Simons. Histamine and H1-antihistamines: Celebrating a century of progress. *Journal of Allergy and Clinical Immunology*, 128(6):1139–1150.e4, 2011.

[97] Sherry H Yu, Aaron M Drucker, Mark Lebwohl, and Jonathan I Silverberg. A systematic review of the safety and efficacy of systemic corticosteroids in atopic dermatitis. *Journal of the American Academy of Dermatology*, 78(4):733–740.e11, 2018.

[98] Stephen T Holgate and Riccardo Polosa. Treatment strategies for allergy and asthma. *Nature Reviews Immunology*, 8(3):218–230, 2008.

[99] J A Dantzer and R A Wood. The use of omalizumab in allergen immunotherapy. *Clinical & Experimental Allergy*, 48(3):232–240, 2018.

[100] Laurel Stephenson. Monoclonal Antibody Therapy for Asthma. *Clinical Pulmonary Medicine*, 24(6):250–257, 2017.

[101] O Pfaar, H Lou, Y Zhang, L Klimek, and L Zhang. Recent Developments and Highlights in Allergen Immunotherapy. *Allergy*, 73(12):2274–2289, 2018.

[102] Cezmi A Akdis and Mübeccel Akdis. Mechanisms of allergen-specific immunotherapy and immune tolerance to allergens. *The World Allergy Organization journal*, 8(1):17, 2015.

[103] Christine James and David I Bernstein. Allergen immunotherapy: an updated review of safety. *Current opinion in allergy and clinical immunology*, 17(1):55–59, 2017.

[104] Emily C McGowan and Robert A Wood. Sublingual (SLIT) versus oral immunotherapy (OIT) for food allergy. *Current allergy and asthma reports*, 14(12):486, 2014.

[105] S Dhami, H Zaman, E-M Varga, G J Sturm, A Muraro, C A Akdis, D Antolín-Amérigo, M B Bilò, D Bokanovic, M A Calderon, E Cichocka-Jarosz, J N G Oude Elberink, R Gawlik, T Jakob, M Kosnik, J Lange, E Mingomataj, D I Mitsias, H Mosbech, M Ollert, O Pfaar, C Pitsios, V Pravettoni, G Roberts, F Ruëff, B A Sin, M Asaria, G Netuveli, and A Sheikh. Allergen immunotherapy for insect venom allergy: a systematic review and meta-analysis. *Allergy*, 72(3):342–365, 2017.

[106] Fardous Musa, Mona Al-Ahmad, Nermina Arifhodzic, and Waleed Al-Herz. Compliance with allergen immunotherapy and factors affecting compliance among patients with respiratory allergies. *Human Vaccines & Immunotherapeutics*, 13(3):514–517, 2016.

[107] OPTN/SRTR 2018 Annual Data Report: Introduction. *American journal of transplantation : official journal of the American Society of Transplantation and the American Society of Transplant Surgeons*, 20 Suppl s1(s1):11–19, 2020.

[108] Thomas M Williams. Human Leukocyte Antigen Gene Polymorphism and the Histocompatibility Laboratory. *The Journal of Molecular Diagnostics*, 3(3):98–104, 2001.

[109] Fumiko Yamamoto, Shingo Suzuki, Akiko Mizutani, Atsuko Shigenari, Sayaka Ito, Yoshie Kametani, Shunichi Kato, Marcelo Fernandez-Viña, Makoto Murata, Satoko Morishima, Yasuo Morishima, Masafumi Tanaka, Jerzy K Kulski, Seiamak Bahram, and Takashi Shiina. Capturing Differential Allele-Level Expression and Genotypes of All Classical HLA Loci and Haplotypes by a New Capture RNA-Seq Method. *Frontiers in Immunology*, 11:941, 2020.

[110] E Thorsby. A short history of HLA. *Tissue Antigens*, 74(2):101–116, 2009.

[111] A Djamali, D B Kaufman, T M Ellis, W Zhong, A Matas, and M Samaniego. Diagnosis and management of antibody-mediated rejection: current status and novel approaches. *American journal of transplantation : official journal of the American Society of Transplantation and the American Society of Transplant Surgeons*, 14(2):255–71, 2014.

[112] Curtis D Holt. Overview of Immunosuppressive Therapy in Solid Organ Transplantation. *Anesthesiology clinics*, 35(3):365–380, 2017.

[113] Miae Kim, Spencer T Martin, Keri R Townsend, and Steven Gabardi. Antibody-mediated rejection in kidney transplantation: a review of pathophysiology, diagnosis, and treatment options. *Pharmacotherapy*, 34(7):733–44, 2014.

[114] Douglas J Norman and Michael R Leone. The role of OKT3 in clinical transplantation. *Pediatric Nephrology*, 5(1):130–136, 1991.

[115] Mitchell L Henry and Amer Rajab. The use of basiliximab in solid organ transplantation. *Expert Opinion on Pharmacotherapy*, 3(11):1657–1663, 2002.

[116] Russell H Wiesner and John J Fung. Present state of immunosuppressive therapy in liver transplant recipients. *Liver Transplantation*, 17(S3):S1–S9, 2011.

[117] Florence Herr, Melanie Brunel, Nathalie Roders, and Antoine Durrbach. Co-stimulation Blockade Plus T-Cell Depletion in Transplant Patients: Towards a Steroid- and Calcineurin Inhibitor-Free Future? *Drugs*, 76(17):1589–1600, 2016.

[118] Jacinda Ristov, Pascal Espie, Peter Ulrich, Denise Sickert, Thierry Flandre, Mirela Dimitrova, Dorothee Müller-Ristig, Doris Weider, Gautier Robert, Patrick Schmutz, Barbara Greutmann, Francisco Cordoba-Castro, Martin A Schneider, Max Warncke, Frank Kolbinger, Serge Cote, Christoph Heusser, Christian Bruns, and James S Rush. Characterization of the in vitro and in vivo properties of CFZ533, a blocking and non-depleting anti-CD40 monoclonal antibody. *American journal of transplantation : official journal of the American Society of Transplantation and the American Society of Transplant Surgeons*, 18(12):2895–2904, 2018.

[119] B Nashan, H Tedesco, MW van den Hoogen, SP Berger, D Cibrik, S Mulgaonkar, D Leeser, R Alloway, A Patel, J Pratschke, C Sommerer, A Wiseman, A van Zuilen, U Laessing, J Rush, B Haraldsson, and O Witzke. CD40 Inhibition with CFZ533 - A New, Fully Human, Non-Depleting, Fc Silent mAB - Improves Renal Allograft Function While Demonstrating Comparable Efficacy vs. Tacrolimus in De-Novo CNI-Free Kidney Transplant Recipients. *Transplantation*, 102(&NA;):S366, 2018.

[120] Kentaro Ide, Yuka Tanaka, Yu Sasaki, Hiroyuki Tahara, Masahiro Ohira, Kohei Ishiyama, Hirotaka Tashiro, and Hideki Ohdan. A Phased Desensitization Protocol With Rituximab and Bortezomib for Highly Sensitized Kidney Transplant Candidates. *Transplantation direct*, 1(5):e17, 2015.

[121] Mauro Di Ianni, Franca Falzetti, Alessandra Carotti, Adelmo Terenzi, Flora Castellino, Elisabetta Bonifacio, Beatrice Del Papa, Tiziana Zei, Roberta Iacucci Ostini, Debora Cecchini, Teresa Aloisi, Katia Perruccio, Loredana Ruggeri, Chiara Balucani, Antonio Pierini, Paolo Sportoletti, Cynthia Aristei, Brunangelo Falini, Yair Reisner, Andrea Velardi, Franco Aversa, and Massimo F Martelli. Tregs prevent GVHD and promote immune reconstitution in HLA-haploidentical transplantation. *Blood*, 117(14):3921–8, 2011.

[122] Satoru Todo, Kenichiro Yamashita, Ryoichi Goto, Masaaki Zaitsu, Akihisa Nagatsu, Tetsu Oura, Masaaki Watanabe, Takeshi Aoyagi, Tomomi Suzuki, Tsuyoshi Shimamura, Toshiya Kamiyama, Norihiro Sato, Junichi Sugita, Kanako Hatanaka, Hisashi Bashuda, Sonoko Habu, Anthony J Demetris, and Ko Okumura. A pilot study of operational tolerance with a regulatory T-cell-based cell therapy in living donor liver transplantation. *Hepatology*, 64(2):632–643, 2016.

[123] Dawn M Ecker, Susan Dana Jones, and Howard L Levine. The therapeutic monoclonal antibody market. *mAbs*, 7(1):9–14, 2015.

[124] Vibha Jawa, Frances Terry, Jochem Gokemeijer, Shibani Mitra-Kaushik, Brian J. Roberts, Sophie Tourdot, and Anne S. De Groot. T-Cell Dependent Immunogenicity of Protein Therapeutics Pre-clinical Assessment and Mitigation–Updated Consensus and Review 2020. *Frontiers in Immunology*, 11:1301, 2020.

[125] Matthew Baker, Helen M Reynolds, Brooke Lumicisi, and Christine J Bryson. Immunogenicity of protein therapeutics: The key causes, consequences and challenges. *Self/Nonself*, 1(4):314–322, 2010.

[126] Carlos Pineda, Gilberto Castañeda Hernández, Ira A. Jacobs, Daniel F. Alvarez, and Claudio Carini. Assessing the Immunogenicity of Biopharmaceuticals. *BioDrugs*, 30(3):195–206, 2016.

[127] William Y Hwang and Jefferson Foote. Immunogenicity of engineered antibodies. *Methods (San Diego, Calif.)*, 36(1):3–10, 2005.

[128] Anne S De Groot, Frances Terry, Leslie Cousens, and William Martin. Beyond humanization and de-immunization: tolerization as a method for reducing the immunogenicity of biologics. *Expert Review of Clinical Pharmacology*, 6(6):651–662, 2014.

[129] François Blanchette and Oliver Neuhaus. Glatiramer Acetate: Evidence for a dual mechanism of action. *Journal of Neurology*, 255(S1):26–36, 2008.

[130] Pau Serra and Pere Santamaria. Antigen-specific therapeutic approaches for autoimmunity. *Nature Biotechnology*, 37(3):238–251, 2019.

[131] Emma L Smith and Mark Peakman. Peptide Immunotherapy for Type 1 Diabetes—Clinical Advances. *Frontiers in Immunology*, 9:392, 2018.

[132] Antonio Di Sabatino, Marco V Lenti, Gino R Corazza, and Carmen Gianfrani. Vaccine Immunotherapy for Celiac Disease. *Frontiers in medicine*, 5:187, 2018.

[133] Eva C Koffeman, Mark Genovese, Diane Amox, Elissa Keogh, Ernesto Santana, Eric L Matteson, Arthur Kavanaugh, Jerry A Molitor, Michael H Schiff, James O Posever, Joan M Bathon, Alan J Kivitz, Rodrigo Samodal, Francis Belardi, Carolyn Dennehey, Theo van den Broek, Femke van Wijk, Xiao Zhang, Peter Zieseniss, Tho Le, Berent A Prakken, Gary C Cutter, and Salvatore Albani. Epitope-specific immunotherapy of rheumatoid arthritis: clinical responsiveness occurs with immune deviation and relies on the expression of a cluster of molecules associated with T cell tolerance in a double-blind, placebo-controlled, pilot phase II trial. *Arthritis and rheumatism*, 60(11):3207–16, 2009.

[134] Robert Zimmer, Hugo R Scherbarth, Oscar Luis Rillo, Juan Jesus Gomez-Reino, and Sylviane Muller. Lupuzor/P140 peptide in patients with systemic lupus erythematosus: a randomised, double-blind, placebo-controlled phase IIb clinical trial. *Annals of the rheumatic diseases*, 72(11):1830–5, 2012.

[135] Amit Bar-Or, Timothy Vollmer, Jack Antel, Douglas L Arnold, Caroline Anita Bodner, Denise Campagnolo, Jill Gianettoni, Farzaneh Jalili, Norman Kachuck, Yves Lapierre, Masaaki Niino, Joel Oger, Mary Price, Susan Rhodes, William H Robinson, Fu-Dong Shi, Paul J Utz, Frank Valone, Leslie Weiner, Lawrence Steinman, and Hideki Garren. Induction of Antigen-Specific Tolerance in Multiple Sclerosis After Immunization With DNA Encoding Myelin Basic Protein in a Randomized, Placebo-Controlled Phase 1/2 Trial. *Archives of Neurology*, 64(10):1407, 2007.

[136] Hideki Garren, William H Robinson, Eva Krasulová, Eva Havrdová, Congor Nadj, Krzysztof Selmaj, Jacek Losy, Ilinka Nadj, Ernst-Wilhelm Radue, Brian A Kidd, Jill Gianettoni, Karen Tersini, Paul J Utz, Frank Valone, Lawrence Steinman, and BHT-3009 Study Group. Phase 2 trial of a DNA vaccine encoding myelin basic protein for multiple sclerosis. *Annals of neurology*, 63(5):611–20, 2008.

[137] Peggy P Ho, Paulo Fontoura, Pedro J Ruiz, Lawrence Steinman, and Hideki Garren. An Immunomodulatory GpG Oligonucleotide for the Treatment of Autoimmunity via the Innate and Adaptive Immune Systems. *The Journal of Immunology*, 171(9):4920–4926, 2003.

[138] B O Roep, N Solvason, P A Gottlieb, J R F Abreu, L C Harrison, G S Eisenbarth, L Yu, M Leviten, W A Hagopian, J B Buse, M von Herrath, J Quan, R S King, W H Robinson, P J Utz, H Garren, The BHT-3021 Investigators, and L Steinman. Plasmid-Encoded Proinsulin Preserves C-Peptide While Specifically Reducing Proinsulin-Specific CD8+ T Cells in Type 1 Diabetes. *Science Translational Medicine*, 5(191):191ra82–191ra82, 2013.

[139] Courtney A Iberg and Daniel Hawiger. Natural and Induced Tolerogenic Dendritic Cells. *Journal of immunology (Baltimore, Md. : 1950)*, 204(4):733–744, 2020.

[140] Irati Zubizarreta, Georgina Flórez-Grau, Gemma Vila, Raquel Cabezón, Carolina España, Magi Andorra, Albert Saiz, Sara Llufriu, Maria Sepulveda, Nuria Sola-Valls, Elena H Martinez-Lapiscina, Irene Pulido-Valdeolivas, Bonaventura Casanova, Marisa Martinez Gines, Nieves Tellez, Celia Oreja-Guevara, Marta Español, Esteve Trias, Joan Cid, Manel Juan, Miquel Lozano, Yolanda Blanco, Lawrence Steinman, Daniel Benitez-Ribas, and Pablo Villoslada. Immune tolerance in multiple sclerosis and neuromyelitis optica with peptide-loaded tolerogenic dendritic cells in a phase 1b trial. *Proceedings of the National Academy of Sciences of the United States of America*, 116(17):8463–8470, 2019.

[141] G M Bell, A E Anderson, J Diboll, R Reece, O Eltherington, R A Harry, T Fouweather, C MacDonald, T Chadwick, E McColl, J Dunn, A M Dickinson, C M U Hilkens, and John D Isaacs. Autologous tolerogenic dendritic cells for rheumatoid and inflammatory arthritis. *Annals of the Rheumatic Diseases*, 76(1):227–234, 2016.

[142] Helen Benham, Hendrik J Nel, Soi Cheng Law, Ahmed M Mehdi, Shayna Street, Nishta Ramnoruth, Helen Pahau, Bernett T Lee, Jennifer Ng, Marion E G Brunck, Claire Hyde, Leendert A Trouw, Nadine L Dudek, Anthony W Purcell, Brendan J O'Sullivan, John E Connolly, Sanjoy K Paul, Kim-Anh Lê Cao, and Ranjeny Thomas. Citrullinated peptide dendritic cell immunotherapy in HLA risk genotype–positive rheumatoid arthritis patients. *Science Translational Medicine*, 7(290):290ra87–290ra87, 2015.

[143] A Lutterotti, S Yousef, A Sputtek, K H Sturner, J P Stellmann, P Breiden, S Reinhardt, C Schulze, M Bester, C Heesen, S Schippling, S D Miller, M Sospedra, and R Martin. Antigen-Specific Tolerance by Autologous Myelin Peptide-Coupled Cells: A Phase 1 Trial in Multiple Sclerosis. *Science Translational Medicine*, 5(188):188ra75–188ra75, 2013.

[144] David H. Sachs, Tatsuo Kawai, and Megan Sykes. Induction of Tolerance through Mixed Chimerism. *Cold Spring Harbor Perspectives in Medicine*, 4(1):a015529, 2014.

[145] Tatsuo Kawai, A. Benedict Cosimi, Thomas R. Spitzer, Nina Tolkoff-Rubin, Manikkam Suthanthiran, Susan L. Saidman, Juanita Shaffer, Frederic I. Preffer, Ruchuang Ding, Vijay Sharma, Jay A. Fishman, Bimalangshu Dey, Dicken S.C. Ko, Martin Hertl, Nelson B. Goes, Waichi Wong, Winfred W. Williams, Robert B. Colvin, Megan Sykes, and David H. Sachs. HLA-Mismatched Renal Transplantation without Maintenance Immunosuppression. *The New England Journal of Medicine*, 358(4):353–361, 2008.

[146] Kristen M Lorentz, Stephan Kontos, Giacomo Diaceri, Hugues Henry, and Jeffrey A Hubbell. Engineered binding to erythrocytes induces immunological tolerance to E. coli asparaginase. *Science advances*, 1(6):e1500112, 2015.

[147] Stephan Kontos, Iraklis C Kourtis, Karen Y Dane, and Jeffrey A Hubbell. Engineering antigens for in situ erythrocyte binding induces T-cell deletion. *Proceedings of the National Academy of Sciences of the United States of America*, 110(1):E60–8, 2013.

[148] Novalia Pishesha, Angelina M Bilate, Marsha C Wibowo, Nai-Jia Huang, Zeyang Li, Rhogerry Dhesycka, Djenet Bousbaine, Hojun Li, Heide C Patterson, Stephanie K Dougan, Takeshi Maruyama, Harvey F Lodish, and Hidde L Ploegh. Engineered erythrocytes covalently linked to antigenic peptides can protect against autoimmune disease. *Proceedings of the National Academy of Sciences of the United States of America*, 114(12):3157–3162, 2017.

[149] Zoe Hunter, Derrick P McCarthy, Woon Teck Yap, Christopher T Harp, Daniel R Getts, Lonnie D Shea, and Stephen D Miller. A biodegradable nanoparticle platform for the induction of antigen-specific immune tolerance for treatment of autoimmune disease. *ACS nano*, 8(3):2148–60, 2014.

[150] Tobias L Freitag, Joseph R Podojil, Ryan M Pearson, Frank J Fokta, Cecilia Sahl, Marcel Messing, Leif C Andersson, Katarzyna Leskinen, Päivi Saavalainen, Lisa I Hoover, Kelly Huang, Deborah Phippard, Sanaz Maleki, Nicholas J C King, Lonnie D Shea, Stephen D Miller, Seppo K Meri, and Daniel R Getts. Gliadin Nanoparticles Induce Immune Tolerance to Gliadin in Mouse Models of Celiac Disease. *Gastroenterology*, 158(6):1667–1681.e12, 2020.

[151] Ryan Galea, Hendrik J Nel, Meghna Talekar, Xiao Liu, Joshua D Ooi, Megan Huynh, Sara Hadjigol, Kate J Robson, Yi Tian Ting, Suzanne Cole, Karyn Cochlin, Shannon Hitchcock, Bijun Zeng, Suman Yekollu, Martine Boks, Natalie Goh, Helen Roberts, Jamie Rossjohn, Hugh H Reid, Ben J Boyd, Ravi Malaviya, David J Shealy, Daniel G Baker, Loui Madakamutil, A Richard Kitching, Brendan J O'Sullivan, and Ranjeny Thomas. PD-L1- and calcitriol-dependent liposomal antigen-specific regulation of systemic inflammatory autoimmune disease. *JCI insight*, 4(18), 2019.

[152] Takashi Kei Kishimoto. Development of ImmTOR Tolerogenic Nanoparticles for the Mitigation of Anti-drug Antibodies. *Frontiers in Immunology*, 11:969, 2020.

[153] Omar Duramad, Amy Laysang, Jun Li, Natalie Nguyen, Yasuyuki Ishii, and Reiko Namikawa. A Liposomal Formulation of KRN7000 (RGI-2001) Potently Reduces GvHD Lethality through the Expansion of CD4+Foxp3+ Regulatory T Cells in Murine Models. *Blood*, 112(11):3500–3500, 2008.

[154] Ada Yeste, Meghan Nadeau, Evan J Burns, Howard L Weiner, and Francisco J Quintana. Nanoparticle-mediated codelivery of myelin antigen and a tolerogenic small molecule suppresses experimental autoimmune encephalomyelitis. *Proceedings of the National Academy of Sciences of the United States of America*, 109(28):11270–5, 2012.

[155] Jeremy A Goettel, Roopali Gandhi, Jessica E Kenison, Ada Yeste, Gopal Murugaiyan, Sharmila Sambanthamoorthy, Alexandra E Griffith, Bonny Patel, Dror S Shouval, Howard L Weiner, Scott B Snapper, and Francisco J Quintana. AHR Activation Is Protective against Colitis Driven by T Cells in Humanized Mice. *Cell reports*, 17(5):1318–1329, 2016.

[156] D Scott Wilson, Martina Damo, Sachiko Hirosue, Michal M Raczy, Kym Brünggel, Giacomo Diaceri, Xavier Quaglia-Thermes, and Jeffrey A Hubbell. Synthetically glycosylated antigens induce antigen-specific tolerance and prevent the onset of diabetes. *Nature Biomedical Engineering*, 3(10):817–829, 2019.

[157] Antonella Carambia, Barbara Freund, Dorothee Schwinge, Oliver T Bruns, Sunhild C Salmen, Harald Ittrich, Rudolph Reimer, Markus Heine, Samuel Huber, Christian Waurisch, Alexander Eychmüller, David C Wraith, Thomas Korn, Peter Nielsen, Horst Weller, Christoph Schramm, Stefan Lüth, Ansgar W Lohse, Joerg Heeren, and Johannes Herkel. Nanoparticle-based autoantigen delivery to Treg-inducing liver sinusoidal endothelial cells enables control of autoimmunity in mice. *Journal of hepatology*, 62(6):1349–56, 2015.

[158] Edward Fox, Daniel Wynn, Stanley Cohan, Donna Rill, Dawn McGuire, and Clyde Markowitz. A randomized clinical trial of autologous T-cell therapy in multiple sclerosis: subset analysis and implications for trial design. *Multiple sclerosis (Houndmills, Basingstoke, England)*, 18(6):843–52, 2011.

[159] Marco Romano, Giorgia Fanelli, Caraugh Jane Albany, Giulio Giganti, and Giovanna Lombardi. Past, Present, and Future of Regulatory T Cell Therapy in Transplantation and Autoimmunity. *Frontiers in immunology*, 10:43, 2019.

[160] Jonathan H Esensten, Yannick D Muller, Jeffrey A Bluestone, and Qizhi Tang. Regulatory T cell therapy for autoimmune and autoinflammatory diseases: the next frontier. *The Journal of allergy and clinical immunology*, 142(6):1710–1718, 2018.

[161] Stefan Floess, Jennifer Freyer, Christiane Siewert, Udo Baron, Sven Olek, Julia Polansky, Kerstin Schlawe, Hyun-Dong Chang, Tobias Bopp, Edgar Schmitt, Stefan Klein-Hessling, Edgar Serfling, Alf Hamann, and Jochen Huehn. Epigenetic Control of the foxp3 Locus in Regulatory T Cells. *PLoS Biology*, 5(2):e38, 2007.

[162] D A Boardman, C Philippeos, G O Fruhwirth, M A A Ibrahim, R F Hannen, D Cooper, F M Marelli-Berg, F M Watt, R I Lechler, J Maher, L A Smyth, and G Lombardi. Expression of a Chimeric Antigen Receptor Specific for Donor HLA Class I Enhances the Potency of Human Regulatory T Cells in Preventing Human Skin Transplant Rejection. *American Journal of Transplantation*, 17(4):931–943, 2017.

[163] Qunfang Zhang, Weihui Lu, Chun-Ling Liang, Yuchao Chen, Huazhen Liu, Feifei Qiu, and Zhenhua Dai. Chimeric Antigen Receptor (CAR) Treg: A Promising Approach to Inducing Immunological Tolerance. *Frontiers in Immunology*, 9:2359, 2018.

[164] Xavier Clemente-Casares, Jesus Blanco, Poornima Ambalavanan, Jun Yamanouchi, Santiswarup Singha, Cesar Fandos, Sue Tsai, Jinguo Wang, Nahir Garabatos, Cristina Izquierdo, Smriti Agrawal, Michael B Keough, V Wee Yong, Eddie James, Anna Moore, Yang Yang, Thomas Stratmann, Pau Serra, and Pere Santamaria. Expanding antigen-specific regulatory networks to treat autoimmunity. *Nature*, 530(7591):434–40, 2016.

[165] Sue Tsai, Afshin Shameli, Jun Yamanouchi, Xavier Clemente-Casares, Jinguo Wang, Pau Serra, Yang Yang, Zdravka Medarova, Anna Moore, and Pere Santamaria. Reversal of Autoimmunity by Boosting Memory-like Autoregulatory T Cells. *Immunity*, 32(4):568–580, 2010.

[166] Simone Arienti, Nicole D Barth, David A Dorward, Adriano G Rossi, and Ian Dransfield. Regulation of Apoptotic Cell Clearance During Resolution of Inflammation. *Frontiers in pharmacology*, 10:891, 2019.

[167] G Cox, J Crossley, and Z Xing. Macrophage engulfment of apoptotic neutrophils contributes to the resolution of acute pulmonary inflammation in vivo. *American journal of respiratory cell and molecular biology*, 12(2):232–7, 1995.

[168] C. Haslett, J. S. Savill, M. K. B. Whyte, M. Stern, I. Dransfield, and L. C. Meagher. The Role of Apoptosis in Development, Tissue Homeostasis and Malignancy, Death from inside out. pages 91–97, 1995.

[169] Sandra Hodge, Greg Hodge, Raffaele Scicchitano, Paul N Reynolds, and Mark Holmes. Alveolar macrophages from subjects with chronic obstructive pulmonary disease are deficient in their ability to phagocytose apoptotic airway epithelial cells. *Immunology & Cell Biology*, 81(4):289–296, 2003.

[170] Konosuke Morimoto, William J Janssen, and Mayumi Terada. Defective efferocytosis by alveolar macrophages in IPF patients. *Respiratory medicine*, 106(12):1800–3, 2012.

[171] Carla V Rothlin, Eugenio A Carrera-Silva, Lidia Bosurgi, and Sourav Ghosh. TAM Receptor Signaling in Immune Homeostasis. *Annual Review of Immunology*, 33(1):355–391, 2015.

[172] Philip L. Cohen, Roberto Caricchio, Valsamma Abraham, Todd D. Camenisch, J. Charles Jennette, Robert A.S. Roubey, H. Shelton Earp, Glenn Matsushima, and Elizabeth A. Reap. Delayed Apoptotic Cell Clearance and Lupus-like Autoimmunity in Mice Lacking the c-mer Membrane Tyrosine Kinase. *The Journal of Experimental Medicine*, 196(1):135–140, 2002.

[173] Zaida G Ramirez-Ortiz, William F Pendergraft, Amit Prasad, Michael H Byrne, Tal Iram, Christopher J Blanchette, Andrew D Luster, Nir Hacohen, Joseph El Khoury, and Terry K Means. The scavenger receptor SCARF1 mediates the clearance of apoptotic cells and prevents autoimmunity. *Nature Immunology*, 14(9):917–926, 2013.

[174] Ana Lleo, Carlo Selmi, Pietro Invernizzi, Mauro Podda, and M. Eric Gershwin. The consequences of apoptosis in autoimmunity. *Journal of Autoimmunity*, 31(3):257–262, 2008.

[175] International Multiple Sclerosis Genetics Consortium, Wellcome Trust Case Control Consortium 2, Stephen Sawcer, Garrett Hellenthal, Matti Pirinen, Chris C A Spencer, Nikolaos A Patsopoulos, Loukas Moutsianas, Alexander Dilthey, Zhan Su, Colin Freeman, Sarah E Hunt, Sarah Edkins, Emma Gray, David R Booth, Simon C

Potter, An Goris, Gavin Band, Annette Bang Oturai, Amy Strange, Janna Saarela, Céline Bellenguez, Bertrand Fontaine, Matthew Gillman, Bernhard Hemmer, Rhian Gwilliam, Frauke Zipp, Alagurevathi Jayakumar, Roland Martin, Stephen Leslie, Stanley Hawkins, Eleni Giannoulatou, Sandra D'alfonso, Hannah Blackburn, Filippo Martinelli Boneschi, Jennifer Liddle, Hanne F Harbo, Marc L Perez, Anne Spurkland, Matthew J Waller, Marcin P Mycko, Michelle Ricketts, Manuel Comabella, Naomi Hammond, Ingrid Kockum, Owen T McCann, Maria Ban, Pamela Whittaker, Anu Kemppinen, Paul Weston, Clive Hawkins, Sara Widaa, John Zajicek, Serge Dronov, Neil Robertson, Suzannah J Bumpstead, Lisa F Barcellos, Rathi Ravindrarajah, Roby Abraham, Lars Alfredsson, Kristin Ardlie, Cristin Aubin, Amie Baker, Katharine Baker, Sergio E Baranzini, Laura Bergamaschi, Roberto Bergamaschi, Allan Bernstein, Achim Berthele, Mike Boggild, Jonathan P Bradfield, David Brassat, Simon A Broadley, Dorothea Buck, Helmut Butzkueven, Ruggero Capra, William M Carroll, Paola Cavalla, Elisabeth G Celius, Sabine Cepok, Rosetta Chiavacci, Françoise Clerget-Darpoux, Katleen Clysters, Giancarlo Comi, Mark Cossburn, Isabelle Cournu-Rebeix, Mathew B Cox, Wendy Cozen, Bruce A C Cree, Anne H Cross, Daniele Cusi, Mark J Daly, Emma Davis, Paul I W de Bakker, Marc Debouverie, Marie Beatrice D'hooghe, Katherine Dixon, Rita Dobosi, Bénédicte Dubois, David Ellinghaus, Irina Elovaara, Federica Esposito, Claire Fontenille, Simon Foote, Andre Franke, Daniela Galimberti, Angelo Ghezzi, Joseph Glessner, Refujia Gomez, Olivier Gout, Colin Graham, Struan F A Grant, Franca Rosa Guerini, Hakon Hakonarson, Per Hall, Anders Hamsten, Hans-Peter Hartung, Rob N Heard, Simon Heath, Jeremy Hobart, Muna Hoshi, Carmen Infante-Duarte, Gillian Ingram, Wendy Ingram, Talat Islam, Maja Jagodic, Michael Kabesch, Allan G Kermode, Trevor J Kilpatrick, Cecilia Kim, Norman Klopp, Keijo Koivisto, Malin Larsson, Mark Lathrop, Jeannette S Lechner-Scott, Maurizio A Leone, Virpi Leppä, Ulrika Liljedahl, Izaura Lima Bomfim, Robin R Lincoln, Jenny Link, Jianjun Liu, Aslaug R Lorentzen, Sara Lupoli, Fabio Macciardi, Thomas Mack, Mark Marriott, Vittorio Martinelli, Deborah Mason, Jacob L McCauley, Frank Mentch, Inger-Lise Mero, Tania Mihalova, Xavier Montalban, John Mottershead, Kjell-Morten Myhr, Paola Naldi, William Ollier, Alison Page, Aarno Palotie, Jean Pelletier, Laura Piccio, Trevor Pickersgill, Fredrik Piehl, Susan Pobywajlo, Hong L Quach, Patricia P Ramsay, Mauri Reunanen, Richard Reynolds, John D Rioux, Mariaemma Rodegher, Sabine Roesner, Justin P Rubio, Ina-Maria Rückert, Marco Salvetti, Erika Salvi, Adam Santaniello, Catherine A Schaefer, Stefan Schreiber, Christian Schulze, Rodney J Scott, Finn Sellebjerg, Krzysztof W Selmaj, David Sexton, Ling Shen, Brigid Simms-Acuna, Sheila Skidmore, Patrick M A Sleiman, Cathrine Smestad, Per Soelberg Sørensen, Helle Bach Søndergaard, Jim Stankovich, Richard C Strange, Anna-Maija Sulonen, Emilie Sundqvist, Ann-Christine Syvänen, Francesca Taddeo, Bruce Taylor, Jenefer M Blackwell, Pentti Tienari, Elvira Bramon, Ayman Tourbah, Matthew A Brown, Ewa Tronczynska, Juan P Casas, Niall Tubridy, Aiden Corvin, Jane Vickery, Janusz Jankowski, Pablo Villoslada, Hugh S Markus, Kai Wang, Christopher G Mathew, James Wason, Colin N A Palmer, H-Erich Wichmann, Robert Plomin, Ernest Willoughby, Anna Rautanen, Juliane Winkelmann, Michael Wittig, Richard C Trembath, Jacqueline Yaouanq, Ananth C Viswanathan, Haitao Zhang, Nicholas W Wood, Rebecca Zuvich, Panos Deloukas, Cordelia Langford, Audrey Duncanson, Jorge R Ok-

senberg, Margaret A Pericak-Vance, Jonathan L Haines, Tomas Olsson, Jan Hillert, Adrian J Ivinson, Philip L De Jager, Leena Peltonen, Graeme J Stewart, David A Hafler, Stephen L Hauser, Gil McVean, Peter Donnelly, and Alastair Compston. Genetic risk and a primary role for cell-mediated immune mechanisms in multiple sclerosis. *Nature*, 476(7359):214–9, 2011.

[176] Jason G Weinger, Celia F Brosnan, Olivier Loudig, Michael F Goldberg, Fernando Macian, Heather A Arnett, Anne L Prieto, Vladislav Tsiperson, and Bridget Shafit-Zagardo. Loss of the receptor tyrosine kinase Axl leads to enhanced inflammation in the CNS and delayed removal of myelin debris during Experimental Autoimmune Encephalomyelitis. *Journal of Neuroinflammation*, 8(1):49, 2011.

[177] V A Fadok, D L Bratton, A Konowal, P W Freed, J Y Westcott, and P M Henson. Macrophages that have ingested apoptotic cells in vitro inhibit proinflammatory cytokine production through autocrine/paracrine mechanisms involving TGF-beta, PGE2, and PAF. *The Journal of clinical investigation*, 101(4):890–8, 1998.

[178] Mai-Lan N L Huynh, Valerie A Fadok, and Peter M Henson. Phosphatidylserine-dependent ingestion of apoptotic cells promotes TGF-beta1 secretion and the resolution of inflammation. *The Journal of clinical investigation*, 109(1):41–50, 2002.

[179] Carla V. Rothlin, Sourav Ghosh, Elina I. Zuniga, Michael B.A. Oldstone, and Greg Lemke. TAM Receptors Are Pleiotropic Inhibitors of the Innate Immune Response. *Cell*, 131(6):1124–1136, 2007.

[180] S D Miller, R P Wetzig, and H N Claman. The induction of cell-mediated immunity and tolerance with protein antigens coupled to syngeneic lymphoid cells. *The Journal of Experimental Medicine*, 149(3):758–773, 1979.

[181] Subramaniam Sriram, Gary Schwartz, and Lawrence Steinman. Administration of myelin basic protein-coupled spleen cells prevents experimental allergic encephalitis. *Cellular Immunology*, 75(2):378–382, 1983.

[182] Xunrong Luo, Kathryn L. Pothoven, Derrick McCarthy, Mathew DeGutes, Aaron Martin, Daniel R. Getts, Guliang Xia, Jie He, Xiaomin Zhang, Dixon B. Kaufman, and Stephen D. Miller. ECDI-fixed allogeneic splenocytes induce donor-specific tolerance for long-term survival of islet transplants via two distinct mechanisms. *Proceedings of the National Academy of Sciences*, 105(38):14527–14532, 2008.

[183] Daniel R Getts, Danielle M Turley, Cassandra E Smith, Christopher T Harp, Derrick McCarthy, Emma M Feeney, Meghann Teague Getts, Aaron J Martin, Xunrong Luo, Rachael L Terry, Nicholas J C King, and Stephen D Miller. Tolerance induced by apoptotic antigen-coupled leukocytes is induced by PD-L1+ and IL-10-producing splenic macrophages and maintained by T regulatory cells. *Journal of immunology (Baltimore, Md. : 1950)*, 187(5):2405–17, 2011.

[184] Buvana Ravishankar, Haiyun Liu, Rahul Shinde, Phillip Chandler, Babak Baban, Masato Tanaka, David H Munn, Andrew L Mellor, Mikael C I Karlsson, and Tracy L

McGaha. Tolerance to apoptotic cells is regulated by indoleamine 2,3-dioxygenase. *Proceedings of the National Academy of Sciences of the United States of America*, 109(10):3909–14, 2012.

[185] Alizée J J Grimm, Stephan Kontos, Giacomo Diaceri, Xavier Quaglia-Thermes, and Jeffrey A Hubbell. Memory of tolerance and induction of regulatory T cells by erythrocyte-targeted antigens. *Scientific reports*, 5:15907, 2015.

[186] Frederic A Fellouse, Kaori Esaki, Sara Birtalan, Demetrios Raptis, Vincenzo J Cancasci, Akiko Koide, Parkash Jhurani, Mark Vasser, Christian Wiesmann, Anthony A Kossiakoff, Shohei Koide, and Sachdev S Sidhu. High-throughput Generation of Synthetic Antibodies from Highly Functional Minimalist Phage-displayed Libraries. *Journal of Molecular Biology*, 373(4):924–940, 2007.

[187] Meredith Safford, Samuel Collins, Michael A Lutz, Amy Allen, Ching-Tai Huang, Jeanne Kowalski, Amanda Blackford, Maureen R Horton, Charles Drake, Ronald H Schwartz, and Jonathan D Powell. Egr-2 and Egr-3 are negative regulators of T cell activation. *Nature Immunology*, 6(5):472–480, 2005.

[188] Randeep Singh, Tizong Miao, Alistair L J Symonds, Becky Omodho, Suling Li, and Ping Wang. Egr2 and 3 Inhibit T-bet–Mediated IFN- Production in T Cells. *The Journal of Immunology*, 198(11):4394–4402, 2017.

[189] John E Harris, Kenneth D Bishop, Nancy E Phillips, John P Mordes, Dale L Greiner, Aldo A Rossini, and Michael P Czech. Early Growth Response Gene-2, a Zinc-Finger Transcription Factor, Is Required for Full Induction of Clonal Anergy in CD4 + T Cells. *The Journal of Immunology*, 173(12):7331–7338, 2004.

[190] Yan Zheng, Yuanyuan Zha, Gregory Driessens, Frederick Locke, and Thomas F Gajewski. Transcriptional regulator early growth response gene 2 (Egr2) is required for T cell anergy in vitro and in vivo. *Journal of Experimental Medicine*, 209(12):2157–2163, 2012.

[191] Giuliana P Mognol, Roberto Spreafico, Victor Wong, James P Scott-Browne, Susan Togher, Alexander Hoffmann, Patrick G Hogan, Anjana Rao, and Sara Trifari. Exhaustion-associated regulatory regions in CD8(+) tumor-infiltrating T cells. *Proceedings of the National Academy of Sciences of the United States of America*, 114(13):E2776–E2785, 2017.

[192] Selena Viganò, Riddhima Banga, Florence Bellanger, Céline Pellaton, Alex Farina, Denis Comte, Alexandre Harari, and Matthieu Perreau. CD160-associated CD8 T-cell functional impairment is independent of PD-1 expression. *PLoS pathogens*, 10(9):e1004380, 2014.

[193] Ellen M Ross, Dorothée Bourges, Thea V Hogan, Paul A Gleeson, and Ian R van Driel. Helios defines T cells being driven to tolerance in the periphery and thymus. *European journal of immunology*, 44(7):2048–58, 2014.

[194] Stefano Caserta, Norman Nausch, Amy Sawtell, Rebecca Drummond, Tom Barr, Andrew S Macdonald, Francisca Mutapi, and Rose Zamoyska. Chronic infection drives expression of the inhibitory receptor CD200R, and its ligand CD200, by mouse and human CD4 T cells. *PloS one*, 7(4):e35466, 2012.

[195] Jason B Williams, Brendan L Horton, Yan Zheng, Yukan Duan, Jonathan D Powell, and Thomas F Gajewski. The EGR2 targets LAG-3 and 4-1BB describe and regulate dysfunctional antigen-specific CD8+ T cells in the tumor microenvironment. *The Journal of experimental medicine*, 214(2):381–400, 2017.

[196] Anna Brewitz, Sarah Eickhoff, Sabrina Dähling, Thomas Quast, Sammy Bedoui, Richard A Kroczek, Christian Kurts, Natalio Garbi, Winfried Barchet, Matteo Iannacone, Frederick Klauschen, Waldemar Kolanus, Tsuneyasu Kaisho, Marco Colonna, Ronald N Germain, and Wolfgang Kastenmüller. CD8+ T Cells Orchestrate pDC-XCR1+ Dendritic Cell Spatial and Functional Cooperativity to Optimize Priming. *Immunity*, 46(2):205–219, 2017.

[197] Alison Crawford, Jill M Angelosanto, Charlly Kao, Travis A Doering, Pamela M Odorizzi, Burton E Barnett, and E J Wherry. Molecular and transcriptional basis of CD4 T cell dysfunction during chronic infection. *Immunity*, 40(2):289–302, 2014.

[198] E J Wherry, Sang-Jun J Ha, Susan M Kaech, W N Haining, Surojit Sarkar, Vandana Kalia, Shruti Subramaniam, Joseph N Blattman, Daniel L Barber, and Rafi Ahmed. Molecular signature of CD8+ T cell exhaustion during chronic viral infection. *Immunity*, 27(4):670–84, 2007.

[199] L Baitsch, P Baumgaertner, and Devêvre -E of .... Exhaustion of tumor-specific CD8+ T cells in metastases from melanoma patients. 2011.

[200] Samad A Ibitokou, Brian E Dillon, Mala Sinha, Bartosz Szczesny, Añahi Delgadillo, Doaa Reda Abdelrahman, Csaba Szabo, Lutfi Abu-Elheiga, Craig Porter, Demidmaa Tuvdendorj, and Robin Stephens. Early Inhibition of Fatty Acid Synthesis Reduces Generation of Memory Precursor Effector T Cells in Chronic Infection. *The Journal of Immunology*, 200(2):643–656, 2017.

[201] Ian A Parish, Sudha Rao, Gordon K Smyth, Torsten Juelich, Gareth S Denyer, Gayle M Davey, Andreas Strasser, and William R Heath. The molecular signature of CD8+ T cells undergoing deletional tolerance. *Blood*, 113(19):4575–85, 2009.

[202] Y Jiang, Y Li, and B Zhu. T-cell exhaustion in the tumor microenvironment. *Cell death & disease*, 6(6):e1792, 2015.

[203] Koki Makabe, Valentina Tereshko, Grzegorz Gawlak, Shude Yan, and Shohei Koide. Atomic-resolution crystal structure ofBorrelia burgdorferiouter surface protein A via surface engineering. *Protein Science*, 15(8):1907–1914, 2006.

[204] Alena M Gallegos, Huizhong Xiong, Ingrid M Leiner, Bože Sušac, Michael S Glickman, Eric G Pamer, and Jeroen W J van Heijst. Control of T cell antigen reactivity via programmed TCR downregulation. *Nature immunology*, 17(4):379–86, 2016.

[205] Nicholas J Maurice, M Juliana McElrath, Erica Andersen-Nissen, Nicole Frahm, and Martin Prlic. CXCR3 enables recruitment and site-specific bystander activation of memory CD8+ T cells. *Nature Communications*, 10(1):4987, 2019.

[206] Leo M. Carlin, Kumiko Yanagi, Adrienne Verhoef, Esther N. M. Nolte-'t Hoen, John Yates, Leanne Gardner, Jonathan Lamb, Giovanna Lombardi, Margaret J. Dallman, and Daniel M. Davis. Secretion of IFN- and not IL-2 by anergic human T cells correlates with assembly of an immature immune synapse. *Blood*, 106(12):3874–3879, 2005.

[207] Nicholas Schwab, Tilman Schneider-Hohendorf, and Heinz Wiendl. Therapeutic uses of anti-$\alpha$4-integrin (anti-VLA-4) antibodies in multiple sclerosis. *International immunology*, 27(1):47–53, 2015.

[208] Thomas R Klei, Sanne M Meinderts, Timo K van den Berg, and Robin van Bruggen. From the Cradle to the Grave: The Role of Macrophages in Erythropoiesis and Erythrophagocytosis. *Frontiers in immunology*, 8:73, 2017.

[209] Tracy L McGaha and Mikael C Karlsson. Apoptotic cell responses in the splenic marginal zone: a paradigm for immunologic reactions to apoptotic antigens with implications for autoimmunity. *Immunological reviews*, 269(1):26–43, 2016.

[210] Igor V Pivkin, Zhangli Peng, George E Karniadakis, Pierre A Buffet, Ming Dao, and Subra Suresh. Biomechanics of red blood cells in human spleen and consequences for physiology and disease. *Proceedings of the National Academy of Sciences of the United States of America*, 113(28):7804–9, 2016.

[211] L M VAN PUTTEN and Fineke Croon. The Life Span of Red Cells in the Rat and the Mouse as Determined by Labeling with DFP32 in Vivo. *Blood*, 13(8):789–794, 1958.

[212] A Viola and A Lanzavecchia. T Cell Activation Determined by T Cell Receptor Number and Tunable Thresholds. *Science*, 273(5271):104–106, 1996.

[213] Chun-Hong H Qiu, Yasunobu Miyake, Hitomi Kaise, Hiroshi Kitamura, Osamu Ohara, and Masato Tanaka. Novel subset of CD8{alpha}+ dendritic cells localized in the marginal zone is responsible for tolerance to cell-associated antigens. *Journal of immunology (Baltimore, Md. : 1950)*, 182(7):4127–36, 2009.

[214] Kai Hildner, Brian T Edelson, Whitney E Purtha, Mark Diamond, Hirokazu Matsushita, Masako Kohyama, Boris Calderon, Barbara U Schraml, Emil R Unanue, Michael S Diamond, Robert D Schreiber, Theresa L Murphy, and Kenneth M Murphy. Batf3 deficiency reveals a critical role for CD8alpha+ dendritic cells in cytotoxic T cell immunity. *Science (New York, N.Y.)*, 322(5904):1097–100, 2008.

[215] Henrique Borges da Silva, Raíssa Fonseca, Rosana Moreira Pereira, Alexandra Dos Anjos Cassado, José Maria Álvarez, and Maria Regina D'Império Lima. Splenic Macrophage Subsets and Their Function during Blood-Borne Infections. *Frontiers in immunology*, 6:480, 2015.

[216] Jeanne E Hendrickson, Traci E Chadwick, John D Roback, Christopher D Hillyer, and James C Zimring. Inflammation enhances consumption and presentation of transfused RBC antigens by dendritic cells. *Blood*, 110(7):2736–2743, 2007.

[217] Y Gottlieb, O Topaz, LA Cohen, LD Yakov, T Haber, A Morgenstern, A Weiss, Chait K Berman, E Fibach, and EG Meyron-Holtz. Physiologically aged red blood cells undergo erythrophagocytosis in vivo but not in vitro. *Haematologica*, 97(7):9941002, 2012.

[218] Tracy L McGaha, Yunying Chen, Buvana Ravishankar, Nico van Rooijen, and Mikael C Karlsson. Marginal zone macrophages suppress innate and adaptive immunity to apoptotic cells in the spleen. *Blood*, 117(20):5403–12, 2011.

[219] Buvana Ravishankar, Rahul Shinde, Haiyun Liu, Kapil Chaudhary, Jillian Bradley, Henrique P Lemos, Phillip Chandler, Masato Tanaka, David H Munn, Andrew L Mellor, and Tracy L McGaha. Marginal zone CD169+ macrophages coordinate apoptotic cell-driven cellular recruitment and tolerance. *Proceedings of the National Academy of Sciences of the United States of America*, 111(11):4215–20, 2014.

[220] Nico van Rooijen and Esther Hendrikx. Methods in Molecular Biology. *Methods in molecular biology (Clifton, N.J.)*, 605:189–203, 2009.

[221] Marika Enders, Lars Franken, Marie-Sophie S Philipp, Nina Kessler, Ann-Kathrin K Baumgart, Melanie Eichler, Emmanuel J H JH Wiertz, Natalio Garbi, and Christian Kurts. Splenic Red Pulp Macrophages Cross-Prime Early Effector CTL That Provide Rapid Defense against Viral Infections. *Journal of immunology (Baltimore, Md. : 1950)*, 204(1):87–100, 2020.

[222] Yingping Xu, Yi Liu, Chunqing Yang, Li Kang, Meixiang Wang, Jingxia Hu, Hao He, Wengang Song, and Hua Tang. Macrophages transfer antigens to dendritic cells by releasing exosomes containing dead-cell-associated antigens partially through a ceramide-dependent pathway to enhance CD4(+) T-cell responses. *Immunology*, 149(2):157–71, 2016.

[223] Ronald Backer, Timo Schwandt, Mascha Greuter, Marije Oosting, Frank Jüngerkes, Thomas Tüting, Louis Boon, Tom O'Toole, Georg Kraal, Andreas Limmer, and Joke M M den Haan. Effective collaboration between marginal metallophilic macrophages and CD8+ dendritic cells in the generation of cytotoxic T cells. *Proceedings of the National Academy of Sciences of the United States of America*, 107(1):216–21, 2010.

[224] Joanna Grabowska, Miguel A Lopez-Venegas, Alsya J Affandi, and Joke M M MM den Haan. CD169+ Macrophages Capture and Dendritic Cells Instruct: The Interplay of the Gatekeeper and the General of the Immune System. *Frontiers in immunology*, 9:2472, 2018.

[225] Catherine Lynch, Maria Panagopoulou, and Christopher D Gregory. Extracellular Vesicles Arising from Apoptotic Cells in Tumors: Roles in Cancer Pathogenesis and Potential Clinical Applications. *Frontiers in Immunology*, 8:1174, 2017.

[226] Wiebke Nahrendorf, Philip J Spence, Irene Tumwine, Prisca Lévy, William Jarra, Robert W Sauerwein, and Jean Langhorne. Blood-stage immunity to Plasmodium chabaudi malaria following chemoprophylaxis and sporozoite immunization. *eLife*, 4:e05165, 2015.

[227] Augustina Frimpong, Kwadwo Asamoah Kusi, Dennis Adu-Gyasi, Jones Amponsah, Michael Fokuo Ofori, and Wilfred Ndifon. Phenotypic Evidence of T Cell Exhaustion and Senescence During Symptomatic Plasmodium falciparum Malaria. *Frontiers in immunology*, 10:1345, 2019.

[228] Rachel J Lundie, Tania F de Koning-Ward, Gayle M Davey, Catherine Q Nie, Diana S Hansen, Lei Shong Lau, Justine D Mintern, Gabrielle T Belz, Louis Schofield, Francis R Carbone, Jose A Villadangos, Brendan S Crabb, and William R Heath. Blood-stage Plasmodium infection induces CD8+ T lymphocytes to parasite-expressed antigens, largely regulated by CD8alpha+ dendritic cells. *Proceedings of the National Academy of Sciences of the United States of America*, 105(38):14509–14, 2008.

[229] Sven Burgdorf, Veronika Lukacs-Kornek, and Christian Kurts. The Mannose Receptor Mediates Uptake of Soluble but Not of Cell-Associated Antigen for Cross-Presentation. *The Journal of Immunology*, 176(11):6770–6776, 2006.

[230] Marcus Buggert, Johanna Tauriainen, Takuya Yamamoto, Juliet Frederiksen, Martin A Ivarsson, Jakob Michaëlsson, Ole Lund, Bo Hejdeman, Marianne Jansson, Anders Sönnerborg, Richard A Koup, Michael R Betts, and Annika C Karlsson. T-bet and Eomes Are Differentially Linked to the Exhausted Phenotype of CD8+ T Cells in HIV Infection. *PLoS Pathogens*, 10(7):e1004251, 2014.

[231] Günther Schönrich, Ulrich Kalinke, Frank Momburg, Marie Malissen, Anne-Marie Schmitt-Verhulst, Bernard Malissen, Günter J Hämmerling, and Bernd Arnold. Downregulation of T cell receptors on self-reactive T cells as a novel mechanism for extrathymic tolerance induction. *Cell*, 65(2):293–304, 1991.

[232] Minh Ngoc Duong, Efe Erdes, Michael Hebeisen, and Nathalie Rufer. Chronic TCR-MHC (self)-interactions limit the functional potential of TCR affinity-increased CD8 T lymphocytes. *Journal for immunotherapy of cancer*, 7(1):284, 2019.

[233] E John Wherry, Joseph N Blattman, Kaja Murali-Krishna, Robbert van der Most, and Rafi Ahmed. Viral Persistence Alters CD8 T-Cell Immunodominance and Tissue Distribution and Results in Distinct Stages of Functional Impairment. *Journal of Virology*, 77(8):4911–4927, 2003.

[234] Hendrik Streeck, Zabrina L Brumme, Michael Anastario, Kristin W Cohen, Jonathan S Jolin, Angela Meier, Chanson J Brumme, Eric S Rosenberg, Galit Alter, Todd M Allen, Bruce D Walker, and Marcus Altfeld. Antigen load and viral sequence diversification determine the functional profile of HIV-1-specific CD8+ T cells. *PLoS medicine*, 5(5):e100, 2008.

[235] Alexander Dobin, Carrie A Davis, Felix Schlesinger, Jorg Drenkow, Chris Zaleski, Sonali Jha, Philippe Batut, Mark Chaisson, and Thomas R Gingeras. STAR: ultrafast universal RNA-seq aligner. *Bioinformatics*, 29(1):15–21, 2012.

[236] Artem Tarasov, Albert J Vilella, Edwin Cuppen, Isaac J Nijman, and Pjotr Prins. Sambamba: fast processing of NGS alignment formats. *Bioinformatics*, 31(12):2032–2034, 2015.

[237] Yang Liao, Gordon K Smyth, and Wei Shi. The Subread aligner: fast, accurate and scalable read mapping by seed-and-vote. *Nucleic Acids Research*, 41(10):e108–e108, 2013.

[238] Nicolas L Bray, Harold Pimentel, Páll Melsted, and Lior Pachter. Near-optimal probabilistic RNA-seq quantification. *Nature Biotechnology*, 34(5):525–527, 2016.

[239] M D Robinson, D J McCarthy, and G K Smyth. edgeR: a Bioconductor package for differential expression analysis of digital gene expression data. *Bioinformatics*, 26(1):139–140, 2009.

[240] Di Wu, Elgene Lim, François Vaillant, Marie-Liesse Asselin-Labat, Jane E. Visvader, and Gordon K. Smyth. ROAST: rotation gene set tests for complex microarray experiments. *Bioinformatics*, 26(17):2176–2182, 2010.

[241] Craig N Jenne and Paul Kubes. Immune surveillance by the liver. *Nature immunology*, 14(10):996–1006, 2013.

[242] Shishir Shetty, Patricia F Lalor, and David H Adams. Liver sinusoidal endothelial cells - gatekeepers of hepatic immunity. *Nature reviews. Gastroenterology & hepatology*, 2018.

[243] Shishir Shetty, Patricia F. Lalor, and David H. Adams. Lymphocyte recruitment to the liver: Molecular insights into the pathogenesis of liver injury and hepatitis. *Toxicology*, 254(3):136–146, 2008.

[244] Zuxing Kan and David Madoff. Liver Anatomy: Microcirculation of the Liver. *Seminars in Interventional Radiology*, 25(2):077–085, 2008.

[245] Allan I Jacob, Philip K Goldberg, Norman Bloom, George A Degenshein, and Philip J Kozinn. Endotoxin and Bacteria in Portal Blood. *Gastroenterology*, 72(6):1268–1270, 1977.

[246] Emmanuel A Tsochatzis, Jaime Bosch, and Andrew K Burroughs. Liver cirrhosis. *Lancet (London, England)*, 383(9930):1749–61, 2014.

[247] RY Calne, RA Sells, JR Pena, DR Davis, and PR Millard. Induction of immunological tolerance by porcine liver allografts. 1969.

[248] Nicole Simpson, Yong W. Cho, James C. Cicciarelli, R Rick Selby, and Tse-Ling Fong. Comparison of Renal Allograft Outcomes in Combined Liver-Kidney Transplantation Versus Subsequent Kidney Transplantation in Liver Transplant Recipients: Analysis of UNOS Database. *Transplantation*, 82(10):1298–1303, 2006.

[249] Lucile E. Wrenshall, Jeffrey D. Ansite, Peter M. Eckman, Michelle J. Heilman, R. Brian Stevens, and David E.R. Sutherland. MODULATION OF IMMUNE RESPONSES AFTER PORTAL VENOUS INJECTION OF ANTIGEN1. *Transplantation*, 71(7):841–850, 2001.

[250] Rong Yang, Qi Liu, Jay L. Grosfeld, and Mark D. Pescovitz. Intestinal venous drainage through the liver is a prerequisite for oral tolerance induction. *Journal of Pediatric Surgery*, 29(8):1145–1148, 1994.

[251] B Smedsrød, P J De Bleser, F Braet, P Lovisetti, K Vanderkerken, E Wisse, and A Geerts. Cell biology of liver endothelial and Kupffer cells. *Gut*, 35(11):1509, 1994.

[252] Percy A Knolle and Dirk Wohlleber. Immunological functions of liver sinusoidal endothelial cells. *Cellular & molecular immunology*, 13(3):347–53, 2016.

[253] Ekta Pandey, Aiah S Nour, and Edward N Harris. Prominent Receptors of Liver Sinusoidal Endothelial Cells in Liver Homeostasis and Disease. *Frontiers in Physiology*, 11:873, 2020.

[254] Marta Bermejo-Jambrina, Julia Eder, Leanne C Helgers, Nina Hertoghs, Bernadien M Nijmeijer, Melissa Stunnenberg, and Teunis B H Geijtenbeek. C-Type Lectin Receptors in Antiviral Immunity and Viral Escape. *Frontiers in Immunology*, 9:590, 2018.

[255] Seyed Ali Mousavi, Marita Sporstøl, Cathrine Fladeby, Rune Kjeken, Nicolas Barois, and Trond Berg. Receptor-mediated endocytosis of immune complexes in rat liver sinusoidal endothelial cells is mediated by FcRIIb2. *Hepatology*, 46(3):871–884, 2007.

[256] J Borvak, J Richardson, C Medesan, F Antohe, C Radu, M Simionescu, V Ghetie, and E S Ward. Functional expression of the MHC class I-related receptor, FcRn, in endothelial cells of mice. *International Immunology*, 10(9):1289–1298, 1998.

[257] A Limmer, J Ohl, C Kurts, H G Ljunggren, Y Reiss, M Groettrup, F Momburg, B Arnold, and P A Knolle. Efficient presentation of exogenous antigen by liver endothelial cells to CD8+ T cells results in antigen-specific T-cell tolerance. *Nature medicine*, 6(12):1348–54, 2000.

[258] Jun Wu, Zhongji Meng, Min Jiang, Ejuan Zhang, Martin Trippler, Ruth Broering, Agnes Bucchi, Frank Krux, Ulf Dittmer, Dongliang Yang, Michael Roggendorf, Guido Gerken, Mengji Lu, and Joerg F Schlaak. Toll-like receptor-induced innate immune responses in non-parenchymal liver cells are cell type-specific. *Immunology*, 129(3):363–74, 2010.

[259] Montserrat Martin-Armas, Jaione Simon-Santamaria, Ingvild Pettersen, Ugo Moens, Bård Smedsrød, and Baldur Sveinbjørnsson. Toll-like receptor 9 (TLR9) is present in murine liver sinusoidal endothelial cells (LSECs) and mediates the effect of CpG-oligonucleotides. *Journal of hepatology*, 44(5):939–46, 2006.

[260] Jia Liu, Min Jiang, Zhiyong Ma, Kirsten K Dietze, Gennadiy Zelinskyy, Dongliang Yang, Ulf Dittmer, Joerg F Schlaak, Michael Roggendorf, and Mengji Lu. TLR1/2 ligand-stimulated mouse liver endothelial cells secrete IL-12 and trigger CD8+ T cell immunity in vitro. *Journal of immunology (Baltimore, Md. : 1950)*, 191(12):6178–90, 2013.

[261] Xiang Yu, Lu Chen, Jianqiao Liu, Bolei Dai, Guoqiang Xu, Guanxin Shen, Qingming Luo, and Zhihong Zhang. Immune modulation of liver sinusoidal endothelial cells by melittin nanoparticles suppresses liver metastasis. *Nature Communications*, 10(1):574, 2019.

[262] Antonella Carambia, Barbara Freund, Dorothee Schwinge, Markus Heine, Alena Laschtowitz, Samuel Huber, David C Wraith, Thomas Korn, Christoph Schramm, Ansgar W Lohse, Joerg Heeren, and Johannes Herkel. TGF-$\beta$-dependent induction of CD4CD25Foxp3 Tregs by liver sinusoidal endothelial cells. *Journal of hepatology*, 61(3):594–9, 2014.

[263] Nils Kruse, Katrin Neumann, Arnhild Schrage, Katja Derkow, Eckart Schott, Ulrike Erben, Anja Kühl, Christoph Loddenkemper, Martin Zeitz, Alf Hamann, and Katja Klugewitz. Priming of CD4+ T cells by liver sinusoidal endothelial cells induces CD25low forkhead box protein 3- regulatory T cells suppressing autoimmune hepatitis. *Hepatology (Baltimore, Md.)*, 50(6):1904–13, 2009.

[264] Antonella Carambia, Christian Frenzel, Oliver T. Bruns, Dorothee Schwinge, Rudolph Reimer, Heinrich Hohenberg, Samuel Huber, Gisa Tiegs, Christoph Schramm, Ansgar W. Lohse, and Johannes Herkel. Inhibition of inflammatory CD4 T cell activity by murine liver sinusoidal endothelial cells. *Journal of Hepatology*, 58(1):112–118, 2013.

[265] Bastian Höchst, Frank A Schildberg, Jan Böttcher, Christina Metzger, Sebastian Huss, Andreas Türler, Markus Overhaus, Andreas Knoblich, Berthold Schneider, Dimitrios Pantelis, Christian Kurts, Jörg C C Kalff, Percy Knolle, and Linda Diehl. Liver sinusoidal endothelial cells contribute to CD8 T cell tolerance toward circulating carcinoembryonic antigen in mice. *Hepatology (Baltimore, Md.)*, 56(5):1924–33, 2012.

[266] Frank A Schildberg, Silke I Hegenbarth, Beatrix Schumak, Kai Scholz, Andreas Limmer, and Percy A Knolle. Liver sinusoidal endothelial cells veto CD8 T cell activation by antigen-presenting dendritic cells. *European journal of immunology*, 38(4):957–67, 2008.

[267] Anja Uhrig, Ramin Banafsche, Michael Kremer, Silke Hegenbarth, Alf Hamann, Markus Neurath, Guido Gerken, Andreas Limmer, and Percy A Knolle. Development and functional consequences of LPS tolerance in sinusoidal endothelial cells of the liver. *Journal of leukocyte biology*, 77(5):626–33, 2005.

[268] Yuriko Higuchi, Makiya Nishikawa, Shigeru Kawakami, Fumiyoshi Yamashita, and Mitsuru Hashida. Uptake characteristics of mannosylated and fucosylated bovine serum albumin in primary cultured rat sinusoidal endothelial cells and Kupffer cells. *International Journal of Pharmaceutics*, 287(1-2):147–154, 2004.

[269] Sheena A Linehan. The mannose receptor is expressed by subsets of APC in non-lymphoid organs. *BMC Immunology*, 6(1):4, 2005.

[270] Wanli Liu, Li Tang, Ge Zhang, Handong Wei, Yufang Cui, Lihai Guo, Zikuan Gou, Xiaoxiao Chen, Daifeng Jiang, Yunping Zhu, Gefei Kang, and Fuchu He. Characterization of a novel C-type lectin-like gene, LSECtin: demonstration of carbohydrate binding and expression in sinusoidal endothelial cells of liver and lymph node. *The Journal of biological chemistry*, 279(18):18748–58, 2004.

[271] Jeremy Meyer, Carmen Gonelle-Gispert, Philippe Morel, and Léo Bühler. Methods for Isolation and Purification of Murine Liver Sinusoidal Endothelial Cells: A Systematic Review. *PLOS ONE*, 11(3):e0151945, 2016.

[272] Rajkumar Cheluvappa. Standardized Isolation and Culture of Murine Liver Sinusoidal Endothelial Cells. *Current Protocols in Cell Biology*, 65(1):2.9.1–8, 2014.

[273] Arnhild Schrage, Christoph Loddenkemper, Ulrike Erben, Uta Lauer, Gert Hausdorf, Peter R Jungblut, Judith Johnson, Percy A Knolle, Martin Zeitz, Alf Hamann, and Katja Klugewitz. Murine CD146 is widely expressed on endothelial cells and is recognized by the monoclonal antibody ME-9F1. *Histochemistry and cell biology*, 129(4):441–51, 2008.

[274] Claus Kordes, Iris Sawitza, Silke Götze, and Dieter Häussinger. Hepatic Stellate Cells Support Hematopoiesis and are Liver-Resident Mesenchymal Stem Cells. *Cellular Physiology and Biochemistry*, 31(2-3):290–304, 2013.

[275] Martin Falkowski, Kai Schledzewski, Berit Hansen, and Sergij Goerdt. Expression of stabilin-2, a novel fasciclin-like hyaluronan receptor protein, in murine sinusoidal endothelia, avascular tissues, and at solid/liquid interfaces. *Histochemistry and Cell Biology*, 120(5):361–369, 2003.

[276] Lin Wang, Xiangdong Wang, Guanhua Xie, Lei Wang, Colin K Hill, and Laurie D DeLeve. Liver sinusoidal endothelial cell progenitor cells promote liver regeneration in rats. *The Journal of clinical investigation*, 122(4):1567–73, 2012.

[277] Jeremy Meyer, Stéphanie Lacotte, Philippe Morel, Carmen Gonelle-Gispert, and Léo Bühler. An optimized method for mouse liver sinusoidal endothelial cell isolation. *Experimental cell research*, 349(2):291–301, 2016.

[278] Sonya A MacParland, Jeff C Liu, Xue-Zhong Ma, Brendan T Innes, Agata M Bartczak, Blair K Gage, Justin Manuel, Nicholas Khuu, Juan Echeverri, Ivan Linares, Rahul Gupta, Michael L Cheng, Lewis Y Liu, Damra Camat, Sai W Chung, Rebecca K Seliga, Zigong Shao, Elizabeth Lee, Shinichiro Ogawa, Mina Ogawa, Michael D Wilson, Jason E Fish, Markus Selzner, Anand Ghanekar, David Grant, Paul Greig, Gonzalo Sapisochin, Nazia Selzner, Neil Winegarden, Oyedele Adeyi, Gordon Keller, Gary D Bader, and Ian D McGilvray. Single cell RNA sequencing of human liver reveals distinct intrahepatic macrophage populations. *Nature Communications*, 9(1):4383, 2018.

[279] Chen Ding, Yanyan Li, Feifei Guo, Ying Jiang, Wantao Ying, Dong Li, Dong Yang, Xia Xia, Wanlin Liu, Yan Zhao, Yangzhige He, Xianyu Li, Wei Sun, Qiongming Liu, Lei Song, Bei Zhen, Pumin Zhang, Xiaohong Qian, Jun Qin, and Fuchu He. A Cell-type-resolved Liver Proteome. *Molecular & cellular proteomics : MCP*, 15(10):3190–3202, 2016.

[280] Angeles Dominguez-Soto, Laura Aragoneses-Fenoll, Enrique Martin-Gayo, Lorena Martinez-Prats, Maria Colmenares, Marisa Naranjo-Gomez, Francesc E Borras, Pilar Munoz, Mercedes Zubiaur, Maria L Toribio, Rafael Delgado, and Angel L Corbi. The DC-SIGN–related lectin LSECtin mediates antigen capture and pathogen binding by human myeloid cells. *Blood*, 109(12):5337–5345, 2007.

[281] Zaopeng Yang, Qian Li, Xin Wang, Xuepei Jiang, Dianyuan Zhao, Xin Lin, Fuchu He, and Li Tang. C-type lectin receptor LSECtin-mediated apoptotic cell clearance by macrophages directs intestinal repair in experimental colitis. *Proceedings of the National Academy of Sciences*, 115(43):201804094, 2018.

[282] Teunis B H Geijtenbeek and Sonja I Gringhuis. Signalling through C-type lectin receptors: shaping immune responses. *Nature Reviews Immunology*, 9(7):465–479, 2009.

[283] Nelson B Cole. Site-Specific Protein Labeling with SNAP-Tags. *Current Protocols in Protein Science*, 73(1):Unit 30.1, 2013.

[284] Nazlı Eda Kaleli, Murat Karadag, and Sibel Kalyoncu. Phage display derived therapeutic antibodies have enriched aliphatic content: Insights for developability issues. *Proteins*, 87(7):607–618, 2019.

[285] Hedda Wardemann, Sergey Yurasov, Anne Schaefer, James W. Young, Eric Meffre, and Michel C. Nussenzweig. Predominant Autoantibody Production by Early Human B Cell Precursors. *Science*, 301(5638):1374–1377, 2003.

[286] Beth A Tamburini, Matthew A Burchill, and Ross M Kedl. Antigen capture and archiving by lymphatic endothelial cells following vaccination or viral infection. *Nature communications*, 5:3989, 2014.

[287] Martin L Biniossek, Dorit K Nägler, Christoph Becker-Pauly, and Oliver Schilling. Proteomic identification of protease cleavage sites characterizes prime and non-prime specificity of cysteine cathepsins B, L, and S. *Journal of proteome research*, 10(12):5363–73, 2011.

[288] Jacqueline Staring, Matthijs Raaben, and Thijn R Brummelkamp. Viral escape from endosomes and host detection at a glance. *Journal of Cell Science*, 131(15):jcs216259, 2018.

[289] Dakota J Brock, Helena M Kondow-McConaghy, Elizabeth C Hager, and Jean-Philippe Pellois. Endosomal Escape and Cytosolic Penetration of Macromolecules Mediated by Synthetic Delivery Agents. *Bioconjugate chemistry*, 30(2):293–304, 2018.

[290] A J G Pötgens, S Drewlo, M Kokozidou, and P Kaufmann. Syncytin: the major regulator of trophoblast fusion? Recent developments and hypotheses on its action. *Human Reproduction Update*, 10(6):487–496, 2004.

[291] Faranak S Nouri, Xing Wang, Mania Dorrani, Zahra Karjoo, and Arash Hatefi. A recombinant biopolymeric platform for reliable evaluation of the activity of pH-responsive amphiphile fusogenic peptides. *Biomacromolecules*, 14(6):2033–40, 2013.

[292] Sascha Drewlo, Simone Leyting, Maria Kokozidou, François Mallet, and Andy J Pötgens. C-Terminal truncations of syncytin-1 (ERVWE1 envelope) that increase its fusogenicity. *Biological chemistry*, 387(8):1113–20, 2006.

[293] Kristina Najjar, Alfredo Erazo-Oliveras, and Jean-Philippe Pellois. Delivery of Proteins, Peptides or Cell-impermeable Small Molecules into Live Cells by Incubation with the Endosomolytic Reagent dfTAT. *Journal of Visualized Experiments*, (103), 2015.

[294] Evan A Scott, Armando Stano, Morgane Gillard, Alexandra C Maio-Liu, Melody A Swartz, and Jeffrey A Hubbell. Dendritic cell activation and T cell priming with adjuvant- and antigen-loaded oxidation-sensitive polymersomes. *Biomaterials*, 33(26):6211–6219, 2012.

[295] Yi-Nan Zhang, Wilson Poon, Anthony J Tavares, Ian D McGilvray, and Warren C W Chan. Nanoparticle-liver interactions: Cellular uptake and hepatobiliary elimination. *Journal of controlled release : official journal of the Controlled Release Society*, 240:332–348, 2016.

[296] Shuo-Wang W Qiao, Kanna Kobayashi, Finn-Eirik E Johansen, Ludvig M Sollid, Jan T Andersen, Edgar Milford, Derry C Roopenian, Wayne I Lencer, and Richard S Blumberg. Dependence of antibody-mediated presentation of antigen on FcRn. *Proceedings of the National Academy of Sciences of the United States of America*, 105(27):9337–42, 2008.

[297] Thomas Gramberg, Elizabeth Soilleux, Tanja Fisch, Patricia F Lalor, Heike Hofmann, Sophie Wheeldon, Andrew Cotterill, Anja Wegele, Thomas Winkler, David H Adams, and Stefan Pöhlmann. Interactions of LSECtin and DC-SIGN/DC-SIGNR with viral ligands: Differential pH dependence, internalization and virion binding. *Virology*, 373(1):189–201, 2008.

[298] Yi Li, Bingtao Hao, Xuezhang Kuai, Guichun Xing, Juntao Yang, Jie Chen, Li Tang, Lingqiang Zhang, and Fuchu He. C-type lectin LSECtin interacts with DC-SIGNR and is involved in hepatitis C virus binding. *Molecular and cellular biochemistry*, 327(1-2):183–90, 2009.

[299] Thomas Gramberg, Heike Hofmann, Peggy Möller, Patricia F Lalor, Andrea Marzi, Martina Geier, Mandy Krumbiegel, Thomas Winkler, Frank Kirchhoff, David H Adams, Stephan Becker, Jan Münch, and Stefan Pöhlmann. LSECtin interacts with filovirus glycoproteins and the spike protein of SARS coronavirus. *Virology*, 340(2):224–36, 2005.

[300] Li Tang, Juntao Yang, Xiaoming Tang, Wantao Ying, Xiaohong Qian, and Fuchu He. The DC-SIGN family member LSECtin is a novel ligand of CD44 on activated T cells. *European journal of immunology*, 40(4):1185–91, 2010.

[301] Feng Xu, Jing Liu, Di Liu, Biao Liu, Min Wang, Zhiyuan Hu, Xuemei Du, Li Tang, and Fuchu He. LSECtin expressed on melanoma cells promotes tumor progression by inhibiting antitumor T-cell responses. *Cancer research*, 74(13):3418–28, 2014.

[302] Jun Wu, Mengji Lu, Zhongji Meng, Martin Trippler, Ruth Broering, Agnes Szczeponek, Frank Krux, Ulf Dittmer, Michael Roggendorf, Guido Gerken, and Joerg F Schlaak. Toll-like receptor-mediated control of HBV replication by nonparenchymal liver cells in mice. *Hepatology (Baltimore, Md.)*, 46(6):1769–78, 2007.

[303] Sean Allen, Omar Osorio, Yu-Gang Liu, and Evan Scott. Facile assembly and loading of theranostic polymersomes via multi-impingement flash nanoprecipitation. *Journal of Controlled Release*, 262:91–103, 2017.

[304] T Wang, E B Ahmed, L Chen, J Xu, J Tao, C R Wang, M L Alegre, and A S Chong. Infection with the Intracellular Bacterium, Listeria monocytogenes, Overrides Established Tolerance in a Mouse Cardiac Allograft Model: Infection with Listeria Overrides Established Tolerance. *American Journal of Transplantation*, 10(7):1524–1533, 2010.

[305] M Rios, S Daniel, C Chancey, I K Hewlett, and S L Stramer. West Nile Virus Adheres to Human Red Blood Cells in Whole Blood. *Clinical Infectious Diseases*, 45(2):181–186, 2007.

[306] Mark Lyons, David Onion, Nicky K Green, Kriss Aslan, Ratna Rajaratnam, Miriam Bazan-Peregrino, Sue Phipps, Sarah Hale, Vivien Mautner, Leonard W Seymour, and Kerry D Fisher. Adenovirus Type 5 Interactions with Human Blood Cells May Compromise Systemic Delivery. *Molecular Therapy*, 14(1):118–128, 2006.

[307] Takashi Kei Kishimoto and Roberto A Maldonado. Nanoparticles for the Induction of Antigen-Specific Immunological Tolerance. *Frontiers in immunology*, 9:230, 2018.

[308] Eddie A James, Massimo Pietropaolo, and Mark J Mamula. Immune Recognition of $\beta$-Cells: Neoepitopes as Key Players in the Loss of Tolerance. *Diabetes*, 67(6):1035–1042, 2018.

[309] Ako Ishihara, Jun Ishihara, Elyse A. Watkins, Andrew C. Tremain, Mindy Nguyen, Ani Solanki, Kiyomitsu Katsumata, Aslan Mansurov, Erica Budina, Aaron T. Alpar, Peyman Hosseinchi, Lea Maillat, Joseph W. Reda, Takahiro Kageyama, Melody A. Swartz, Eiji Yuba, and Jeffrey A. Hubbell. Prolonged residence of an albumin–IL-4 fusion protein in secondary lymphoid organs ameliorates experimental autoimmune encephalomyelitis. *Nature Biomedical Engineering*, pages 1–12, 2020.

[310] Yvonne M Mueller, Stephen C De Rosa, Justin A Hutton, James Witek, Mario Roederer, John D Altman, and Peter D Katsikis. Increased CD95/Fas-Induced Apoptosis of HIV-Specific CD8+ T Cells. *Immunity*, 15(6):871–882, 2001.

[311] Norihisa Mikami, Ryoji Kawakami, Kelvin Y Chen, Atsushi Sugimoto, Naganari Ohkura, and Shimon Sakaguchi. Epigenetic conversion of conventional T cells into regulatory T cells by CD28 signal deprivation. *Proceedings of the National Academy of Sciences of the United States of America*, 117(22):12258–12268, 2020.

[312] Masahiko Akamatsu, Norihisa Mikami, Naganari Ohkura, Ryoji Kawakami, Yohko Kitagawa, Atsushi Sugimoto, Keiji Hirota, Naoto Nakamura, Satoru Ujihara, Toshio Kurosaki, Hisao Hamaguchi, Hironori Harada, Guliang Xia, Yoshiaki Morita, Ichiro Aramori, Shuh Narumiya, and Shimon Sakaguchi. Conversion of antigen-specific effector/memory T cells into Foxp3-expressing T reg cells by inhibition of CDK8/19. *Science Immunology*, 4(40):eaaw2707, 2019.

[313] David Leslie, Peter Lipsky, and Abner Louis Notkins. Autoantibodies as predictors of disease. *Journal of Clinical Investigation*, 108(10):1417–1422, 2001.

[314] Matthew S. Macauley, Fabian Pfrengle, Christoph Rademacher, Corwin M. Nycholat, Andrew J. Gale, Annette von Drygalski, and James C. Paulson. Antigenic liposomes displaying CD22 ligands induce antigen-specific B cell apoptosis. *Journal of Clinical Investigation*, 123(7):3074–3083, 2013.

[315] Shetal A Patel and Andy J Minn. Combination Cancer Therapy with Immune Checkpoint Blockade: Mechanisms and Strategies. *Immunity*, 48(3):417–433, 2018.